AD-A082 616 UNITED TECHNOLOGIES CORP WINDSOR LOCKS CONN HAMILTON --ETC F/G 20/1
V/STOL ROTARY PROPULSOR NOISE PREDICTION MODEL UPDATE AND EVALU--ETC(U)
DEC 79 B MAGLIOZZI

UNCLASSIFIED FAA-RD-79-187 NL

1 of 3

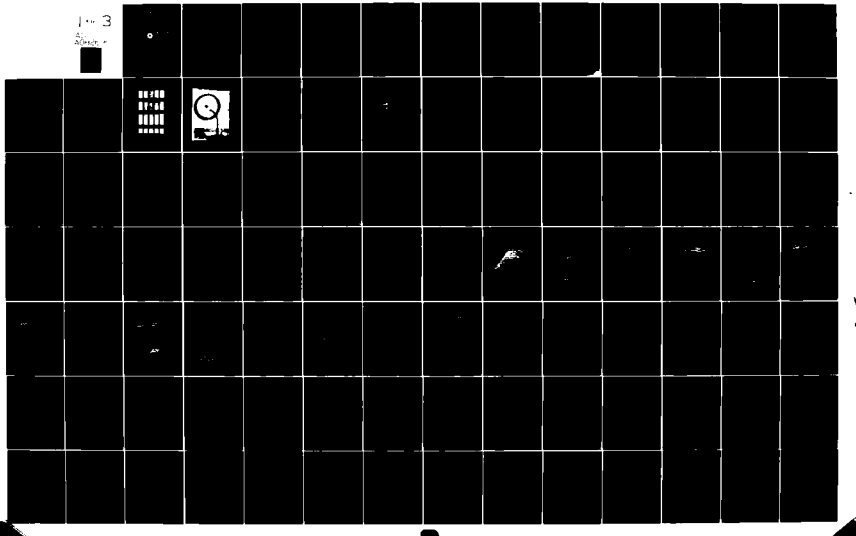

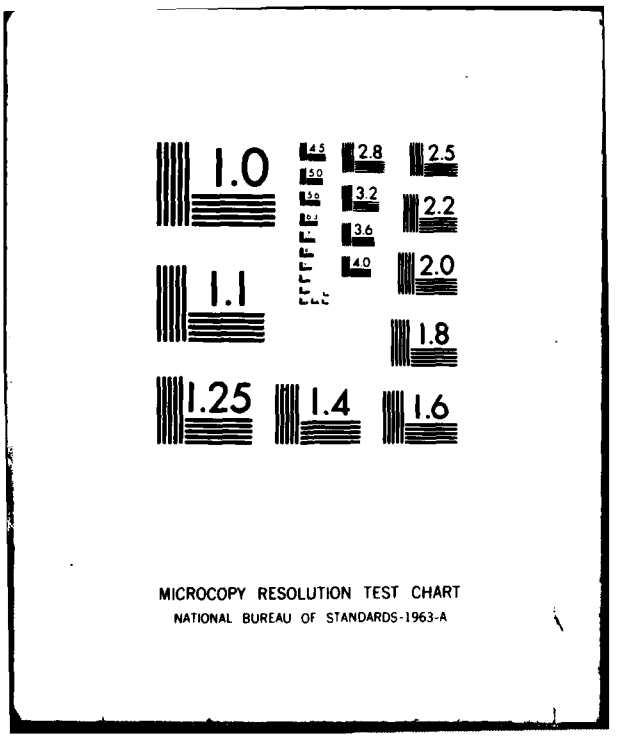
1.0
1.1
1.25
1.4
1.6
1.8
2.0
2.2
2.5
2.8
3.2
3.6
4.0
4.5
5.0
5.6
MICROCOPY RESOLUTION TEST CHART
NATIONAL BUREAU OF STANDARDS-1963-A

REPORT NO. FAA-RD-79-107

LEVEL II

V/STOL ROTARY PROPULSOR NOISE PREDICTION MODEL UPDATE AND EVALUATION

B. Magliozzi

December, 1979

Final Report

Prepared for

U.S. DEPARTMENT OF TRANSPORTATION
FEDERAL AVIATION ADMINISTRATION
Systems Research & Development Service
Washington, D.C. 20590

NOTICE

This document is disseminated under the sponsorship of the Department of Transportation in the interest of information exchange. The United States Government assumes no liability for its contents or use thereof.

1. Report No.	2. Government Accession No.	3. Recipient's Catalog No.
FAA-RD-79-167		

4. Title and Subtitle	5. Report Date
V/STOL Rotary Propulsor Noise Prediction Model, Update and Evaluation	December 1979
	6. Performing Organization Code
7. Author(s) B. Magliozzi	8. Performing Organization Report No. 253
9. Performing Organization Name and Address Hamilton Standard Division of United Technologies Corp. Windsor Locks, Connecticut 06096	10. Work Unit No. (TRAIS)
	11. Contract or Grant No. DOT-FA77WA-4067
12. Sponsoring Agency Name and Address U.S. Department of Transportation Federal Aviation Administration Systems Research and Development Service Washington, D.C. 20590	13. Type of Report and Period Covered Final Report
	14. Sponsoring Agency Code ARD-650 (2015-607)

15. Supplementary Notes

16. Abstract

The V/STOL Rotary Propulsor Noise Prediction Model developed under contract DOT-FA74WA-3477 was updated and evaluated. A three-phase program was conducted. In the first phase, a literature review was conducted to identify and evaluate high quality noise measurements of propeller, variable pitch fan, fixed pitch fan, helicopter, lift fan, core engine, and jet noise for the preparation of a data base with emphasis on recent measurements of in-flight propulsors. In the second phase, the effects of forward flight on V/STOL propulsor noise were evaluated and the noise prediction model was improved to give better agreement with current measurements. ~~In the third phase,~~ Lastly, the performance of the noise prediction methodology was evaluated by comparison of calculations with measurements of propulsor noise from the data base.

Although certain aspects of the measured propulsor noise, such as installation and ground reflection effects, caused discrepancies between measured and calculated levels (the calculations assume uninstalled propulsors under free-field conditions), the general correlation was good. Typical correlation between measured and calculated one-third octave band levels was ±5 dB and between measured and calculated dB(A), PNL, PNLT, and EPNL was ±8 dB.

17. Key Words	18. Distribution Statement
Propeller Noise/Variable Pitch Fan Noise/Helicopter Noise/Jet Noise/ Helicopter Noise/Noise Prediction/ Fixed Pitch Fan Noise/ Forward Flight Effects on Noise	This document is available to the public through the National Technical Information Service, Springfield, Virginia 22151

19. Security Classif. (of this report)	20. Security Classif. (of this page)	21. No. of Pages	22. Price
Unclassified	Unclassified	230	

METRIC CONVERSION FACTORS

Approximate Conversions to Metric Measures

Symbol	When You Know	Multiply by	To Find	Symbol
	LENGTH			
in	inches	*2.5	centimeters	cm
ft	feet	30	centimeters	cm
yd	yards	0.9	meters	m
mi	miles	1.6	kilometers	km
	AREA			
in^2	square inches	6.5	square centimeters	cm^2
ft^2	square feet	0.09	square meters	m^2
yd^2	square yards	0.8	square meters	m^2
mi^2	square miles	2.6	square kilometers	km^2
	acres	0.4	hectares	ha
	MASS (weight)			
oz	ounces	28	grams	g
lb	pounds	0.45	kilograms	kg
	short tons (2000 lb)	0.9	tonnes	t
	VOLUME			
tsp	teaspoons	5	milliliters	ml
Tbsp	tablespoons	15	milliliters	ml
fl oz	fluid ounces	30	milliliters	ml
c	cups	0.24	liters	l
pt	pints	0.47	liters	l
qt	quarts	0.95	liters	l
gal	gallons	3.8	liters	l
ft^3	cubic feet	0.03	cubic meters	m^3
yd^3	cubic yards	0.76	cubic meters	m^3
	TEMPERATURE (exact)			
°F	Fahrenheit temperature	5/9 (after subtracting 32)	Celsius temperature	°C

*1 in = 2.54 (exactly). For other exact conversions and more detailed tables, see NBS Misc. Publ. 286, Units of Weights and Measures, Price $2.25, SD Catalog No. C13.10:286.

Approximate Conversions from Metric Measures

Symbol	When You Know	Multiply by	To Find	Symbol
	LENGTH			
mm	millimeters	0.04	inches	in
cm	centimeters	0.4	inches	in
m	meters	3.3	feet	ft
m	meters	1.1	yards	yd
km	kilometers	0.6	miles	mi
	AREA			
cm^2	square centimeters	0.16	square inches	in^2
m^2	square meters	1.2	square yards	yd^2
km^2	square kilometers	0.4	square miles	mi^2
ha	hectares (10,000 m^2)	2.5	acres	
	MASS (weight)			
g	grams	0.035	ounces	oz
kg	kilograms	2.2	pounds	lb
t	tonnes (1000 kg)	1.1	short tons	
	VOLUME			
ml	milliliters	0.03	fluid ounces	fl oz
l	liters	2.1	pints	pt
l	liters	1.06	quarts	qt
l	liters	0.26	gallons	gal
m^3	cubic meters	35	cubic feet	ft^3
m^3	cubic meters	1.3	cubic yards	yd^3
	TEMPERATURE (exact)			
°C	Celsius temperature	9/5 (then add 32)	Fahrenheit temperature	°F

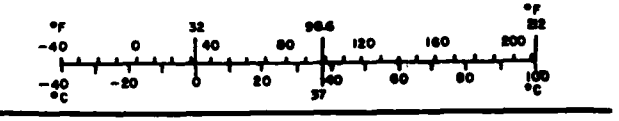

TABLE OF CONTENTS

	Page
INTRODUCTION	1
BACKGROUND	3
INTRODUCTION	3
REVIEW OF NOISE GENERATING MECHANISMS	3
Free-Air Propellers	3
Variable-Pitch Fans	4
Fixed-Pitch Fans	5
Helicopter Rotors	5
Tilt-Propellers	5
Lift-Fans	5
Jets	6
INSTALLATION EFFECTS	6
FORWARD-FLIGHT EFFECTS	10
Free-Air Propellers	10
Variable-Pitch Fans	11
Fixed-Pitch Fans	11
Helicopter Rotors	13
Tilt-Propellers	13
Lift-Fans	13
Jets	14
PROPAGATION AND GROUND REFLECTIONS	14
Introduction	14
Propagation Effects	14
Ground Reflection	15
PHASE I - DATA BASE EXPANSION	21
INTRODUCTION	21
LITERATURE SEARCH	21
DATA EVALUATION	22

TABLE OF CONTENTS (Cont)

	Page
DATA BASE PREPARATION	22
GENERAL OBSERVATIONS ON THE AVAILABLE DATA	38
PHASE II - EVALUATION OF V/STOL ROTARY PROPULSOR FORWARD FLIGHT EFFECTS	39
INTRODUCTION	39
FORWARD-FLIGHT EFFECTS EVALUATION	39
Introduction	39
Free-Air Propellers	40
Variable-Pitch Fans	55
Fixed-Pitch Fans	57
Helicopter Rotors	72
Tilt-Propellers and Lift-Fans	81
Jets	81
SUMMARY OF FORWARD FLIGHT EFFECTS EVALUATION	87
PHASE III - EVALUATION OF V/STOL ROTARY PROPULSOR NOISE PREDICTION METHODOLOGY	91
INTRODUCTION	91
EVALUATION OF PROPELLER NOISE PREDICTION	91
Uninstalled Propellers	91
Installed Propellers	97
Summary for Propellers	111
EVALUATION OF VARIABLE-PITCH FAN NOISE PREDICTION	111
Introduction	111
Comparisons of Measured and Calculated Variable-Pitch Fan Noise	112
Summary for Variable-Pitch Fans	120

TABLE OF CONTENTS (Cont)

	Page
EVALUATION OF FIXED-PITCH FAN NOISE PREDICTION	120
Introduction	120
Methodology Evaluation Using Isolated Static Fan Data	122
Methodology Evaluation Using Real-Engine Data	135
Methodology Evaluation Using the Generalized Engine	144
Summary for Fixed-Pitch Fans	146
EVALUATION OF HELICOPTER NOISE PREDICTION	147
Introduction	147
Comparison of Measured and Calculated Helicopter Noise	149
Summary for Helicopters	170
EVALUATION OF CORE ENGINE NOISE PREDICTION	173
Introduction	173
Comparison of Measured and Calculated Core Engine Noise	173
Summary for Core Engines	177
EVALUATION OF JET NOISE PREDICTION	177
Introduction	177
Comparison of Measured and Calculated Model Jet Noise	177
Comparison of Measured and Calculated Full-Scale Jet Noise	200
Summary for Jets	203
SUMMARY OF NOISE PREDICTION METHODOLOGY EVALUATION	206
CONCLUSIONS	209
RECOMMENDATIONS	211

TABLE OF CONTENTS (Cont)

	Page
APPENDIX A. - COMPUTER PROGRAM CHANGES	213
INTRODUCTION	213
PROGRAM CHANGES	213
Program Corrections	213
Methodology Changes	214
Changes in the Input List	214
USER'S MANUAL REVISIONS	216
APPENDIX B. - GRAPHICAL PROCEDURE CHANGES	219
INTRODUCTION	219
REVISED CHARTS	219
Free-Air Propellers	219
Variable-Pitch Fans with IGVs	219
Variable-Pitch Fans with OGVs	219
Helicopter Rotors	225
Jets	225
REFERENCES	229

INTRODUCTION

Both rotary propulsors and jets have noise generating mechanisms which are strongly influenced by forward flight. Open and shrouded rotors ingest normally occurring atmospheric turbulence which gives rise to unsteady loading noise. The characteristics of the ingested turbulence are strongly influenced by forward-flight effects. Thus, the noise generating mechanisms of rotary propulsors in flight differ from those which occur statically. These different mechanisms result in changes in generated noise levels, spectrum shapes, and source directivity as the propulsor makes the transition from static (take-off) to flight.

Jet noise is caused by fluctuating forces due to viscous shear gradients between the highly turbulent high speed gas stream and the lower velocity ambient medium. The sound intensity is related to the velocity of the jet relative to that of the ambient air. The relative velocity is greatest statically and decreases as forward speed is increased. Thus, in the case of jet noise forward-flight also affects the amplitude, frequency spectrum, and directivity of the generated noise.

Current and proposed aircraft noise certification regulations indicate that the noise level limits will be established under flight conditions. It is thus important for aircraft manufacturers, operators, and regulating agencies to be able to assess the noise levels of present and future propulsor designs to establish trade-offs for designing low-noise propulsors. Since the noise generating mechanisms at static conditions differ substantially from those that occur in flight, useful noise prediction methodology must address the flight regime.

A02 73 89
370

In 1976, Hamilton Standard completed work under FAA contract DOT-FA74WA-3477 363
to develop V/STOL rotary propulsion system noise prediction procedures. The result of this effort, published as a three-volume report (FAA-RD-76-49), included both graphical and computerized noise prediction methods for free-air propellers, shrouded propellers, variable-pitch fans, fixed-pitch fans, tilt-propellers, helicopter rotors, lift-fans, gearboxes, core (drive) engines and jets (primary and bypass). All of these, with the exception of gearboxes and core engines, have noise generating mechanisms which are affected by forward flight. In this previous work, forward-flight effects were incorporated. However, due to the lack of good, high quality data, the forward-flight effects were not fully evaluated. Also, in recent acoustic research work throughout the world, emphasis has been placed on understanding forward-flight effects and this knowledge was not available in the previous study.

In this study, the forward-flight effects included in the methodology from the previous study were reviewed and, where justified, were improved based on currently available measurements of static and in-flight noise. Extensive comparisons between high quality data and calculations using the procedures revised in this contract were made to evaluate the noise prediction methodology accuracy. These comparisons showed generally good agreement, thus confirming that the noise prediction procedures should be useful for noise assessment of potential new aircraft on a preliminary design basis.

BACKGROUND

INTRODUCTION

As background for the discussion of the work performed under this contract, the important noise generating mechanisms and how they are influenced by forward-flight, installation and other considerations will be presented. Thus, a brief review of the significant noise generating mechanisms for the propulsors under consideration will be given below. This discussion is abstracted from Volume I of reference 1. Following this, forward-flight and installation effects will be discussed. Finally, other considerations, such as atmospheric absorption and ground reflection effects, will also be discussed.

REVIEW OF NOISE GENERATING MECHANISMS

The propulsors for which noise prediction methodology is contained in the noise estimating procedures of reference 1 include: free-air propellers, variable-pitch fans, fixed-pitch fans, helicopter rotors, core engines, gearboxes and jets. Although there are variations within each category, such as variable-pitch fans which may have inlet guide vanes or outlet guide vanes, these usually have similar noise generating mechanisms. Also, some noise generating mechanisms are common to several propulsors. Finally, the noise generating mechanisms of core engines and gearboxes are not generally affected by forward flight.

Free-Air Propellers

The major noise sources in propellers are rotor self-noise and inflow/rotor interaction noise. Rotor self-noise consists of thickness (monopole) noise, loading (dipole) noise, non-linear source (quadrupole) noise and broadband noise (also characterized as dipoles). Thickness noise is important only at higher tip speeds for lightly loaded propellers. Quadrupole sources are significant only at transonic tip speeds. Thus, for V/STOL propellers, which are typically moderately to highly loaded at moderate tip speeds, the most significant self-noise sources are loading and broadband noise.

The mechanism of steady loading noise generation is the lift forces on the blades which are steady in a coordinate system fixed to the blades. As the blades rotate they produce periodically oscillating forces in the air. These result in tones at blade passing frequency (rotation rate x number of blades) and integer multiples thereof. The lift vector can be split into a thrust component (usually normal to the plane of rotation) and a torque component (usually in the plane of rotation).

The mechanisms of broadband noise have not been substantiated but are generally conjectured to be vortex shedding, tip vortex interaction, and boundary layer radiation. The original concept of vortex shedding noise was that the blade turbulent boundary layer sheds vortices into the airfoil wakes, resulting in the generation of oscillating random forces at the blade trailing edge. The tip vortex interaction is explained as

a vortex originating at the leading edge interacting with the trailing edge of the same airfoil. Finally, the turbulent boundary layer results in random pressure fluctuations on the airfoil surface which cause noise to be generated. None of these mechanisms has been substantiated satisfactorily. Prediction methods are based on empirical formulas.

Inflow/rotor interaction noise occurs through the mechanisms of non-uniform inflow into the propeller causing fluctuating blade loading. A disturbance in the inflow causes changes in the local resultant air flow velocity. This in turn causes an effective change in the blade angle of attack, which in turn causes a change in the blade lift. Depending on the structure of the inflow disturbance, the noise is generated as tones, broadband, or both. Although the mechanism has *not* been fully substantiated, there is enough indirect evidence, in the form of measured inflow distortion and blade surface pressures, to support the current hypotheses.

Variable-Pitch Fans

Variable-pitch fans, which are defined to be subsonic tip speed devices, have the same noise generating mechanisms as those for free-air propellers plus some additional sources due to inlet or outlet guide vanes. Although in variable-pitch fans the noise generating mechanisms described for free-air propellers are modified, primarily due to the effect of the shroud, they remain qualitatively the same.

Shroud-support/swirl-recovery/preswirl vanes result in an additional source of noise. Wakes from upstream vanes result in fluctuating loads on the rotor blades. Wakes from the *rotor* result in fluctuating loads on the downstream vanes. Thus, fluctuating pressures appear on the rotor blades in one case and on the stator vanes in the other which result in additional noise. Since the separate wakes from the upstream blade row are not exactly equal and are distorted by turbulence in the flow, they do *not* appear at the downstream blade row as a series of identical pulses. Instead, the pulse amplitude and position is modulated in a random manner. The periodic portion gives rise to pure tones, which also occur at blade passing frequencies, while the random portion results in broadband noise.

The shroud also has an effect on the propagation of the noise components generated at the rotor and/or stator. This occurs because the shroud provides an impedance which is dependent on its geometry and varies with duct modes. In general, subsonic modes will decay very rapidly, while those which are supersonic will propagate. Thus, the steady loading and thickness sources in a variable-pitch fan will always decay, as the rotor tip speed is always subsonic. Inflow/rotor and rotor/stator interaction modes may or may not propagate depending on their wall speed (see reference 1 for a more detailed discussion).

A final effect that the shroud produces is to nozzle the discharge flow. Through-flow velocities are generally high enough at the discharge to produce significant jet noise.

In general, the noise sources for a variable-pitch fan are inflow/rotor interaction, rotor broadband, rotor/stator interaction and jet noise.

Fixed-Pitch Fans

The only major difference between fixed-pitch fans and variable-pitch fans are that fixed-pitch fans have higher tip speed, higher pressure ratio, and greater number of blades and vanes. Thus, the fan noise sources summarized above also apply to fixed-pitch fans.

An additional source for fixed-pitch fans is combination tones, which are harmonic of shaft rotation frequency, that occur at supersonic tip speed for fans without inlet guide vanes. The mechanism for this source is the rotating shock pattern from the supersonic blades. As the blades are not identical to one another, the shock pattern is not uniform and the non-blade-passing-frequency harmonics are not cancelled. Thus, the shaft rotation frequency appears as the fundamental frequency of the harmonic series.

Thus, the major sources of noise in fixed-pitch fans include inflow/rotor interaction, rotor/stator interaction, rotor broadband, combination tones (supersonic rotors without inlet guide vanes), and jet noise.

Helicopter Rotors

The noise generating mechanisms of hovering helicopter rotors are similar to those already described for propellers. In addition, interaction between tip vortex filaments can occur. This occurs when the tip vortex of a blade is intersected by the following blade. This results in a lift pulse on the intersecting blade which is similar to that which occurs during turbulence ingestion. In this case also, many harmonics of blade passing frequency are generated.

Tilt-Propellers

Tilt-propellers at lift-off have similar noise generating mechanisms to those of propellers, previously described, except for the effects of cyclic pitch.

In general, cyclic pitch will introduce a certain amount of inflow distortion which may move around the propeller disc to follow the cyclic input location. This inflow distortion will enhance primarily the low frequency tones, since the cyclic input provides a sinusoidal modulation of the blade angle at a rate of one cycle per revolution.

Lift-Fans

In lift-fans, the noise sources and generating mechanisms are the same as for the axial flow fans used for forward flight propulsion. For transonic-tip-speed, fixed-pitch lift fans, however, the combination tones are not as important as in propulsion fans. This

is because this source of noise does not appear in the fan exhaust and the typical lift-fan has a short inlet duct which does not promote the formation of the strong shocks which result in combination tones.

Some lift-fans also have tip turbine drives, which are another noise source.

Jets

Jet noise is generated outside the physical envelope of the propulsor. Although not a significant contributor to the total V/STOL rotary propulsor noise except for low bypass ratio fans, it may become significant when noise suppression is incorporated in the propulsor design.

Jet noise is generally described as a quadrupole source due to the turbulent shear stresses which occur in the boundary between the moving gases and the surrounding medium. The most influential parameter affecting jet noise is jet velocity, as the noise level varies as the velocity raised to the 8th power.

In coaxial jets, as occur in most propulsion fans, the central jet (exhaust from the core engine) is surrounded by a second jet (fan discharge). This provides two shear boundaries: one between the bypass flow and the core engine exhaust and one between the bypass flow and the ambient air. This produces several effects. First, since in general the bypass flow velocity is lower than that of the core engine exhaust, the relative velocities at the interfaces are lower than that for a single jet. Second, the acoustic pressure generated by the primary jet has to propagate through the bypass flow and thereby is attenuated. Finally, the bypass flow jet noise is of a lower intensity due to its lower relative velocity and of lower frequency due to the larger fan nozzle area. Thus, the effects on jet noise for coaxial configuration is to reduce the generated noise primarily by moving a greater mass of air at a lower velocity.

INSTALLATION EFFECTS

The foregoing discussion addressed the noise generating mechanisms for uninstalled propulsors. Uninstalled propulsors are totally isolated and therefore operate with uniform inflow (except for naturally occurring atmospheric turbulence). In reality, it is not possible to test under ideal conditions, i.e., even a very aerodynamically clean drive system introduces some blockage effects. For actual installation on aircraft, the effects are even stronger. Since these effects can have significant influence on the noise generated, they are important. The noise prediction methodology described in reference 1, which was evaluated in this study, was developed for uninstalled propulsors. Thus, for a valid evaluation, only test data from configurations which are free from installation effects should be used. In the present study, acquiring this type of data turned out to be a difficult task. The following summary of installation effects is presented to put the problem in perspective.

The installation effects usually encountered either distort or interact with the propulsor flow-field. For example, a propeller with a small tip clearance to the fuselage or a fan mounted near a fuselage will operate in distorted inflow due to the blockage from the fuselage and possible ingestion of the fuselage boundary layer. Figure 2-1 shows blade surface pressures measured on a static propeller abstracted from reference 2. During the static portion of the run (first 50 revolutions), a strong disturbance appears in the vicinity of the 40th circumferential sample number. This coincides with the instrumented blade being closest to the airplane fuselage. It is conjectured that this disturbance is due to a vortex originating on the fuselage.

A second disturbance is apparent in figure 2-1 near circumferential sample 80. This occurs when the instrumented blade is closest to the ground. Again, it is conjectured that this indicates a vortex, but now originating at the ground. Such vortices have been observed and documented. Figure 2-2 is a photograph which clearly shows a ground vortex being ingested into a fixed-pitch fan.

As seen in this figure, the vortex is of small transverse scale relative to the fan diameter. Thus, when a blade intersects the vortex, a sharp blade loading pulse, as seen in figure 2-1, is generated. Due to the large amplitude and short duration of the pulse, high levels of noise extending into the high frequencies are generated. Since each blade intersects the vortex once per revolution, the noise generated is at harmonics of blade passing frequency. The data from reference 2 shows many harmonics of blade passing frequency extending well into the mid-frequencies for the static runs. It is apparent from this data that the ingestion of a vortex will result in tone-like noise which is dominant over the other sources, including normally occurring atmospheric turbulence inflow interaction noise, steady loading noise, and rotor/stator interaction noise.

Another flow-field interaction, encountered in helicopters, is that between the main rotor(s) and the tail rotor. Tandem main rotors usually have some degree of overlap. Thus, the wake from the upper rotor is convected downward into the lower rotor, producing local turbulence which is intercepted by the second rotor blades. Similarly, the main rotor wake may be convected into the tail rotor. This causes noise to be generated due to inflow distortion interaction. The relative importance of this mechanism, of course, depends on the proximity of the two rotors, the rotor operating conditions, and the vehicle operating condition.

A third installation effect is distortion of the flow-field due to blockage. Wings, nacelles, fuselages, etc. produce distortion by blocking part of the inflow so that the rotor sees a periodic variation in the flow-field once per revolution. The significance of this mechanism depends on the intensity of the distortion as well as its harmonic content. A low-order distortion, as might be produced by fuselage blockage, would not result in significant noise generation for a many-bladed rotor.

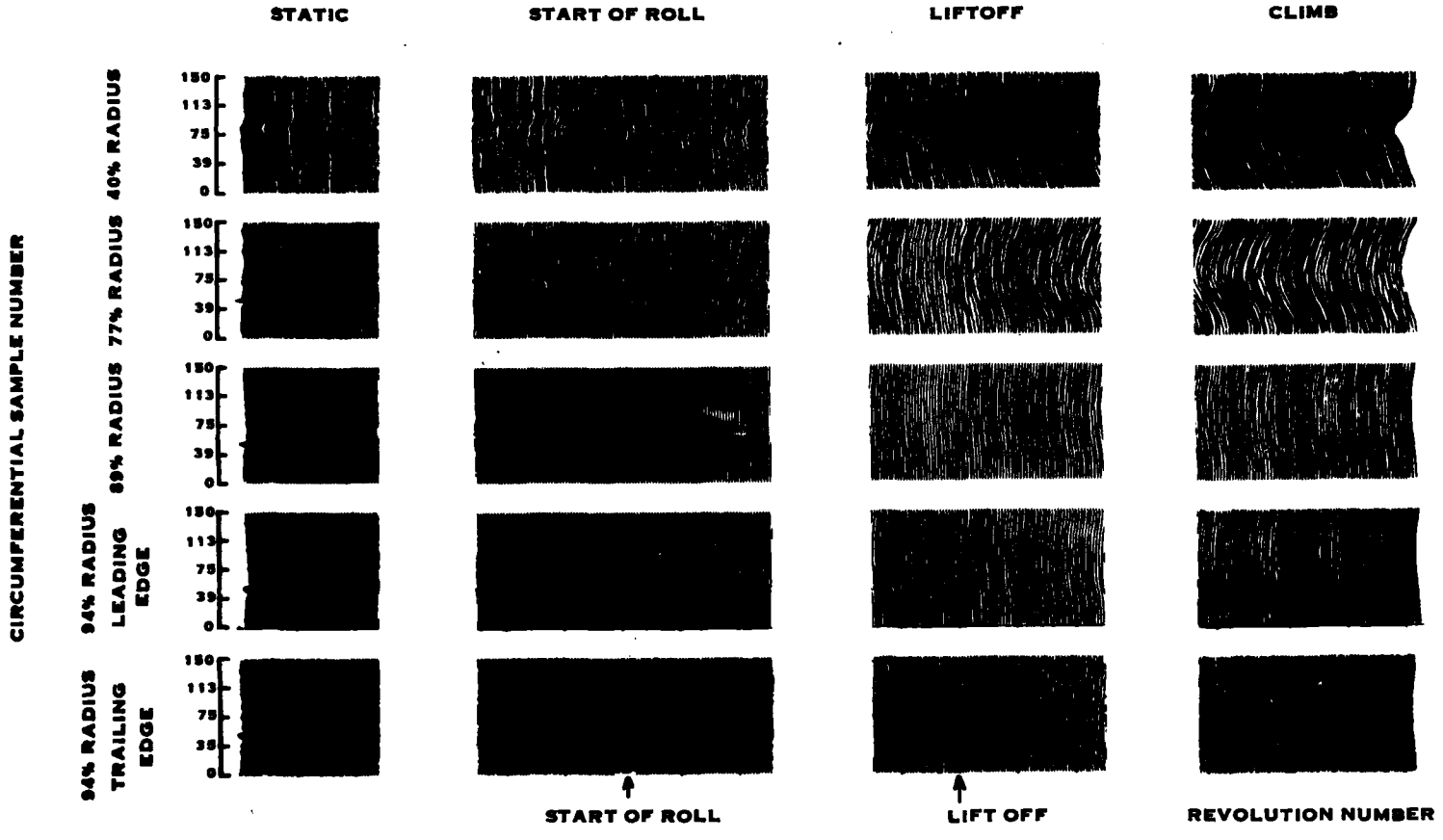

FIGURE 2-1. PROPELLER BLADE SURFACE PRESSURE TIME HISTORIES UNDER STATIC CONDITIONS

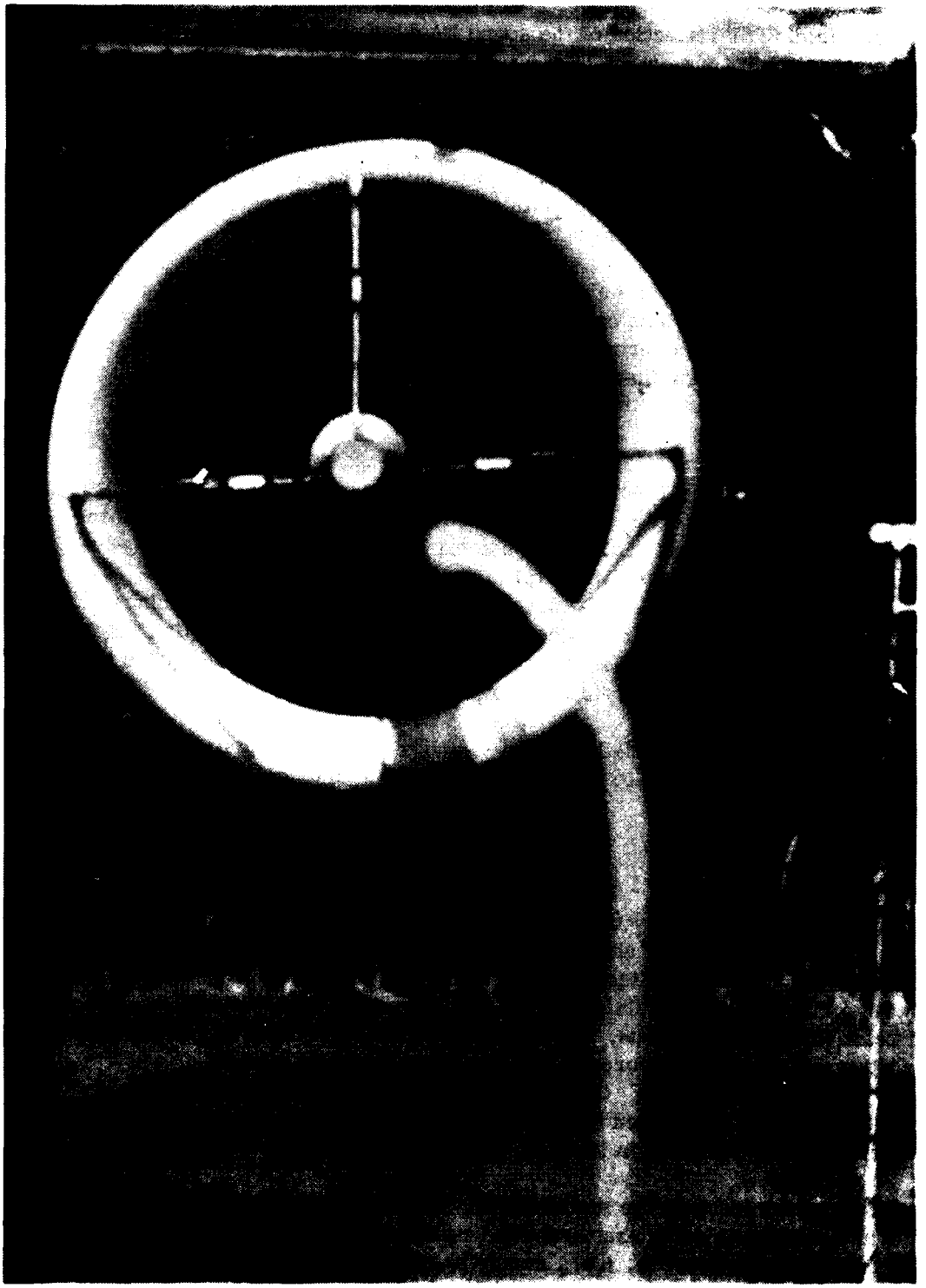

FIGURE 2-2. GROUND VORTEX INGESTION

A final effect is shielding or reflection of the sound field by wings, fuselage, tail surfaces, etc. As an example, one engine of an airplane with aft-mounted turbofans is shielded by the fuselage to an observer located to the side of the airplane. Also, the noise from the engine on the observer side will be reflected by the fuselage. Thus, the noise measured to the side will differ from that measured above or below the airplane, as would be the case during flyover. Other possibilities include the shielding of the engine inlet by the wings, shielding of an aft center mounted engine inlet by the fuselage, and engine shielding by a helicopter fuselage.

In summary, installation effects can be significant and may be the dominant propulsor noise generating mechanism in some cases. Since the current methodology under evaluation applies only to isolated propulsors, the data for correlation must be carefully screened for evidence of any installation effects.

FORWARD-FLIGHT EFFECTS

Forward-flight effects on V/STOL rotary propulsors can be generally classified into two categories. In the first category are those effects which result from changes in operating conditions due to flight. This includes, for example, the reduction in propeller thrust, reduction in helicopter rotor torque, and reduction in jet relative velocity which occur as forward speed is increased. The second category includes changes in the noise sources due to the effects of flight on the noise generating mechanisms. An example of these effects is the modification of inflow turbulence due to flight with a resulting change in rotor/inflow interaction noise.

In the following sections the forward-flight effects and their implementation in the noise prediction methodology prior to this evaluation will be discussed in turn for each propulsor.

Free-Air Propellers

Steady loading noise is conveniently divided into torque noise and thrust noise. During a normal take-off, the power input and rpm are held constant. However, the propeller thrust decreases with increasing flight speed. Thus, the thrust component of the noise decreases. As forward speed is further increased, the noise may increase due to the increase in relative tip speed. Thus, as forward speed is increased, the steady loading noise is expected to initially decrease slightly, then increase slightly.

Since the broadband noise is believed to be related to the propeller thrust, broadband noise is also expected to decrease in level as forward flight is increased.

These two effects are implicit in the methodology, as the formulations for steady loading noise and broadband noise use thrust and tip speed as inputs. Thus, forward-flight effects on self-noise sources, i.e., steady loading and broadband noise, are built into the methodology. The inflow/rotor interaction noise, however, requires

definition of the inflow, which is conjectured to be influenced by the propeller potential flow field. Figure 2-3 depicts the current understanding of the differences in inflow between static and flight. Statically, the rotor potential field extends over a large area, both in front and behind the plane of rotation. Thus, a turbulent eddy captured by the propeller flow field is greatly contracted as it enters the disc. To conserve angular momentum, the transverse turbulence is increased and the eddy is transformed into a long, thin region of high intensity turbulence which moves through the rotor. This is the cause of the high levels of higher frequency harmonics generated statically as previously described. In flight, the inflow contraction is much less, so that the patches of turbulence are relatively unaffected. Thus, the noise due to inflow/rotor interaction will be much lower in flight than statically.

It is also apparent that installation effects in flight will differ from those at static conditions. For instance, vortices from the fuselage (if any are formed in flight) will be convected downstream without passing through the propeller disc. Ground vortices, of course, are not formed at all. This can appear as a significant effect of forward flight on noise which would not be apparent for uninstalled propellers. In contrast, inflow distortion due to blockage from the nacelles, wing upwash, fuselage boundary layer, etc. is more severe in flight than statically, thus causing an opposite effect.

Variable-Pitch Fans

In general, the forward-flight effects previously discussed for free-air propellers also apply to variable-pitch fans. It should be noted, however, that the rotor steady loading and broadband noise and the stator noise are relatively unaffected by forward flight, as the rotor operating conditions are constant due to the effects of the shroud. The influence of forward flight on rotor/inflow interaction noise and installation effects are expected to be similar to those previously described.

Fixed-Pitch Fans

The forward-flight effects on fixed-pitch fan noise depend on the fan configuration. It is generally assumed that the noise generated in fans with inlet guide vanes is due primarily to stator/rotor interaction. As stator/rotor interaction is unaffected by forward-flight, the noise generated by a fixed-pitch fan with inlet guide vanes does not change with forward flight. Fixed-pitch fans without inlet guide vanes generate noise by inflow-turbulence/rotor interaction. At subsonic relative tip speed, the fan steady loading noise and thickness noise are not totally dominant over the inflow-turbulence/rotor interaction noise. Thus, forward-flight will result in reduction of fan tone noise at subsonic tip speeds. As the tip speed approaches sonic velocity, the steady rotor sources become dominant and the forward-flight effects become insignificant.

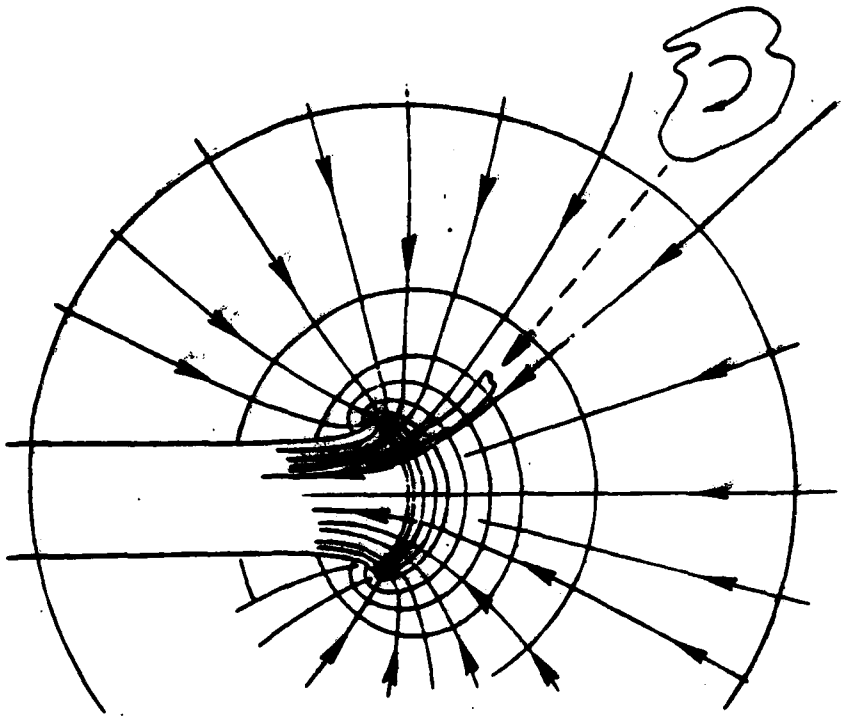

STATIC

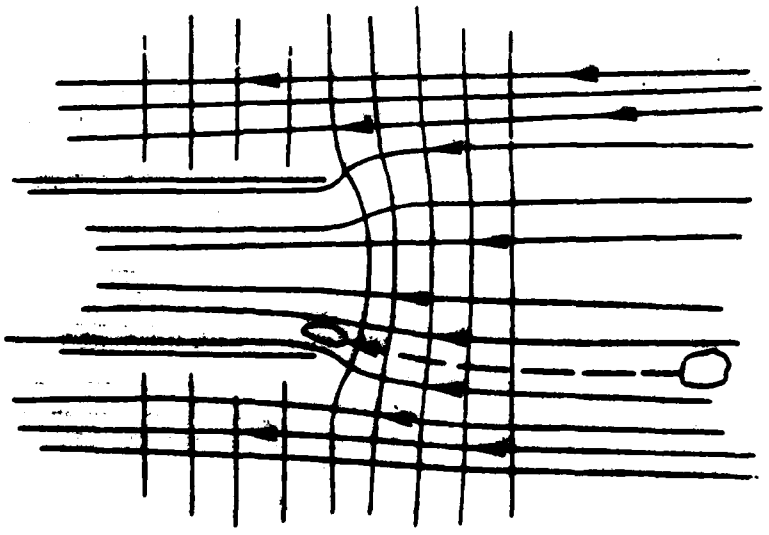

FLIGHT

FIGURE 2-3. COMPARISON OF TURBULENCE INGESTION UNDER STATIC AND FLIGHT CONDITIONS

Helicopter Rotors

There are three major forward flight effects on helicopter rotor noise. First, the turbulence in the inflow is modified. This is a similar effect to that described under propellers. Second, the paths of the tip vortices are modified. During ascent and cruise, the vortices may be convected out of the path of the following blades. During descent, the vortices may be convected into the path of the following blades. Thus, a helicopter rotor which does not exhibit impulsive noise (often called "blade slap") during hover or cruise may exhibit it during descent. Third, during cruise, the inflow is not normal to the rotor disc. This creates an inplane (transverse) velocity component. Thus, the blade which is advancing (i.e., during the half of a revolution when it is moving in the flight direction) experiences a velocity which is the sum of the rotational velocity and a component of the flight velocity. The retreating blade will experience the component of the flight velocity subtracted from the rotational velocity. If the two components are large (i.e., high tip speed and high flight speed) the advancing blade can approach or even exceed sonic velocity with an abrupt change in loading. This will result in impulsive noise generation. If the two components are not too large, the blade will still experience a change in loading as it goes through a revolution. However, this is a low order distortion and couples only with the low frequency harmonics.

A final effect can be conjectured, although it is presently difficult to substantiate with the available data. Since the broadband noise level is dependent on the blade section speed to the sixth power, the advancing blade will make more broadband noise than the retreating blade. As this fluctuating blade section speed varies periodically at the rotor revolution rate, the ear or a frequency analyzer will tend to read an average. Since the noise level is dependent on velocity to the sixth power, the integrated average will be higher than that using the mean velocity (zero flight speed). At representative tip speeds, this effect could result in an increase in broadband noise of about 4 dB at 60 kts compared to that during hover.

Tilt-Propellers

The noise from tilt-propellers will be affected by flight as was described for free-air propellers. In addition, the skewed inflow may generate low order fluctuating blade loads as described for helicopter rotors.

Lift-Fans

Lift-fans will show forward-flight effects comparable to those which were described for the like propulsion fans. In addition, skewed inflow may give rise to low order inflow distortion, but that is not particularly significant in lift-fans due to the large number of rotor blades. However, severe skewed inflow can cause the flow to separate in the inlet duct. As this produces local patches of high level turbulence, it can be a significant source of noise.

Jets

Inasmuch as jet noise is generated in the boundary between the moving gases and the surrounding medium, the level of jet noise is dependent on relative velocity. Thus, as flight speed is increased, relative velocity decreases, and jet noise decreases. Although there is some disagreement on the strength of the flight effect, it is generally conceeded that the jet noise is proportional to $(V_j-V_a)^n V_j^{8-n}$, where V_j is the jet velocity, V_a is the flight velocity and n is an exponent equal to 6 or 7.

PROPAGATION AND GROUND REFLECTIONS

Introduction

As a final section in this background discussion, it is appropriate to describe two additional effects which affect measured noise levels. In contrast to the phenomena described in previous sections, which affect the noise which is generated, the ones to be described in this section relate to how the noise is affected after it is generated and in transit to the observer. The first item is propagation effects and includes atmospheric absorption, refraction, Doppler frequency shift and shielding. The second item relates to reflections from a ground plane, usually present when noise measurements are made.

Propagation Effects

Atmospheric Absorption. - The atmosphere is not a perfect noise propagating medium, and therefore has losses. Thus, in addition to reduction in sound intensity due to spherical spreading, the source noise will decay with distance due to atmospheric losses. A current widely accepted procedure for calculating atmospheric absorption (also called excess attenuation) is given in reference 3. This procedure provides values of absorption as functions of frequency, temperature, and relative humidity. These vary from about 0.1 dB/1000 ft at low frequencies to more than 20 dB/1000 ft at high frequencies, depending on the temperature and relative humidity.

Although a temperature and relative humidity profile between source and observer can be defined and the atmospheric absorption calculated incrementally, it is usually calculated assuming constant temperature and humidity over the propagation path. The data acquired for correlations typically had propagation distances of 500 to 1500 ft and were obtained under normal atmospheric conditions (i.e., no temperature inversions, stable atmosphere). For a normal atmosphere, an altitude change of 1500 ft results in a change of about 6 degrees in temperature and 3 percent in relative humidity. On a standard day (77 degrees Farenheit and 70 percent relative humidity), the variation in atmospheric absorption rate over an altitude change of 1500 ft is only a few tenths of a dB below 5000 Hz, increasing to about 2 dB at 10,000 Hz. Even for ambient conditions for which large values of atmospheric attenuation are calculated (up to about 60 dB per 1000 ft for 50 degrees Farenheit and 30 percent relative humidity), the change in atmospheric absorption is from about 1 dB at 1000 Hz to 15 dB at 10,000 Hz over the 1500 ft

distance. Thus, the assumption of constant temperature and humidity over the propagation path is not considered a serious problem for this study, as for most cases the resulting "error" is less than one dB (and that only at very high frequencies) with a possible maximum "error" of less than 8 dB at 10,000 Hz.

Refraction. - Refraction occurs when a propagating wave encounters a temperature gradient at a non-normal angle. This phenomenon results in an apparent change in directivity and a change in the actual transmission path length. Again, for the purpose of this study, this effect is not particularly significant as the data was acquired relatively close to the source with normal atmospheric conditions.

Doppler Frequency Shift. - Motion of a source relative to an observer causes an apparent source frequency shift. This is readily calculated and can be easily corrected for. It does present a problem, however, when attempting narrow-band analyses of flyover data as the frequency may shift from one band to another and cause "smearing" of tones. Also, the change in wavelength affects ground reflection effects (to be described later). A second effect of the Doppler shift is to cause an increase in the apparent sound level at the observer as the source is approaching and a decrease in the level as the source is receding. These apparent changes in the source directivity are usually called convective or dynamic amplification effects.

Shielding. - A barrier between the source and the observer will affect the noise propagation. Although diffraction may prevent total blockage of the sound, large surfaces such as wings can effectively block the transmission of high frequency noise. Thus, the wing on an airplane with aft mounted engines may shield the engine inlet noise from an observer on the ground during a flyover, as illustrated in figure 2-4. It may be noted that for the configuration depicted in figure 2-4, an observer to the side of the airplane will hear only the engine on his side of the airplane. The engine on the opposite side is shielded by the fuselage. The fuselage and wing will reflect noise back to the observer. Thus, the effective transmission paths for engine noise for this installation are vastly different to the side as compared with engine noise heard below the aircraft. Since static data is typically acquired to the side of an airplane or on a test stand, while in-flight data is typically acquired during flyover, significant differences in noise levels measured between static and flight may result from shielding effects.

Ground Reflection

In a typical flyover noise measurement program, as for noise certification, the microphone is located at some distance above the ground. This results in ground reflection effects, which are caused by interference between the direct acoustic wave and that reflected by the ground.

The phenomenon is depicted in figure 2-5. As may be seen in this figure, the source (assumed to be of uniform directivity for this discussion) emits a ray which travels directly to the observer. A second ray is emitted which also travels to the observer,

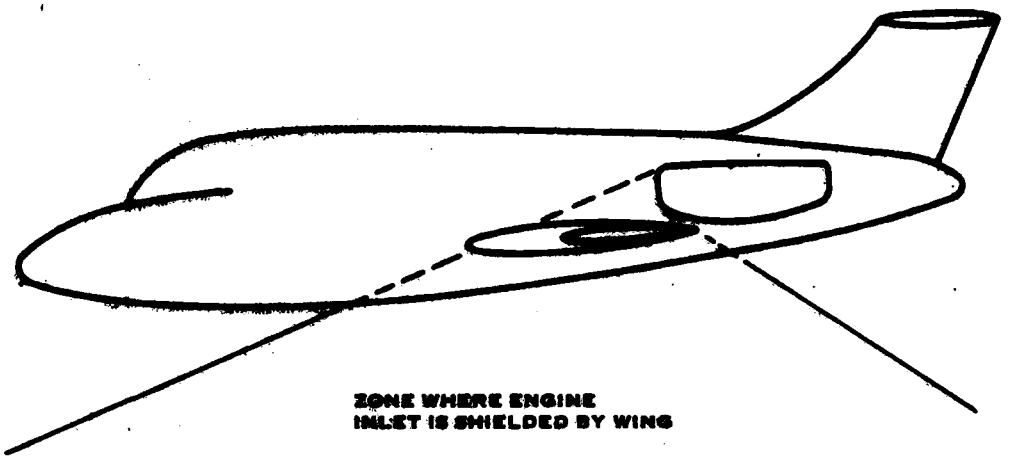

FIGURE 2-4. ENGINE INLET SHIELDING BY AIRPLANE WING

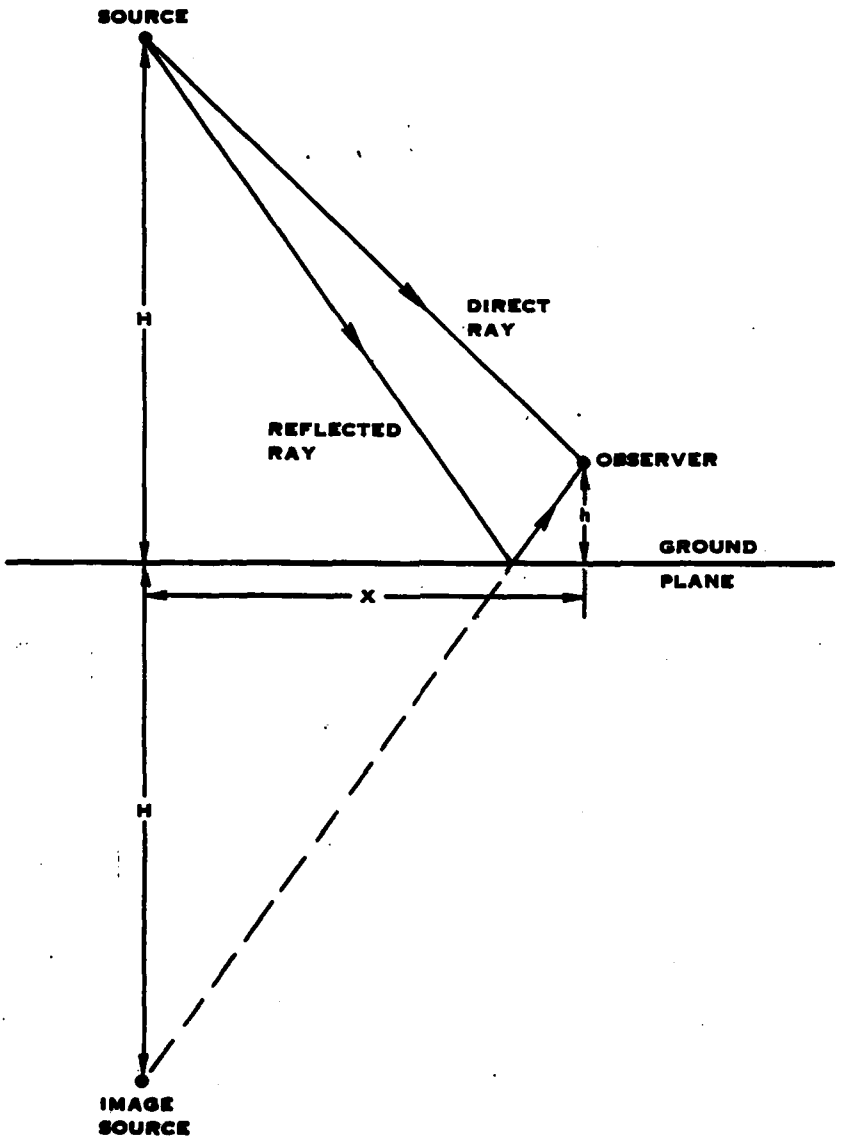

FIGURE 2-5. GROUND REFLECTION GEOMETRY

but this one first hits the ground plane (assumed to be a perfect reflector) which reflects it to the microphone. This is equivalent to there being two sources, the actual source and an image source of equal amplitude and phase to the actual source located beneath the ground plane. It is readily apparent that the distance traveled by the direct ray is $[x^2+(H-h)^2]^{1/2}$ while that traveled by the reflected ray is $[x^2+(H-h)^2]^{1/2}$. It is obvious that when H and h are both greater than zero, the reflected ray will travel a greater distance than the direct ray. When this occurs, the phases of the direct and reflected signal at the observer will generally be different. Specifically, when the path length difference is equal to a half-wavelength, the two signals arrive at the observer exactly out of phase and subtract. Conversely, when the path length is equal to a full wavelength, the two signals arrive in phase and add. Assuming that the path length difference is small compared to the distance between source and observer, a perfect ground plane, and uniform source directivity, when the two signals are out of phase they cancel completely, while when in phase the signal is doubled in amplitude. Thus, for a given geometry, the frequency spectrum at the observer will show peaks at those frequencies where the path length difference is an interger multiple of full wavelengths (full reinforcements) and nulls where the path length difference is an odd multiple of a half-wavelength. Compared to free-field (i.e., no ground plane), the observer will hear an effect equal to: $\Delta dB = 10 \log_{10} (2 + 2 \cos \theta)$, where $\theta = \pi f \Delta r/c$ and f is the signal frequency, Δr is the path length difference, and c is the speed of sound. It is apparent from the above equation that for the theoretical case for single frequencies (i.e., tones) the ΔdB varies from $-\infty$ (full cancellation) to +6 (full reinforcement). The variation for broadband noise integrated over the width of one-third octave bands is less, typically in the range -14 to +6 dB.

In actuality, the above extremes do not occur. Typically, ground reflection effects are seen at low frequencies and result in levels which are 5 dB above to 10 dB below free-field levels. At high frequencies, several reinforcements and cancellations occur within one band and are therefore averaged (giving a constant +3 dB increase over free-field levels). For certification requirements, a microphone height of 4 ft is specified. For flyovers, at the time the source is over the microphone the path length difference is about 8 ft, which gives cancellations at multiples of about 80 Hz. Although this produces a jagged low frequency spectrum for smooth broadband noise such as that from a jet, it has no strong effect on the measured perceived noise level (PNL) except to increase it up to 3 dB over that which would be measured under free-field conditions. However, 80 Hz is in the range where propellers and helicopter rotors have significant tone noise. As these tones usually set the PNL, wide variations can occur, particularly since the cancellation effect on pure tones is very sharp. The application of ground reflection corrections to pure tone sources has not been particularly successful, especially in the regions where cancellations are thought to occur. This task is difficult because the cancellation is very sensitive to small phase differences, which are not generally known with sufficient accuracy.

It is thus apparent that the ground reflection effect will vary during a flyover, as the geometry and frequencies are changing. It is thus not practical to correct the data to free-field conditions for low-frequency tones. Also, since in-flight data is obtained

typically during 1000 ft altitude flyovers while static data is obtained with the source at a few feet above the ground, the two sets of data will show significant differences in the measured low-frequency tone noise levels.

One way which appears promising for reducing the ground reflection problem for sources of low frequency tones during flyovers is to use a ground level microphone. In this approach, the microphone is located flush with or as near as possible to an ideal reflecting surface (i.e., a large, flat, and hard area, such as a concrete or asphalt pad). With this configuration, the direct and reflected low frequency signals remain in phase, giving a correction to free-field of nearly -6 dB which is independent of frequency and aircraft position.

PHASE I - DATA BASE EXPANSION

INTRODUCTION

Forward-flight affects the noise produced by rotary propulsors in two ways. The first way is a change in noise generating mechanisms which affects the noise sources directly. The second way is an effective change in aerodynamic loading conditions, particularly important for open rotors such as propellers and helicopter rotors. This is not due to change in the noise generation mechanisms, but rather an aerodynamic change which results in a change in the inputs to the noise calculation procedures.

The work reported in reference 1 includes the forward-flight effects of the second type, as these are inherent in the methodology. Forward-flight effects of the first type were not treated rigorously, but an attempt was made to include them for each propulsor, where applicable. Limited data availability precluded evaluation of these effects at the time that reference 1 was written.

In the time since reference 1 was completed, additional data has become available. Thus, by using this data the forward-flight effects could be investigated in more detail and the methodology evaluated.

As a first task in this study, therefore, a literature search was conducted to identify, collect, catalog and evaluate data which could be used to evaluate the methodology with emphasis on recent measurements of noise in flight.

LITERATURE SEARCH

A literature search was conducted using the Engineering Index and STAR abstract catalogs and the United Technologies Corporation library system listings. Also, papers from recent technical society meetings, which might not have reached the abstract indices, and data from the Hamilton Standard unpublished data base were included. Personal contacts with some authors and others in the aircraft industry were made to seek out unpublished data.

Data was sought first to evaluate forward-flight effects on the noise of those sources in the V/STOL noise prediction methodology which were expected to be affected by flight, and second to establish a base of high quality data for the methodology evaluation, including that from free-air propellers, variable-pitch fans, fixed-pitch fans, helicopters, lift-fans, jets, core engines and gearboxes. Standardization methods were also sought, so that the available data could be adjusted for ground reflection, atmospheric absorption and variance of flight path for comparison with calculations.

DATA EVALUATION

All data was subjected to a preliminary evaluation. Items which passed the preliminary evaluation are listed in tables 3-Ia and 3-Ib. Data which were found in the open literature are listed in table 3-Ia, while data in the Hamilton Standard data bank are listed in table 3-Ib. These data were selected because they were recent, the measurements were made using modern techniques, and they were believed suited to the requirements of this study. In some cases, however, data were included because they were the only samples available for certain noise sources. For example, wind tunnel model data for variable pitch fans and lift fans were included because there were no outdoor flyover data.

DATA BASE PREPARATION

Each item in table 3-I was examined in some detail to determine its suitability for evaluation of forward-flight effects and for comparison with calculations made using the prediction methodology. These data were considered useful only if they included all the operating and test parameters at the time of data acquisition. These parameters are needed as inputs to the prediction procedure. This included information on aircraft speed and position, engine operating conditions, atmospheric conditions and instrumentation used in test, including microphone height (for ground reflection effects corrections). It may be noted that most of the items do not include all the information needed to perform the calculations, but if general engine operating conditions, such as take-off, approach, 80% power, etc. were identified, then the specific data could be obtained from the engine manufacturer.

Preferred data was that in which both static and flight noise were measured for a particular propulsor. Also, data presentation in the form of narrowband, or at least one-third octave band, spectra was desired for diagnosis of the methodology in the case of aircraft with multiple sources. Some data originally considered promising were eliminated because noise from the different sources could not be separated. Finally, for each type of rotary propulsor, data from several configurations covering a range of design and operating parameters were obtained where possible. For example, data on low-bypass-ratio multiple-stage fans, low-bypass-ratio single-stage fans, and high-bypass-ratio fans were sought to cover a range of fixed-pitch fan parameters.

The data which was selected as being the best qualified for the needs of this study following the above criteria is identified in table 3-II. It may be noted that for a few propulsor types only relative levels obtained under static and flight conditions are available. These data are used only for evaluation of forward-flight effects. The remaining data identified in table 3-II were used both for evaluation of forward flight effects and for methodology evaluation.

TABLE 3-Ia

FAA V/STOL ROTARY PROPULSOR NOISE PREDICTION - DATA CATALOG

PROPELLERS

1)	Magliozzi Feb. 1977	The Influence of Forward Flight on Propeller Noise NASA CR-145105
2)	Galloway Mar. 1976	Investigation of Propeller Noise as a Function of Engine Power and Test Density Altitude BBN Report 3170
3)	Conner, Hilton, Copeland, and Clark Apr. 1975 (1966 Data)	Noise Characteristics of the O-1 Airplane and Some Approaches to Noise Reduction NASA TMX-72638
4)	Hilton, Conner, Copeland, and Dibble Apr. 1975 (1967 Data)	Noise Reduction Studies for the OV-1 Airplane NASA TMX-72639
5)	Hilton, Conner, Hubbard, and Dingeldein Apr. 1975 (1967 Data)	Noise Reduction Studies for the U-10 Airplane TMX-72640
6)	Conner, Hilton, and Dingeldein Apr. 1975 (1969 Data)	Noise Reduction Studies for the CESSNA Model 337 (O-2) Airplane NASA TMX-74641
7)	Hilton, Henderson, and Lawton Apr. 1975 (1969 Data)	Ground Noise Measurements During Static and Flyby Operations of the CESSNA 02-T Turbine Powered Airplane NASA TMX-72642
8)	Hilton, Henderson, and Maglieri Dec. 1971	Ground Noise Measurements During Landing, Takeoff, and Flyby Operations of a Four-Engine Turbo-propeller STOL Airplane NASA TND 6486
9)	Pegg, Magliozzi, and Farassat Mar. 1977	Some Measured and Calculated Effects of Forward Velocity on Propeller Noise ASME 77-GT-70
10)	Cicci and Toplis Apr. 1976	Noise Level Measurements on a Quiet Short Haul Turboprop Transport SAE 760455

TABLE 3-Ia
FAA V/STOL ROTARY PROPULSOR NOISE PREDICTION - DATA CATALOG

PROPELLERS

11)	Metzger, Magliozzi, and Pegg April 1976	Progress Report on Propeller Aircraft Flyover Noise Research SAE 760454
12)	Gray Dec. 1972	Results of Noise Surveys of Seventeen General Aviation Type Aircraft FAA-EQ-73-1
13)	Bishop Mar. 1971	Variability of Flyover Noise Measures for Repeated Flights of Turbojet and Piston Engine Transport Aircraft NASA CR-1752
14)	Atencio, Soderman June 1972	Comparisons of Wind Tunnel and Flyover Noise Measurements of the YOV-10A STOL Aircraft NASA TMX-62166
15)	Falarski, Koenig, Soderman June 1972	Aspects of Investigating STOL Noise Using Large Scale Wind Tunnel Models NASA TMX-62164
16)	Flemming, Scholten Jan. 1978	Measurements in the Course of the German/Swiss Research Program (BMV 8/75) Results Delivered by DFVLR Braunschweig-Private Communication
17)	Tanner (Date not given)	Noise Characteristics of Several General Aviation Aircraft Hydrospace - Challenger Report TR-S-235
18)	Bartels, Borchers, Scholten, Uhse Oct. 1977	Studies of the Noise Generation of Light Aircraft Propellers AIAA 77-1320

VARIABLE PITCH FANS

1)	Edkins, Hirschkron, Lee 1972	TF34 Turbofan Engine Study NASA CR-120914
2)	Heidmann and Feiler Oct. 1973	Noise Comparisons from Full-Scale Fan Tests at NASA-Lewis Research Center AIAA 73-1017
3)	Heidmann and Dietrich Nov. 1976	Simulation of Flight-Type Engine Fan Noise in the NASA-Lewis 9X15 Anechoic Wind Tunnel NASA TMX-73540
4)	Heidmann, Dietrich Oct. 1977	Effects of Simulated Flight on Fan Noise AIAA 77-1334
5)	Shaw, Woodward, Glaser, and Dastoli Oct. 1977	Inlet Turbulence and Fan Noise Measured in an Anechoic Wind Tunnel and Statically with an Inlet Flow Control Device AIAA 77-1345

TABLE 3-Ia

FAA V/STOL ROTARY PROPULSOR NOISE PREDICTION - DATA CATALOG

VARIABLE PITCH FANS (cont.)

6)	Glaser, Woodward, Lucas Feb. 1977	Acoustic and Aerodynamic Performance of a Variable Pitch 1.83 Meter (6 ft) Diameter 1.20 Pressure Ratio Fan Stage (QF9) NASA TND-8402
7)	Demers, Metzger, Smith, Wainauski Mar. 1973	Testing of the Hamilton Standard Q-Fan™ Demonstrator NASA CR-121265
8)	Metzger, Hanson Jan. 1973	Low Pressure Ratio Fan Noise - Experiment and Theory ASME Journal of Engineering for Power - Jan. 1973

FIXED PITCH FANS

1)	Cumpsty and Lowrie July 1974	The Cause of Tone Generation by Aero-Engine Fans at High Subsonic Tip Speeds and the Effect of Forward Speed ASME 73-WA/GT-4
2)	Kester Oct. 1974	Status of the JT8D Refan Noise Reduction Program Internoise - 1974
3)	Lowrie Mar. 1975	Simulation of Flight Effects on Aero-Engine Fan Noise AIAA 75-463
4)	Feiler and Merriman Aug. 1974	Effects of Forward Velocity and Acoustic Treatment on Inlet Fan Noise NASA TMX-71591
5)	Merriman and Good Mar. 1975	Effect of Forward Motion on Fan Noise AIAA 75-464
6)	Strout Jan. 1976	Flight Effects on Noise Generated by the JT8D-17 Engine in a Quiet Nacelle and a Conventional Nacelle as Measured in the NASA-Ames 40X80 Wind Tunnel NASA CR-137797
7)	Hodder Dec. 1976	Further Studies of Static to Flight Effects on Fan Tone Noise Using Inlet Distortion Control for Source Identification TMX-73183
8)	Feiler and Groeneweg Oct. 1977	Summary of Forward Velocity Effects on Fan Noise NASA TM 73722
9)	Motsinger, et al Feb. 1969	Low Tip Speed Fan Noise Demonstration Program NASA CR-72456

TABLE 3-1a
FAA V/STOL ROTARY PROPULSOR NOISE PREDICTION - DATA CATALOG

FIXED PITCH FANS (cont.)

10)	Hosier June 1972	A Comparison of Two Independent Measurements and Analysis of Jet Aircraft Flyover Noise NASA TND 8379
11)	Hastings, et al May 1977	Noise Data for a Twin-Engine Commercial Jet Aircraft Flying Conventional, Steep and Two-Segment Approaches NASA TND 8441
12)	McCollough, True Sept. 1975	Effect of Temperature and Humidity on Aircraft Noise Propagation FAA-RD-75-100
13)	Burdsall, Brochu, Scaramella Nov. 1975	Results of Acoustic Testing of the JT8D-109 Refan NASA CR-134875
14)	Anon., Douglas Aircraft July 1975	DC-9 Flight Demonstration Program with Refanned JT8D Engines - Final Report, Vol. IV, Flyover Noise NASA CR-134860
15)	Strout June 1976	Flight Effects on Noise Generated by the JT8D-17 Engine in a Quiet Nacelle and a Conventional Nacelle as Measured in the NASA-Ames 40X80 Foot Wind Tunnel - Summary Report NASA CR-2576
16)	Goodman, et al Aug. 1973	Aircraft Noise Definition Phase I - Analysis of Existing Data for DC-8, DC-9 and DC-10 Aircraft FAA-EQ-73-5
17)	Sofrin, Riloff Sept. 1975	Two Stage Low Noise Advanced Technology Fan, Vol. III Acoustic Data NASA CR-134829
18)	DeLapp Aug. 1974	Aircraft Noise Definition, Phase II Analysis of Flyover Noise FAA-EQ-74-5
19)	Sofrin, Riloff Sept. 1975	Two Stage Low Noise Advanced Technology Fan Vol. V Acoustic Final Report NASA CR-134831
20)	Munoz Aug. 1976	727/JT8D Jet and Fan Noise Flight Effects Study FAA-RD-76-110
21)	Woodward, Lucas, Balombin Apr. 1977	Acoustic and Aerodynamic Performance of a 1.5 Pressure Ratio, 1.83 Meter (6 ft) Diameter Fan Stage for Turbofan Engines NASA TMX-3521

TABLE 3-Ia
FAA V/STOL ROTARY PROPULSOR NOISE PREDICTION - DATA CATALOG

FIXED PITCH FANS (cont.)

22)	Goldstein, Lucas, and Balombin Nov. 1970	Acoustic and Aerodynamic Performance of a 6-Foot Diameter Fan for Turbofan Engines II-Performance of QF-1 Fan in Nacelle without Acoustic Suppression NASA TND-6080
23)	Juttras May 1976	Single Stage Low Noise Advanced Technology Fan Vol. 5 Fan Acoustics NASA-CR-134895
24)	Blankenship, Low, Watkins, Merriman Oct. 1977	Effects of Forward Motion on Engine Noise NASA-CR-134954
25)	Montegani Mar. 1972	Noise Generated by Quiet Fans NASA TMX-2528
26)	Roundhill, Schaut Mar. 1975	Model and Full Scale Test Results Relating to Fan Noise In-Flight Effects AIAA 75-465
27)	Merriman, Good, Low, Lee, and Blankenship July 1976	Forward Motion and Installation Effects on Engine Noise AIAA 76-584
28)	Kazin, Minzer, Paas (No date given)	Acoustic Testing of a 1.5 Pressure Ratio, Low Tip Speed Fan (QEP Fan B Scale Model) NASA-CR-120789
29)	Bishop Aug. 1976	Descriptions of Flyover Noise Signals Produced by Various Jet Aircraft FAA-DS-67-18
30)	Plucinsky Apr. 1973	Quiet Aspects of the Pratt & Whitney Aircraft JT15D Turbofan SAE 730289
31)	Blankenship Oct. 1977	Effect of Forward Motion on Turbomachinery Noise AIAA 77-1346

HELICOPTERS

1)	Bowes Mar. 1973	Test and Evaluation of a Quiet Helicopter Configuration HH-43B - JASA V.54 N.5
2)	Henderson, Pegg, and Hilton Sep. 1973	Results of the Noise Measurement Program on a Standard and Modified OH-6A Helicopter NASA TND-7216
3)	True and Rickley July 1977	Noise Characteristics of Eight Helicopters FAA RD-77-94

TABLE 3-Ia

FAA V/STOL ROTARY PROPULSOR NOISE PREDICTION - DATA CATALOG

HELICOPTERS (cont.)

4)	True, Rickley, and Letty Apr. 1977	Helicopter Noise Measurements Data Report Vols. I and II - FAA-RD-77-57
5)	Leverton and Pollard Feb. 1973	A Comparison of the Overall and Broad Band Noise Characteristics of Full Scale and Model Helicopter Rotors JSV (30) 2
6)	Hilton, Henderson, Pegg Feb. 1971	Ground Noise Measurements During Flyover, Hover, Landing and Takeoff Operations of a Standard and Modified HH-43B Helicopter NASA TMX-2226
7)	Pegg, Henderson, Hilton Dec. 1973	Results of the Flight Noise Measurement Program Using a Standard and Modified SH-3A Helicopter NASA TND-7330
8)	Widnall, Bauer, Lee Oct. 1972	Experimental Studies of Rotational Noise in Forward Flight Mideast Region Symposium, American Helicopter Society, Oct. 1972
9)	Cox June 1969	Rotor Noise Measurements in Wind Tunnels, Proceedings 3rd Cal/AVLABS Symposium, Vol. I Aerodynamics of Rotary Wing and VSTOL Aircraft
10)	d'Ambra, Dedieu, Julienne Sept. 1972	Measures De Bruit D'Helicopteres En Vol AGARD CP-111
11)	Barlow, McCluskey, Ferris Sept. 1972	OH-6A Phase II Quiet Helicopter Program USAAMRDL TR-72-29
12)	Leverton, Pollard, Wills Aug. 1975	Main Rotor Wake/Tail Rotor Interaction Vertica 1977 Vol. I

LIFTING FANS

1)	Krishnappa Jan. 1972	Lifting Fan Noise Studies with Superimposed Cross Flows AIAA 72-128
2)	Krishnappa Sept. 1973	Noise Characteristics of an Experimental Lifting Fan Under Crossflow Conditions AGARD CP-135
3)	Stimpert Feb. 1973	Effect of Crossflow Velocity on VTOL Lift Fan Blade Passing Frequency Noise Generation NASA CR-114566
4)	Claes July 1973	Acoustic Evaluation of LF 336/E GE TM73-355

TABLE 3-Ia
FAA V/STOL ROTARY PROPULSOR NOISE PREDICTION - DATA CATALOG

LIFTING FANS (cont.)

5)	Krishnappa Feb. 1974	Acoustic Tests on a Fan-In-Wing Model: Effects of an Extended Inlet National Research Council of Canada DME LR-576
6)	Atencio	Noise Measurements From a Large-Scale Lift Fan Transport in the 40X80 Foot Wind Tunnel NASA TMX-62284
7)	Stimpert, Fogg Feb. 1973	Effect of Crossflow Velocity on the Generation of Lift Fan Jet Noise in VTOL Aircraft NASA CR-114571

JETS

1)	Jaeck Aug. 1977	Empirical Jet Noise Predictions for Single and Dual Flow Jets with and without Suppressor Nozzles Vol. II, Dual Flow Subsonic and Supersonic Jets, Boeing Document D6-42929-2
2)	Drevet, DuPonchel, and Jacques July 1976	The Effect of Flight on Jet Noise as Observed on the Bertin Aerotrain JSV 54(2)
3)	Hoch, Berthelot July 1976	Use of the Bertin Aerotrain for the Investigation of Flight Effects on Aircraft Engine Noise JSV 54(2), AIAA 76-534
4)	Stone Nov. 1976	Flight Effects on Exhaust Noise for Turbojet and Turbofan Engines - Comparison of Experimental Data with Prediction NASA TMX-73552
5)	Stone, Miles, and Sargent Nov. 1976	Effects of Forward Velocity on Noise for a J85 Turbojet Engine with Multitube Suppressors from Wind Tunnel and Flight Tests NASA TMX-73542
6)	Dahlen June 1972	Some Experiments on the Noise Emission of Coaxial Jets. Presented at 1st INT Symposium on Air Breathing Engines Marseille 1972
7)	Bushell Sept. 1970	A Survey of Low Velocity and Coaxial Jet Noise with Application to Jet Prediction. Symposium on Aerodynamic Noise. Loughborough Univ. of Technology, Paper B.3
8)	Bushell Mar. 1975	Measurement and Prediction of Jet Noise in Flight AIAA 75-461

TABLE 3-Ia

FAA V/STOL ROTARY PROPULSOR NOISE PREDICTION - DATA CATALOG

JETS (cont.)

9)	Jaeck Sept. 1976	Static and Wind Tunnel Near-Field/Far-Field Jet Noise Measurements from Model Scale Single-Flow Baseline and Suppressor Nozzles. Vol. 1. Noise Source Locations and Extrapolation of Static Free-Field Jet Noise Data - NASA CR-137913 Vol. 2 Forward Speed Effects NASA CR-137914
10)	Burley and Karabinus Jan. 1973	Flyover and Static Tests to Investigate External Flow Effect on Jet Noise for Nonsuppressor and Suppressor Exhaust Nozzles AIAA 73-190
11)	Beulke, Clapper, McCann, Morozumi	A Forward Speed Effects Study on Jet Noise from Several Suppressor Nozzles in the NASA/Ames 40X80 Wind Tunnel NASA CR-114741
12)	Strout, Atencio July 1976	Flight Effects on JT8D Engine Jet Noise Measured in a 40X80 Tunnel J. Aircraft (14) 8
13)	Packman, Ng, Paterson June 1975	Effect of Simulated Forward Flight on Subsonic Jet Exhaust Noise AIAA 75-869
14)	Belleval, Chen, Perulli Sept. 1975	Investigation of In-Flight Jet Noise Based on Measurements in an Anechoic Wind Tunnel: Presented at the Sixth International Congress on Instrumentation for Aerospace Test Installations Ottawa
15)	Chamberlin Aug. 1973	Flyover and Static Tests to Study Flight Velocity Effects on Jet Noise of Suppressed and Unsuppressed Plug Nozzle Configurations NASA TMX-2856
16)	Jaeck June 1977	Static and Wind Tunnel Near-Field/Far-Field Jet Noise Measurements from Model Scale Single-Flow Baseline and Suppressor Nozzles - Summary Report NASA CR-2841
17)	Atencio Feb. 1977	The Effect of Forward Speed on J85 Engine Noise from Suppressor Nozzles as Measured in the NASA-Ames 40X80 Foot Wind Tunnel NASA TND-8426
18)	Burley, Johns Jan. 1974	Flight Velocity Effects on Jet Noise of Several Variations of a 12-Chute Suppressor Installed on a Plug Nozzle NASA TMX-2918

TABLE 3-Ia
FAA V/STOL ROTARY PROPULSOR NOISE PREDICTION - DATA CATALOG

JETS (cont.)

19)	Brausch Aug. 1972	Flight Velocity Influence on Jet Noise of Conical Ejector, Annular Plug and Segmented Suppressor Nozzles NASA CR-120961
20)	Glass	Noise Characteristics of Several Executive Jet Aircraft Hydrospace - Challenger Report TR-S-236
21)	Zwieback Sept. 1973	Flyover Noise Testing of Commercial Jet Airplanes J. Aircraft (10) 9
22)	Atencio, Kirk, Soderman, Hall Oct. 1972	Comparison of Flight and Wind Tunnel Measurements of Jet Noise for the XV-5B Aircraft NASA TMX 62182
23)	Brooks, Woodrow Mar. 1975	The Effects of Forward Speed on a Number of Turbojet Exhaust Silencers AIAA 75-506
24)	Cocking, Bryce Mar. 1975	Subsonic Jet Noise In Flight Based on Some Recent Wind Tunnel Results AIAA 75-462
25)	Cocking Oct. 1976	The Effect of Flight on the Noise of Subsonic Jets National Gas Turbine Establishment (NGTE Report 343)
26)	Larson, McColgan, Packman Mar. 1978	Jet Noise Source Modification Due to Forward Flight AIAA Journal (16)3
27)	Reed Aug. 1974	Effect of Forward Velocity on the Noise Characteristics Dual-Flow Jet Nozzles ASME 74-WA/AERO-4

CORE ENGINE

1)	Mathews, Rekos July 1976	Direct Combustion Generated Noise in Turbo-propulsion Systems - Prediction and Measurement AIAA 76-579
2)	Low Oct. 1977	Effects of Forward Motion on Jet and Core Noise AIAA 77-1330
3)	Reshotko, Karchmer, Penko, and McArdle	Core Noise Measurements on a YF-102 Turbofan Engine NASA TMX-73587
4)	Kazin, et al Aug. 1974	Core Engine Noise Control Program Vols. I, II, and III FAA-RD-74-125

TABLE 3-Ia
FAA V/STOL ROTARY PROPULSOR NOISE PREDICTION - DATA CATALOG

CORE ENGINE (cont.)

5) Grande Oct. 1973	Core Engine Noise AIAA 73-1026
6) Grande Dec. 1972	Exhaust Noise Field Generated in the JT8D Core Engine - Noise Floor Presented by the Internal Noise Sources JASA (55) 1
7) Cumpsty, Marble May 1977	Core Noise from Gas Turbines JSV (54) 2
8) Sowers, Coward Dec. 1977	Quiet Clean Short-Haul Experimental Engine (QCSEE) Core Engine Noise Measurements NASA CR-135160
9) Von Glahn, Goodykoontz Nov. 1972	Forward Velocity Effects on Jet Noise with Dominant Internal Noise Source NASA TMX-71348
10) Mathews, Rekos, Nagel Feb. 1977	Combustion Noise Investigation FAA-RD-77-3
11) Kazin, Emmerling July 1974	Low Frequency Core Engine Noise ASME 74-WA/AERO-2

GEARBOX

1) Bowes, Giansante, Bossler, Berman June 1977	Helicopter Transmission Vibration and Noise Program USAAMRDL-TR-77-14
2) Badgley, Hartman June 1973	Gearbox Noise Reduction: Prediction and Measurement of Mesh-Frequency Vibrations within an Operating Helicopter Rotor-Drive Gearbox ASME 73-DET-31
3) Hartman May 1973	A Dynamics Approach to Helicopter Transmission Noise Reduction and Improved Reliability AHS #772

DATA STANDARDIZATION

1) Miles Apr. 1975	Analysis of Ground Reflection of Jet Noise Obtained with Various Microphone Arrays Over Asphalt Surface NASA TMX-71696
2) Miles, Stevens, and Leininger Nov. 1975	Analysis and Correction of Ground Reflection Effects in Measured Narrow Band Sound Spectra Using Cepstral Techniques NASA TMX-71810

TABLE 3-Ia

FAA V/STOL ROTARY PROPULSOR NOISE PREDICTION - DATA CATALOG

DATA STANDARDIZATION (cont.)

3)	Miles Jan. 1974	Rational Function Representation of Flap Noise Spectra Including Correction for Reflection Effects AIAA 74-193
4)	Kraft Oct. 1970	Acoustic Grbund Reflection Correction of Broadband Noise Based on Empirical Determination of Ground Impedance GE TM 70-815
5)	Smith Oct. 1977	International Aircraft Noise Measurement Procedures - Expensive Acquisition of Poor Quality Data AIAA 77-1371
6)	Society of Automotive Engineers, Committee A-21 Sept. 1975	Acoustic Effects Produced by a Plane SAE Aerospace Information Report AIR-1327
7)	Society of Automotive Engineers, Committee A-21 Oct. 1973	Standard Values of Atmospheric Absorption as a Function of Temperature and Humidity SAE Aerospace Recommended Practice ARP-866A
8)	Sutherland May 1975	Review of Experimental Data in Support of a Proposed New Method for Computing Atmospheric Absorption Losses DOT-TST-75-87
9)	Bass, Evans, Marsh May 1976	Background for Theoretical Equations Used to Calculate Atmospheric Absorption of Sound Prepared for Working Group S1-57 American National Standards Institute
10)	DeLoach May 1977	A Review of Current Procedures for Normalizing Aircraft Flyover Noise Data to Reference Meteorological Conditions NASA TND-8406
11)	Kajland Aug. 1974	Measured Variations in Aircraft Noise Near Arlanda JASA (56) 2
12)	Soderman, Noble Mar. 1975	Directional Microphone Array for Acoustic Studies of Wind Tunnel Models J. Aircraft (12) 3
13)	Copeland, Hilton, Huckel, Dibble, Maglieri Dec. 1966	Noise Measurement Evaluations of Various Take-off - Climbout Profiles of a Four-Engine Turbojet Transport Airplane NASA TND-3715

TABLE 3-Ia
FAA V/STOL ROTARY PROPULSOR NOISE PREDICTION - DATA CATALOG

DATA STANDARDIZATION (cont.)

14)	McCollough, True Sept. 1975	Effect of Temperature and Humidity on Aircraft Noise Propagation FAA-RD-75-100
15)	Watkins Oct. 1977	Investigation of Excess Attenuation of Noise in the Atmosphere AIAA 77-1347

TABLE 3-Ib

V/STOL ROTARY PROPULSOR NOISE PREDICTION METHODOLOGY

Hamilton Standard Unpublished Data Bank

Unshrouded Propellers	Data Source	Static or Forward Flight
Brequet 94 1S	Hamilton Standard	Forward Flight
DeHavilland DHC-5 Buffalo	Hamilton Standard	Static and Forward Flight
DeHavilland DHC-6 Twin Otter	NASA/Hamilton Standard*	Static and Forward Flight
DeHavilland DHC-7	Hamilton Standard	Static and Forward Flight
Lockheed L188 Electra	Hamilton Standard	Forward Flight
V/STOL Propeller Model	United Technologies Research Center	Static
Shrouded Propellers		
Bell X22	Hamilton Standard	Static
Variable Pitch Fans		
1.14 Pressure Ratio 1.75 Ft. Fan Model	NASA/Hamilton Standard*	Static
1.18 Pressure Ratio 1.5 Ft. Fan Model	NASA/Hamilton Standard*	Static
1.18 Pressure Ratio 4.6 Ft. Fan	NASA/Hamilton Standard*	Static and Forward Flight (Wind Tunnel)
1.20 Pressure Ratio 6 Ft. Fan	NASA	Static
Fixed Pitch Fans		
Boeing 727	Hamilton Standard	Forward Flight
Douglas DC9	Hamilton Standard	Forward Flight

*Tapes were obtained in joint programs with NASA and Hamilton Standard; tapes are currently at NASA Langley Research Center.

TABLE 3-Ib

V/STOL ROTARY PROPULSOR NOISE PREDICITON METHODOLOGY

Hamilton Standard Unpublished Data Bank

Helicopter Rotors	Data Source	Static or Forward Flight	
Sikorsky	NASA	Forward Flight	
Kaman	NASA	Forward Flight	
Hughes	NASA	Forward Flight	
Westland	Westland	Forward Flight	
Miscellaneous	FAA	Forward Flight	
Lift Fans			
LF 336	NASA	Static and Forward Flight (Wind Tunnel)	
Core Engine			
DDA Allison	Hamilton Standard	Static	Unaffected by Flight
Lycoming T55	Hamilton Standard	Static	
Pratt & Whitney PT6	Hamilton Standard	Static	
Lycoming PLT26	U.S. Army	Static	

TABLE 3-II

DATA TO BE USED FOR METHODOLOGY EVALUATION

	Catalog Item	Author(s)	Aircraft Type
Propeller	1)	Magliozzi	DeHavilland DHC-6 Twin Otter
	7)	Hilton, et al	Cessna 337 02-T
	16)	Flemming, Scholten	Pilatus Porter PC-6
	Hamilton Standard Data Bank		DeHavilland DHC-6 Twin Otter
	Hamilton Standard Data Bank		DeHavilland DHC-7 DASH-7
Variable Pitch Fan	4)	Heidmann, Dietrich	NASA Rotor 55 (20 inch)
	7)	Demers, et al	Hamilton Standard Q-Fan(TM) (4.6 ft.)
	Hamilton Standard Data Bank		Hamilton Standard Q-Fan(TM) (1.5 ft.)
Fixed Pitch Fan	1)	Cumpsty, Lowrie	Rolls-Royce RB211
	3)	Lowrie	Rolls-Royce RB211
	4)	Fieler, Merriman	Pratt & Whitney Aircraft JT3D-3B, JT9D-20, JT8D-9 General Electric CF6-6
	6)	Strout	Wind Tunnel P&WA JT8D-17
	13)	Burdsall, et al	Test Stand P&WA JT8D-109
	14)	McDonnell-Douglas	DC-9 - P&WA JT8D-109
	20)	Munoz	B-727 - P&WA JT8D-109
	24)	Blankenship, et al	DC-9-30 - P&WA JT8D-109 DC-10-40 - P&WA JT9D-59A DC-10-10 - G.E. CF6-6D
	30)	Plucinsky	Cessna Citation - P&WA JT15D
Helicopter	2)	Henderson, et al	Hughes OH-6A
	3)	True, Rickley	Hughes 300C Hughes 500C Bell 47-G Bell 206-L Bell 212 (UH1N) Sikorsky S-61 (SH-3A) Sikorsky S-64 (CH-54B) Boeing Vertol CH-47C
	7)	Pegg, et al	Sikorsky SH-3A
Lift Fans	2)	Krishnappa	12 Inch Model Fan
	6)	Atencio	G.E. X376-B
Jets	2)	Drevet, et al	Aerotrain - G.E. J85
	9)	Jaeck	Wind Tunnel - G.E. J85 Nozzles
	13)	Packman, et al	Wind Tunnel Model Jet
	23)	Brooks, Woodrow	Rolls-Royce Viper 601
	25)	Cocking	Wind Tunnel Model Jet
Core Engine	2)	Low	P&WA JT8D-109, JT9D-59A
	9)	Von Glahn, Goodykoontz	Model Jet

GENERAL OBSERVATIONS ON THE AVAILABLE DATA

Although the data listed in table 3-II are the best that were found in the literature and in the Hamilton Standard data bank, there are numerous limitations which prevent full evaluation of the V/STOL rotary propulsor noise prediction methodology.

As may be recalled, the subject noise prediction methodology was developed for uninstalled propulsors and calculates free-field noise levels. The data, particularly those for propulsors in flight, contain measurements of noise from aircraft, which may contain several sources as well as have significant installation effects. Also, although attempts were made to correct the data for ground reflection effects, these were not always successful, particularly for the propulsors having strong low frequency tones (propellers and helicopter rotors). These problems, as well as a more complete evaluation of the data, will be described in more detail in the appropriate sections of the Phase II and Phase III discussions.

PHASE II - EVALUATION OF V/STOL ROTARY PROPULSOR FORWARD FLIGHT EFFECTS

INTRODUCTION

The forward flight effects on V/STOL rotary propulsor noise sources derived under the previous contract (reference 1) were evaluated in the present program using the selected data described earlier in the Data Base Expansion discussion. This was done typically by calculating the noise for a propulsor statically and in flight for the configuration and operating conditions for which the test data was acquired.

The changes in noise levels calculated for forward flight effects vs. those measured indicate the performance of the forward-flight effects methodology.

The methodology indicates the sources which are calculated to be affected by forward flight. It is not generally possible to derive the forward-flight effects from the data, as it is not possible to separate the sources. For instance, propeller noise tones may consist of steady loading, unsteady loading, and thickness noise, each of which cannot be separated in the test data. Thus, the forward-flight effects which will be seen are the results of the combined effects on all the tone noise sources. In some cases, noise from different propulsor components cannot be separated. Broadband noise in flight could be generated by the propeller, the engine, or the airframe. The noise prediction methodology will calculate the flight effects on the propeller and engine noise and compute a total spectrum. If this does not match the test data, it is not possible to determine if this is due to incorrectly calculated propeller or engine noise, or to strong contribution of airframe noise. Thus, the available test data cannot be used to identify which portions of the methodology are deficient, but only to indicate how well the overall forward-flight effects are calculated.

Some of the data which was selected for evaluation of forward-flight effects and for methodology evaluation was found upon further examination to be of only limited usefulness. This was due to either strong installation effects or, in the case of propellers and helicopters, strong ground reflection effects on tones. As the correlations are discussed in subsequent sections, these specific problems will be identified.

FORWARD-FLIGHT EFFECTS EVALUATION

Introduction

In this section, forward-flight effects on the noise generated by V/STOL rotary propulsors will be discussed and the methodology evaluated using the data from the data base. The data used for the evaluation of a specific propulsor will be identified by its data catalog number which can be found in table 3-I.

Free-Air Propellers

The forward-flight effects on propeller noise included in the methodology are the changes in steady loading and broadband noise due to the changes in blade loading, which occur due to changes in the inflow velocity distribution, and to changes in the inflow turbulence ingested by the propeller caused by changes in the inflow contraction ratio. The change in noise due to blade loading is contained in the analytic methodology for the propeller noise theory. Turbulence interaction effects are based on empirical formulations of the turbulence amplitude and length scale changes with changes in the inflow contraction ratio.

As the changes in steady loading noise are relatively small between static and low-to-moderate flight speed, only a small change in the level of the noise where this source dominates would be expected. Unsteady loading noise, however, is expected to change dramatically from static to forward flight. Thus, at low frequency for the first few harmonics of blade passing frequency the methodology will show only a small change in level from static to flight. The higher frequency harmonics, which are dominated by unsteady loading noise, will show large reductions.

As the broadband noise prediction method uses thrust as an input, the calculated effects of forward-flight on broadband noise will show a decrease in flight due to the propeller thrust lapse. This will appear in the measurements as a decrease in the mid-to-high frequency noise, assuming that the test data is not contaminated by engine or airframe noise.

The following sections will describe the evaluation of forward-flight which was done using the data identified in the data catalog under propellers.

Data Catalog Item 1. - The data contained in this report was acquired on the DeHavilland Twin Otter, a two-engine turboprop airplane. Noise measurements were made using two wing-tip microphones as well as a ground based system. The general arrangement of the airplane and wing-tip microphone system is shown in figure 4-1. The ground-based microphone system included a microphone which was flush with the ground, so that varying ground reflection effects during the flyover were avoided.

The aircraft has 8.5 ft. diameter 3-bladed propellers. The design take-off operating condition is 2200 rpm (979 ft/sec) and 550 SHP/propeller. Since the engines are the free-turbine type, the propeller rpm can be varied. For the purposes of this evaluation, the data at lower rpm was used, as at the take-off condition the light loading and high tip speed result in high levels of thickness noise. The methodology in the V/STOL Rotary Propulsor Noise Prediction computer program does not include thickness noise, as new V/STOL propellers are expected to operate at low tip speeds, where thickness noise is negligible.

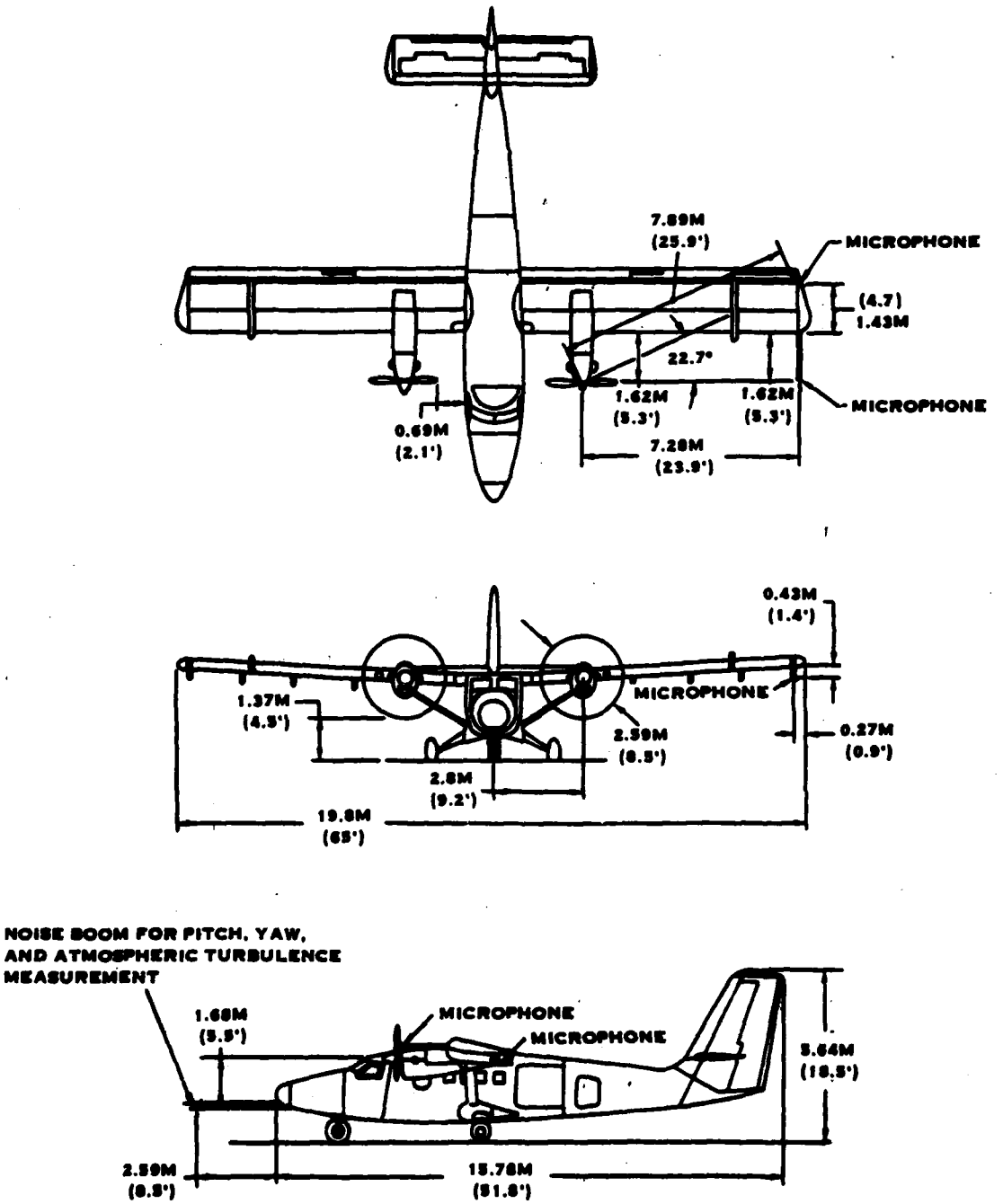

FIGURE 4-1. THREE-VIEW OF FORWARD FLIGHT PROPELLER NOISE RESEARCH AIRPLANE

The wing-tip microphone data is useful for evaluation of forward-flight effects on propeller noise harmonic levels, as there is no relative motion between the source and the microphone. For a qualitative evaluation of forward-flight effects, the narrow-band carpet plot of propeller noise vs. time during a take-off shown in figure 4-2 was generated. In this figure, the airplane is static at time 0. At this time, the spectrum is seen to contain many harmonics of blade passing frequency. At about time equal 2 secs., the airplane starts to roll. Almost immediately, the levels of the upper harmonics decrease significantly. Shortly after the start of the take-off roll, only the first 6 or 7 harmonics of blade passing frequency are discernible.

Figure 4-3 shows the comparison between the measured and calculated differences in harmonic levels static-minus-flight for several propeller operating conditions for the in-plane wing-tip microphone. Figure 4-4 shows the same data for the aft wing-tip microphone. As these figures show, the measured levels show a difference of about 10 dB between the static and flight levels at the fundamental. This decreases to 3 to 4 dB at the third harmonic, then increases again to about 25 dB at the tenth harmonic. The calculated differences between static and flight harmonic levels show similar trends above the second harmonic. At the fundamental it is conjectured that the high level of static noise is an installation effect. This can be substantiated using the blade-surface pressure traces contained in the report. Figure 4-5 shows a sample of the blade-surface pressures measured statically and in-flight for the same propeller operating condition. As may be seen, a sharp pulse appears near the circumferential sample point number 38 in the static data. This occurs when the instrumented blade is close to the fuselage. A second pulse is seen near circumferential sample point 75, which is when the instrumented blade is close to the ground. In-flight, both pulses have disappeared. It is conjectured that this is evidence of vortices originating on the fuselage and on the ground, which is an installation effect. This sharp blade loading pulse gives rise to many intense higher frequency harmonics, as shown in figure 4-6. These extend well beyond the 30th harmonic (2987 Hz). It may also be seen in figure 4-6 that the first eight harmonics define an envelope which is consistent with the exponential harmonic roll-off resulting from unsteady loading. Beyond the eighth harmonic, the harmonic levels rise and show a peak in the harmonic envelope near the tenth to eleventh harmonic (at around 1000 Hz). It is believed that this mid-frequency peak is a result of the installation effects and would not appear in the harmonic spectrum of an isolated static propeller. This will be explained in more detail in the discussion of the noise prediction methodology evaluation.

If it is assumed that the fuselage vortex raises the tone noise levels by about 5 dB (i.e., by the difference between measured and calculated static-minus-flight levels at the fundamental) the agreement between the calculated and the measured changes in noise level from static to flight is good.

Figures 4-7 and 4-8 show one-third octave band spectra which are comparable to the static-minus-flight harmonic spectra shown in figures 4-3 and 4-4. As may be seen, the agreement between calculated and measured spectra is good at the low frequencies. At above about 400 Hz, the measured differences are much greater than those calcu-

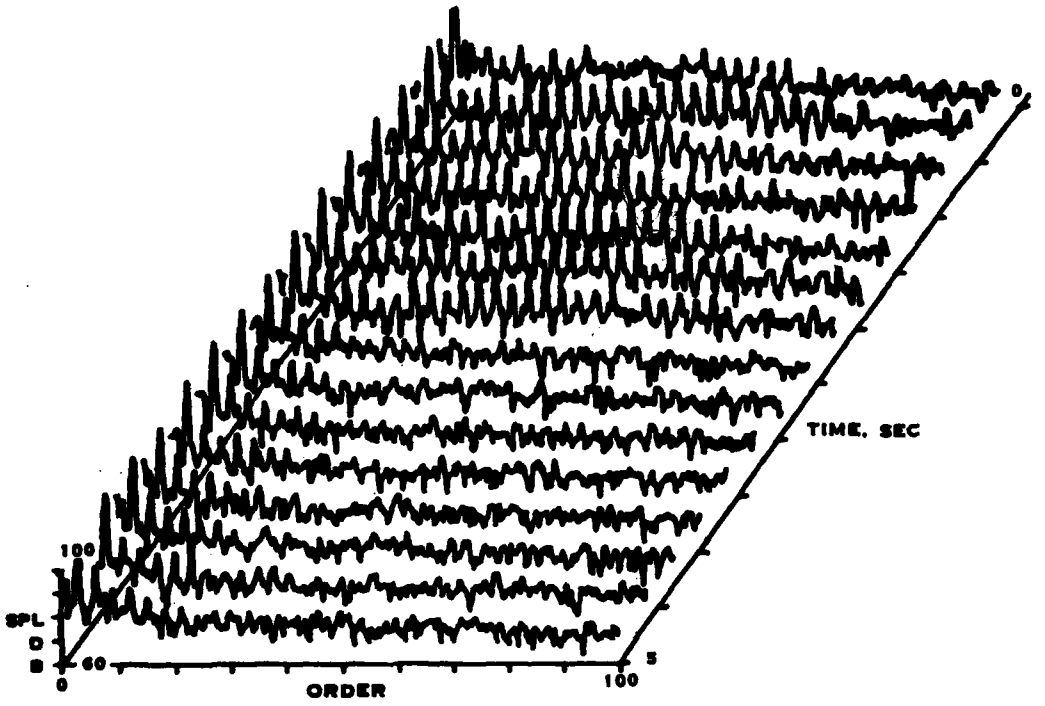

FIGURE 4-2. NARROW-BAND CARPET PLOT OF PROPELLER NOISE DURING TAKE-OFF

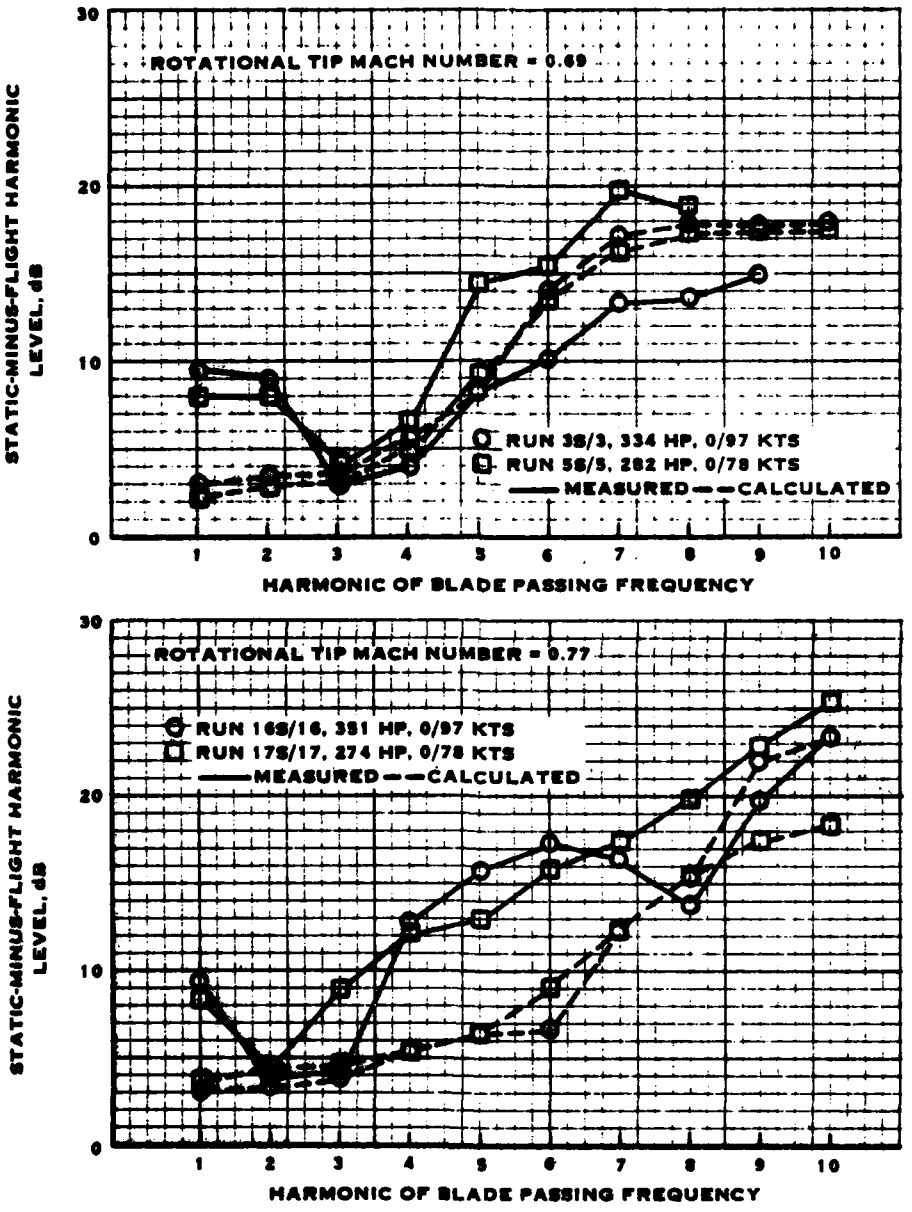

FIGURE 4-3. COMPARISON OF MEASURED AND CALCULATED DIFFERENCES IN HARMONIC LEVELS - STATIC MINUS FLIGHT - FOR THE FRONT WINGTIP MICROPHONE FROM DATA BASE ITEM PROPELLER -1

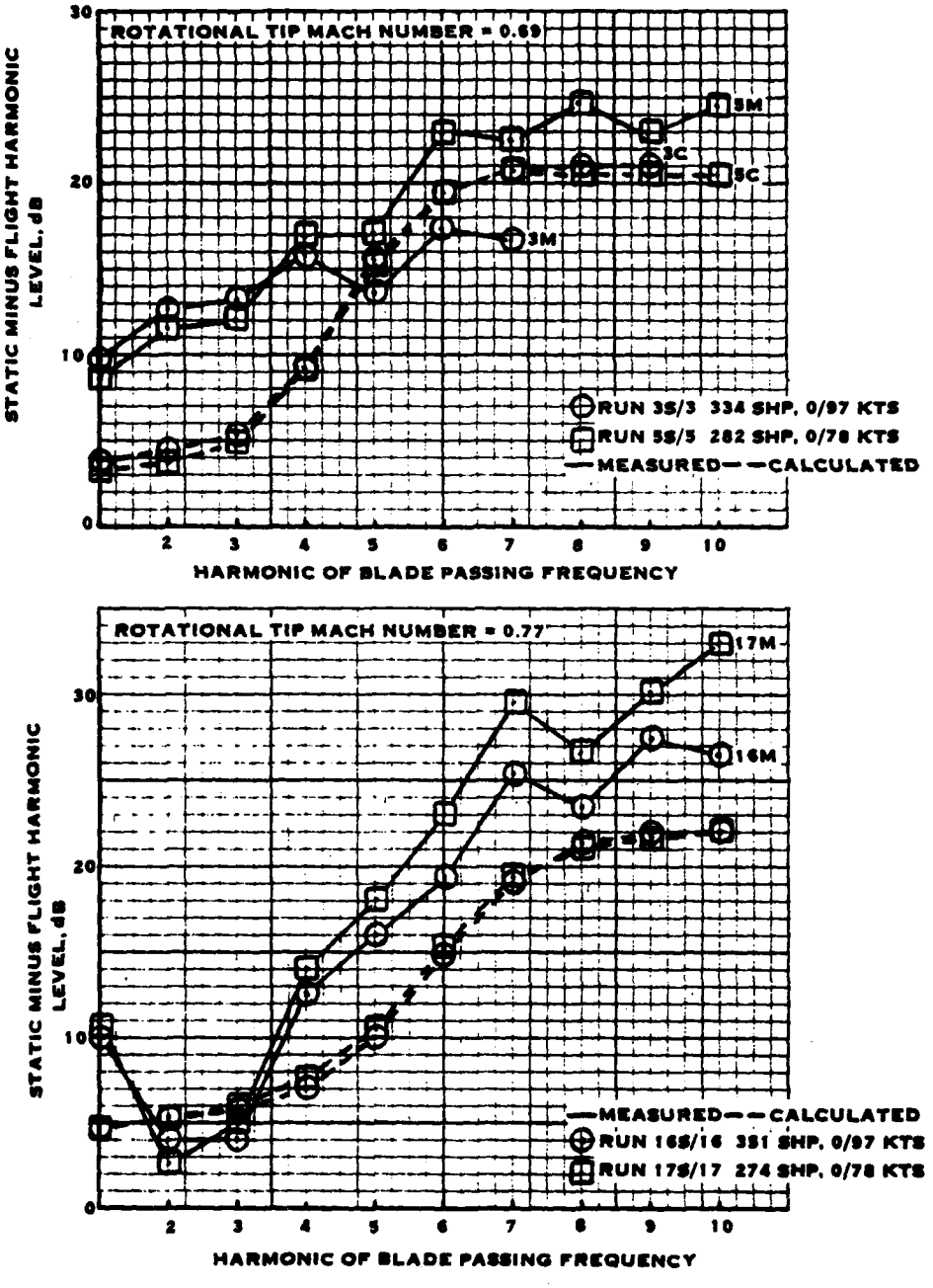

FIGURE 4-4. COMPARISON BETWEEN MEASURED AND CALCULATED DIFFERENCES IN HARMONIC LEVELS - STATIC MINUS FLIGHT - FOR THE AFT MICROPHONE IN DATA BASE ITEM PROPELLER -1

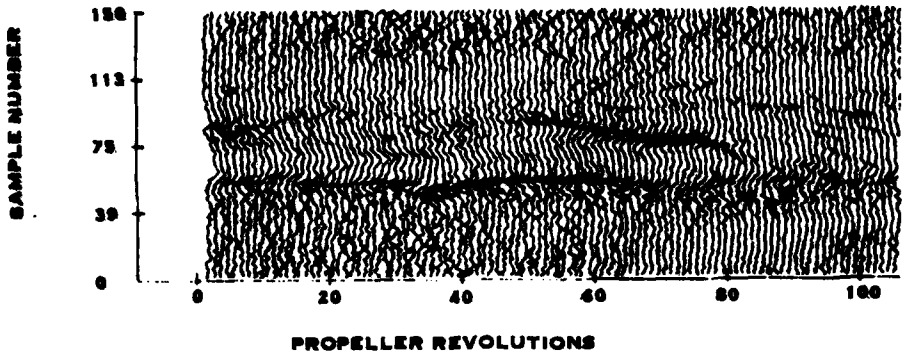

A) STATIC

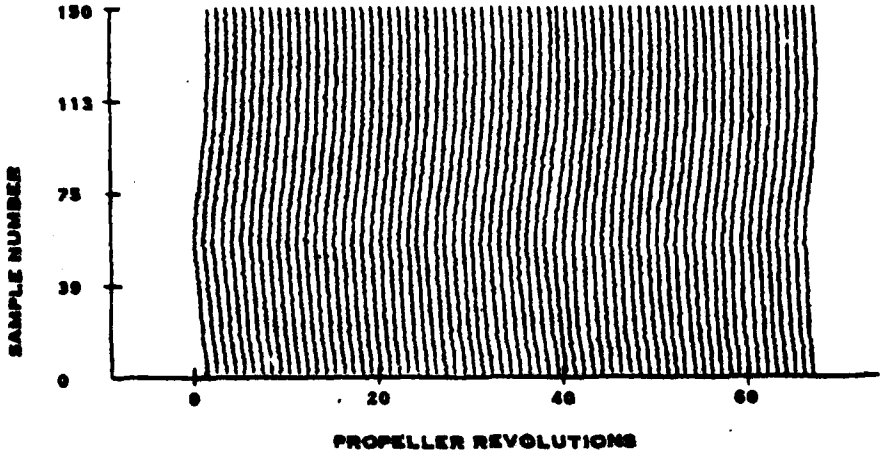

B) IN FLIGHT

FIGURE 4-8. PROPELLER BLADE SURFACE PRESSURES FOR STATIC AND IN-FLIGHT CONDITIONS.

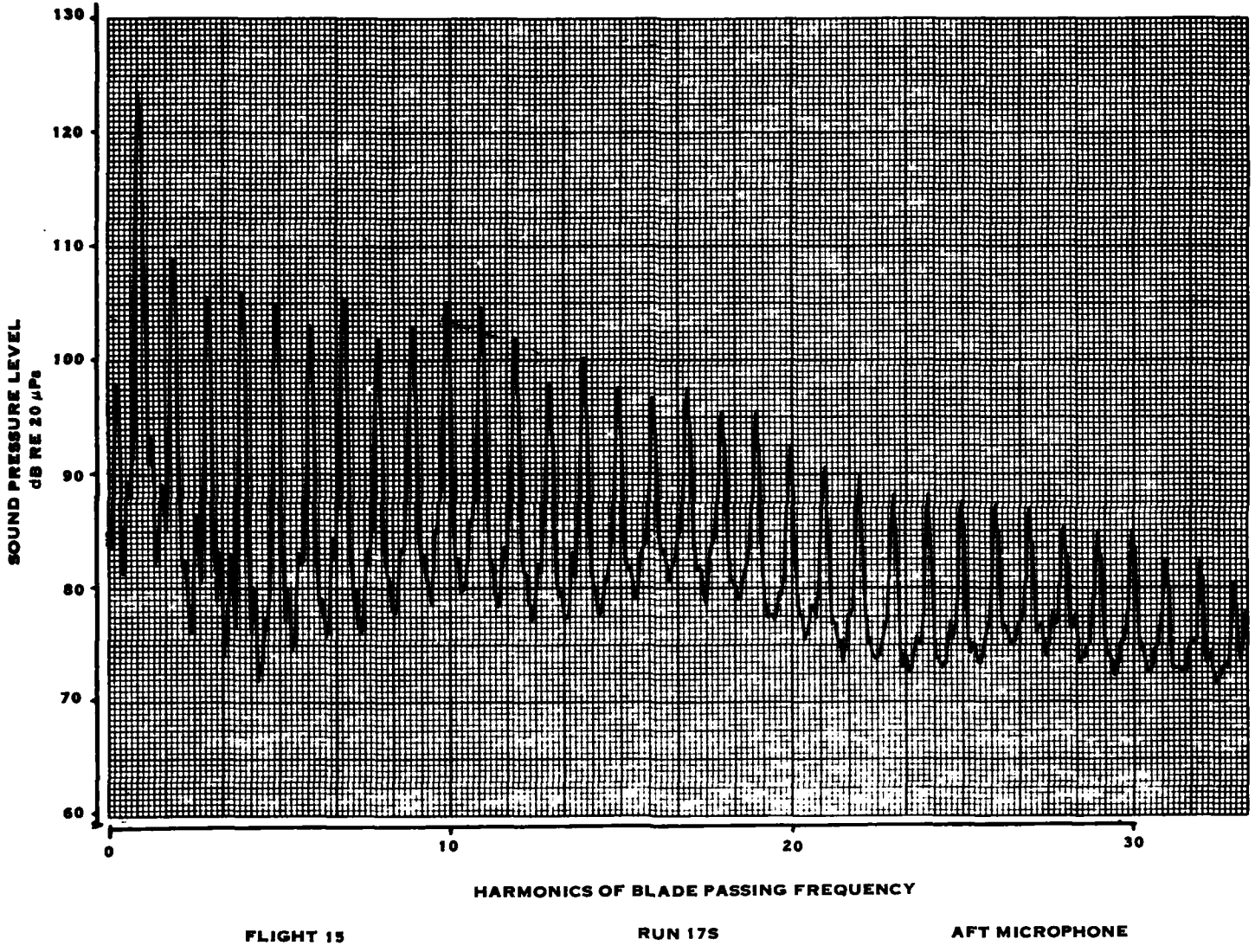

FIGURE 4-6. TYPICAL NOISE SPECTRUM FOR A PROPELLER OPERATING UNDER STATIC CONDITIONS.

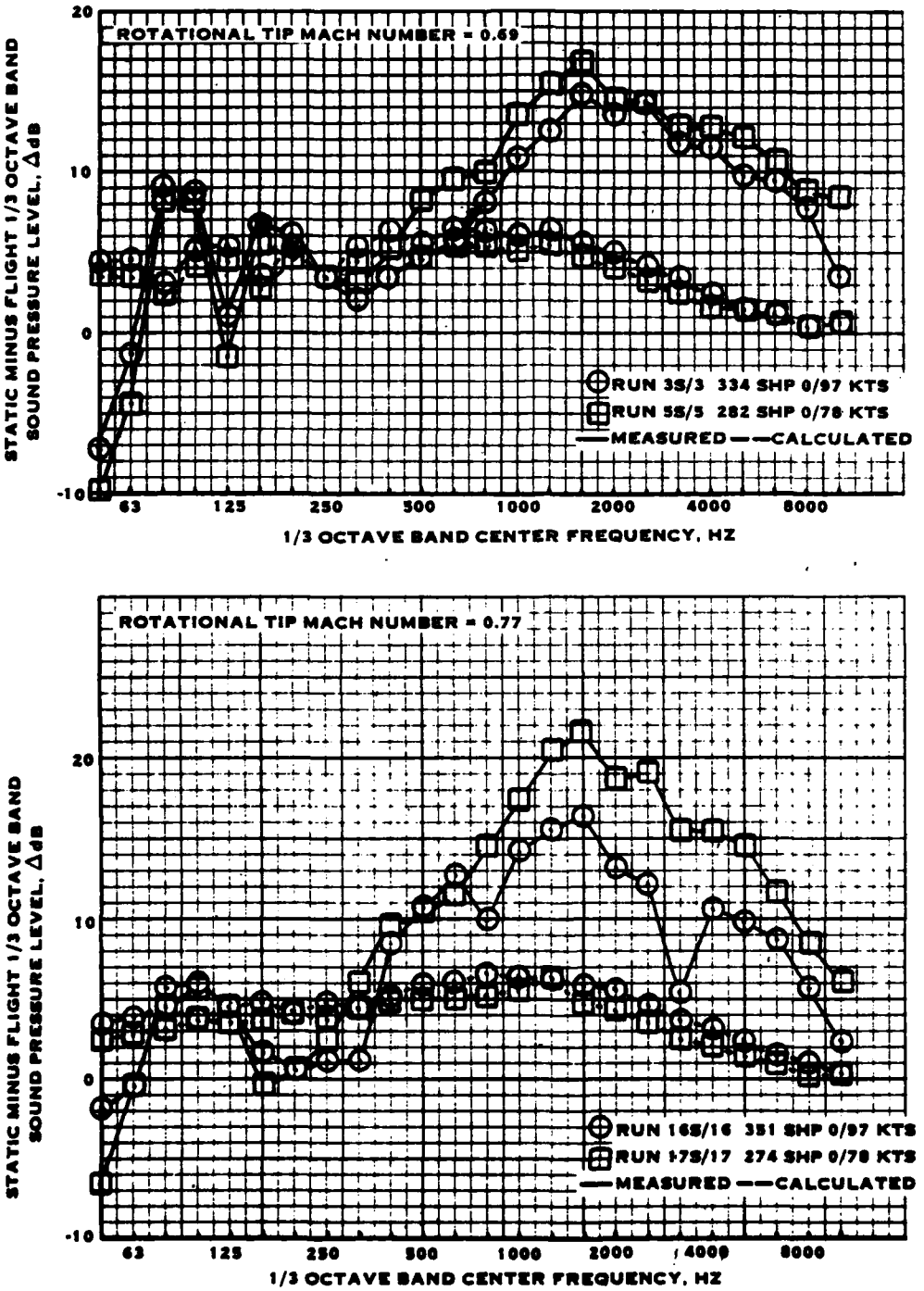

FIGURE 4-7. COMPARISON OF MEASURED AND CALCULATED DIFFERENCES IN 1/3 OCTAVE BAND LEVELS - STATIC MINUS FLIGHT - FOR THE FRONT WING TIP MICROPHONE IN DATA BASE ITEM PROPELLER -1

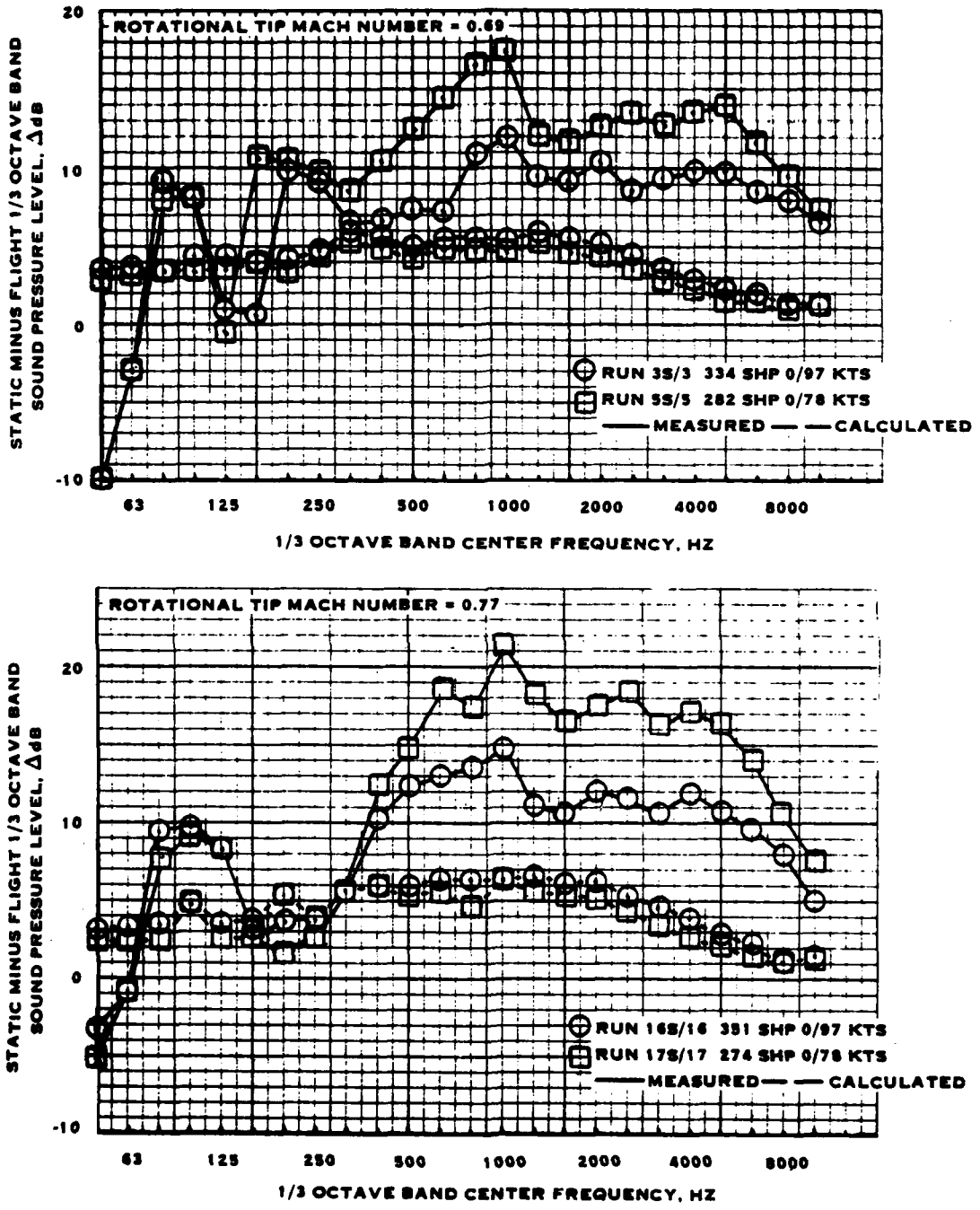

FIGURE 4-8. COMPARISON OF MEASURED AND CALCULATED DIFFERENCES IN 1/3 OCTAVE BAND LEVELS - STATIC MINUS FLIGHT - FOR THE AFT WING TIP MICROPHONE IN DATA BASE ITEM PROPELLER -1

lated. This occurs because the static spectrum is totally dominated by the higher harmonics which result from the ingestion of the fuselage and ground vortices. The one-third octave band spectra also confirm this, as the agreement between the calculated and measured in-flight noise levels is quite good.

It is possible to get a comparison in broadband noise level change utilizing the narrow band spectra from the Data Base Item 1 report by looking at the levels between harmonics. This was done for the aft wing-tip microphone and is summarized in figure 4-9. A problem with this data is that there is wind noise on the microphone in flight. This appears as high levels of low frequency broadband noise which decrease in level with increasing frequency. Thus, the significance of the negative values of measured static-minus-flight levels shown in figure 4-9 is that the in-flight low frequency broadband noise is dominated by wind noise on the microphone. Beyond about 500 Hz, the propulsion system broadband noise becomes dominant. Since broadband noise is non-descript, it is not possible to determine its source -- it could originate at the propeller, the engine, or the airframe (in-flight). To isolate the broadband noise source, two comparisons are shown in figure 4-9. The change in calculated propeller broadband noise without engine broadband noise is plotted along with the change in calculated total propulsor broadband noise. It is apparent that the engine noise is calculated to be significant, as the difference between static and flight for the total propulsor is less than that for the propeller alone. The test results show closer agreement with the propeller-alone trends. This could indicate that the engine noise is overpredicted or that the propeller noise is underpredicted. However, the magnitude of the calculated change in broadband noise is in general agreement with the measured change.

Data Catalog Item 7. - This report presents data measured on a Cessna 02-T airplane. Noise measurements were made statically and in-flight with the front propeller, aft propeller, and both propellers operating at several power settings. For the purposes of this evaluation, only the data acquired with the front propeller will be used, as the aft propeller has significant installation effects due to fuselage blockage, ingestion of wing wakes, and inflow interaction with the front propeller wake. Although narrowband analyses are given for the static data, the flight data are presented as octave bands.

Figure 4-10 shows the comparison between measured and calculated static-minus-flight octave band levels for cruise power (175 SHP) and partial power (100 SHP), both at 1519 rpm (0.51 tip Mach number). Since the static data was acquired at a 50 ft. distance, while the flyover data was acquired at a nominal 300 ft. altitude, one set of measurements was adjusted by 15.5 dB to eliminate the distance effects.

The comparison between measurement and calculation for the 125 to 1000 Hz bands is quite good for the cases where the noise from the core engine was included in the calculations. At the higher frequencies, the agreement is better for the cases without the core engine noise. This indicates that the higher frequency core engine noise is overpredicted, the static propeller noise is underpredicted, or the in-flight propeller noise

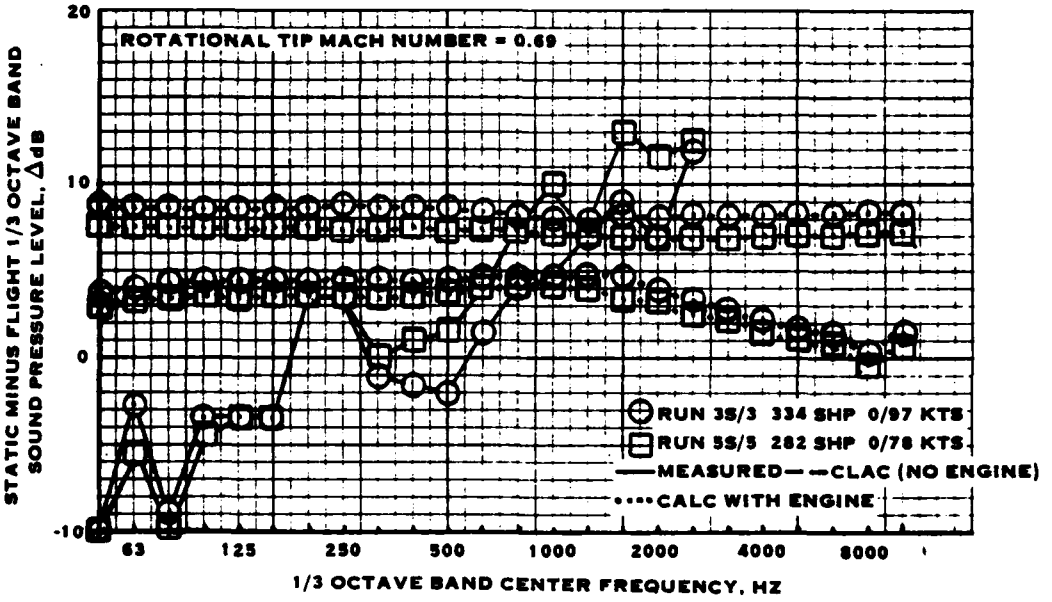

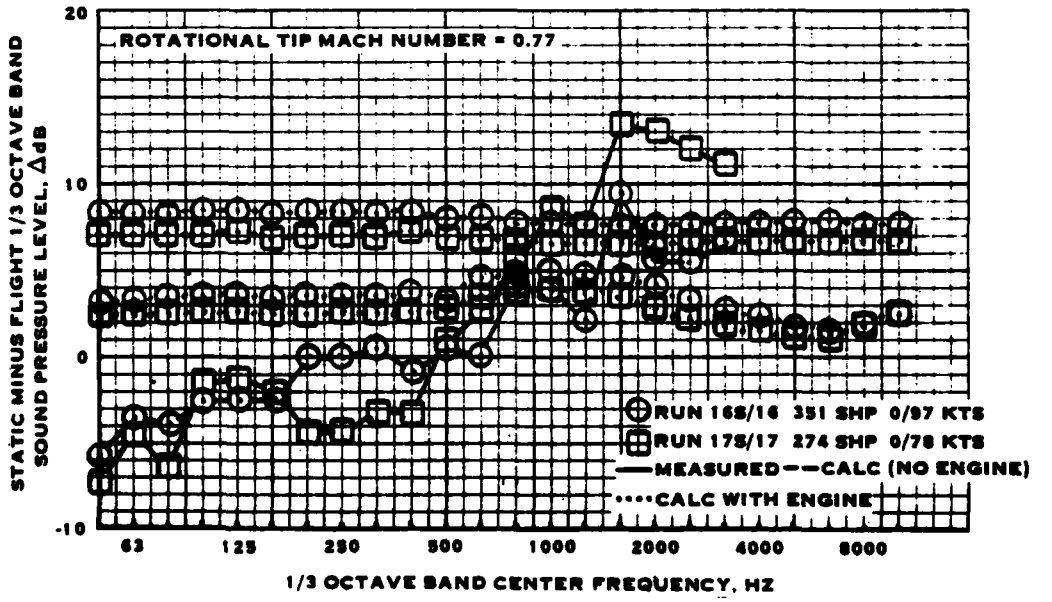

FIGURE 4-9. COMPARISON OF MEASURED AND CALCULATED DIFFERENCES IN 1/3 OCTAVE BAND BROADBAND NOISE LEVELS - STATIC MINUS FLIGHT - FOR THE AFT WING TIP MICROPHONE IN DATA BASE ITEM PROPELLER -1

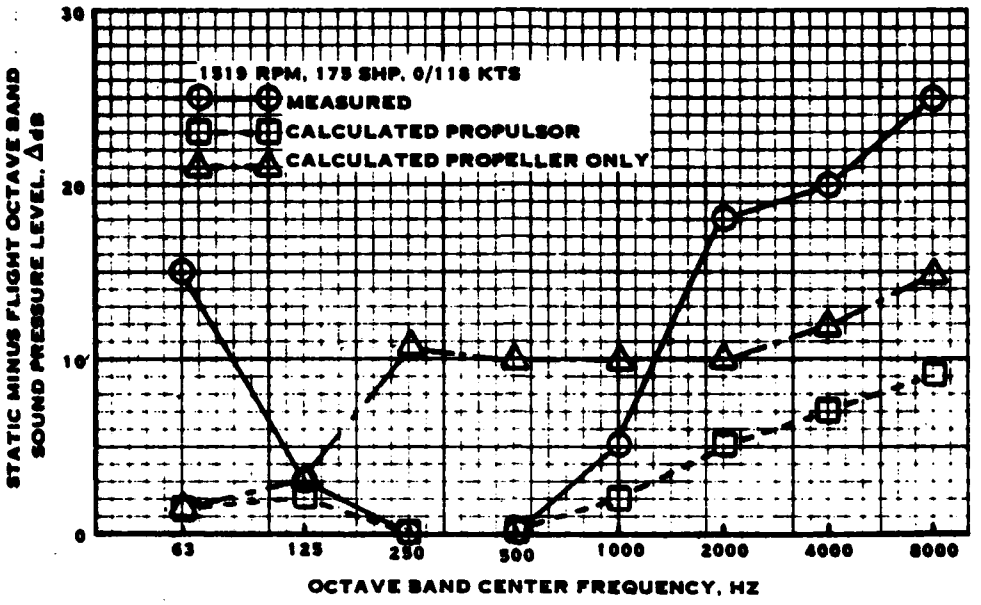

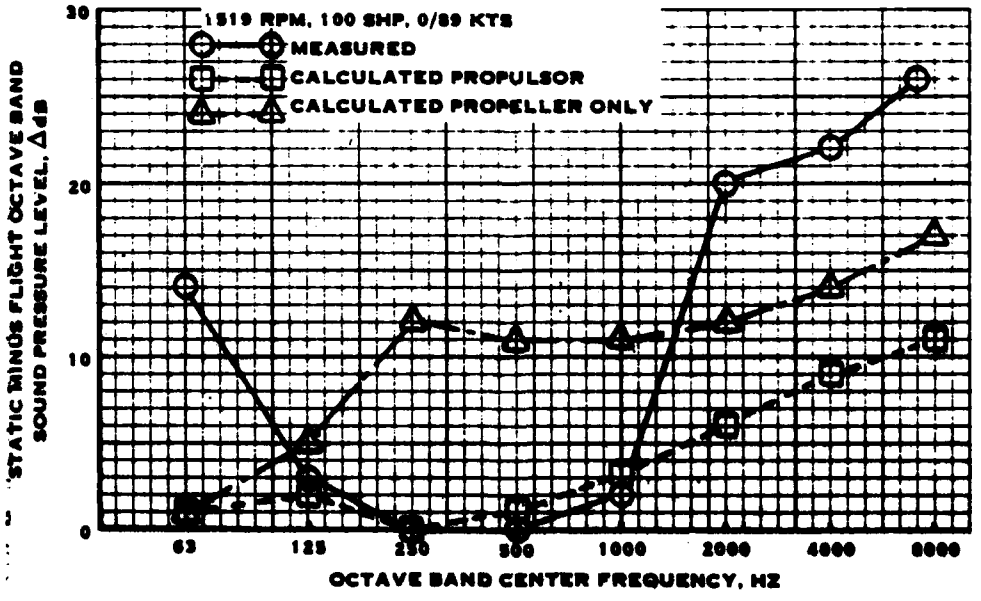

FIGURE 4-10. COMPARISON OF MEASURED AND CALCULATED DIFFERENCES BETWEEN STATIC AND FLIGHT NOISE LEVELS FOR DATA BASE ITEM PROPELLER -7

is overpredicted. Since the noise data is presented in octave bands, it is not possible to establish the engine noise contribution. Also, the engine design and operating parameters were not known, so that the calculations were made for a generalized engine. It is also apparent from the individual spectra that the high-frequency noise under static condition is slightly underpredicted while that in-flight is slightly overpredicted. This results in the 10 dB discrepancy between the measured and calculated differences at high frequency. It is thus concluded that for this airplane, the generalized engine noise prediction overestimates the high frequency engine noise. The static propeller noise is underestimated and the in-flight propeller noise is overestimated; but it is not possible to determine which of the components of propeller noise are incorrectly calculated. However, since the general trend is in good agreement, the correlation between calculated and measured forward-flight effects for this data is considered acceptable.

DeHavilland DHC-7. - The comparison of calculated and measured static-minus-flight noise for this airplane is shown in figure 4-11. The static data was acquired on an aerodynamic test stand for a single propeller. As this was driven by an electric motor, the noise measured is representative of an isolated propeller. The in-flight data was acquired during airplane flyover. The respective data were adjusted for distance and number of propellers.

As for the previous comparison, it may be seen that the agreement between measurements and calculations is better with engine noise included (flight only in this case) at the low frequencies and without engine noise at the high frequencies. Since the one-third octave band analyses, which is all that is available for the flight data, do not permit identification of components in the noise spectra, it must be assumed that the engine noise is overpredicted at high frequencies. If this assumption is accepted, then the correlation between measured and calculated forward-flight effects on the noise of the DeHavilland DHC-7 propeller is quite good.

Summary for Free-Air Propellers. - It is apparent that the major problem in evaluating the forward flight effects on propeller noise is two-fold: installation effects and the lack of available detailed (i.e., narrow-band) analyses of the flight data. In addition, the effect of forward-flight on propeller noise is difficult to assess, as the flight data includes engine broadband noise, which is indistinguishable from that generated by the propeller.

However, despite these limitations on the data, it is apparent that the current forward-flight effects which are included in the V/STOL noise prediction methodology are qualitatively good and quantitatively acceptable. They are qualitatively good in that the propeller tone higher harmonics are calculated to decrease in level rapidly as forward flight is begun, as was demonstrated by the carpet plot of Twin-Otter noise vs. frequency vs. time. They are also quantitatively acceptable in that for the limited data available the correlation between calculated and measured static-minus-flight noise levels is generally good.

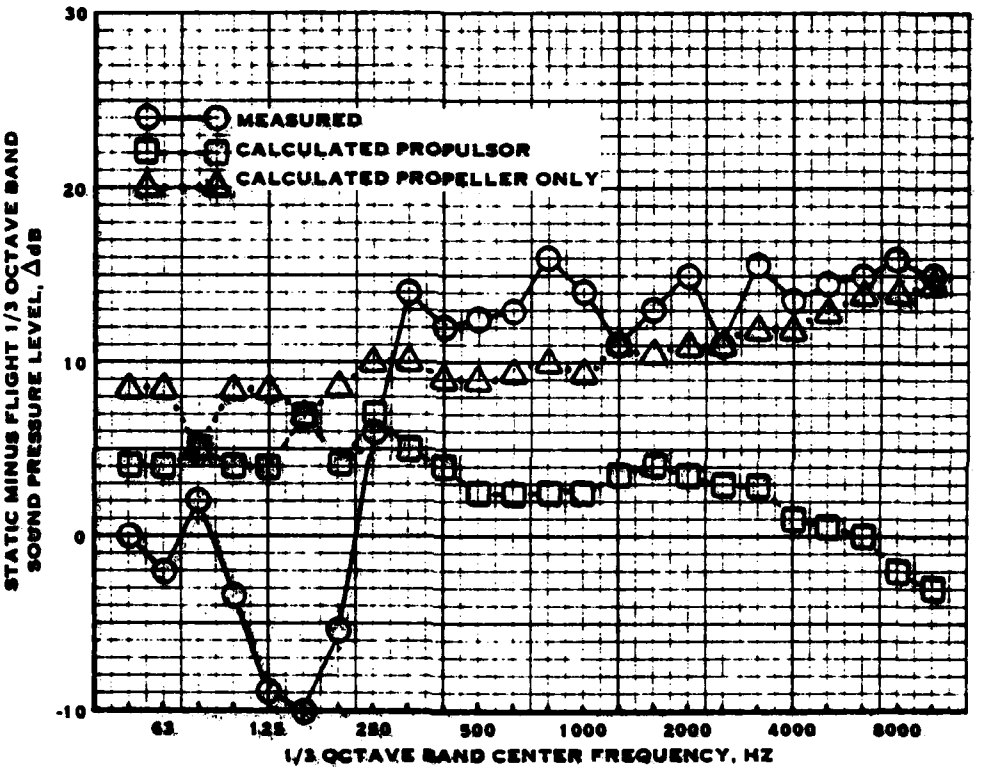

FIGURE 4-11. COMPARISON OF MEASURED AND CALCULATED DIFFERENCES BETWEEN STATIC AND FLIGHT NOISE LEVELS FOR THE DEHAVILLAND DHC-7

Variable-Pitch Fans

The forward flight effects on variable-pitch fan noise included in the methodology are 1) the changes in unsteady loading noise due to the modification in the inflow turbulence ingested by the fan caused by changes in the inflow contraction ratio and 2) the change in the jet noise due to relative velocity changes. Thus, the observed change in variable-pitch noise with forward flight will depend on the relative contribution of unsteady loading noise to the total tone noise (i.e., that from the stator) and the broadband jet noise to the total broadband noise. In particular, it is apparent that for the case where the combination of tip speed and ratio of vane-count to blade-count causes the fundamental (and higher harmonics) to be cut-off, a tone will generally appear at the fundamental under static conditions but will disappear in flight.

The only data which shows the effects of flight on variable-pitch fan noise was found to be that identified as Item 4 under variable-pitch fans in the data catalog. Although this data is limited, it was used as being the only example available. The data is limited to fan inlet noise only and was acquired in a wind tunnel. In addition to high levels of tunnel noise and semi-reverberant acoustic field, the turbulence characteristics in a wind tunnel do not generally represent those that a propulsor in flight in the free atmosphere would encounter, as demonstrated in reference 4. This is particularly true of static conditions. Thus, this data was used as an indicator of the general trends of variable-pitch fan noise with forward-flight, but was not used to revise the methodology for better agreement with measurements.

Figure 4-12 shows the comparison between the measured and calculated static-minus-flight levels of the fundamental and second harmonic tones at 60 degrees azimuth as functions of tunnel speed for two fan tip speeds. As may be seen, the trends for the fundamental show good agreement between calculated and measured. This occurs, in part, because the fundamental tone is cut-off. However, the unsteady loading noise is not and, therefore, dominates at static conditions. In flight, the unsteady loading noise decreases and the change in fan noise at the fundamental is due uniquely to the change in unsteady loading noise. The test data show essentially no effect of flight on the level of the second harmonic. The calculations show about the same effect for the second harmonic as for the fundamental. This is because the second harmonic of the stator noise is calculated to be insignificant compared to that of the unsteady loading noise. Thus, either the test environment is preventing the second harmonic of loading noise from decreasing with flight speed, or the calculations are in error. Both the test data and the calculations show little effect of tunnel speed on the high frequency noise. Thus, considering the differences in assumed environments (measurements in a wind tunnel vs. calculations for a normal atmosphere), the agreement between measured and calculated forward-flight effects on fan noise is quite good, except at the second harmonic.

It is thus concluded that the forward-flight effects which are included in the noise prediction methodology for variable-pitch fans are adequate and that revisions based on the currently available data are not justified.

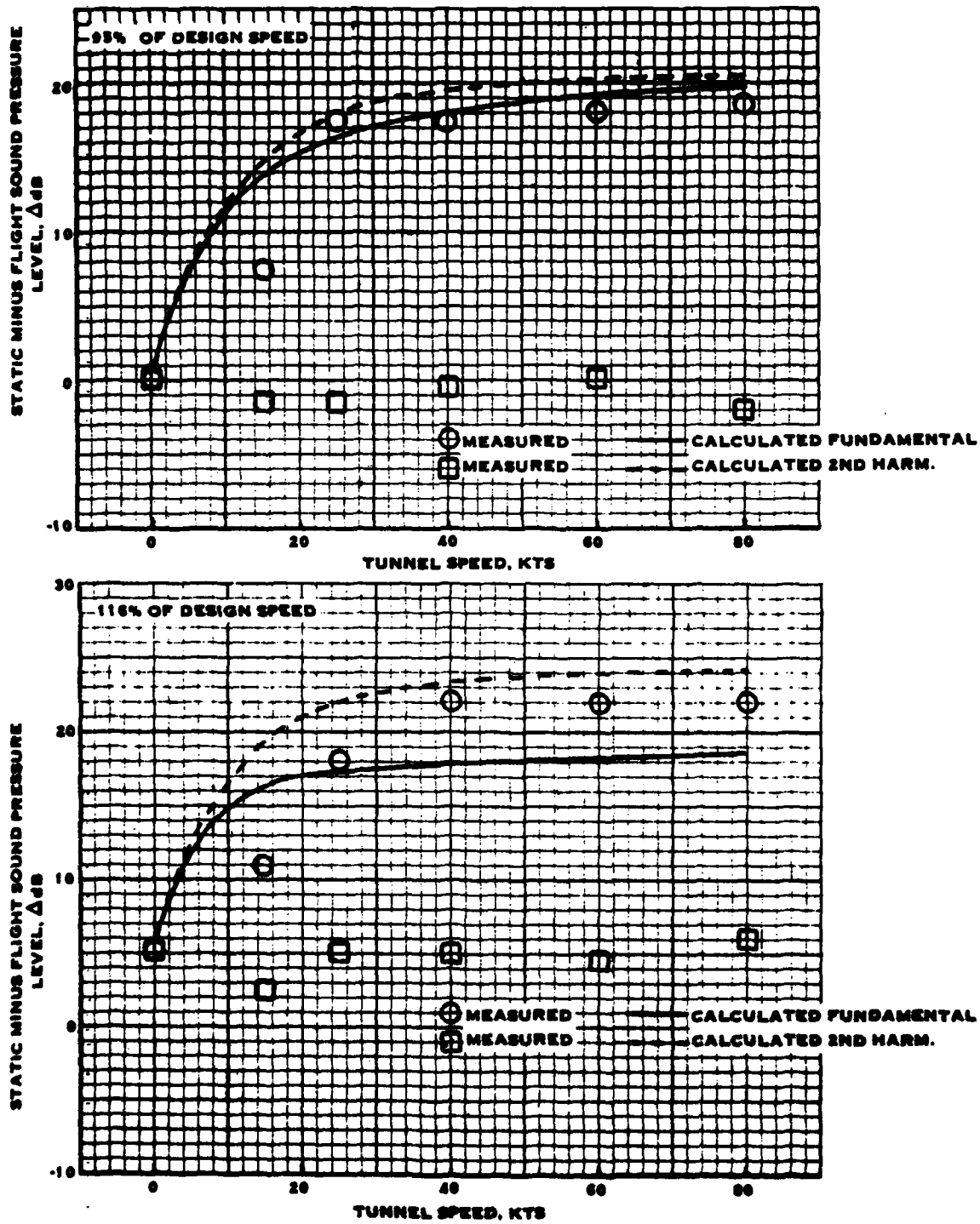

FIGURE 4-12. COMPARISON OF MEASURED AND CALCULATED DIFFERENCES BETWEEN STATIC AND FLIGHT TONE NOISE FOR DATA BASE ITEM VARIABLE PITCH FAN 4

Fixed-Pitch Fans

The forward-flight effects on fixed-pitch fan noise included in the methodology are the reduction in fan tone noise from static to flight and the change in broadband noise due to reduction in relative jet velocity. The reduction in fan tone noise is attributed to the reduction in inflow turbulence interaction and, as such, occurs only when unsteady loading is a significant contributor to the noise. Thus, the reduction in the levels of the tones are formulated in the V/STOL noise prediction procedure to occur only for configurations without inlet guide vanes (IGV's) operating at subsonic tip speeds. The broadband noise reduction is associated with changes in jet noise and will appear only when the jet noise is significant, i.e., for low bypass ratio configurations.

It is particularly important to exclude from the test data extraneous effects, in particular installation effects. As reviewed in reference 5, the ingestion of ground vortices and test stand structure interference in static tests substantially increases the levels of noise at blade passing frequency harmonics. Although these effects disappear in flight, they are not strictly speaking forward-flight effects, but depend primarily on the actual installation of the propulsor.

The data reviewed falls into two general categories. In the first category are those data that show qualitative results on fan noise with forward flight. The second category contains those data which had sufficient information to allow calculations of the noise under static and flight conditions for comparison with the measurements.

Data Catalog Item 1. - These data were acquired with microphones located inside the inlet of a Rolls-Royce RB211 fan. The data from this series of tests is summarized in figure 4-13. As may be seen in figure 4-13a, the level of the fundamental drops significantly between static and flight at a tip relative Mach number of 0.7. The second harmonic is relatively unaffected, but has been identified as a propagating rotor/stator interaction mode. At a tip relative Mach number of 1.0, shown in figure 4-13b, reduction in the tone noise levels with flight is considerably less. It may also be noted that the broadband noise is relatively unaffected by forward flight. Figure 4-13c shows the variation in blade passing frequency (BPF) fundamental between static and flight as a function of tip relative Mach number. As this shows, significant reductions in level were measured for flight vs. static conditions up to a tip relative Mach number of about 1.05, beyond which there was little change.

In summary, the data from this report indicates that for a fixed-pitch fan without IGV's, tone noise decreases with forward flight, showing a significant change for the BPF fundamental below supersonic tip speed and little or no change for the second harmonic. The fan inlet broadband noise is essentially unaffected by flight.

Data Catalog Item 4. - This paper presents results of measurements of JT3D, CF6, and JT9D static and flight engine noise. Static data were acquired on engine test stands at 10 degree intervals at a constant radius. These static data were projected

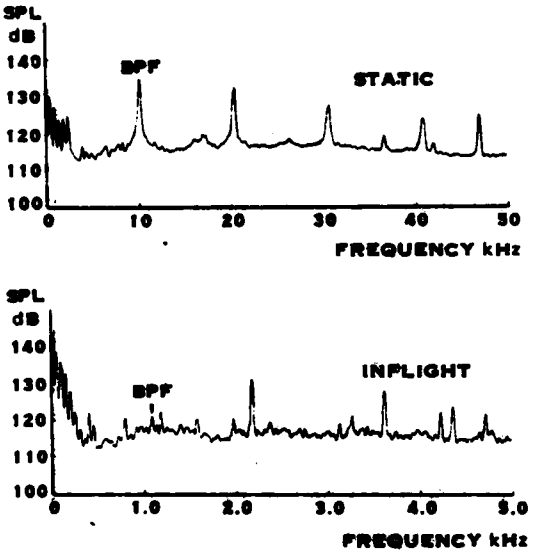

4-13A IN-DUCT SPECTRA OF RB.211 ON VC.10, STATIC AND IN-FLIGHT. FAN TIP RELATIVE MACH NUMBER 0.70.

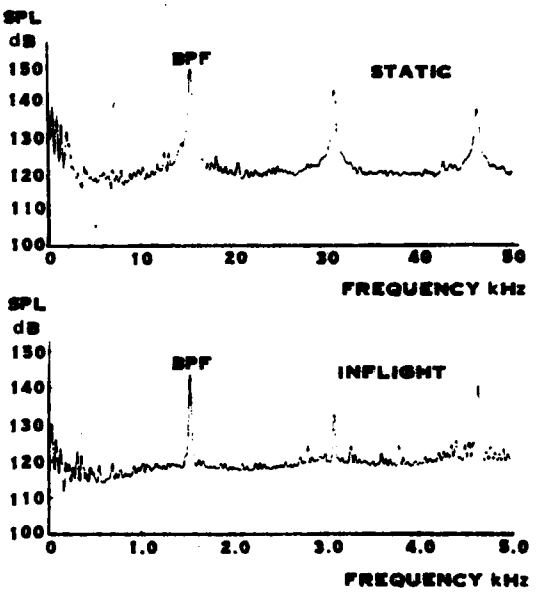

4-13B. IN-DUCT SPECTRA OF RB.211 ON VC.10, STATIC AND IN-FLIGHT. FAN TIP RELATIVE MACH NUMBER 1.00.

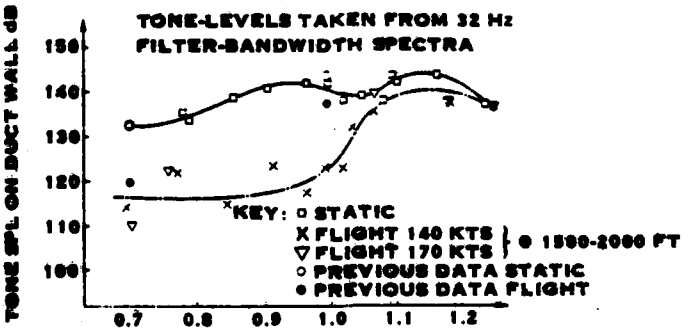

4-13C. VARIATION OF BPF FUNDAMENTAL LEVEL WITH TIP RELATIVE MACH NUMBER, STATIC AND IN-FLIGHT

FIGURE 4-13. SUMMARY OF FAN INLET NOISE FORWARD FLIGHT EFFECTS FROM DATA BASE ITEM FIXED PITCH FAN - 1.

to flight by adjusting for number of engines, flight path, distance, atmospheric absorption, Doppler shift, and altitude. Also, the jet noise components were adjusted for the effects of relative velocity.

Figure 4-14 summarizes the comparison at approach condition for the JT3D engine. As may be seen, both the PNLT vs. time comparison, figure 4-14a, and the inlet noise spectrum comparison, figure 4-14b, show little difference between static and flight conditions. It is also indicated that the maximum PNLT, which occurred after the airplane passed overhead and thus contains aft-radiated engine and fan noise, shows similar spectral agreement to that seen in figure 4-14b.

Figure 4-15 shows the comparison for the CF6 engine. In this case, both the PNLT and the spectrum show significant reductions in flight noise compared to the projected static noise. The most striking difference shown in figure 4-15b is the absence of fan fundamental tone noise in flight. This is reported to be true also at the point of maximum PNLT.

Figure 4-16 shows the same comparisons for the JT9D engine. Similar results to those observed for the CF6 engine may be seen. Although the fan fundamental tone of the JT9D can be seen in the flight data, it is at a reduced level relative to that projected from static measurements. It may also be seen that the level of the second harmonic is reduced by forward flight relative to static conditions; but this reduction is not as great as that of the fundamental.

Finally, Figure 4-17 shows the changes in forward-flight effects which occur for the JT9D with increasing fan speed. As indicated, the flight effects decrease as fan speed is increased.

In summary, this report generally confirms the results which were noted in Data Catalog Item 1. It may also be concluded that fans with IGV's (i.e., JT3D) do not show appreciable forward-flight effects. Fans without IGV's show substantial reduction in the levels of the fan fundamental tone in flight for subsonic tip speed operation. This reduction decreases with increasing tip speed. The second harmonic also shows a decrease in level in flight, but this difference is considerably less than that for the fundamental.

Data Catalog Item 5. - This paper presents measurements made with microphones installed in the inlet and outlet ducts of a CF6-6 fan. Also, a microphone was located on the airplane fuselage at a position forward of the fan inlet. Flyover noise was measured under the flight path. The engines were operated over a range of fan speeds both statically and in flight at 150 to 170 kts.

Figure 4-18 shows a comparison of flight and static spectra for a low fan speed condition. This shows a reduction of about 8 dB at the fundamental fan tone for the inlet noise and about 3 dB at the fundamental fan tone for the discharge noise. A small reduction in broadband noise may also be seen in the inlet, whereas the discharge

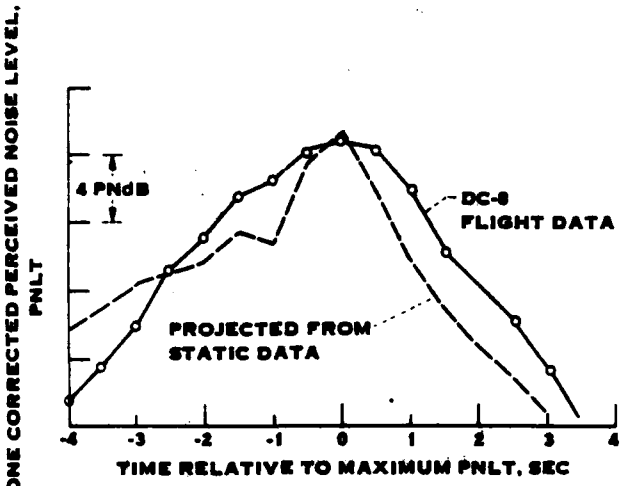

FIGURE 4-14A - COMPARISON OF FLIGHT AND PROJECTED STATIC PNLT HISTORIES FOR JT3D-3B ENGINE AT APPROACH CONDITION (4696 RPM).

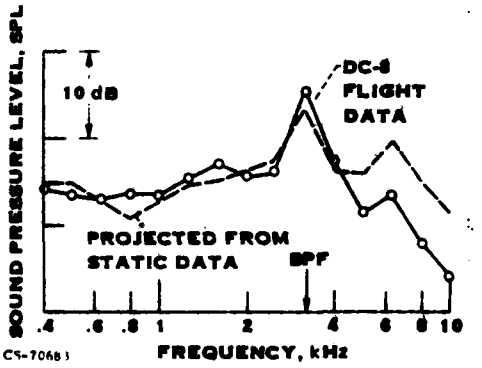

FIGURE 4-14B. - COMPARISON OF FLIGHT AND PROJECTED STATIC INLET SOUND PRESSURE SPECTRA FOR JT3D-3B ENGINE AT APPROACH CONDITION (4696 RPM); 75° INLET ANGLE.

FIGURE 4-14 FORWARD FLIGHT EFFECTS ON JT3D ENGINE NOISE FROM DATA BASE ITEM FIXED PITCH FAN - 4

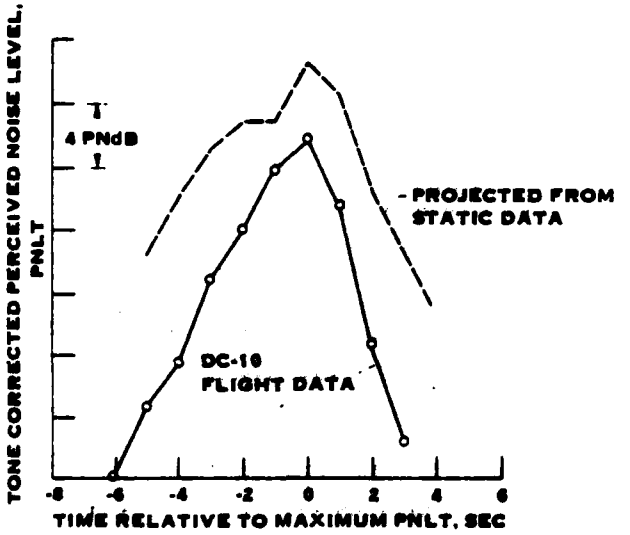

FIGURE 4-15A - COMPARISON OF FLIGHT AND PROJECTED STATIC PNLT HISTORIES FOR CF6-6 ENGINE AT APPROACH CONDITION (2579 RPM).

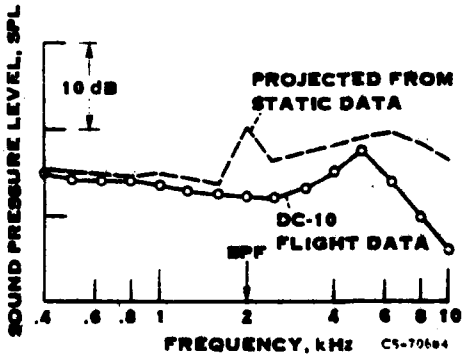

FIGURE 4-15B - COMPARISON OF FLIGHT AND PROJECTED STATIC INLET SOUND PRESSURE SPECTRA FOR CF6-6 ENGINE AT APPROACH CONDITION (2579 RPM); 70° INLET ANGLE.

FIGURE 4-15 FORWARD FLIGHT EFFECTS ON CF6 ENGINE NOISE FROM DATA BASE ITEM FIXED PITCH FAN - 4

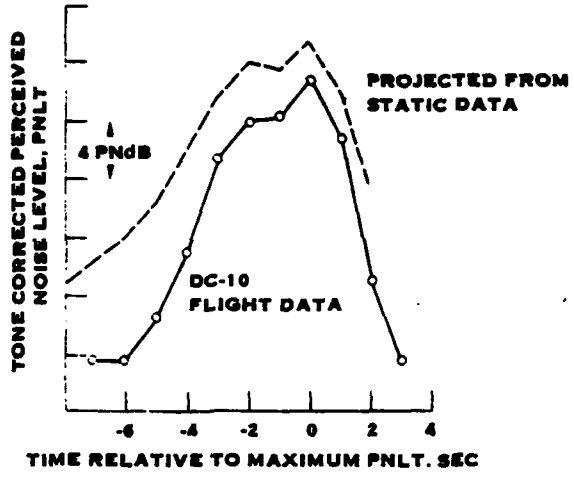

FIGURE 4-16A. - COMPARISON OF FLIGHT AND PROJECTED STATIC PNLT HISTORIES FOR JT9D-20 ENGINE AT APPROACH CONDITION (2666 RPM).

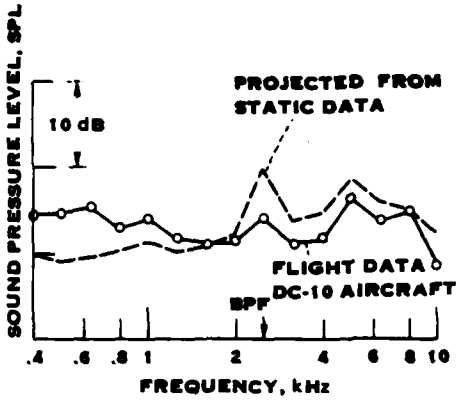

FIGURE 4-16B - COMPARISON OF FLIGHT AND PROJECTED STATIC INLET SOUND PRESSURE SPECTRA FOR JT9D-20 ENGINE AT APPROACH CONDITION (2666 RPM); 60° INLET ANGLE.

FIGURE 4-16. FORWARD FLIGHT EFFECTS ON THE JT9D ENGINE NOISE FROM DATA BASE ITEM FIXED PITCH FAN - 4.

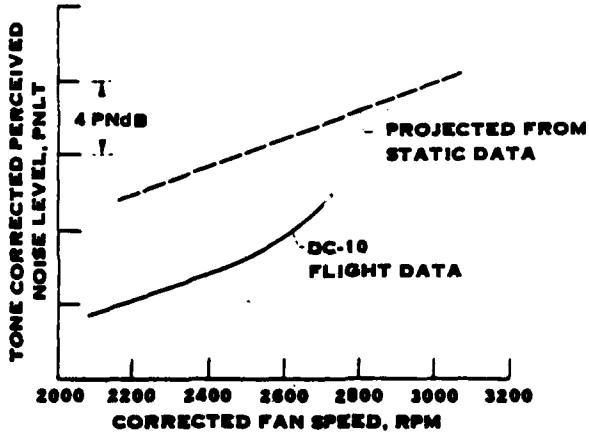

COMPARISON OF FLIGHT AND PROJECTED STATIC TONE CORRECTED PERCEIVED NOISE LEVELS FOR INLET NOISE FROM A JT9D-POWERED DC-10 AT PART 36 APPROACH CONDITION. 60° INLET ANGLE.

FIGURE 4-17. FORWARD FLIGHT EFFECTS VS FAN SPEED FOR THE JT9D ENGINE NOISE FROM DATA BASE ITEM FIXED PITCH FAN - 4.

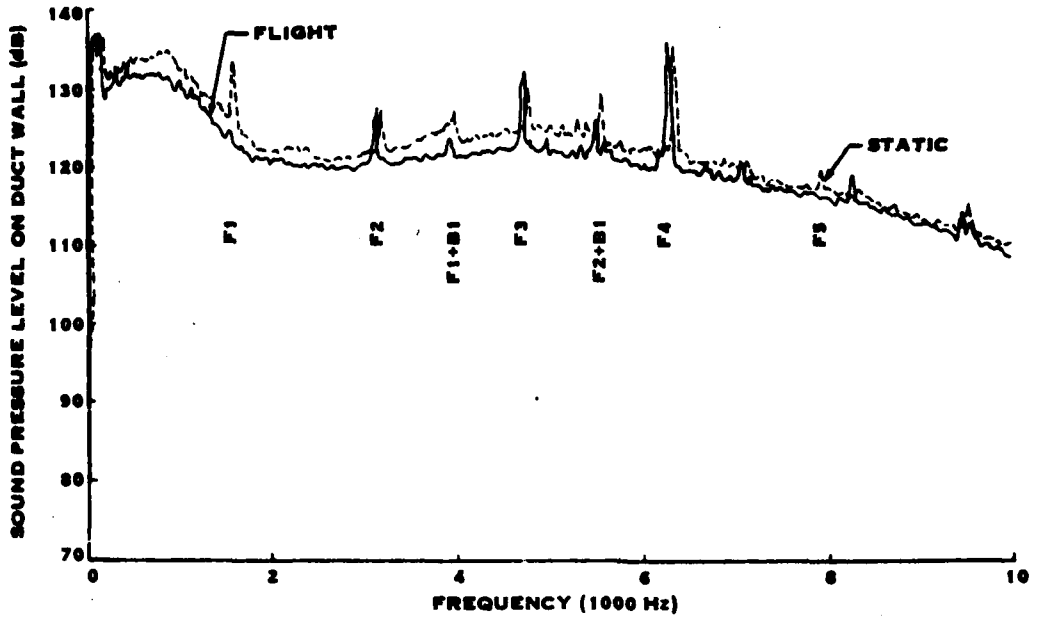

A. COMPARISON OF FLIGHT AND STATIC NARROW-BAND SPECTRA MEASURED ON THE INLET WALL OF THE CF6-6 ENGINE. FAN ROTOR SPEED 2465 RPM

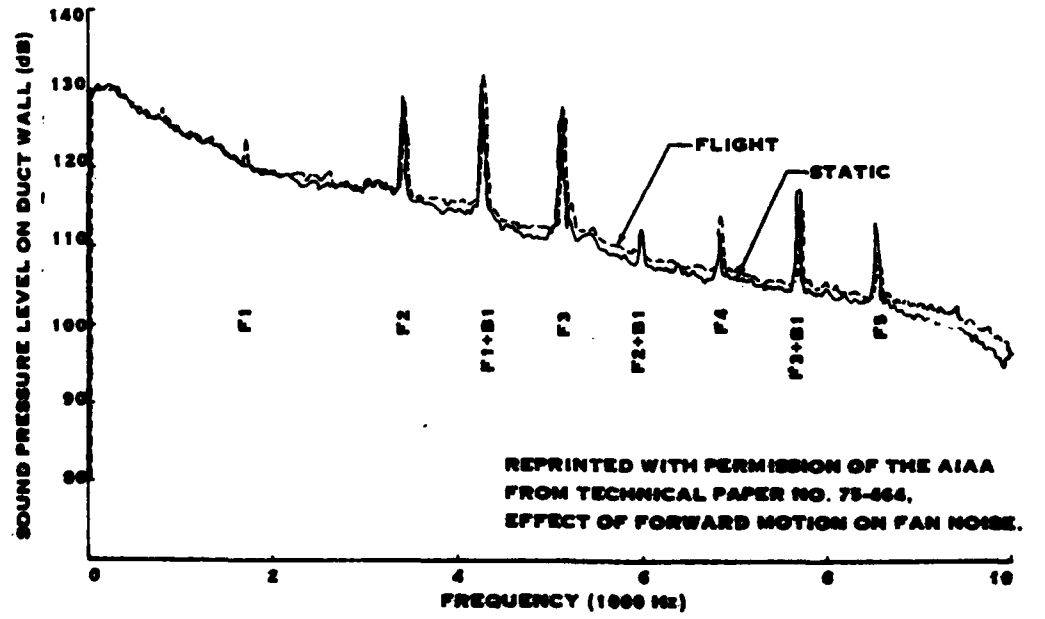

B. COMPARISON OF FLIGHT AND STATIC NARROW-BAND SPECTRA MEASURED ON THE WALL OF THE FAN DISCHARGE DUCT IN THE CF6-6 ENGINE. FAN ROTOR SPEED 2465 RPM

FIGURE 4-18. FORWARD FLIGHT EFFECTS AT LOW FAN SPEEDS FROM DATA BASE ITEM FIXED PITCH FAN-8.

broadband noise is relatively unchanged. The higher harmonics of the fan noise and other tones in the spectra do not appear to change with forward flight.

Figure 4-19 shows a similar comparison made for a high fan speed. There appears to be essentially no difference between the static and flight spectra either in the inlet or the exhaust.

Figure 4-20 summarizes the effects of flight on the level of the fan fundamental tone as a function of fan speed. At the inlet, the flight levels are lower than the static levels until the fan tip speed reaches Mach 1, beyond which the static and flight levels are equal. At low speed, the difference is about 8 dB and decreases almost linearly with increasing tip speed. The fan discharge duct noise levels show a nearly constant 4 dB decrease from static to flight up to a speed of about 3200 rpm, beyond which the difference drops to zero.

The flyover measurements generally confirmed the results measured with the in-duct microphones in terms of reductions of the fundamental fan tones with flight. However, the projected static data show generally higher levels at frequencies above the fan fundamental than those of the flight data. It is suggested that this may be due to mechanisms other than those that affect fan noise generation. These were identified as dynamic amplification effects and differences between actual and assumed propagation through the atmosphere.

In summary, the data from this report is in agreement with that presented in the two previous reports, i.e., the major effect of flight on the noise from fixed-pitch fans without IGV's is to reduce the fundamental tone for subsonic operation.

Data Catalog Item 27. - In this report attempts are made to correct static data to flight condition for a DC-10-10 airplane with CF6-6D engines and a DC-9-30 airplane with JT8D-109 engines. The adjustments included the effects of installation, convective amplification, and propagation effects. The installation effects considered included relative engine location, fuselage and wing shielding, wing/flap/wheel wake sound scattering, jet exhaust scattering, and airframe noise.

The data presented is in general agreement with that from the previously discussed papers, i.e., for the CF-6 at approach condition, the fan fundamental tone is about 8 dB lower in flight than at static conditions. For the CF-6 in take-off and for the JT8D-109 there is no appreciable difference in the fan fundamental tone noise level between static and flight. At mid-frequencies above the fundamental fan tone, the CF-6 flight data is slightly higher than the static-projected data (i.e., static data projected to flight) in the aft quadrant at the approach condition. In the forward quadrants for approach condition and everywhere for the take-off condition for the CF-6, and for all cases of the JT8D, the static-projected data moderately exceeds the flight data. In all cases, the high frequency static-projected data significantly exceeds the flight data. Applying correction for installation, convective amplification, and propagation effects improves the agreement between static-projected and flight data at mid frequencies, but does not reconcile the high frequency noise discrepancy.

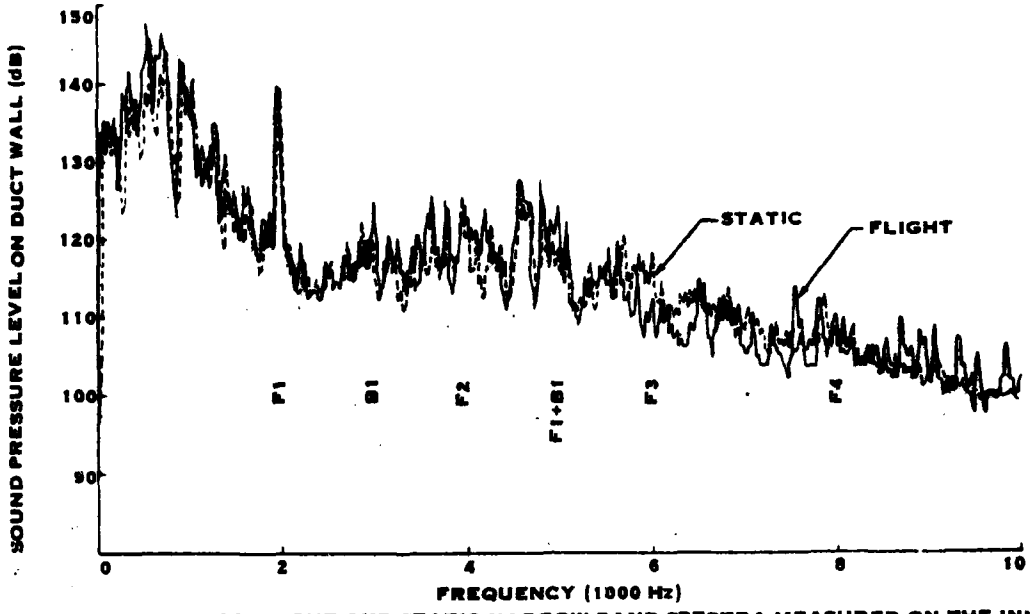

A. COMPARISON OF FLIGHT AND STATIC NARROW-BAND SPECTRA MEASURED ON THE INLET WALL OF THE CF6-6 ENGINE. FAN ROTOR SPEED 3070 RPM

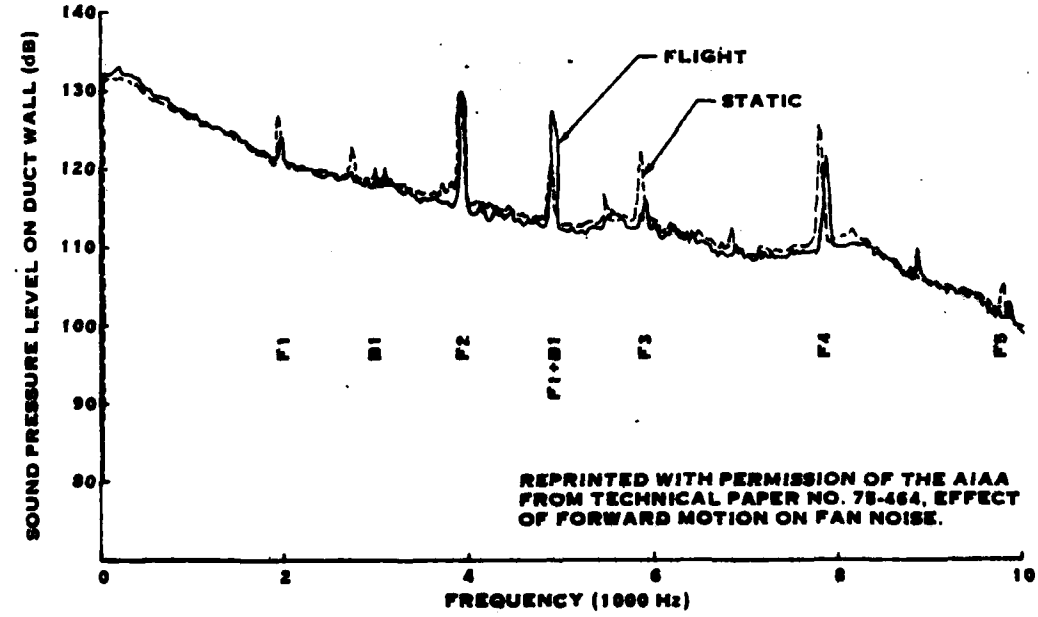

B. COMPARISON OF FLIGHT AND STATIC NARROW-BAND SPECTRA MEASURED ON THE WALL OF THE FAN DISCHARGE DUCT IN THE CF6-6 ENGINE. FAN ROTOR SPEED 3070 RPM

FIGURE 4-19. FORWARD FLIGHT EFFECTS AT HIGH FAN SPEEDS FROM DATA BASE ITEM FIXED PITCH FAN-5.

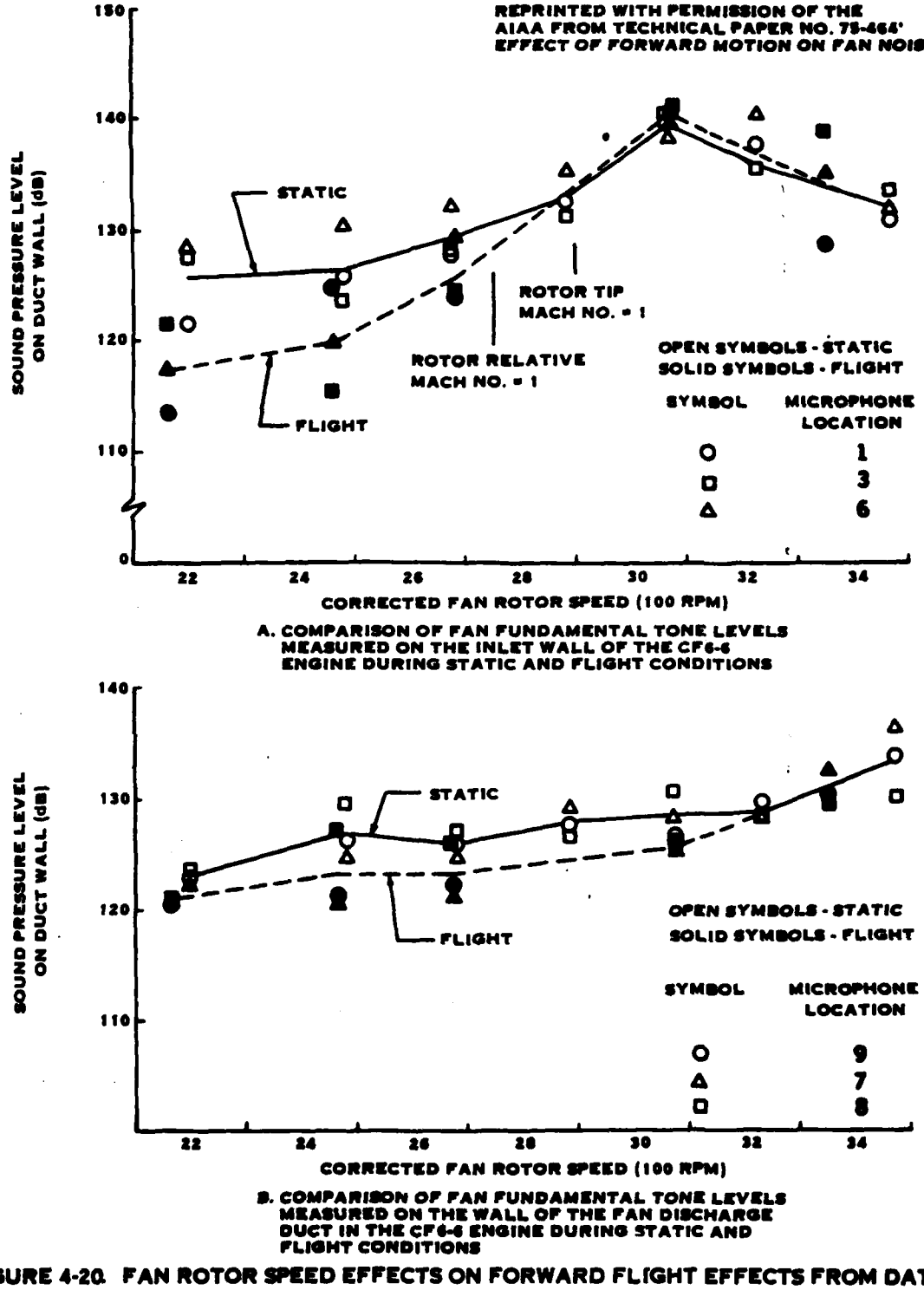

FIGURE 4-20. FAN ROTOR SPEED EFFECTS ON FORWARD FLIGHT EFFECTS FROM DATA BASE ITEM FIXED PITCH FAN - 5.

In summary, the fan noise results presented in this paper generally confirm those noted in previously discussed reports, i.e., the fan tone is reduced as the airplane moves from the static to the flight regime. This paper also indicates that the convective amplification effects noted in the core noise data closely matched the theoretical relationship: $-40 \log (1-M_a \cos \theta)$, where M_a is the airplane flight Mach number and θ is the propagation angle. As this relationship is derived for a moving point source, it is applicable to fan noise as well.

Data Catalog Item 30. - This paper presents static and flyover noise data on a JT15D engine. Figure 4-21a shows a comparison of the static and flight spectra at the maximum sideline noise location. The decrease in the low frequency noise shows the forward-flight effects on jet noise. A large drop in the level of the fan fundamental tone in flight may also be seen. The forward-flight effects on the level of the fan fundamental tone is shown for take-off in figure 4-21b and for approach in figure 4-21c. As can be seen, the difference in the forward quadrant on take-off is up to 18 dB, which is much greater than reported in other studies. It may also be noted that the curves cross in the aft quadrant, indicating that the flight levels are higher than the static levels. However, this could be due to a change in directivity caused by the flight effects. The approach data show similar effects, but the maximum difference between static and flight is only about 10 dB.

The noise level reductions are believed to be due to two effects. On the Cessna Citation, the flight vehicle used in these tests, the engine is located above and slightly aft of the wing, so that the engine inlet is actually over the wing. This configuration is the cause of the two effects which result in the large noise reduction seen in flight compared to the static data. The paper shows a photograph which was taken of the fan inlet under static conditions. This photograph clearly shows two vortices being ingested by the fan. One vortex is believed to have originated on the wing. Thus, under static conditions, the fan experiences inflow distortion caused by its installation in close proximity to the fuselage and the wing. This inflow distortion is similar to that observed for the Twin Otter (discussed under propellers) and gives rise to more intense harmonic noise. In flight, the vortices are not ingested by the fan, thus this mechanism does not occur.

The second effect is due to shielding by the wing. From below the airplane, the engine inlet is shielded by the wing. Thus, in flight, the engine inlet radiated noise is shielded from the microphone by the wing. During static noise measurements, the microphone was located to the side of the airplane, where wing shielding did not occur.

In summary, this paper presents evidence that installation effects on fan noise generation can be more significant than forward-flight effects. Thus, it can be seen that test data must be carefully screened for these other effects in order for comparisons between static and flight data to yield valid forward-flight effects.

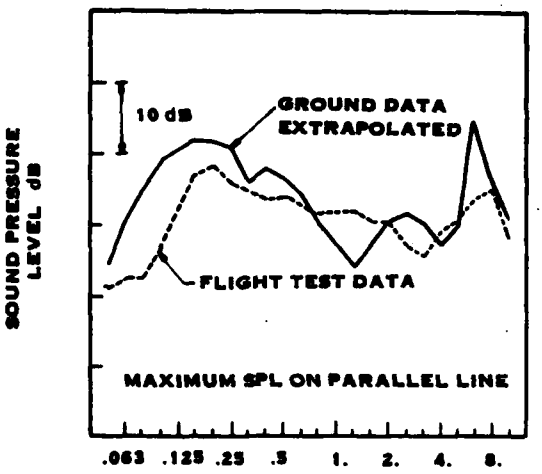

FIGURE 4-21A - COMPARISON OF FLIGHT VERSUS GROUND TEST DATA

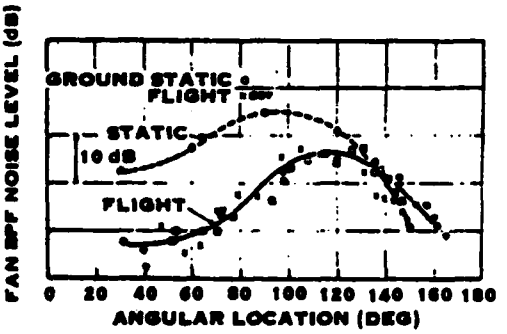

FIGURE 4-21B - FAN BPF VARIATION DURING TAKEOFF

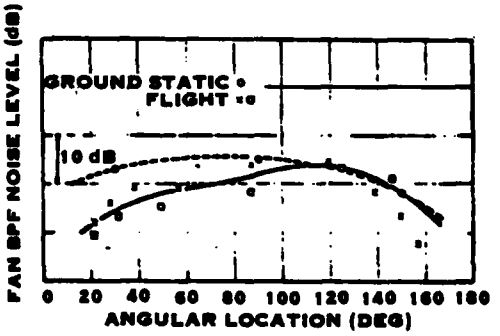

FIGURE 4-21C - FAN BPF VARIATION DURING APPROACH

REPRINTED WITH PERMISSION OF THE SAE FROM TECHNICAL PAPER NO. 730289, "QUIET" ASPECTS OF THE PRATT & WHITNEY AIRCRAFT JT15D TURBOFAN.

FIGURE 4-21. FORWARD FLIGHT EFFECTS FROM DATA BASE ITEM FIXED PITCH FANS - 30.

Data Catalog Item 24. - This report presents in more detail the data already discussed under Data Catalog Items 5 and 27. Although the conclusions presented in this work are in general agreement with those presented in the earlier works, the additional analysis has led to additional conclusions. With respect to this discussion, it was concluded that: 1) the static-to-flight differences for the DC-9-30/JT8D-109 airplane are due to wing shielding, wake sound scattering, and convective amplification (primarily for jet noise), 2) the correlation between static-projected and flight high frequency noise can be improved if excess attenuation in the atmosphere is taken into account, 3) the static-to-flight differences in fan noise are due primarily to differences in noise generation of the fan fundamental tone, 4) measurements suggest that fan higher harmonic and broadband noise are the same at static and flight conditions.

Data Catalog Item 20. - This report presents static and flyover noise measurements made in a JT8D-9 engine. Representative results are shown in figures 4-22 and 4-23. Figure 4-22 shows the comparison between flight and static tone noise levels for the approach condition. In contrast to the data presented previously, these data show large reductions in the flight noise levels compared to the static noise levels. These differences exist over all directivity angles. Figure 4-23 shows the comparison for high frequency broadband noise. The high frequency broadband noise is seen to show small differences between static and flight at 2000 and 4000 Hz and large differences at 6000 Hz.

Although the report does not identify the cause for the high level of noise under static conditions, several effects are mentioned, including high static inlet turbulence intensity due to ingestion of atmospheric turbulence, flow separation inside the inlet, and ingestion of wakes from obstructions around the inlet. Ingestion of ground vortices, shielding of wings and fuselage, and scattering of sound as it passes through wing and landing gear wakes are also possible culprits.

It is thus concluded that the extremely large forward-flight effects presented in this report are due mostly to installation effects, including test facility and ground plane interference effects on the static data, and not due to the changes in the noise generating mechanisms which are accounted for in the current noise prediction methodology.

Data Catalog Item 6. - This report presents results of noise measurements made on a JT8D-17 engine tested in a large wind tunnel. The data acquired in the wind tunnel are compared to data acquired statically on an outdoor test stand, in flight on a B727 airplane, and in a smaller wind tunnel.

The comparison relevant to fan noise forward-flight effects was made for fan inlet noise measured statically on the outdoor test stand and at several tunnel speeds in the wind tunnel. On an average, sound power level (PWL) noise reductions of 8 dB at the first stage fan fundamental tone, 3 dB at the second harmonic, and 1.5 dB at the third harmonic were noted between the wind tunnel data and the outdoor static data. These reductions were observed even at the lowest tunnel speed of 49 ft/sec.

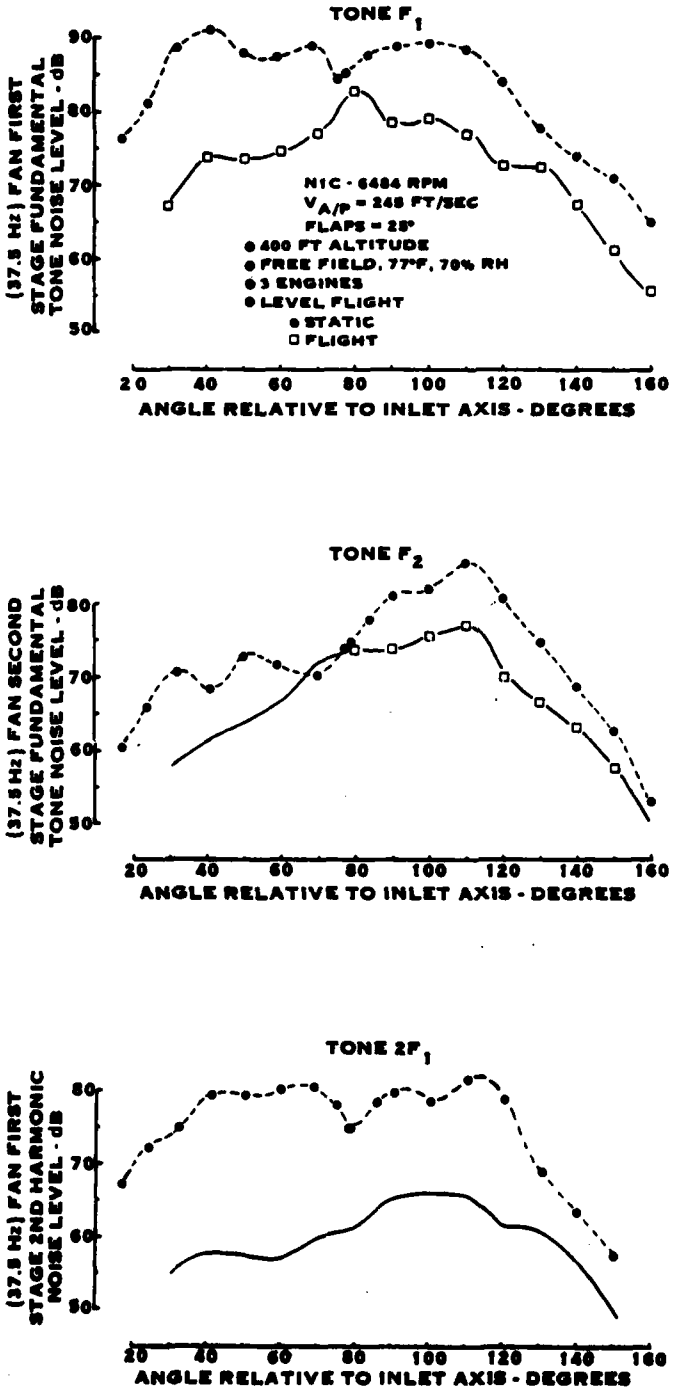

FIGURE 4-22. FORWARD FLIGHT EFFECTS ON FAN TONE NOISE FROM DATA BASE ITEM FIXED PITCH FANS - 20

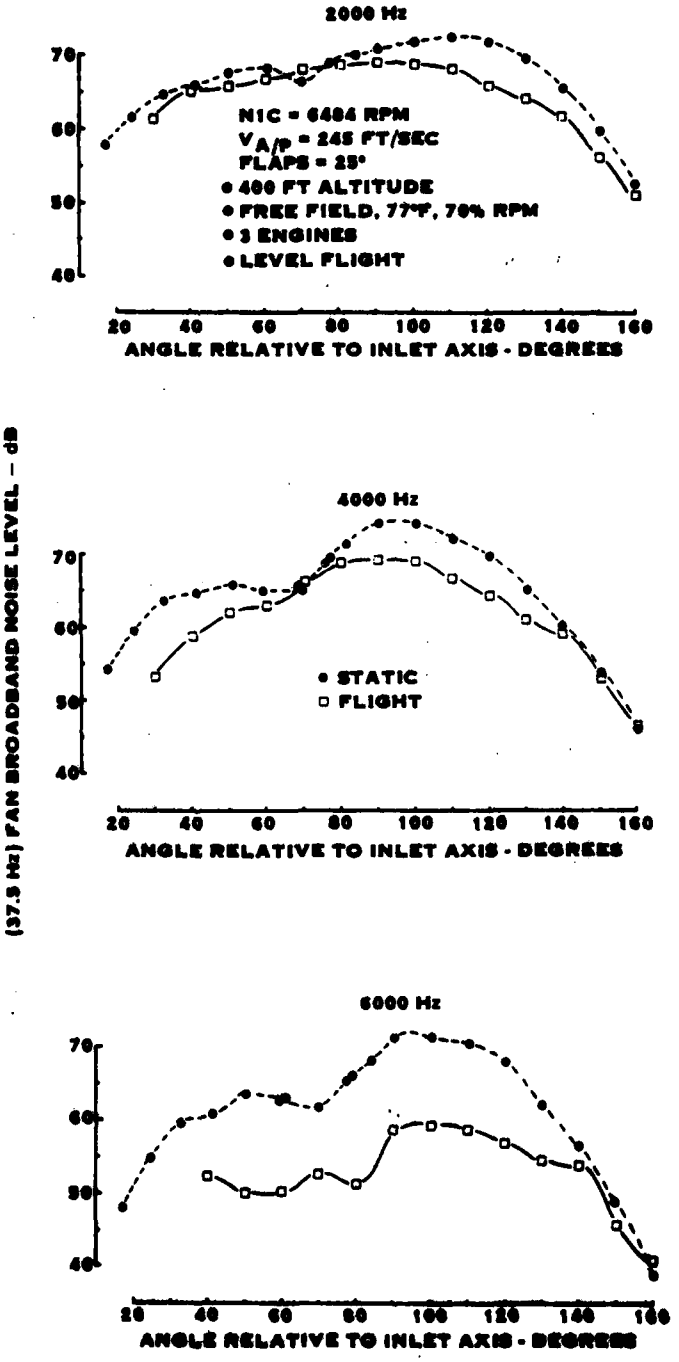

FIGURE 4-21. FORWARD FLIGHT EFFECTS ON HIGH FREQUENCY BROADBAND NOISE FROM DATA BASE ITEM FIXED PITCH FANS - 20.

For an engine with IGV's, the effects on fan noise of inlet "cleanup" due to reduction of inflow distortion was believed to be of secondary importance. The major fan noise source was thought to be IGV/rotor interaction (the JT8D has propagating tones at all operating conditions). The possible explanations for the wind tunnel results noted in this report include: 1) large forward velocity is not required to achieve the static-to-flight fan tone noise reductions, 2) tunnel turbulence is less severe than that in the atmosphere, 3) the ground vortex is more of a significant contributor to the tone noise than the ingested turbulent eddies and is minimized with low forward speed, and 4) combination of any or all of the preceeding.

It should be noted that the lowest tunnel speed was 49 ft/sec, which is high enough to greatly reduce the inflow contraction ratio. Thus, it should not be suprising that the effect identified in 1 above occurs. Also, a speed of 49 ft/sec is probably high enough to prevent ground vortices from being ingested by the fan. Thus, ground vortices in the static test data, as mentioned in 3 above, is a likely strong contributor to the high levels of static fan tone noise reported herein and in Data Catalog Item 20.

Summary of Fixed-Pitch Fan Forward-Flight Effects. - In reviewing these data, the most consistent forward flight effect can be summarized as follows: for fans without IGV's operating at approach power (with the fundamental fan tone cut-off), the in-flight levels of the fundamental fan tone are about 8 dB lower than the static levels; for higher harmonics, all tones of fans with IGV's, and fan broadband noise the forward-flight effects are negligible. Other effects noted include installation effects, fuselage and wing shielding, ingestion of ground vortices, scattering due to wakes from wings and landing gear, and excess atmospheric attenuation. As these effects are not part of the current methodology which is being reviewed, they cannot be included as valid effects.

Dynamic amplification effects on source noise were shown to improve correlations between flight and static-projected mid-frequency fan noise. However, the effect is small and many other adjustments having greater effects were also used to improve the correlations. This effect appears to be more relevant to jet noise than to fan noise.

The current forward-flight effects on fan noise include a fundamental fan tone level reduction of up to 8.1 dB and a second harmonic level reduction of up to 2.7 dB. These are applied to fans without IGV's and the maximum values decrease linearly with fan relative tip Mach number from 0.7 to 1 and increase with airspeed from 0 to the maximum value over the range 10 to 80 kts.

It is thus concluded that the current forward-flight effects are generally representative of the current data on fan noise, if installation effects are removed from the data. Thus, revisions to the methodology are not presently justified.

Helicopter Rotors

The forward-flight effects included in the methodology are only those associated with changes in input parameters, the most notable being the reduction in main rotor input power during transition from hover to low forward speed. Also, in typical operation the tail rotor is unloaded during flight, so that tail rotor noise will be shown to decrease in flight. Two effects which will be shown to occur under actual tests, but which are not accounted for in the methodology, are the increase of rotor impulsive noise (blade slap or banging) with increasing flight speed and the changes in installation effects, including rotor/airframe and rotor/rotor interaction. Impulsive noise generally does not occur in modern helicopter designs during hover and level flight. Thus, formulations of impulsive noise, which are not readily implemented in a simple fashion (i.e., impulsive noise is dependent on parameters such as airfoil geometry, angle of attack, and relative velocities which are not usually readily available to the preliminary design user), were not included in the original methodology on the basis of it being a limited special case. Installation effects were not included for reasons already mentioned in earlier sections.

In contrast to the forward-flight effects on fixed-pitch fan noise, for example, where the effects resulted in reductions of tone noise levels or fan inlet broadband noise levels which were essentially independent of absolute level, the forward-flight effects on helicopter noise are conjectured to be a result of changes in input information and are thus functions of absolute inputs. Also, the noise from helicopters includes contributions from many sources, such as main rotor, tail rotor, and engines, which are not always readily separated in the measured noise. Thus, it is feasible to evaluate forward-flight effects on helicopter noise by comparing measured static vs. flight and calculated static vs. flight noise levels as was done for free-air propellers.

The data presented in the reports were acquired with micorphones located typically 4 ft. above the ground plane. This presents a problem in interpretation of the low frequency tones, as the ground reflection effects produce numerous reinforcements and cancellations. For tones, the cancellation effect can be very sharp and quite sensitive to wavelength; a change of a few percent in wavelength can result in a significant change in the observed tone level. Attempts made to correct the test data for ground reflection effects have generally not been very successful. This will be described in more detail during the description of the methodology evaluation. For the evaluation of forward-flight effects, since both hover and in-flight data were obtained with generally the same microphone height, it was assumed that the ground reflection effects were the same in the comparison of hover and in-flight data.

Data Catalog Item 3, Bell 212. - This data was acquired during helicopter hover and flyover at 60, 99, 110, and 114 kts. flight speed. Although this helicopter exhibits strong blade slap in the forward direction, below and behind it has a normal noise signature. Thus, the comparison made here is for a position directly overhead. Figure 4-24 shows the comparison between measured and calculated levels, hover-minus-flight, for the 60 kts. flyover case. As may be seen from this comparison,

the data shows a reduction in flight noise of up to 12 dB in the mid frequencies, whereas the calculations show a maximum reduction of 1.2 dB. Examination of the calculations show that the dominant noise source is the main rotor, both statically and in-flight. The noise reduction occurs because the power input to the rotor is decreased in flight. The calculated reduction in noise is small, since the rotor thrust and tip speeds are held constant. The test hover-minus-flight noise level differences cannot be explained easily from the available data; e.g., it is not possible to determine if the high levels of mid-frequency noise during hover are due to tones or broadband or whether they originate from the main rotor, tail rotor, or engines. It is stated in the report that the subjective quality of the noise as the helicopter passed overhead was like that of a propeller, indicating that a dominant source was the tail rotor. The calculations, however, place the tail rotor noise levels about 20 dB below those of the main rotor. This is reasonable, as the two have similar tip speeds and the tail rotor operates at about one-tenth the power input of the main rotor. Directivity effects cannot explain high levels of tail rotor noise, since for a rotor in hover, the ingestion of atmospheric tubulence leads to unsteady loading noise which peaks on the axis of rotation, as does the broadband noise. Thus, when the helicopter is directly overhead in hover, the observer is at the main rotor directivity peak and off the tail rotor directivity peak.

The reason for the high levels of tail rotor noise is not obvious from the available data. One possibility is installation effects. Since the tail rotor is mounted on the side of the verical tail, its inflow (or wash, depending on the thrust direction) is blocked by the vertical tail. During flight, the tail provides much of the anti-torque thrust so that the tail rotor is unloaded and also the inflow is much different. This is an installation effect, and is not accounted for in the methodology under evaluation. At this point, this explanation is conjecture and although supported by the available data cannot be proved. To establish the cause of the high levels of mid-frequency noise, narrow-band analyses of data acquired with a ground level microphone (to minimize unknown ground reflection effects) are required to identify the spectral components in the noise. The extensive literature review conducted as part of the present contract indicates that this type of data does not exist in the open literature.

Figure 4-25 shows the calculated flight effects for increased flight speed obtained by comparing the levels at 110 kts. to those at 60 kts. The measurements show an average increase of about 5 dB in the 110 kt. data compared to that at 60 kts. The calculations show an increase of about 1 dB at low frequencies and a slight decrease in level at the mid and high frequencies. Again, it is not clear which noise source is dominant in the data. The calculated noise is dominated by the main rotor, with the tail rotor noise calculated to be about 20 dB below that of the main rotor and the engine noise about 10 dB below that of the main rotor. The calculated main rotor noise at frequencies below about 250 Hz is due to rotational noise, while that above this frequency is due to broadband noise. The calculated change in rotational noise is adequately explained by the necessary increase in main rotor input power as it comes out of the minimum torque region. The broadband noise does not change.

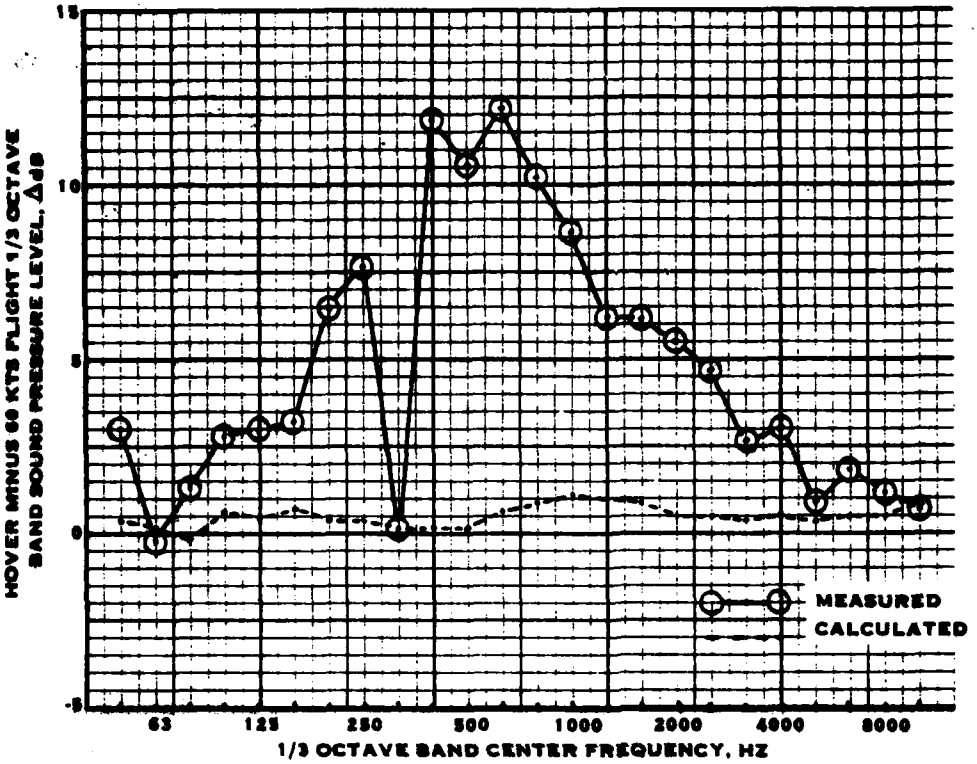

FIGURE 4-24. COMPARISON OF MEASURED AND CALCULATED HOVER-MINUS-FLIGHT NOISE LEVELS AT 60 KTS FOR THE BELL 212

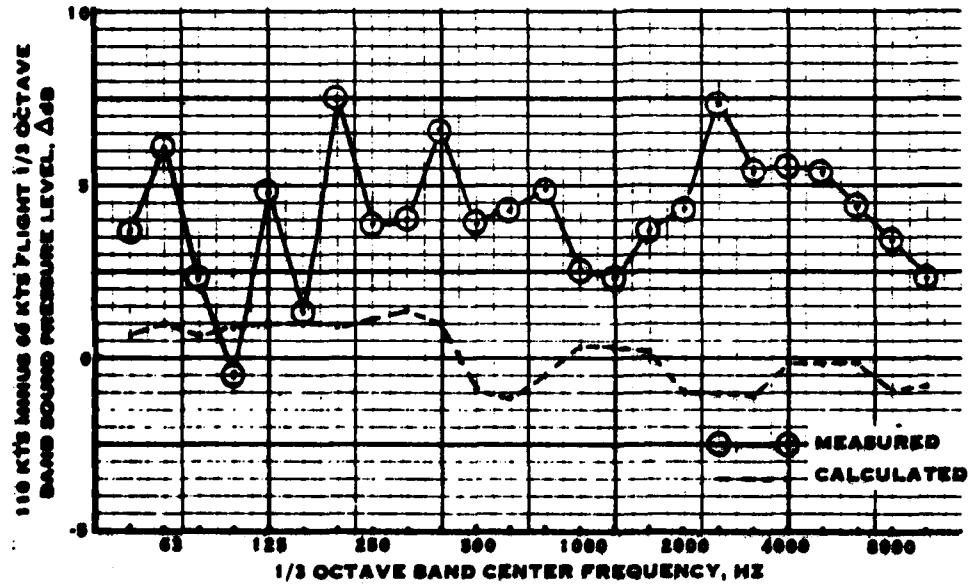

FIGURE 4-25. COMPARISON OF MEASURED AND CALCULATED 110 KTS - MINUS - 60 KTS FLIGHT NOISE LEVELS FOR THE BELL 212

The data presented for this helicopter shows strong forward-flight effects which cannot be matched by the noise calculation methodology. Although the data is insufficient to confirm the cause of the large change in mid-frequency noise between static and flight, it is conjectured that it is due to abnormally high levels of tail rotor noise caused by installation effects.

Data Catalog Item 3, Sikorsky S-61. - The summary of calculated vs. measured forward-flight effects on the noise for the Sikorsky S-61 helicopter is presented in figure 4-26. As this figure shows, the results are similar to those already discussed for the Bell 212 helicopter.

Data Catalog Item 3, Sikorsky S-64. - The comparison of calculated and measured hover-minus-60 kts. flight noise levels for the Sikorsky S-64 helicopter is summarized in figure 4-27. Again, this comparison shows measured flight levels which are significantly lower than the static levels whereas the calculations show only a modest reduction in level.

Data Catalog Item 7. - This report presents noise measurements made on a standard and modified Sikorsky SH-3A helicopter. As the standard SH-3A helicopter is the military designation of the S-61 helicopter, this data can be used for comparison to that given in Data Catalog Item 3. This report gives limited hover noise data, but includes many one-third octave band analyses of flyover noise at 40, 70, 100, and 120 kts. These also extend to the 10 Hz band, so that the main rotor fundamental can be identified.

Figure 4-28 shows the relative levels measured at the maximum noise point during flyovers at nominal altitudes of 200 ft for flight speeds of 40, 69, 98, and 120 kts. The levels shown in this figure were adjusted for variations in actual source to microphone distance. It is apparent that the main rotor tones, in the 16-20 Hz and 32-40 Hz bands, do not change appreciably in level over the flight speed range. The third and fourth harmonics cannot be seen, as they are in the 50 and 63 Hz bands which appear to be strongly influenced by the first ground dip due to the 4 ft. microphone height. Greater variations are seen in the levels of the 100-125 Hz, 200-250 Hz bands, and above. These are clearly due to tail rotor tones (fundamental blade passing frequency of 104 Hz), which appear to dominate the mid-frequencies. Figure 4-29 shows a narrow-band frequency analysis of the noise of the helicopter during a 10 ft. hover. The tail rotor harmonics are clearly evident and dominate the spectrum. It might also be noted that at this low altitude, the helicopter is in ground effect and thus the main rotor is reingesting wakes which are recirculated by the ground plane and would be expected to make more noise than when the helicopter is at a greater distance from the ground. It is thus apparent from this data that the predominant noise source in the mid-frequencies is the tail rotor, as was also documented in the test report which stated that the modified helicopter was quieter than the standard helicopter mainly due to tail-rotor noise reductions. Forward-flight effects on the noise from this helicopter, which are in general agreement with those measured on the S-61 and reported in Data Catalog Item 3, show a variation in mid-to-high-frequency noise which is believed to

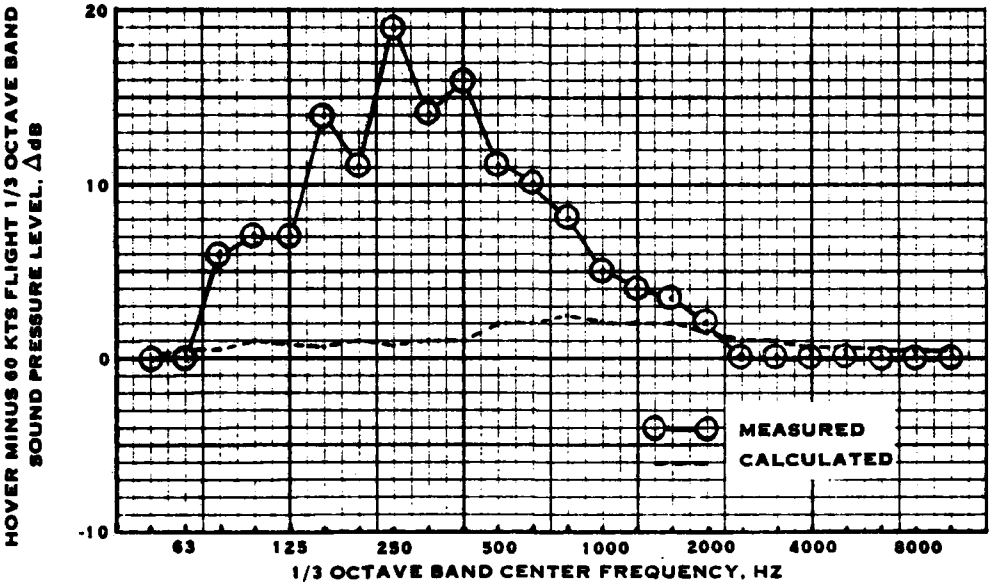

FIGURE 4-26. COMPARISON OF MEASURED AND CALCULATED HOVER-MINUS-FLIGHT NOISE LEVELS AT 60 KTS FOR THE SIKORSKY S-61

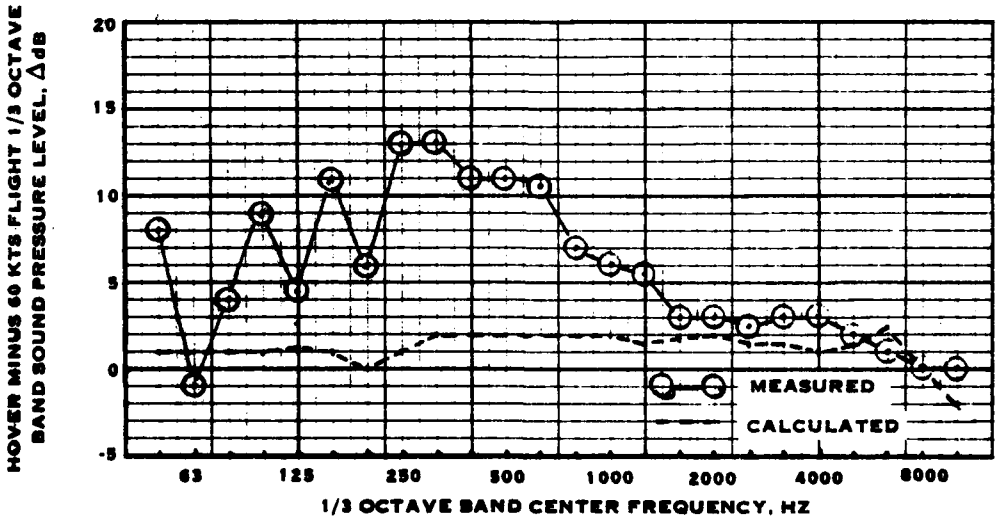

FIGURE 4-27. COMPARISON OF MEASURED AND CALCULATED HOVER-MINUS-FLIGHT NOISE LEVELS AT 60 KTS FOR THE SIKORSKY S-64

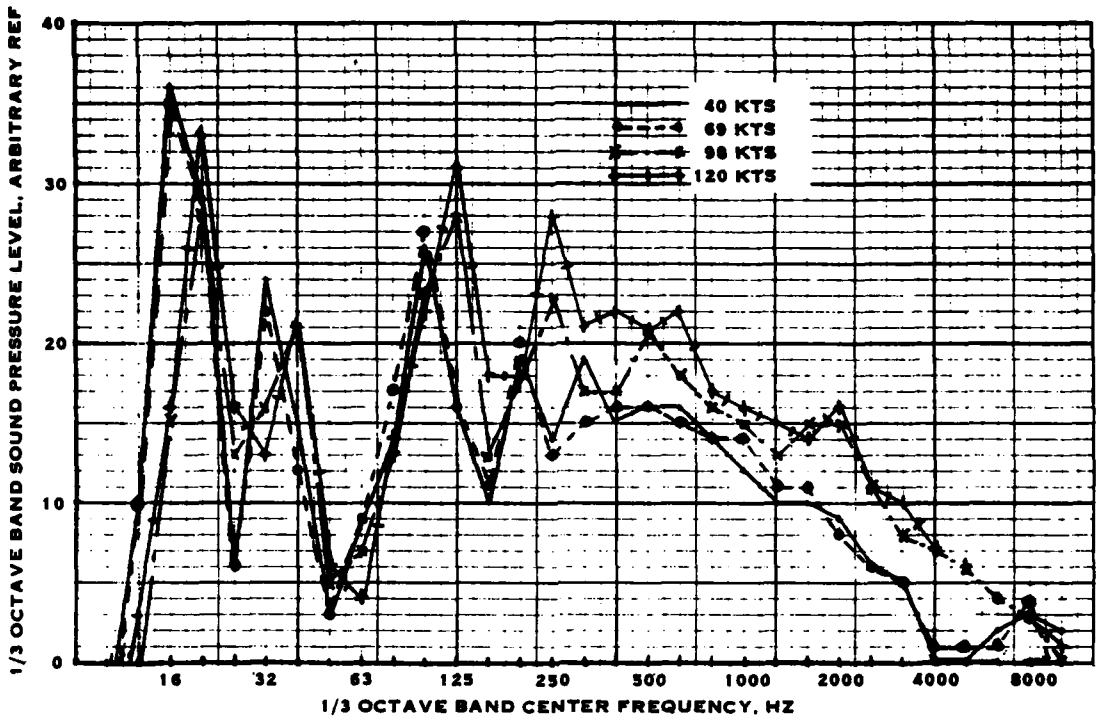

FIGURE 4-28. MEASURED FORWARD FLIGHT EFFECTS ON THE SIKORSKY SH-3A HELICOPTER FROM DATA BASE ITEM HELICOPTER -7

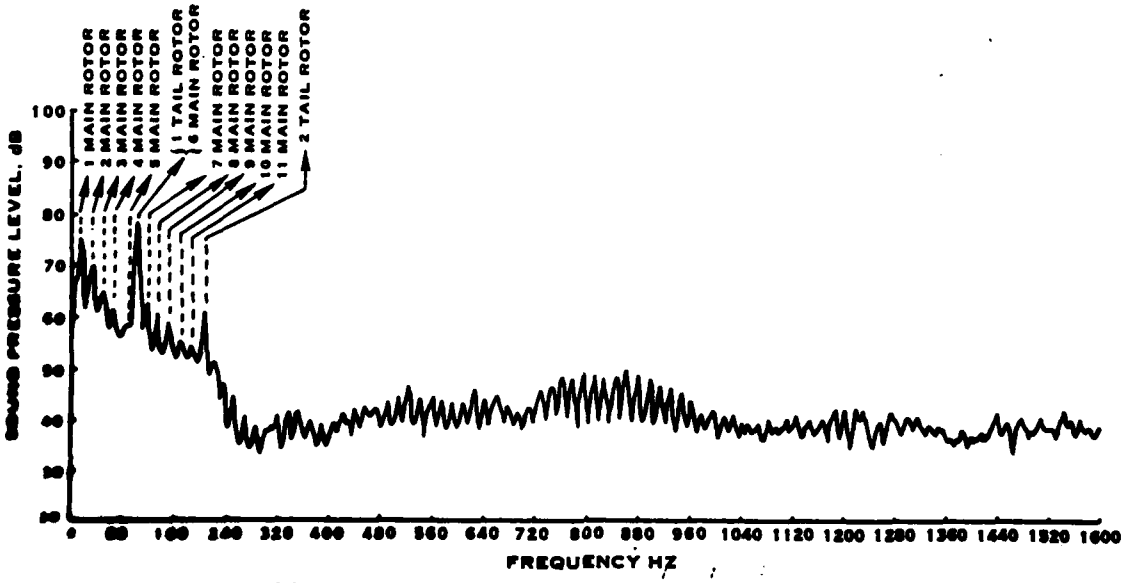

FIGURE 4-29 NARROW BAND SPECTRUM OF THE SH-3A HELICOPTER IN HOVER AT 10 FT ABOVE GROUND PLANE

be caused by tail rotor noise. The high levels of tail rotor noise are believed to be due to installation effects. Thus, for this configuration at least, forward-flight effects on total helicopter noise are governed by the effects on tail rotor noise which are, in turn, due to installation effects. It may be concluded that the measured change in noise with forward flight reflect forward-flight effects on installation effects, rather than on source noise.

Data Catalog Item 6. - This data was acquired on a Kaman HH-43B helicopter which is of particular interest here for comparison with the results discussed for the Bell 212, Sikorsky S-61, and Sikorsky S-64 helicopter as this helicopter does not have a tail rotor. This helicopter has two counter-rotating main rotors, as shown in figure 4-30. The data in this report consists of only full-octave band analyses and does not contain any hover data except for overall noise levels. However, comparisons of noise levels for 60 and 72 kts. relative to noise levels at 43 kts. are shown in figure 4-31 for both measurements and calculations. As may be seen, the measured data show a small effect which is also shown by the calculations. The calculations indicate that the dominant noise source is the rotor with little contribution from the engines.

The overall levels for this helicopter were measured to be 93.8, 92.0, 92.8, and 93.1 dB for hover, 43 kts., 60 kts., and 72 kts., respectively. This confirms that in the absence of installation effects, helicopter rotor noise is not significantly influenced by forward flight.

Data From Reference 6. - This unpublished data was acquired from Kaman Aerospace Corporation in pursuit of the interesting results from Data Catalog Item 6. This data includes measurements made at 200 ft. for the helicopter in hover at 50 ft. and in flyby at 250 ft. to the side of a 50 ft. altitude 80 kts. flight. Figure 4-32 shows the comparison between measured and calculated hover-minus-flight levels for the HH-43B at hover and 80 kts. flight. As may be seen, the agreement is good over the entire frequency range, the greatest discrepancy being 9 dB measured vs. 3.1 dB calculated, i.e., less than 6 dB difference. At all other octave bands but one, the agreement is within 3 dB. This is in sharp contrast to the results for the S-61 and S-64 helicopter which showed discrepancies of up to 18 dB between measured and calculated forward-flight effects.

Summary of Forward-Flight Effects on Helicopter Noise. - Based on the data discussed above, it appears that conventional helicopters (with a main rotor and a tail rotor) show a significant reduction in mid-to-high frequency noise in the transition from hover to low-speed flight then a moderate increase in mid-to-high frequency noise from low- to high-speed flight. Although the evidence from the literature is by no means conclusive, it is apparent that the major change in helicopter noise levels with flight speed is due to changes in tail rotor noise with little effect on main rotor noise. Due to general similarities in tip speed and number of blades between main and tail rotors but much lower power input to the tail rotor, the isolated tail rotor noise would be expected to be about 20 dB lower in level than that of the main rotor, including source directivity effects. The higher-than-anticipated measured levels of tail rotor noise

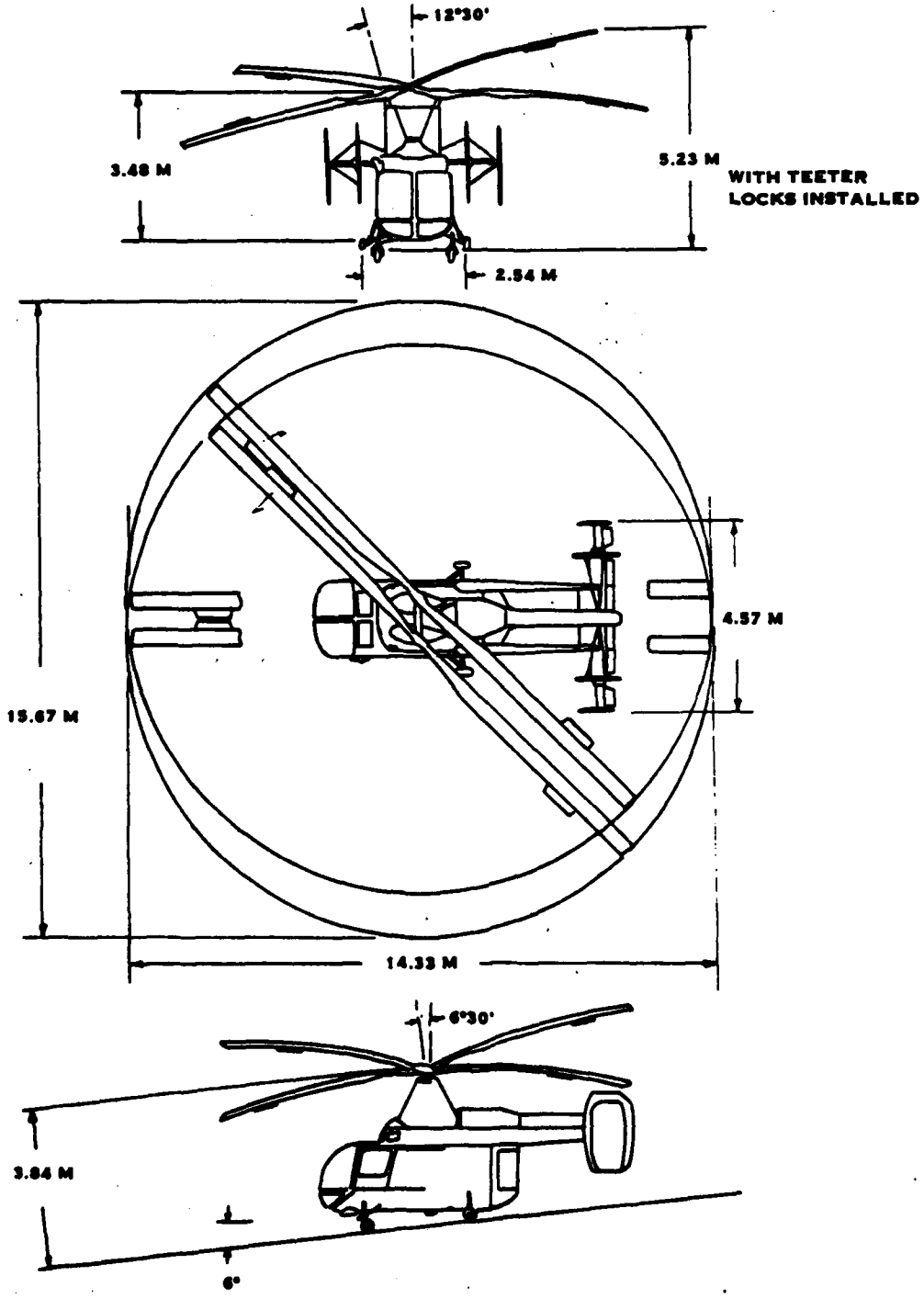

FIGURE 4-30. THREE-VIEW DRAWING OF STANDARD CONFIGURATION OF THE HH-43B TURBINE HELICOPTER.

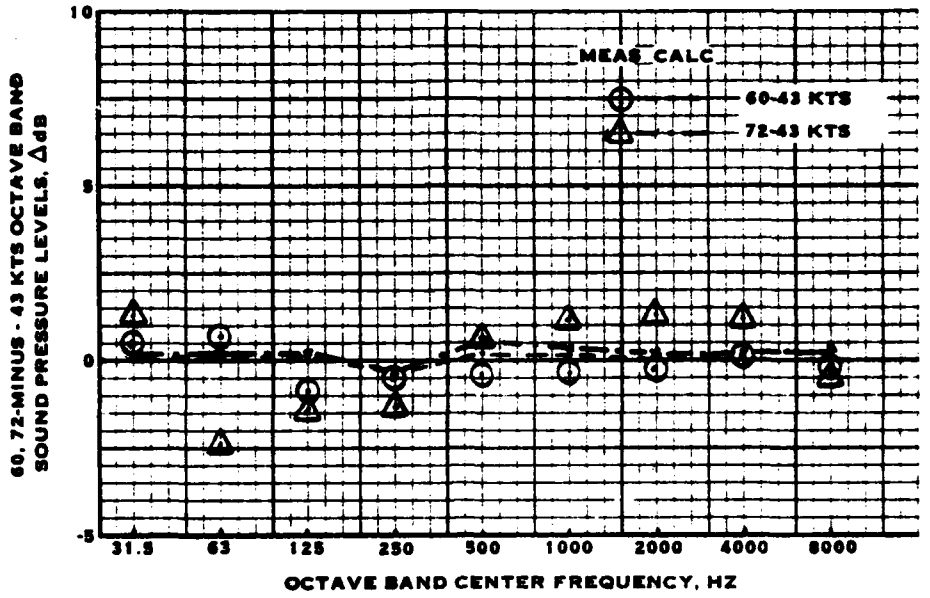

FIGURE 4-31. COMPARISON OF MEASURED AND CALCULATED 60 AND 72 KTS MINUS 43 KTS FLIGHT NOISE LEVELS FOR THE HH-43B

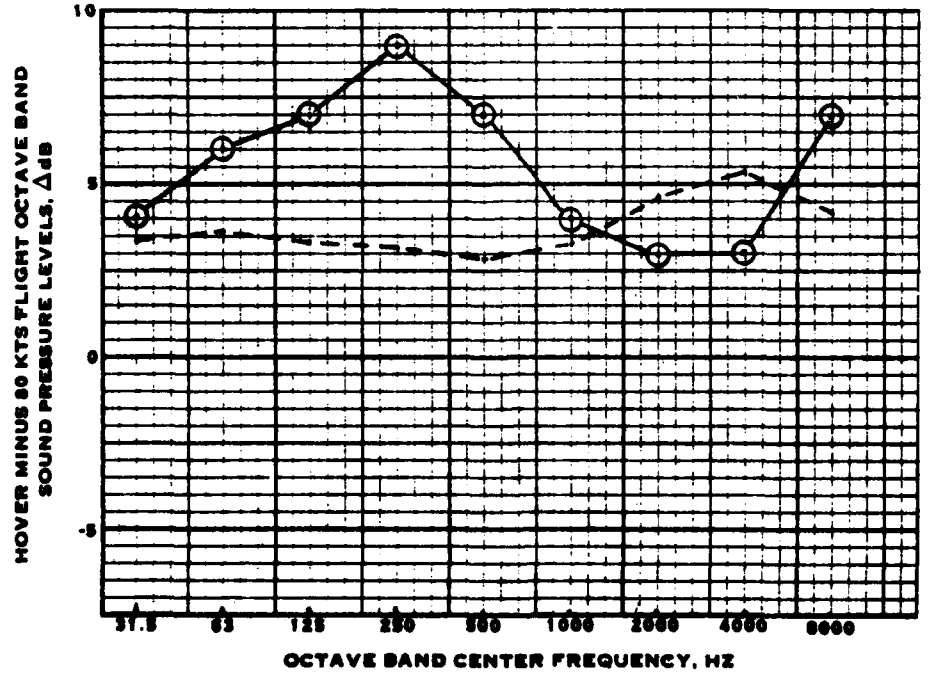

FIGURE 4-32. COMPARISON OF MEASURED AND CALCULATED HOVER-MINUS-FLIGHT NOISE LEVELS FOR THE HH-43B

are believed due to installation effects, in which the inflow to the tail rotor is severly distorted by the vertical tail. Measured noise levels of helicopters having no tail rotors do not show a significant change in noise with forward velocity changes.

The forward-flight effects observed for the configuration without a tail rotor are well predicted by the current methodology. It is thus concluded that the existing methodology adequately predicts forward-flight effects on main rotor noise. Overall helicopter noise levels for the hover case are not adequately predicted by the existing methodology because severe installation effects cause a very significant increase in the noise generated by tail rotors. These installation effects are influenced by flight speed and result in the observed changes in total helicopter noise due to forward-flight. It is beyond the scope of this program to devise and incorporate installation effects on source noise. Thus, the forward-flight effects on helicopter rotors in the absence of installation effects calculated by the current methodology are adequate and do not require revisions.

It is also concluded that the data which were available are not sufficient to identify the installation effects problem and to define the effects of forward-flight on component noise levels. This was because 1) the data lacked resolution of noise components: all data was presented as one-third or full octave band analyses which do not have sufficient frequency resolution, particularly at higher frequencies, to separate main rotor and tail rotor components, and 2) all data were acquired with microphones located at 4 to 5 ft. above the ground plane, where ground reflection effects cause reinforcements and cancellations which make the interpretation of low frequency tonal data extremely difficult. In order to identify the relative contributions from the several noise sources on a helicopter (main rotor, tail rotor, engines, gearboxes) and how they are influenced by flight, narrow-band frequency analyses of noise signatures acquired with a microphone located at ground level are required.

Tilt-Propellers and Lift-Fans

New data on cross-flow effects on tilt-propellers and lift-fans have not been identified in the literature search conducted under this study. Thus, the cross-flow effects which were developed for the methodology of reference 1 are representative of the current empirical procedures for calculating the change in noise due to non-normal inflow.

Jets

The forward-flight effects on the noise produced by jets are a reduction in overall level due to the reduction in relative velocity. The commonly used relationship between the level of jet noise under static and flight conditions is:

$$OASPL_S - OASPL_F = 10 \log_{10}\left[\left(\frac{V_j}{V_j - V_o}\right)^m \left(1 - M_a \cos\theta\right)\right]$$

where OASPL$_S$ and OASPL$_F$ are the jet noise overall levels at static and flight conditions, respectively, V_j is the absolute jet velocity, V_o is the flight velocity, m is the relative velocity exponent, M_a is the flight Mach number, and θ is the angle of noise radiation. Previous studies have derived values of m which are a function of the angle θ. In the current methodology, the values of m from Bushell (reference 7) are used. These values were empirically derived from jet noise measurements made on several engines. These gave values of m from about -2.5 at 30 degrees to about 8 at 160 degrees. It should be noted that a positive value of m results in a reduction in noise from static to flight, while a negative value results in an increase in noise.

Bushell's forward-flight correction was a first-cut procedure at the time when the original V/STOL Noise Prediction Procedure was developed. Since then, additional data have been examined and other forward-flight effects calculation procedures have been derived. It has also been pointed out that m (since it is based on measurements) is sensitive to other sources of low frequency noise (i.e., from core engine internal sources) which are included in real engine noise data. It is thus important to remove the contributions from these other sources to obtain a valid derivation of the exponent for pure jet-mixing noise.

The following reports were reviewed specifically to extract updated computed values of the exponent m and to evaluate other formulations of forward-flight effects on jet noise.

Data Catalog Item 4. - Relative to this study, the highlight of this report is a comprehensive formulation of forward-flight effects on jet-mixing noise. This includes three terms: one for the effects on source strength of forward flight on the external flow field, a second term for dynamic effects due to the change in the velocity of the source relative to that of the ambient air, and a third term for kinematic effects due to the motion of the source relative to the observer. Although this formulation of forward-flight effects is more complete than that currently used in the methodology under evaluation, it is relatively complicated and not readily adaptable to a graphical procedure. Also, these various effects are to a large extent implicit in the current approaches, provided the data used to obtain the exponent m is relatively pure jet-mixing noise.

Data Catalog Fixed-Pitch Fan Item 24. - In addition to the data on fan noise previously discussed, this report presents data on jet noise from the JT8D-109 and JT9D-59A engines and includes derived flight effects. In this report, the jet noise was separated from core noise components. Derivations of the flight velocity exponent m are shown in figure 4-33 for the JT8D-109 and in figure 4-34 for the JT9D-59A. Figure 4-33 shows an exponent varying from about 3.5 in the forward quadrant to about 10 at 150 degrees for the JT8D-109. Figure 4-34 shows the exponents computed from take-off data (open symbols) and approach data (filled symbols) for the JT9D-59A. The ex-

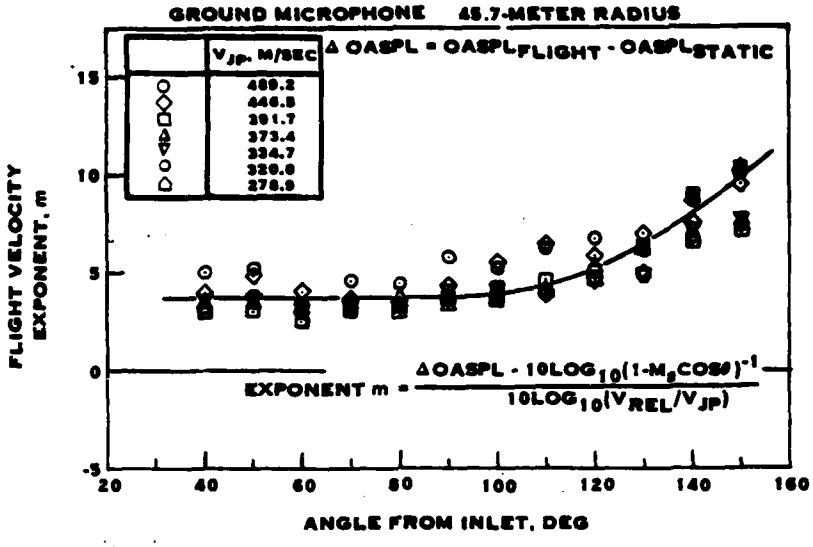

FIGURE 4-33. EFFECT OF CONVECTIVE AMPLIFICATION AND RELATIVE VELOCITY ON DC-9-30/JT8D-109 JET-NOISE FLIGHT VELOCITY EXPONENT

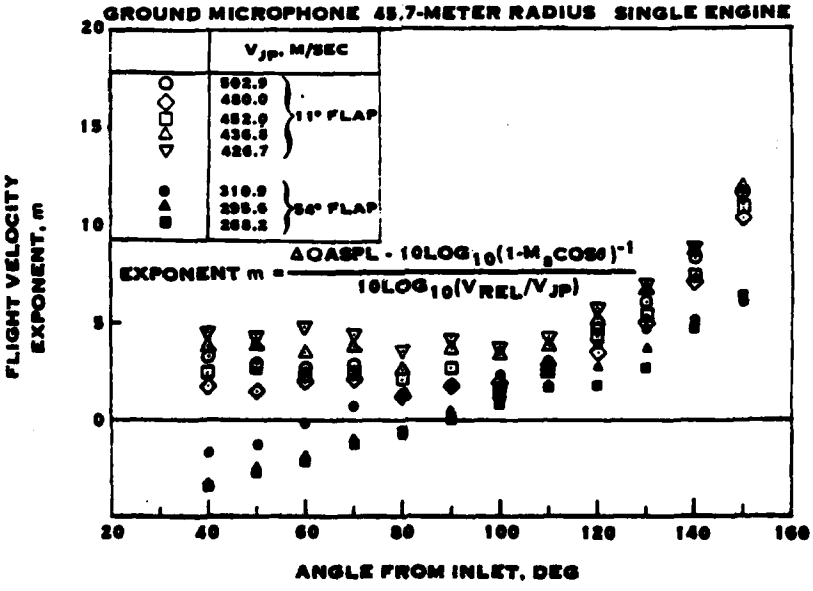

FIGURE 4-34. EFFECT OF CONVECTIVE AMPLIFICATION AND RELATIVE VELOCITY ON DC-10-40/JT9D-59A JET-NOISE FLIGHT VELOCITY EXPONENT

ponents for the take-off data are very similar to those for the JT8D-109 data, but the approach data shows negative values of m in the forward quadrant, indicating that the flight noise data is higher in level than the static noise data. This is attributed to the presence of another low frequency noise source unique to airplane configurations with engines under the wing.

Data Catalog Fixed-Pitch Fan Item 14. - This report presents static and in-flight noise measurements of a DC-9 as part of the JT8D refan program. Figure 4-35 shows a comparison of forward-flight and static data for three jet velocities. At low velocity, the static and flight noise levels in the forward quadrant are essentially the same, indicating that perhaps another low frequency noise source is contributing to the noise. At the two higher velocities, the static data is higher than the flight data at all azimuth angles. The jet noise data for the two highest velocities in figure 4-35 were used to calculate the exponent m, which is shown in figure 4-36. This data is in good agreement with that shown in figures 4-33 and 4-34 and shows only positive values of m.

Data Catalog Item 25. - This data was acquired on single and dual flow model jets in a wind tunnel. The measured jet noise levels at tunnel speeds of 20, 98, and 131 ft/sec were used to derive the flight velocity exponent. These calculations are summarized in figure 4-37. When compared to those calculated previously from real engine data, the model jet data calculations show higher values for m in the front quadrant. This may be due to residual low frequency noise in the real engine data or due to differences between wind tunnel and normal atmosphere environments. Beyond 90 degrees, the agreement among the data is better. It may also be seen that for angles 90 degrees and higher, the flight effects on single and dual jet overall noise levels are essentially the same.

Data Catalog Item 24. - This data was also acquired on model jets in a wind tunnel and show results generally similar to those presented in figure 4-37. Flight velocity exponents of 5.1, 6.0, 6.4, 7.2, and 8.0 are derived from the noise data obtained at 90, 105, 120, 135, and 145 degrees, respectively. It is also suggested that tunnel reverberation effects could contribute about 0.6 to the exponent at 90 degrees, so that a corrected value of 4.5 might be more appropriate. This value is constant over the forward arc.

Data Catalog Item 13. - This paper also presents data from model jets tested in a wind tunnel. In this case, however, the wind tunnel was of the open-jet type. Measurements made on heated jets at several velocities and temperatures showed consistent values for the flight velocity exponent for jet velocities up to 1500 ft/sec over the temperature range 300 to 900 deg. F. A summary correlation is shown in figure 4-38. These data are seen to be in good agreement with the wind tunnel data from Data Catalog Items 24 and 25.

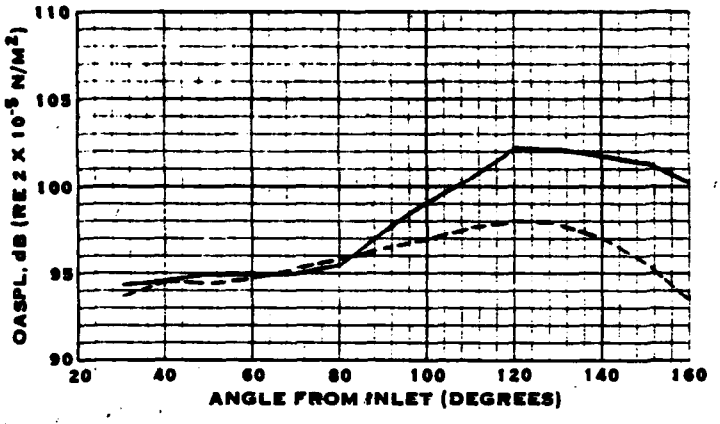

	CONDITION	V_{jp} FT/SEC (M/SEC)
———	STATIC	740 (225.6)
– – – –	FLIGHT	730 (222.5)

- $V_{AIRCRAFT}$ = 235 FT/SEC (71.6 M/SEC)
- FLUSH-MOUNTED GROUND MIC DATA
- 150 FEET (45.7M) POLAR RADIUS
- SINGLE ENGINE

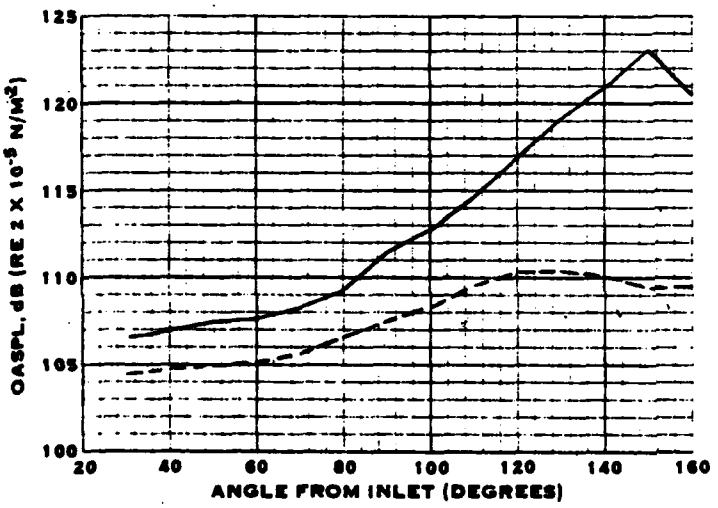

	CONDITION	V_{jp} FT/SEC (M/SEC)
———	STATIC	1310 (399.3)
– – – –	FLIGHT	1308 (398.7)

- $V_{AIRCRAFT}$ = 297 FT/SEC (90.5 M/SEC)
- FLUSH-MOUNTED GROUND MIC DATA
- 150 FEET (46.7M) POLAR RADIUS
- SINGLE ENGINE

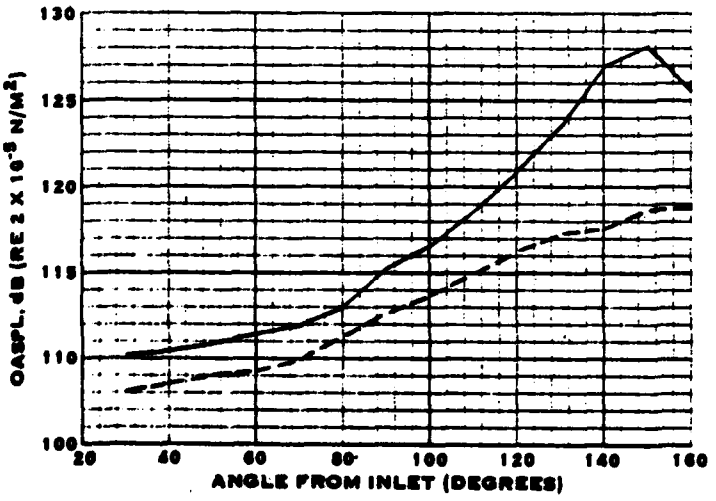

	CONDITION	V_{jp} FT/SEC (M/SEC)
———	STATIC	1530 (466.3)
– – – –	FLIGHT	1600 (487.7)

- $V_{AIRCRAFT}$ = 294 FT/SEC (89.6 M/SEC)
- FLUSH-MOUNTED GROUND MIC DATA
- 150 FEET (45.7M) POLAR RADIUS
- SINGLE ENGINE

FIGURE 4-35. COMPARISON OF STATIC AND FLIGHT LOW FREQUENCY NOISE FROM THE JT8D REFAN PROGRAM

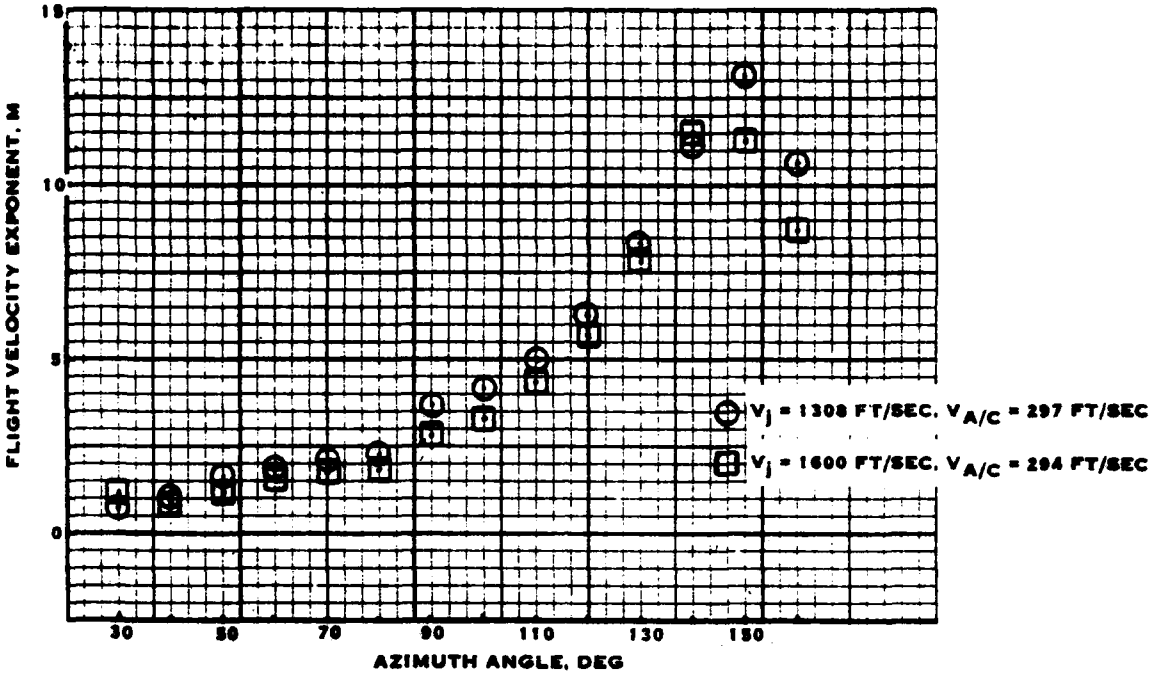

FIGURE 4-36. DERIVED FLIGHT VELOCITY EXPONENT FROM JT8D REFAN PROGRAM DATA.

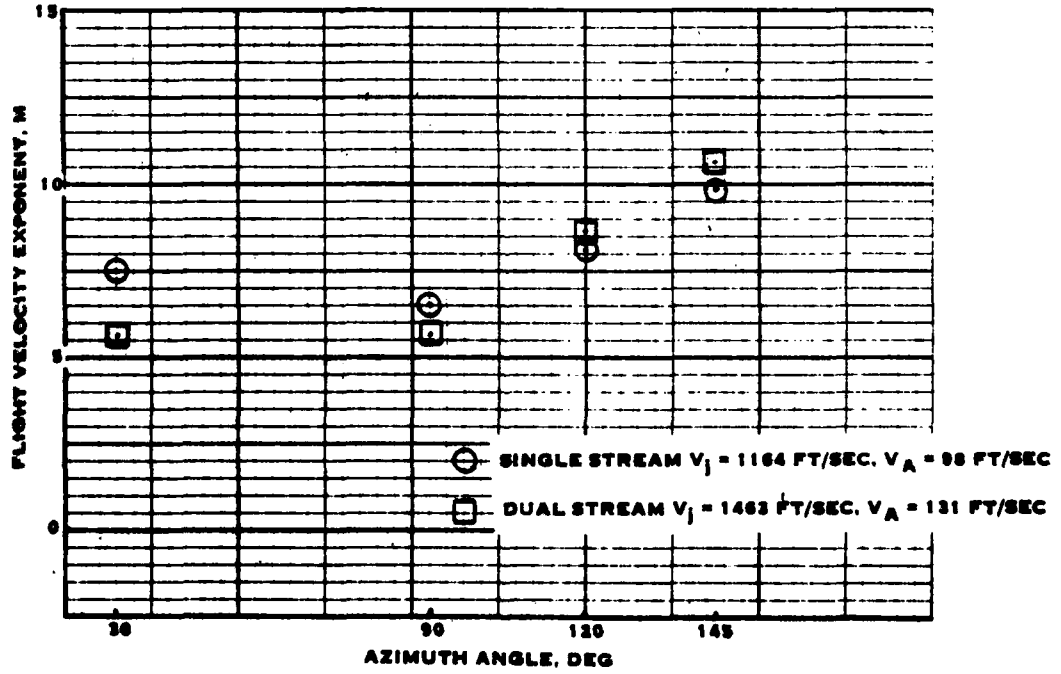

FIGURE 4-37. DERIVED FLIGHT VELOCITY EXPONENT FROM COCKING, DATA BASE ITEM 25

Summary of Forward-Flight Effects on Jet Noise. - The bulk of the literature reviewed indicates that the forward-flight effects on jet noise can be adequately calculated from the relation: $\Delta dB = 10 \log_{10}\left[\left(\frac{V_j}{V_j - V_o}\right)^m \left(1 - M_a \cos\theta\right)\right]$ where m, the flight velocity exponent is a function of the directivity angle θ. Values of m have been derived in more recent studies of test results and are, on the whole, consistent with both real engine data and with data from models in wind tunnels. The current values for m differ from those which were initially proposed by Bushell, particularly in the front quadrant where Bushell's values would show an increase in the noise in flight compared to current values which would show a decrease in noise in flight everywhere. This has been attributed to the early data containing sources of low-frequency noise other than free-jet-mixing noise.

The new values of the exponent m, which are based on the data reviewed above, are shown in figure 4-39 compared to the values which were originally used in the methodology. As may be seen, the new values of m result in reductions in flight noise at all angles, compared to the old values which show an increase in noise at angles forward of 100 degrees. Also, the revised values provide a larger reduction in noise with forward-flight in the aft quadrant than did the former values.

SUMMARY OF FORWARD-FLIGHT EFFECTS EVALUATION

The evaluation of forward-flight effects discussed above are summarized in this section. The conclusions which were reached and changes to the methodology developed in reference 1 are presented. Although the evaluation was directed toward forward-flight effects, certain other conclusions were reached which have an impact on the calculation of absolute noise levels (rather than relative effects such as differences between static and in-flight noise levels). These are mentioned here briefly and described in detail in the section on the evaluation of the noise prediction methodology, including the changes in the resulting methodology.

It was found in the evaluation of forward-flight effects on propeller noise that installation effects produced static noise levels which were higher than those for uninstalled propellers. Further, these installation effects disappear quickly after onset of forward motion. When adjusted to match the levels of static noise for installed propellers, the flight noise levels were overpredicted. When adjusted to match the levels of static noise for uninstalled propellers, the noise levels in flight were well predicted. It also appeared that the core engine noise levels were somewhat overestimated, as correlation of forward-flight effects on broadband noise was better with the mid-to-high-frequency core engine noise omitted. Inclusion of mid-to-high-frequency core engine noise tended to cause overprediction. It was then concluded that with the above adjustments, the forward-flight effects on propeller noise contained in the methodology are adequate.

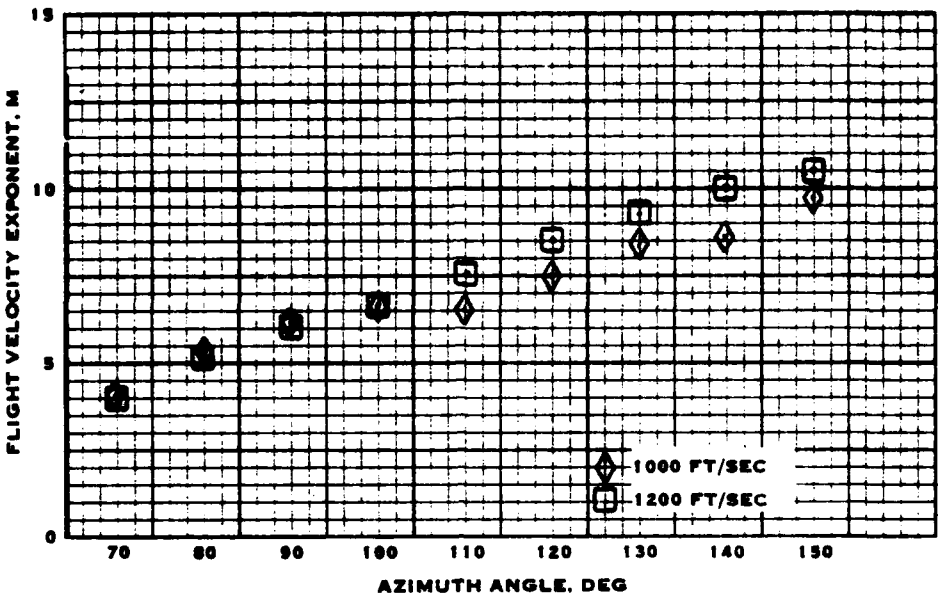

FIGURE 4-38. FLIGHT VELOCITY EXPONENT FROM DATA BASE ITEM 13.

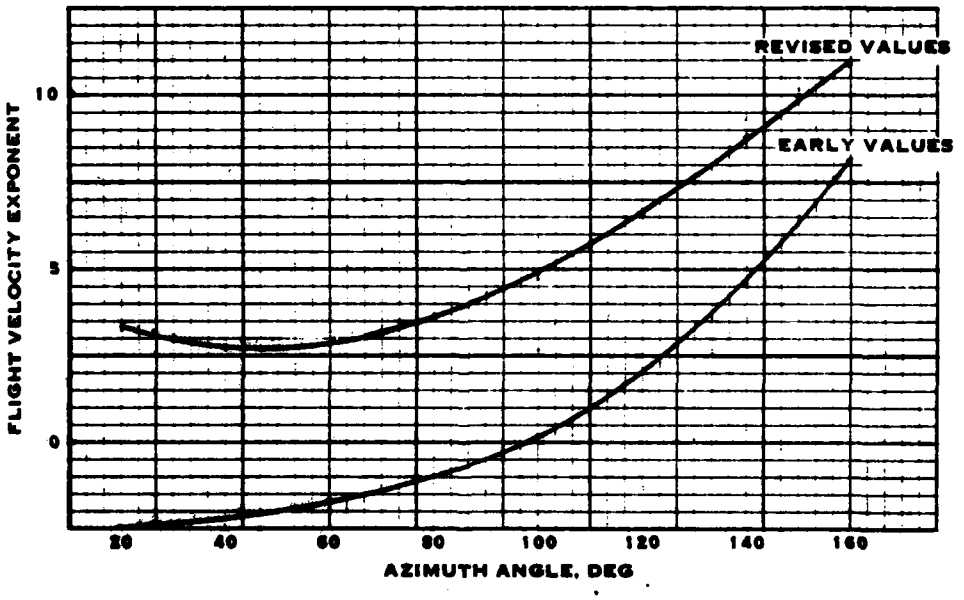

FIGURE 4-39. REVISED VALUES FOR THE FLIGHT VELOCITY EXPONENT COMPARED TO THOSE FORMERLY USED IN JET NOISE PREDICTION

Only limited data was found on forward-flight effects on the noise from variable-pitch fans, and that was for inlet noise of a fan tested in a wind tunnel. Although a wind tunnel does not fully simulate the turbulence environment of the free atmosphere, the general trends in the measurements were well calculated. These included propagation of the fan fundamental tone under static conditions and cut-off under flight conditions.

The calculations also matched the data in that both showed little change in the level of the second harmonic, which is cut-on both statically and in flight, and higher frequencies (both tones and broadband) from static to forward-flight. It was thus concluded that the forward-flight effects in the current methodology for variable-pitch fans are adequate and that revisions based on the currently available data are not justified.

In the area of fixed-pitch fans, it was found again that installation effects play a major role in the observed differences between static and in-flight noise levels. Some data showed strong fundamental tones statically which decreased dramatically in flight, even for fans with IGV's. It was concluded, and can be generally supported in the published literature, that this resulted from the ingestion of vortices originating from the wing, fuselage, and/or ground. Other installation effects included shielding by the wing and fuselage and scattering by the wing/flap/wheel wakes and jet exhaust. Limited data acquired with microphones installed in the fan duct and far-field noise measurements adjusted for convection, shielding, and propagation effects tend to support a significant reduction in the fundamental tone level (up to 8 dB) with little or no change in the levels of the higher harmonics and broadband noise for fans without IGV's operating at subsonic tip speed when static and flight data are compared. As these measured differences agreed within experimental accuracy with the predicted differences from the current methodology, no change in methodology was considered necessary.

Forward-flight effects on helicopters were difficult to establish because of severe installation effects on tail rotor noise and lack of interpretable data to identify the noise sources, whether main rotor, tail rotor, or engine and whether broadband or tone. The difficulty in data interpretation was mainly due to the lack of data acquired with a microphone free from ground reflections and the analyses limited to full and one-third octave bands. It was concluded from the available data that the dominant noise for conventional helicopters was that of the tail rotor. Although the tail rotor operates at substantially the same tip speed and at an order of magnitude lower power input than does the main rotor, its noise level appeared to exceed that of the main rotor, even after accounting for source directivity effects. This was attributed to installation effects due to blockage by the vertical tail. The installation effects appeared to be strongly affected by flight. Data from a helicopter having no tail rotor showed excellent agreement with calculated forward-flight effects. It was thus concluded that the current methodology predicts forward-flight efects on main rotor noise, whereas the effects on tail rotor noise are underpredicted due to installation effects. The dominance of tail rotor noise is supported by the literature. However, verification of this requires data acquired using a ground-level microphone, which is free from ground reflection effects.

No new data on forward-flight effects on tilt-propellers and lift-fans were found. Thus, no evaluation of or revisions to the current methodology were made in this area.

The jet noise forward-flight effects were revised based on more recent real engine and model jet noise measurements. It was concluded that the flight velocity exponent used in the development of the methodology was derived from data which was contaminated by low frequency noise from sources other than free-jet-mixing. The revised values for the exponent show noise reduction at all azimuth angles, compared to former values which produced amplification in the forward quadrant for flight data as compared with noise of static jets.

The above revised forward-flight effects, and others to be described subsequently, have been incorporated into the methodology. This revised methodology was then used for the next phase which is described in the next section.

AD-A082 616 UNITED TECHNOLOGIES CORP WINDSOR LOCKS CONN HAMILTON --ETC F/G 20/1
V/STOL ROTARY PROPULSOR NOISE PREDICTION MODEL UPDATE AND EVALU--ETC(U)
DEC 79 B MAGLIOZZI

UNCLASSIFIED FAA-RD-79-107 NL

2 of 3
AD A082616

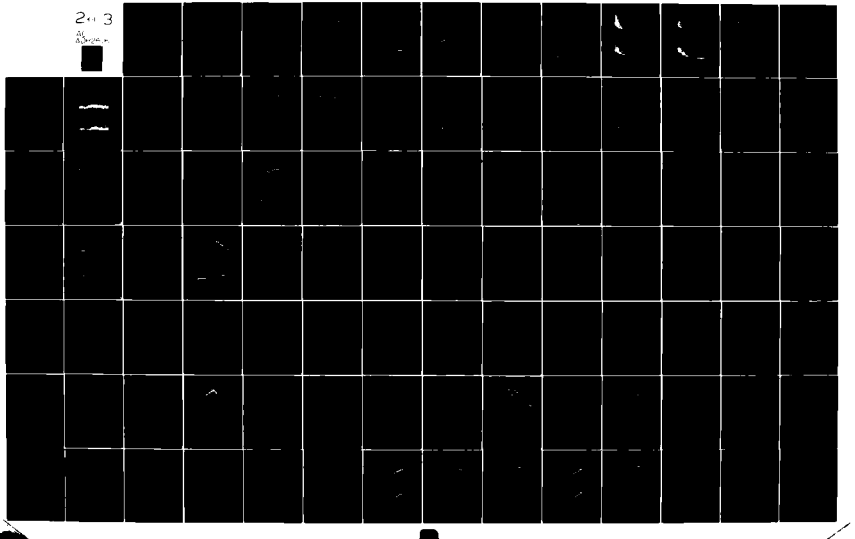

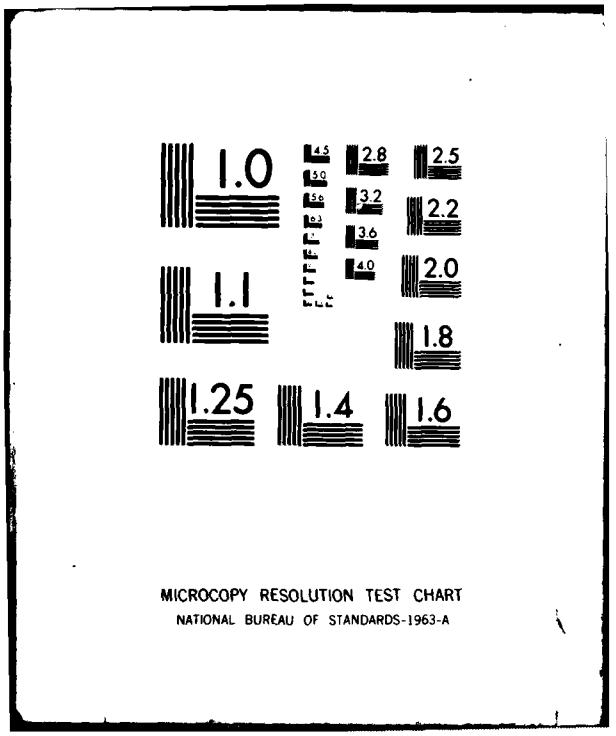
1.0
1.1
1.25
1.4
1.6
1.8
2.0
2.2
2.5
2.8
3.2
3.6
4.0
4.5
5.0
5.6
6.3
MICROCOPY RESOLUTION TEST CHART
NATIONAL BUREAU OF STANDARDS-1963-A

PHASE III - EVALUATION OF V/STOL ROTARY PROPULSOR NOISE PREDICTION METHODOLOGY

INTRODUCTION

As described in the previous section, the forward-flight effects evaluation indicated certain areas where revisions to the methodology were required. These revisions were made prior to the final noise prediction methodology evaluation presented in this section. Thus, the correlations between measurements and calculations presented here represent those which would be obtained using the final revised computer program. They include the revised forward-flight effects, revised adjustments for installation effects which had been included in the orginal formulation (primarily in unsteady loading noise), and corrections of errors in the orginal computer program found during the evaluation.

The empirical data used for the correlations are those identified in table 3-II with certain exceptions. Additional data are presented to emphasize or clarify certain effects, such as the importance of installation effects. Also, some of the data could not be used as the required design and/or operating information for performing the noise calculation was not available. The data actually used will be identified in the appropriate section.

The available data was corrected to the equivalent free-field condition, using the procedures defined in reference 8, where possible. Where the noise was dominated by low frequency tones, corrections for ground reflection effects were generally not successful, especially in the frequency ranges where cancellations were thought to occur. The problem was attributed to uncertainty in the exact direct vs. reflected path length difference (due to uncertainties in source position and microphone height), uncertainty in the exact frequency (including Doppler shift), distributed source, imperfect ground plane, wind shear gradient effects, etc. It is apparent that adjusting the calculations for ground reflection effects rather than correcting the data to equivalent free-field conditions is the better approach. An alternative, of course, is to acquire the data under free-field conditions or with flush microphones, which provide a constant pressure doubling effect.

EVALUATION OF PROPELLER NOISE PREDICTION

Uninstalled Propellers

During the evaluation of forward-flight effects on propeller noise, it was concluded that some of the noise data showed evidence of installation effects. Specifically, the Twin Otter data (reference 2) obtained under static conditions showed high levels of mid-frequency harmonics. These were attributed to the ingestion by the propeller of a vortex originating on the fuselage. This disturbance could be clearly seen in the blade

surface pressure measurements. Since the current methodology does not include installation effects, it is appropriate to make correlations with data which is free from installation effects.

Reference 9 presents noise measurements made on a full-size propeller tested out-of-doors on a very clean test stand with the propeller drive shaft located well above the ground plane. This propeller was tested in a four-and two-blade configuration at tip speeds to about 450 ft/sec. Figure 5-1 summarizes the comparison between measured and calculated harmonic noise levels for five azimuth locations, where zero degrees is on axis in the thrust direction (ahead of the propeller). Although there is scatter in the data, the general trends are in good agreement. At the higher tip speeds, the calculations fit the data reasonably well.

Reference 10 contains noise measurements made on an isolated model propeller. This propeller was designed as a scale model of a V/STOL propeller and was tested over a range of tip speeds and blade angles. Figure 5-2 summarizes the comparison of calculated and measured harmonic noise levels at three rotational tip Mach numbers at the design blade angle of 16 degrees. In general, the correlations are good for all three Mach numbers and at all azimuth locations. Figure 5-3 shows the comparison between measured and calculated one-third octave band spectra for the take-off design condition at four azimuths near the plane of rotation. These would represent the noise near the peak on a sideline. It can be seen that the agreement is good, particularly in annoyance as indicated by the close agreement in PNL values.

As a final comparison of measured vs calculated uninstalled propeller noise, noise measurements made on a 13.5 ft diameter propeller operating statically at 720 ft/sec tip speed and 4000 SHP were analyzed. This propeller was powered by a T56 turboshaft engine. Thus, the noise was calculated for the propeller, engine, engine jet, and gear box for comparison with the measurements. Figure 5-4 shows a narrow band analysis of the noise at an azimuth angle of 112 degrees (near the peak sideline noise). The crosses indicate the calculated levels of the propeller blade passing frequency harmonics. The horizontal bars show the free-field noise levels derived from the measured levels adjusted for ground reflections for the 4 ft high microphone. As can be seen, the ground reflection corrections are not perfect, especially in the frequency range where cancellation is calculated to occur. The fourth harmonic is calculated to be almost completely cancelled, requiring a correction of 57 dB for equivalent free-field level. This apparent discrepancy occurs because the frequency is not exactly known, the ground is not a perfect reflector, the source is not a point, the tone is not pure, etc. The calculated corrections at other frequencies appear more reasonable, but it is not possible to assess their validity, as no free-field measurements are available for comparison. The corrections at the fundamental and second harmonic are probably reasonable, as these are lower in frequency than that of the first ground dip. The agreement between calculated and measured levels is seen to be good - the calculated harmonic levels being generally near the measured levels, and between the

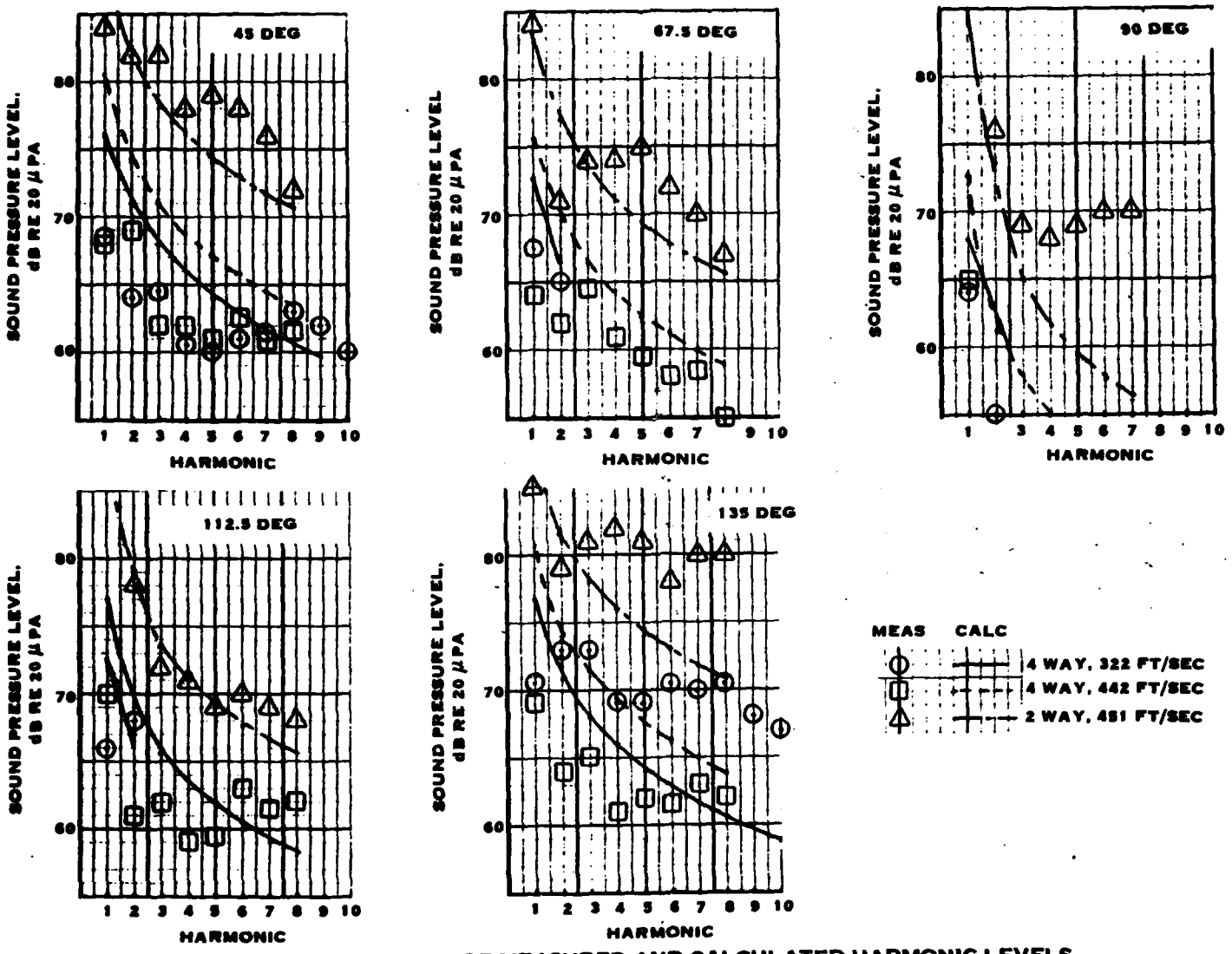

FIGURE 5-1. COMPARISON OF MEASURED AND CALCULATED HARMONIC LEVELS FOR UNINSTALLED, LOW TIP SPEED PROPELLERS

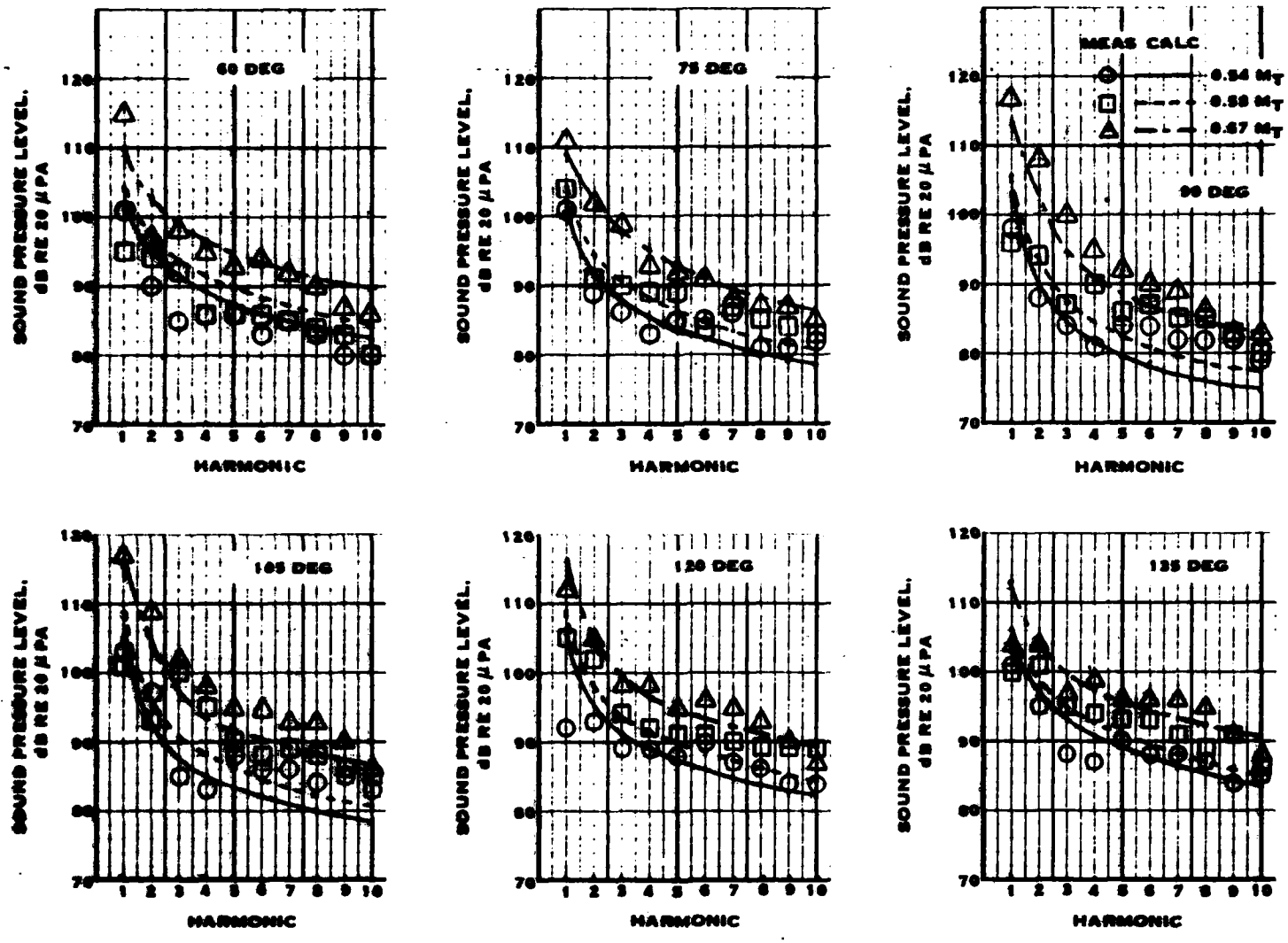

FIGURE 5-2. COMPARISON OF MEASURED AND CALCULATED HARMONIC LEVELS FOR AN UNINSTALLED V/STOL PROPELLER

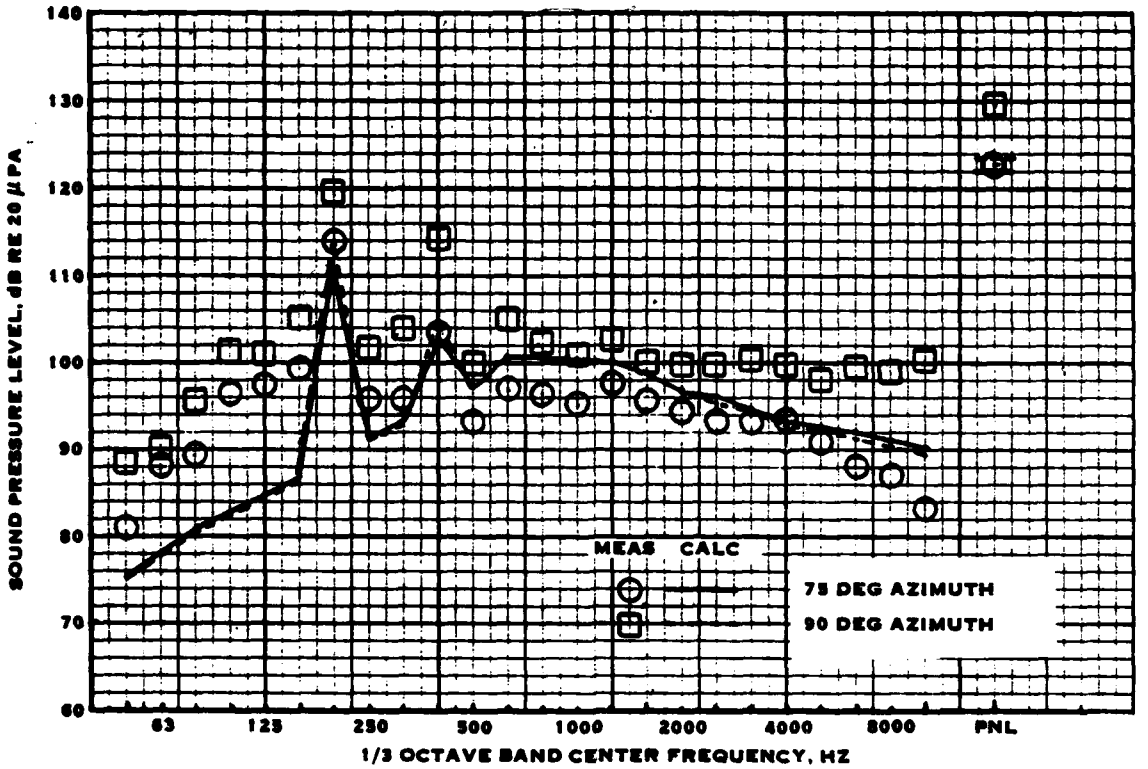

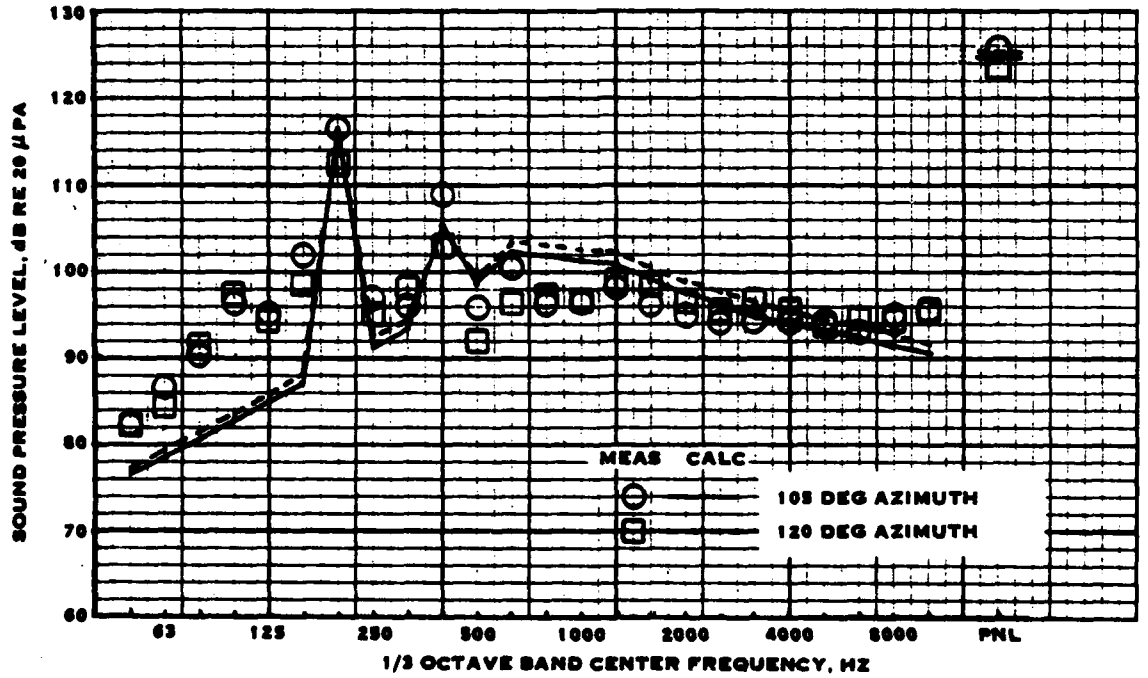

FIGURE 5-3. COMPARISON OF MEASURED AND CALCULATED 1/3 OCTAVE BAND SPECTRA FOR AN UNINSTALLED V/STOL PROPELLER AT 0.67 TIP MACH NUMBER AND 254 SHP

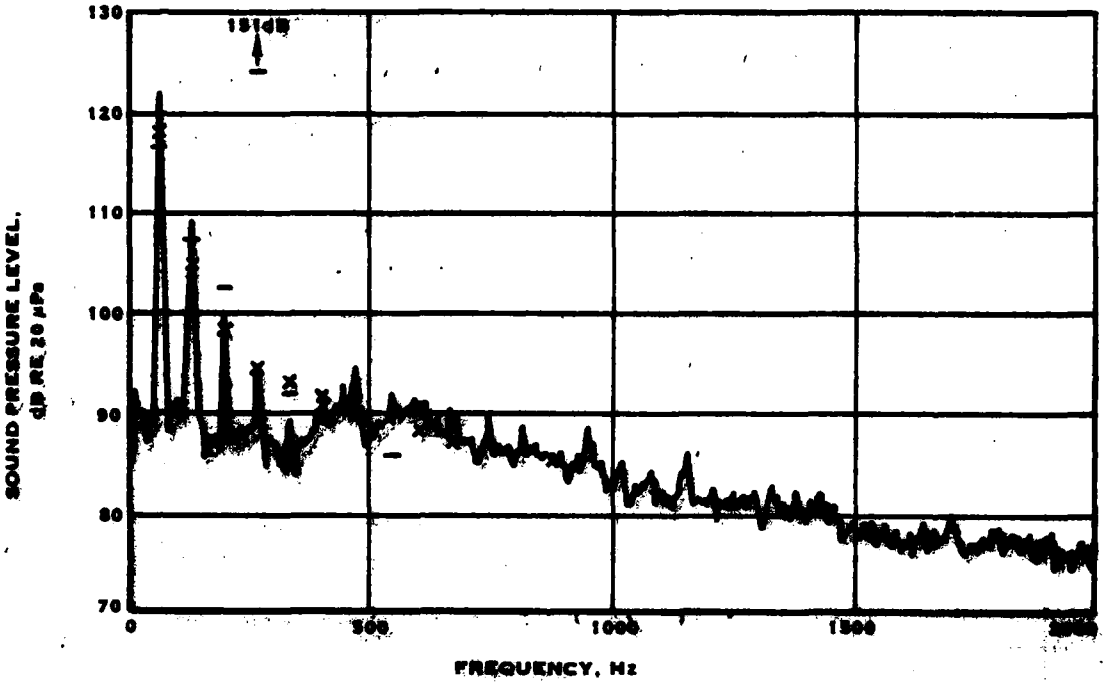

FIGURE 5-4. CALCULATED AND MEASURED HARMONIC LEVELS FOR A FULL SCALE PROPELLER AT STATIC CONDITIONS.

as-measured and free-field corrected levels. Figure 5-5 presents the comparison on a one-third octave band basis, including identification of calculated noise components. The circles indicate the measured levels, while the squares represent the measured levels adjusted to free-field conditions. It is readily apparent that the core engine jet noise is calculated to be negligible. The gearbox noise is of minor importance, showing a few significant peaks at high frequencies. The dominant low frequency noise is clearly that from the propeller. The mid-frequency noise is equally controlled by that from the propeller and the core engine (combustor noise), while the high frequency noise is primarily due to the core engine (turbine noise). The agreement between the measured levels and the calculations is quite good.

It is apparent from these correlations that the current propeller noise methodology is adequate for the calculation of uninstalled propellers under static conditions. No data is available on uninstalled propellers in flight.

Installed Propellers

The data report on static and flight propeller noise measurements on a Twin Otter airplane, Data Catalog Item 1, contains analyses from wing-tip microphones and from ground level microphones. The data used for the evaluation of forward-flight effects indicated severe installation effects during static operation. This was attributed to the ingestion of a fuselage vortex, which resulted in high levels of mid-frequency harmonics. Figure 5-6 shows a representative narrow band analysis for a static condition. The crosses show the calculated levels. The first three and the 22nd to 33rd harmonics are well predicted, but the mid-frequency harmonics are substantially underpredicted. This is in contrast to the previous data for uninstalled propellers which showed good agreement throughout the frequency range. This lack of agreement is believed to be a result of the ingestion of the fuselage vortex. This vortex was seen to disappear rapidly at the onset of forward flight. In flight, the vortex is gone, and good agreement between measurements and calculations is obtained, as shown in figure 5-7. Both of these propeller noise correlations were made in the aft quadrant for a rotational tip Mach number of 0.77, where loading noise dominates. At higher tip speeds, the higher-frequency harmonics become dominated by thickness noise. Since the current methodology does not include thickness noise, lightly loaded, high tip speed propellers will be underpredicted, as shown in figure 5-8. Here, the higher harmonics, beginning at about the fifth, are underpredicted. This is particularly evident in the plane of rotation where thickness noise peaks in directivity, as shown in figure 5-9. At lower tip speeds, figure 5-10, the thickness noise decreases and the noise is more strongly loading-noise controlled. At even lower tip speeds, figure 5-11, the thickness noise becomes insignificant and good correlation between calculated and measured levels is obtained. Figure 5-12 shows the low tip speed correlation for the aft wing-tip microphone. In the formulation of the propeller noise prediction methodology, thickness noise was not included because current and future V/STOL propellers are low tip speed with moderate to high loading and thickness noise is insignificant. Thus, the data for correlation from the Twin Otter will be limited to the low tip speed conditions.

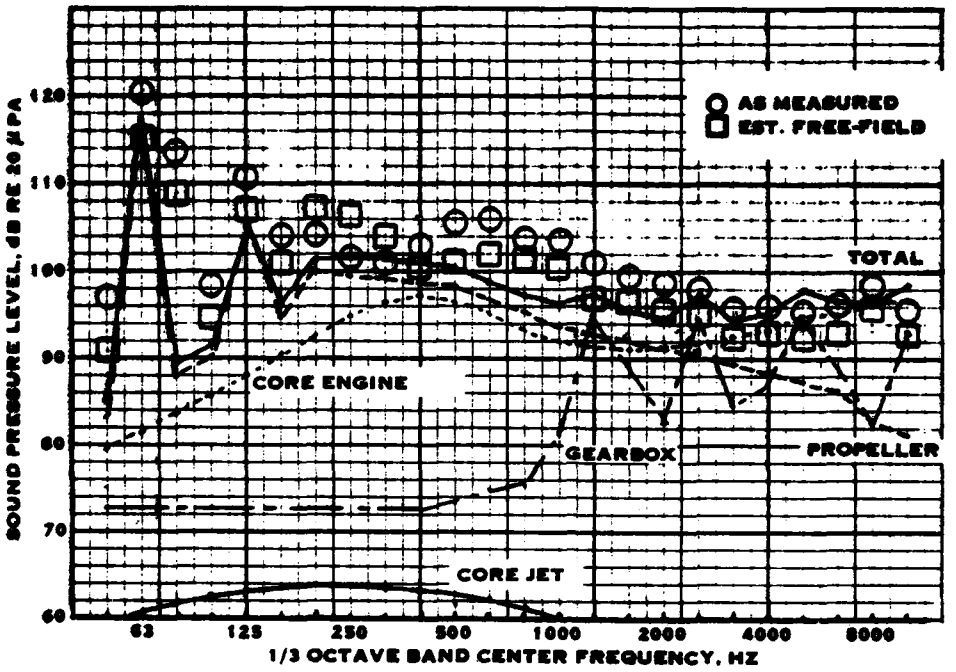

FIGURE 5-5. CALCULATED AND MEASURED NOISE FOR A FULL SCALE PROPELLER, ENGINE, AND GEARBOX AT STATIC CONDITIONS

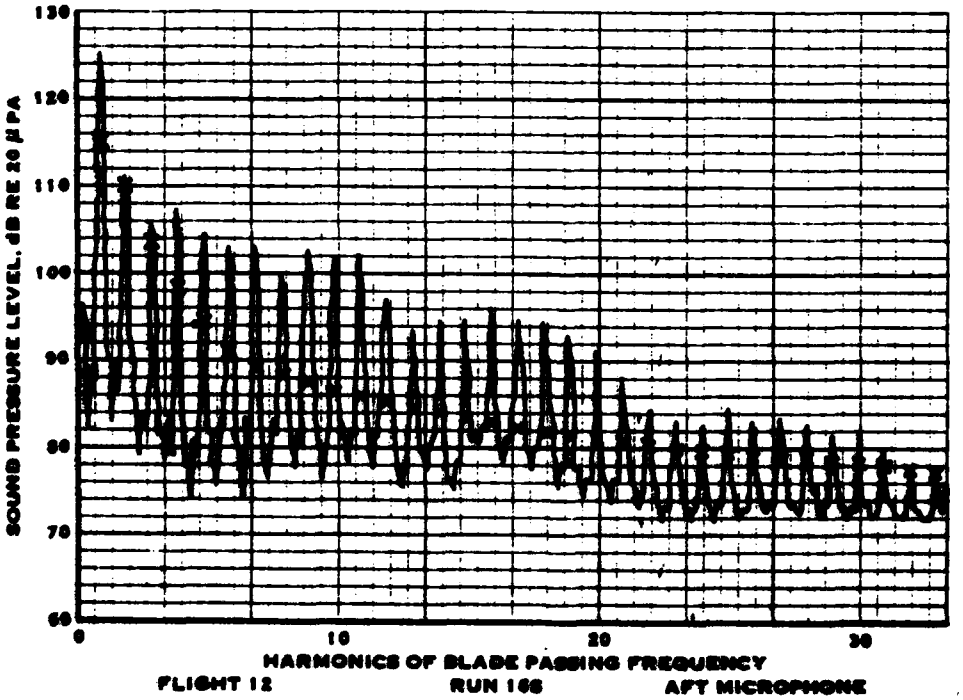

FIGURE 5-6. STATIC PROPELLER HARMONIC NOISE WITH INSTALLATION EFFECTS

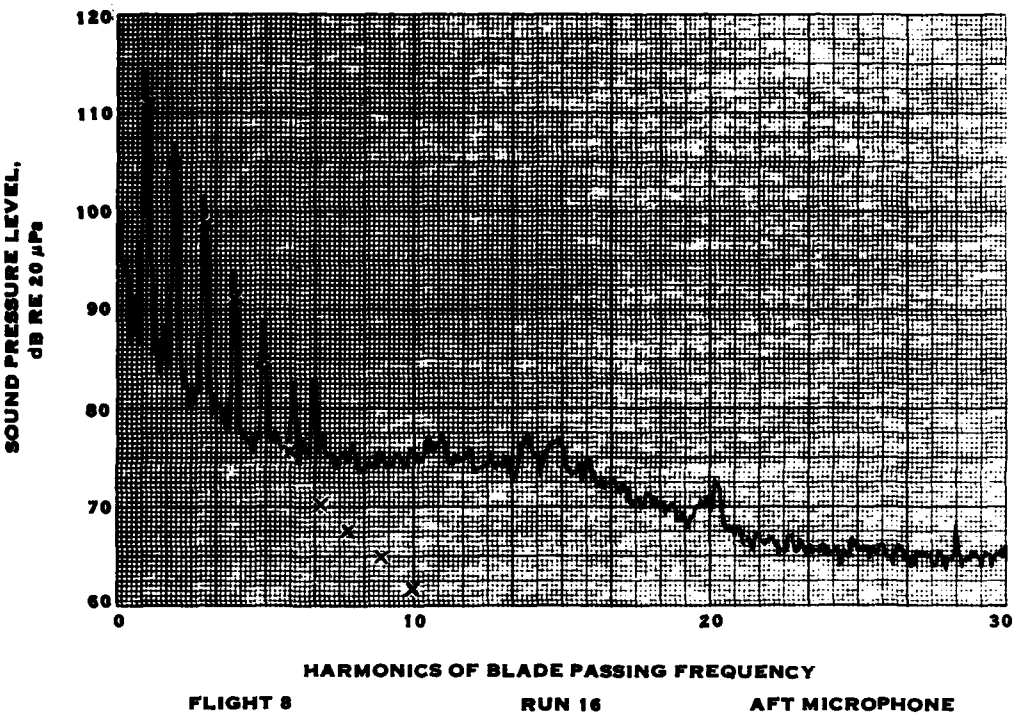

FIGURE 5-7. LOW TIP SPEED PROPELLER NOISE IN FORWARD FLIGHT

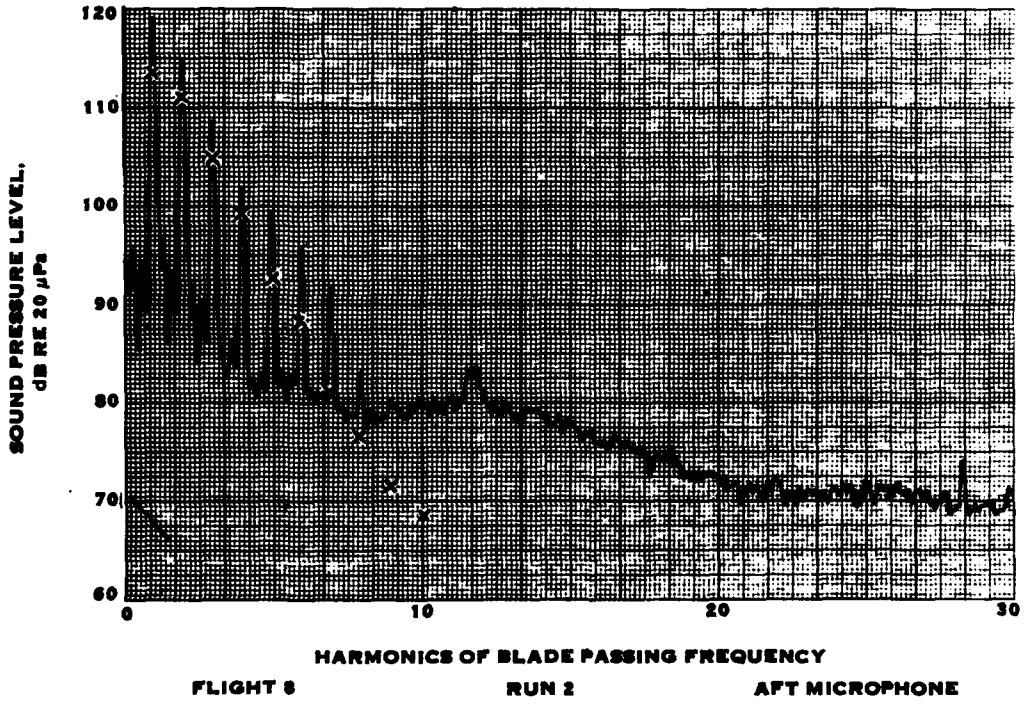

FIGURE 5-8. PROPELLER NOISE LEVELS AT A TIP ROTATIONAL MACH NUMBER OF 0.83 FOR THE AFT WING TIP MICROPHONE.

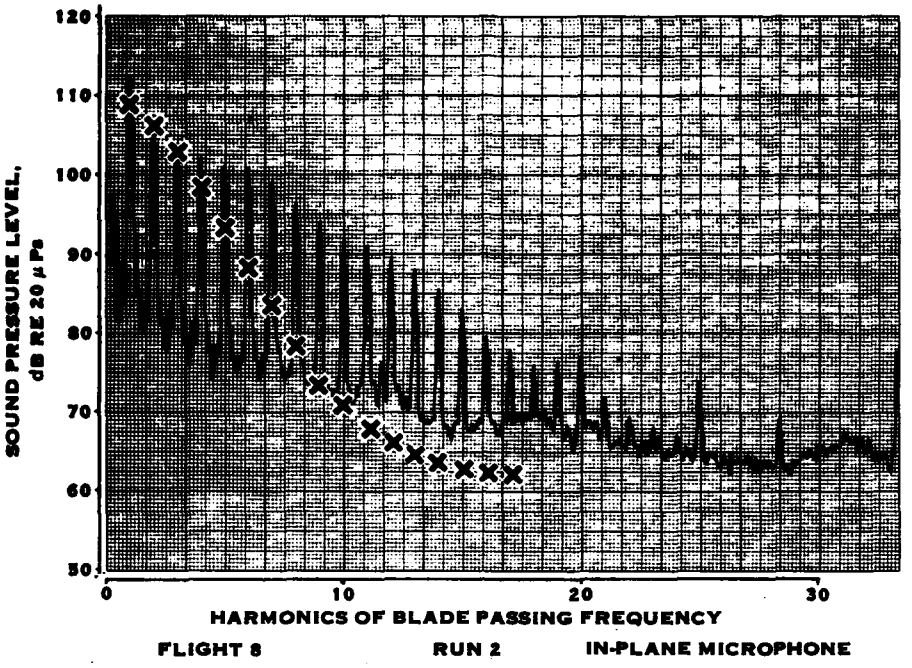

FIGURE 5-9. PROPELLER NOISE LEVELS AT A TIP ROTATIONAL MACH NUMBER OF 0.83 FOR THE IN-PLANE WING TIP MICROPHONE

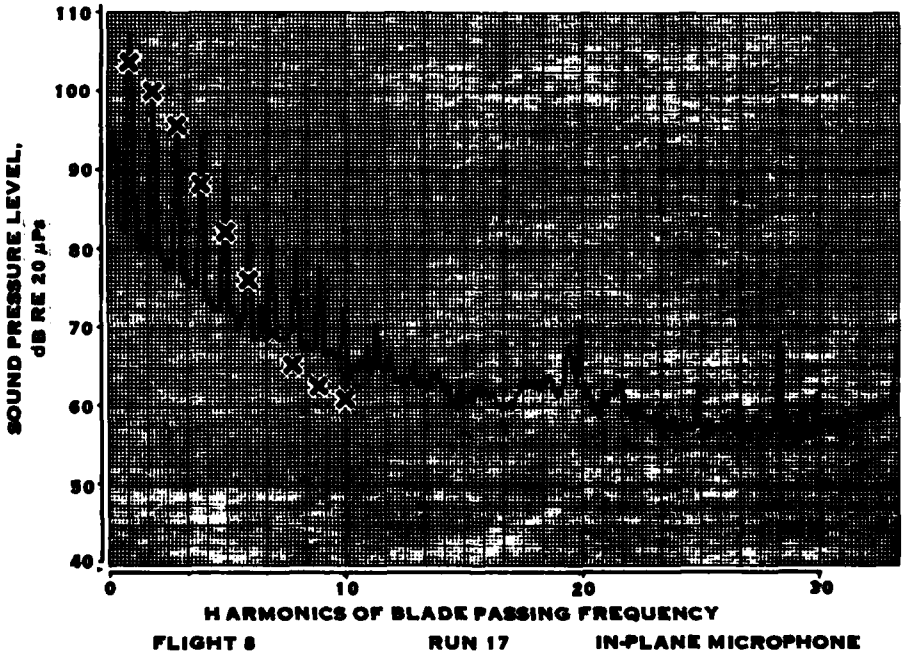

FIGURE 5-10. PROPELLER NOISE LEVELS AT A TIP ROTATIONAL MACH NUMBER OF 0.77 FOR THE IN-PLANE WING TIP MICROPHONE

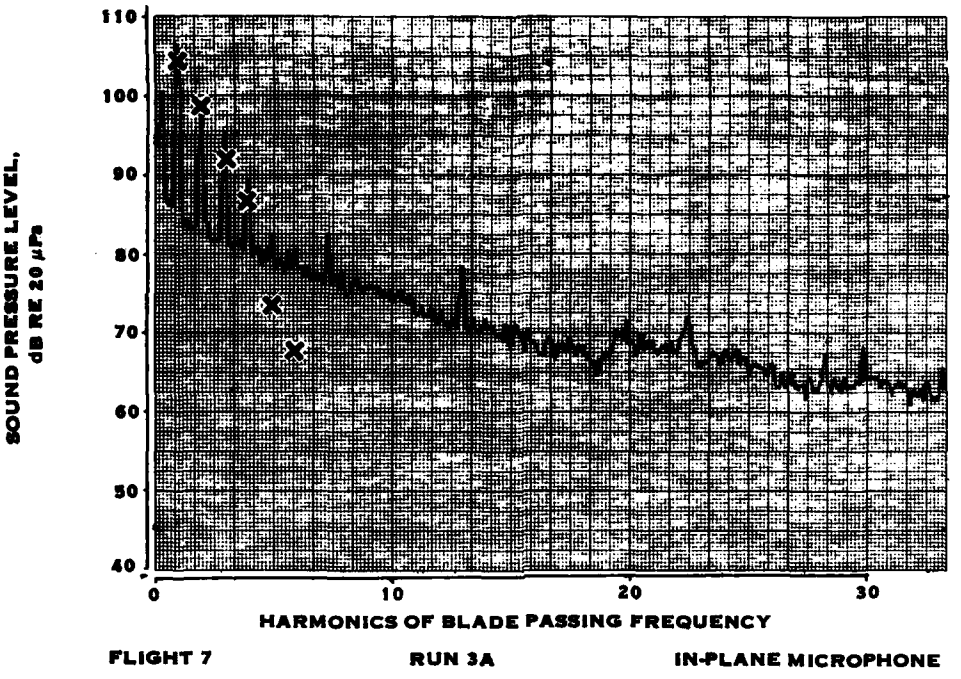

FIGURE 5-11. PROPELLER NOISE LEVELS AT A TIP ROTATIONAL MACH NUMBER OF 0.69 FOR THE IN-PLANE WING TIP MICROPHONE

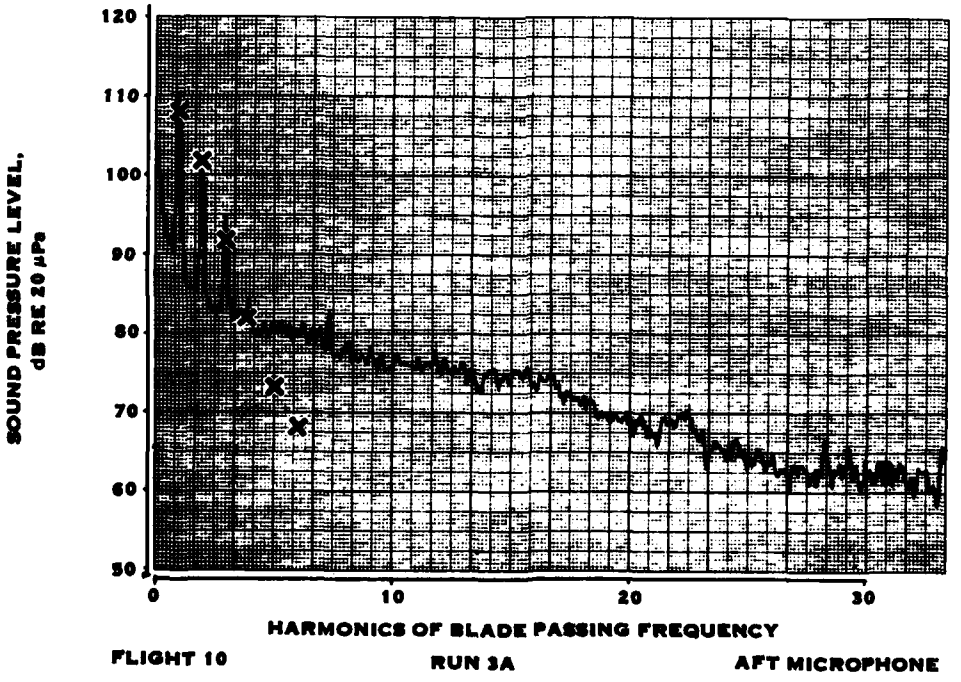

FIGURE 5-12. PROPELLER NOISE LEVELS AT A TIP ROTATIONAL MACH NUMBER OF 0.69 FOR THE AFT WING TIP MICROPHONE.

Figures 5-11 and 5-12 show good correlations between the measured and calculated harmonic noise levels for the two wing-tip microphones in flight. Figures 5-13 and 5-14 show similar comparisons for the entire frequency range. In figure 5-13, it can be seen that the fundamental and second harmonics of blade passing frequency are well predicted. The measurements show the tones split between two bands. This indicates levels of 104.5 and 98.5 dB measured compared to 105 and 99 dB calculated for the fundamental and second harmonics, respectively. The calculated levels do not show the split between the bands, as ideal filters are assumed. It can be seen that the mid- and high-frequency bands are dominated by engine noise. The agreement is good to about 5000 Hz. In the 8000 Hz band, the engine compressor tone is calculated, but does not appear in the measurements. This could be because the tone level is over-predicted or that the gas generator rpm is incorrectly calculated and the tone occurs at higher frequency. The calculated A-weighted overall exceeds the measured level by about 2 dB. However, the over-prediction is caused primarily by the engine compressor tone. Reducing its level by 10 dB (to the measured level) results in very close agreement with the measured levels. The comparison in figure 5-14 shows generally similar results for the aft wing-tip microphone location.

It is thus apparent that, for the Twin Otter data, good correlation between measurements and calculations are obtained at moderate propeller tip speeds in flight. Statically, the propeller mid-frequency harmonics are underpredicted, but this is due to installation effects. The propeller noise in flight is seen to dominate the low frequencies, but mid- to high-frequencies are apparently due to the free-turbine engine.

Data catalog item 7 presents measurements made on a turbine powered Cessna 02T airplane (with propellers fore and aft of the cockpit on the centerline of the aircraft). Because of distortion from the fuselage and wakes from the wings, the aft propeller has substantial inflow distortion. Thus, for the correlation, only the data measured on the front propeller was used. Also, the engine design and operating parameters were not known so that a generalized engine was used in the noise calculations.

Figure 5-15 shows the comparison between measured and calculated 02T propeller tone noise levels for two power inputs at static conditions. Both are for a propeller rotational tip Mach number of 0.51 and are for a location in the plane of rotation. The measurements were also corrected for ground reflection effects. As the source and microphone are close to the ground plane, the first cancellation is calculated to be beyond 800 Hz; thus, the first two propeller harmonics include essentially full pressure doubling. The horizontal bars in figure 5-15 indicate the equivalent measured free-field noise levels. The crosses indicate the calculated free-field noise levels. As can be seen, the calculations and measurements are in excellent agreement.

Figure 5-16 shows the comparison between measured and calculated octave band spectra for the two static operating conditions, also in the plane of rotation. The free-field estimates were made by applying the ground correction effects for the two discernible

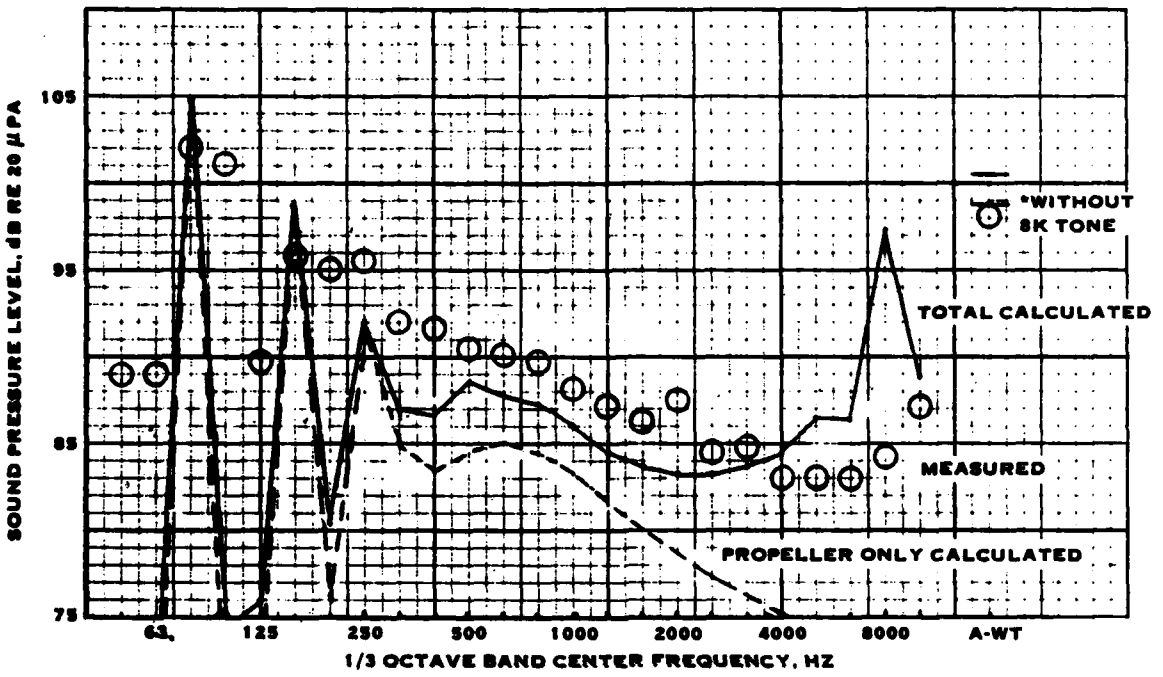

FIGURE 5-13. COMPARISON OF MEASURED AND CALCULATED PROPELLER NOISE FOR THE IN-PLANE WING TIP MICROPHONE

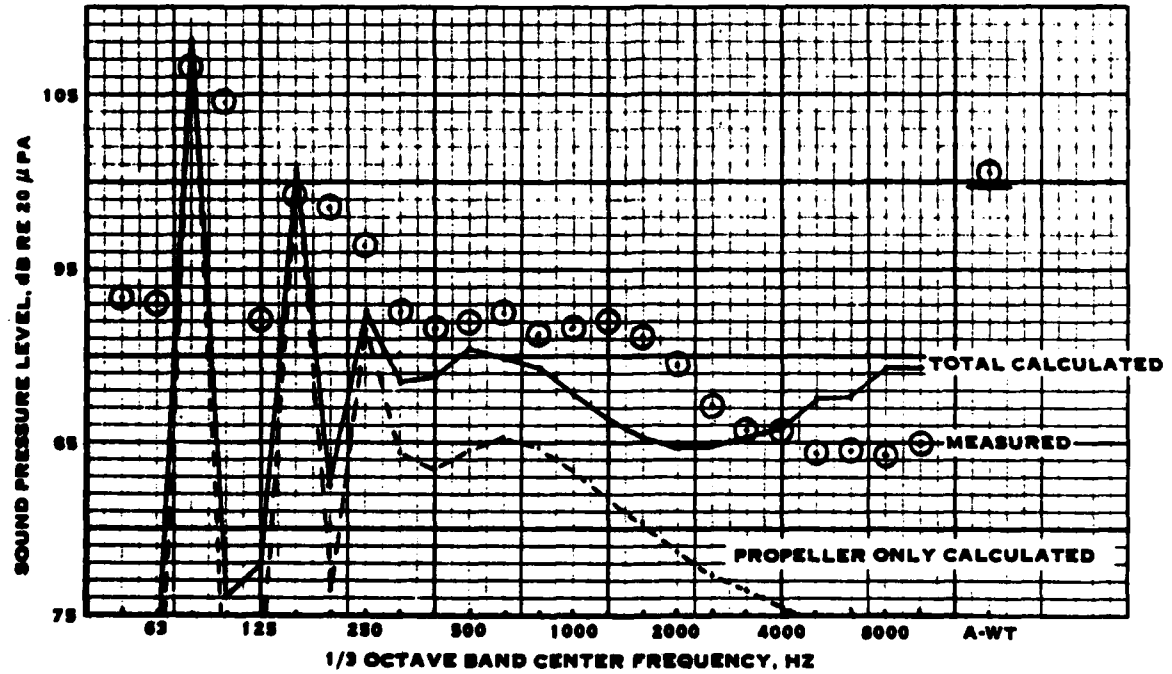

FIGURE 5-14. COMPARISON OF MEASURED AND CALCULATED PROPELLER NOISE FOR THE AFT WING TIP MICROPHONE.

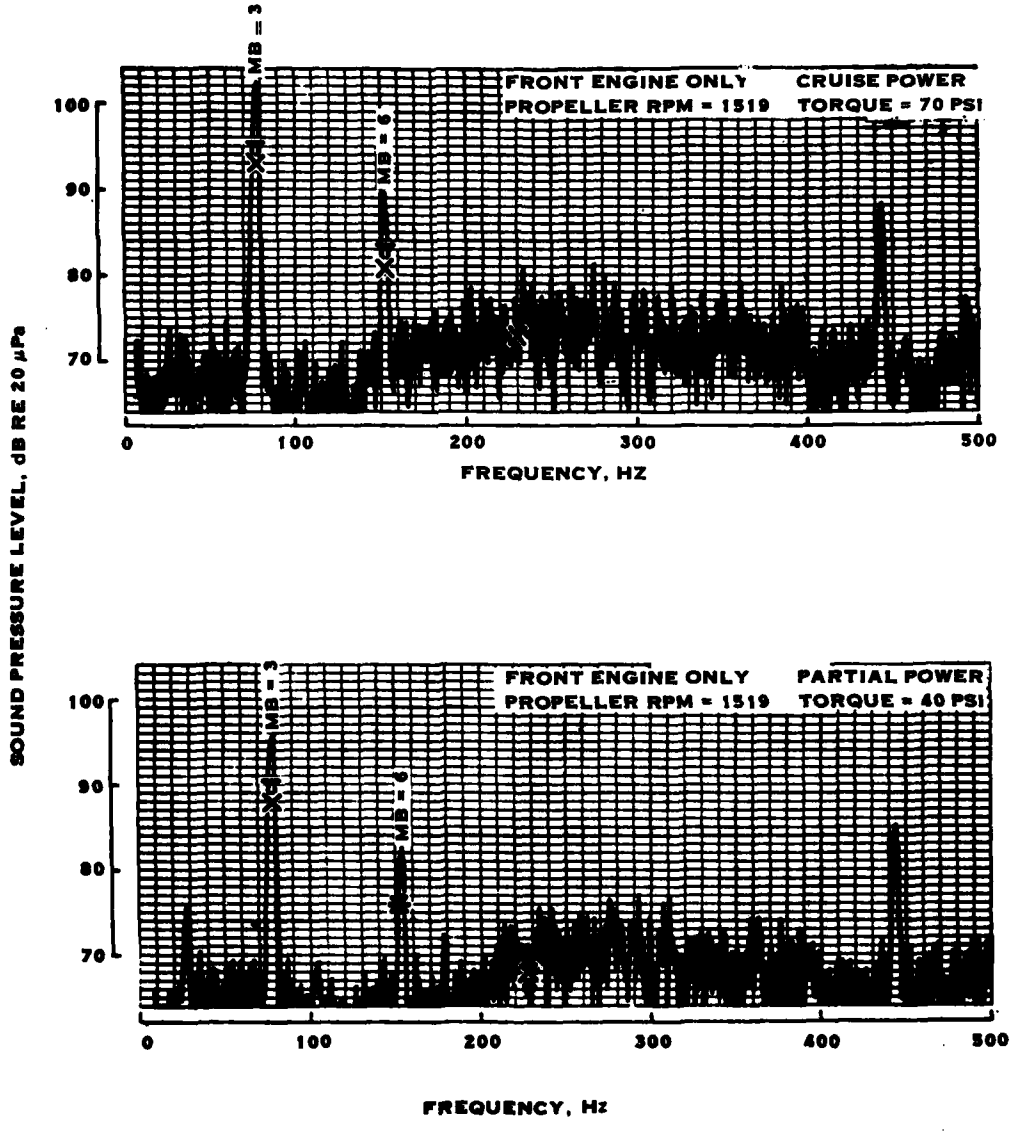

FIGURE 5-15. NARROW BAND ANALYSES OF THE O2T STATIC NOISE AT 90 DEGREES AZIMUTH.

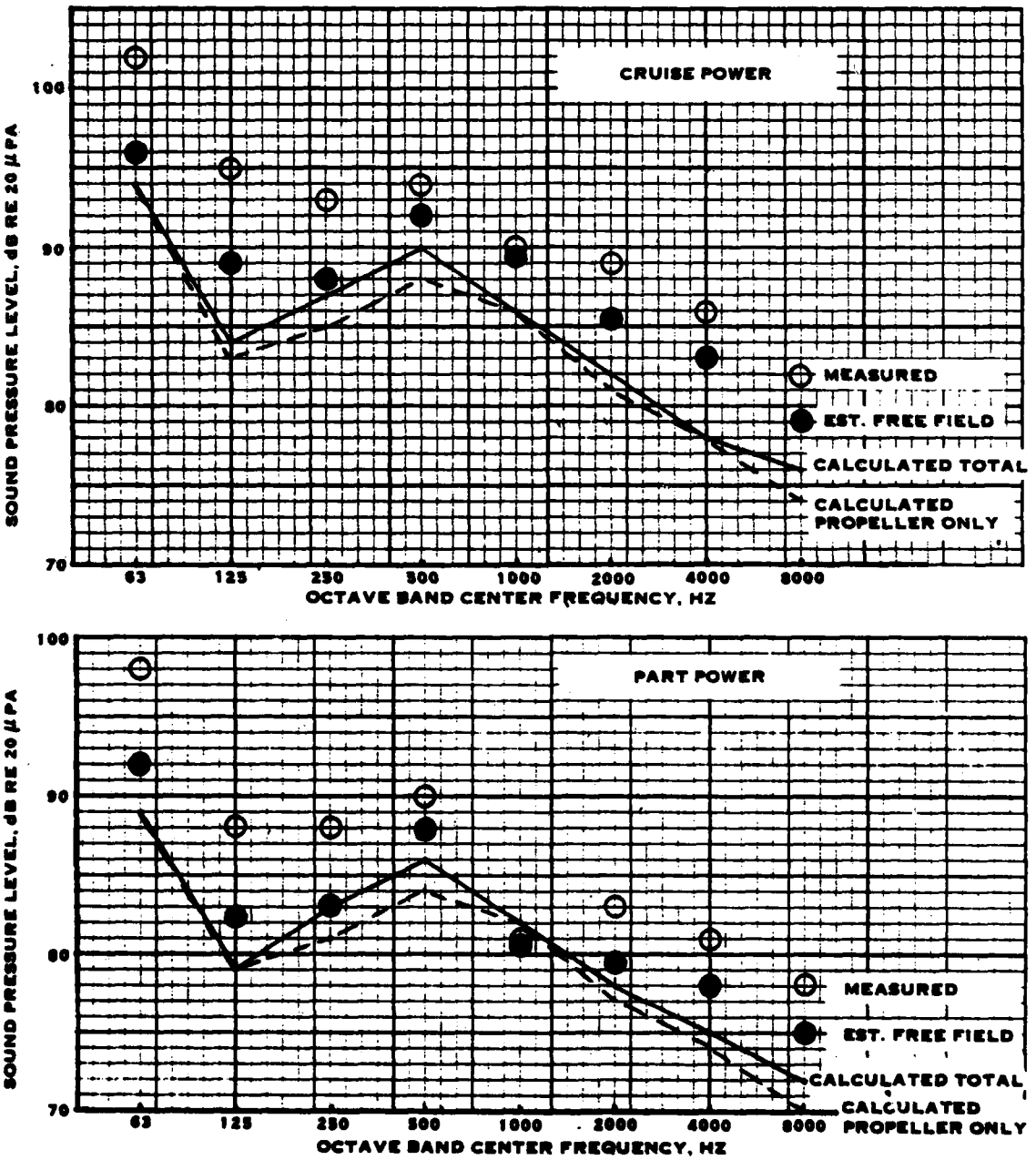

FIGURE 5-16. COMPARISON OF MEASURED AND CALCULATED 02T AIRPLANE NOISE LEVELS AT STATIC CONDITIONS

propeller tones in the 63 and 125 Hz bands (see figure 5-15) and then applying corrections to the other bands assuming broadband noise. It can be seen that the noise is calculated to be predominantly propeller noise, with little contribution from the engine. The agreement is quite good, with a slight underprediction at the high frequencies. Figure 5-17 shows the comparison of measured and calculated overall noise directivities for the cruise and part power conditions. Since the overall noise is dominated by low frequency components, the free-field noise levels were estimated by adding -6 dB, the low-frequency ground reflection correction. The correlation for the cruise power condition is very good, while the part power condition is slightly overestimated. The calculated and measured directivity patterns agree.

Figure 5-18 shows the comparison between calculated and measured 02T peak noise levels during flyover at cruise power. The free-field noise levels were estimated by applying the ground correction to the fundamental and second harmonics for the 63 and 125 Hz bands, respectively, then assuming broadband noise for the other bands. It should be noted that the fundamental was calculated to be in the frequency range of the first cancellation and a correction of 12 dB was derived. This appears to be an overcorrection. Since the cancellation effects on tones are very sensitive to the exact ratio of wavelength to path length difference, the ground correction effects in this case are considered unreliable. The correlation for the 125 to 1000 Hz octave bands is good, although the dominant noise is calculated to be that of the engine. The noise appears to be overpredicted above 1000 Hz. It should be recalled, however, that a generalized engine was used in the noise calculation and not the actual 02T engine, so that judgement of the engine noise calculation procedure based on this correlation is not justified.

Flyover noise measurements on the Lockheed Electra from the Hamilton Standard data bank were also used for methodology evaluation. This data was acquired with a microphone located flush with the ground plane, so that corrections to free-field conditions are essentially independent of frequency and airplane location. A correction of -6 dB was used. The flyover noise was calculated for the total propulsor, including the contribution from the engines, engine jet, and gearboxes. All inputs were available, so that a realistic engine noise estimate was made.

Figure 5-19 shows the comparison between the calculated and measured flyover time history during normal takeoff. The peak PNLT is calculated to be 104.2 PNdB compared to a measured peak of 102.2 PNdB. It is apparent that the calculated tone correction is greater than that from the measurements. On the basis of peak PNL, the comparison is 101.7 calculated vs 100.1 measured. It can also be seen that the shape of the time history is calculated to be close to that measured, except for the one-half to one second near the peak. The calculated EPNL is 97.4 EPNdB compared to a measured EPNL of 96.1 EPNdB.

Figure 5-20 shows a comparison of the measured and calculated one-third octave band spectra for the maximum PNLT. As can be seen, the low frequencies are propeller

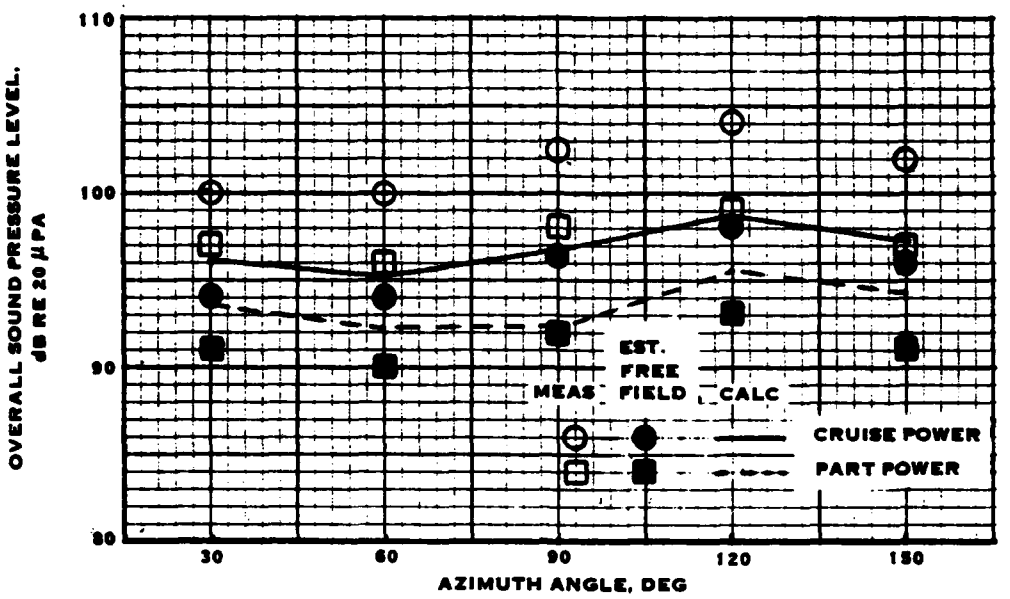

FIGURE 5-17. COMPARISON OF MEASURED AND CALCULATED 02T OVERALL NOISE DIRECTIVITY

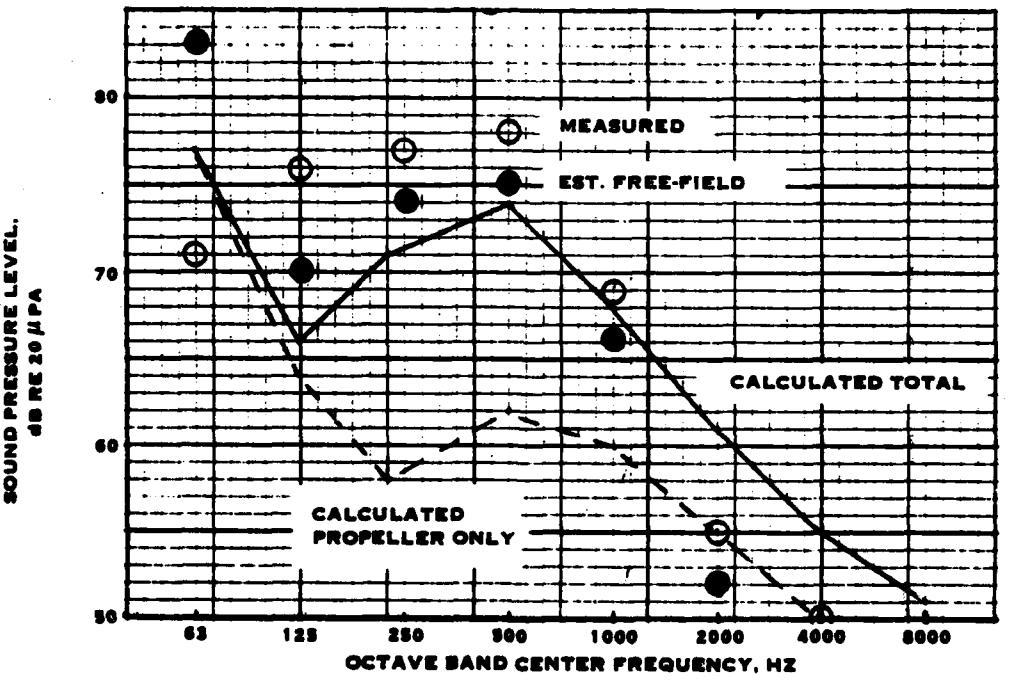

FIGURE 5-18. COMPARISON OF MEASURED AND CALCULATED 02T FLYOVER NOISE AT CRUISE POWER

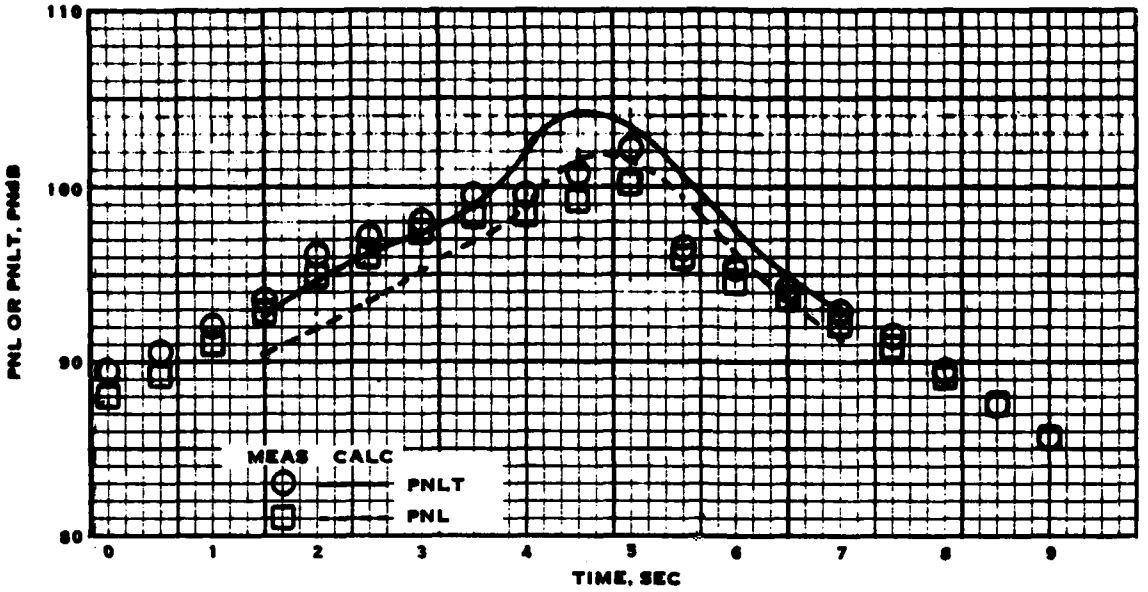

FIGURE 5-19. COMPARISON OF CALCULATED AND MEASURED ELECTRA FLYOVER TIME HISTORY

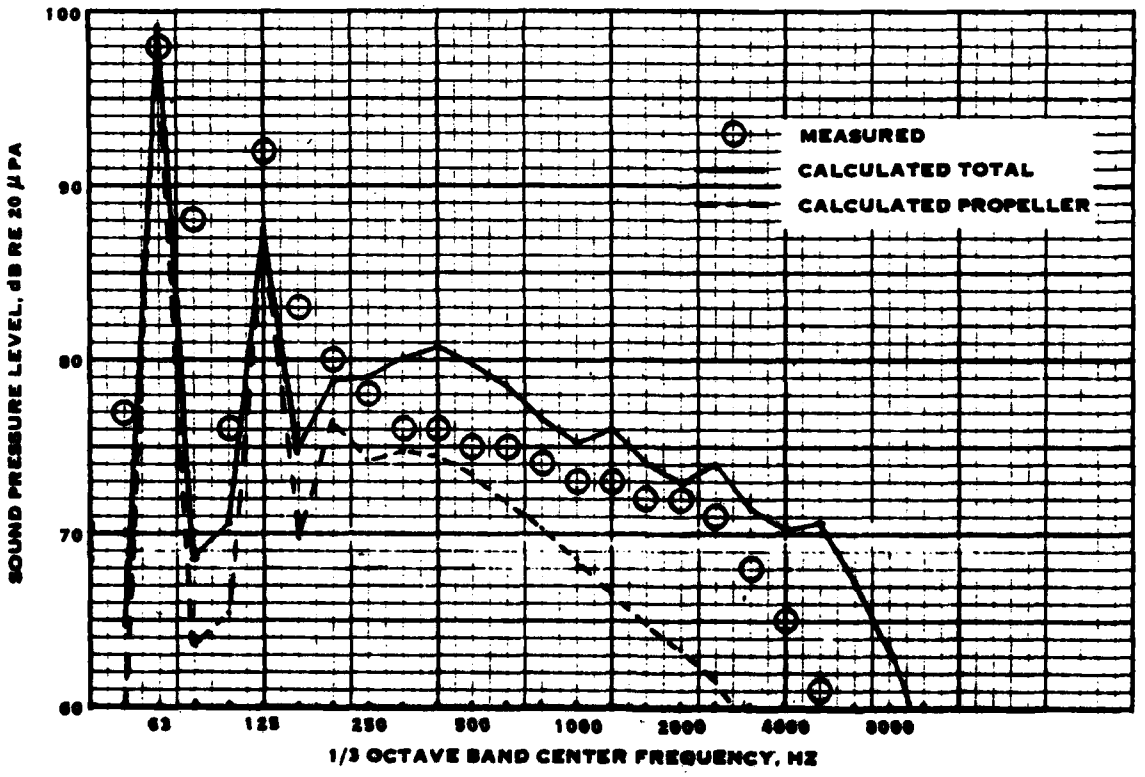

FIGURE 5-20. COMPARISON OF MEASURED AND CALCULATED PEAK PNLT SPECTRA FOR THE ELECTRA

noise dominated, while the mid- and high frequencies are controlled by the drive engine noise. The fundamental is well predicted, but the second harmonic is slightly underpredicted. The mid-frequency (engine) noise is slightly overpredicted. It can also be seen that the high-frequency test spectrum rolls off faster than the calculations. Thus, the 1.5 dB difference between the calculated and measured PNL can be accounted for by an overprediction of about 1 dB at the fundamental (the maximum Noy value is set by it) and slight overprediction of the mid- and high frequencies.

The final propeller noise comparison will be made for the deHavilland DHC-7 airplane. The measurements were made using a microphone located beneath the flight path at a height of six inches above the ground plane. This gives a first ground cancellation frequency of about 570 Hz, so that the first few propeller harmonics show essentially complete pressure doubling. The spectra were corrected to equivalent free-field conditions by subtracting 6 dB from the fundamental and second harmonics, then applying corrections to the remaining part of the spectrum assuming broadband noise. Figure 5-21 shows the comparison of the flyover time histories for the measurements corrected to free-field and calculations. The agreement during the approach part of the flyover is very good, but the peak level is slightly overpredicted. Also, the calculations decrease more rapidly past the peak than do the measurements. The measured EPNL is 95.4 EPNdB compared to a calculated value of 95.8 EPNdB.

Figure 5-22 shows the comparison between the measured spectrum adjusted to free-field and the calculated spectrum at the peak PNLT. The propeller tones are well predicted. The mid-frequency broadband, from 315 to 1250 Hz, is significantly overpredicted. This peak is calculated to be due to engine combustor noise. However, the DHC-7 airplane engine exhaust is above the wing, so that the engine exhaust is shielded from an observer located below. The high-frequency noise is calculated to be turbine noise, which may also be shielded by the wing. The propeller mid-frequency noise appears slightly overpredicted. The circles indicate the measured levels adjusted to free-field assuming a microphone height of exactly six inches (first ground cancellation at 568 Hz). The spectrum shows evidence of incorrect ground reflection corrections, as indicated by the peak at 500 Hz and the valley at 800 Hz, although it is, of course, impossible to confirm that this is actually not the true free-field spectrum. To estimate the sensitivity of the ground reflection correction to microphone height and to see if the shape of the corrected spectrum could be improved, a second set of ground correction values were calculated assuming a microphone height of 5.4 inches. This places the first ground cancellation at 630 Hz. The adjusted spectrum for this assumption is shown by the squares in figure 5-22. As can be seen, the peak at 500 Hz is eliminated and the valley which was seen at 800 Hz is shallower and now appears at 1000 Hz. It is debatable whether the assumed 5.4 inch microphone height resulted in a better estimated free-field spectrum than the assumed 6 inch microphone height; however, the former microphone height assumption results in a smoother, less discontinuous spectrum. It is thus to be concluded that the ground reflection corrections are very sensitive to the input values in the calculation. An assumed change of about one-half inch in microphone height resulted in changes to the corrections for ground

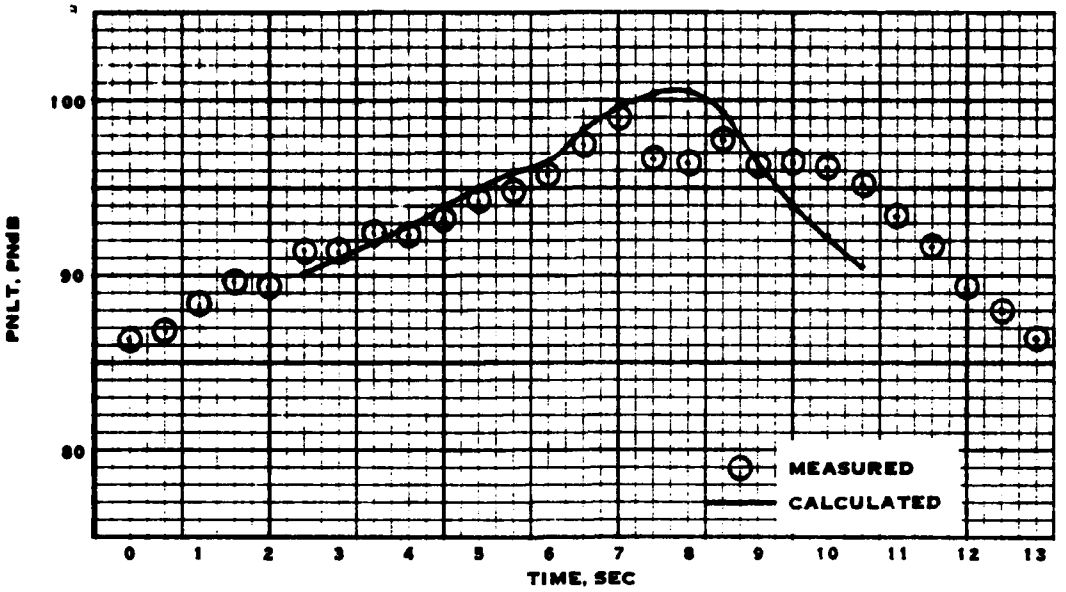

FIGURE 5-21. COMPARISON OF CALCULATED AND MEASURED DHC-7 FLYOVER TIME HISTORY

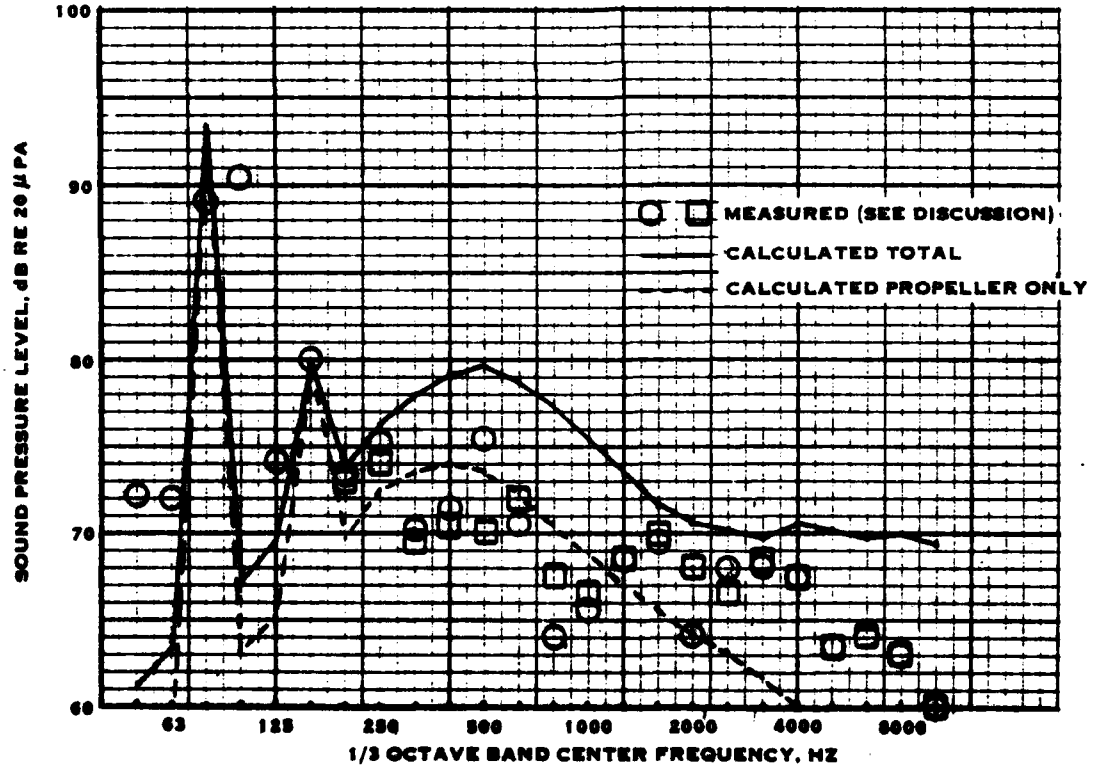

FIGURE 5-22. COMPARISON OF MEASURED AND CALCULATED PEAK PNLT SPECTRA FOR THE DHC-7

reflections of up to 6 dB. In the case of this data, the effect of ground reflection correction on the PNL value is small, as the first ground cancellation occured well above the frequency of the significant propeller tones, which determine the maximum Noy value. However, if the data had been acquired with a more typical four-foot microphone height, the first ground cancellation would have been near 70 Hz, or close to the fundamental blade passing frequency.

For this data on the DHC-7, the high frequency ground reflection corrections have only a small effect on the PNL. The calculated peak PNLT value of 100.7 PNdB agrees closely with the measured value of 99.0 PNdB, as the calculated and measured propeller tone levels are in good agreement. The calculated value is slightly higher than the measured value because of the mid-frequency engine broadband noise overprediction.

Summary for Propellers

Static uninstalled and installed propeller noise data and in-flight installed propeller noise data were used for comparisons of calculated and measured propeller noise. Static uninstalled propeller noise was well predicted throughout the entire frequency spectrum, including the unsteady loading noise which appears as mid-frequency harmonics. Static installed propeller noise was underpredicted, particularly the mid-frequency harmonics. This was due to installation effects, specifically the ingestion of fuselage and/or ground vortices. In flight, the noise of low-to-moderate tip speed, moderately-loaded propellers is well predicted. High tip speed, lightly-loaded propeller noise is underpredicted, as this contains dominant thickness noise components. Thickness noise is not included in the current noise prediction methodology. However, current V/STOL propeller designs operate in the moderate tip speed range so that good noise estimates can be made with the current noise prediction methodology. The in-flight propeller noise data was acquired on airplanes in flight. The calculations indicate that only the low frequencies are due to propeller noise. The mid- to high frequencies are due to turbine drive engines.

Within the range of validity of the propeller noise prediction methodology, i.e. for uninstalled static propellers and low to moderate tip speed propellers in flight, the agreement between measured and calculated one-third octave band levels is generally within ± 5 dB. Agreement between calculated and measured dB(A), overall, PNL, PNLT, and EPNL is typically within ± 3 dB.

EVALUATION OF VARIABLE-PITCH FAN NOISE PREDICTION

Introduction

The available data on variable-pitch fan noise is limited, with very few exceptions, to that from static tests. One such exception is fan inlet noise measurements made on a 20-inch model tested in a wind tunnel. This data was used to evaluate forward-

flight effects and is described in an earlier section of this report. The bulk of the variable-pitch fan noise data was acquired on electrically-driven outdoor static test stands, although some data exists from turbine engine driven systems.

The data used in the following comparisons were selected because the first set of data was acquired in a wind tunnel and includes forward-flight effects, the second set of data was acquired on an electrically-driven fan under free-field conditions, and the third set of data was acquired on a full-scale turbine engine driven fan under free-field conditions.

Comparisons of Measured and Calculated Variable-Pitch Fan Noise

Reference 11. - The data from this report was measured in a wind tunnel under several simulated flight conditions for several fan operating tip speeds. Measurements were made of fan inlet noise only. Figure 5-23 presents the comparison of measured and calculated fan inlet noise at 60 degrees azimuth for four fan tip speeds and two simulated flight speeds.

The correlations at 79 and 95% rpm are good, except for the level of the second harmonic. The calculations show this to be due to unsteady rotor loading noise, which decreases in level to below that of the broadband noise at 80 kts flight. The data show much higher levels, which do not change with speed. At 95% rpm, the measurements show an increase in the level of the third harmonic in flight relative to that at the static condition. In contrast, the data at 106 and 116% rpm show decreases in level of all the harmonics between flight and static conditions. The calculations generally show reductions in the levels of the tones in flight relative to those statically for all operating conditions because the rotor unsteady loading noise is calculated to be dominant over the stator tones. Operations of the fan in forward flight results in reduction in rotor unsteady loading noise, but does not appreciably affect the stator noise. This is supported by the data for the fundamental at all fan speeds. Actually, with 15 rotor blades and 25 stator vanes, the fundamental tone is cut-off; thus, the fundamental tone which is seen in the data must be due to rotor unsteady loading. The higher harmonics are cut-on and, therefore, could be generated at the stator. This might be the case for the second harmonics at the 79 and 95% rpm conditions. However, the tones at 106 and 116% rpm show substantial decreases in noise with forward flight. The correlation of measured and calculated tone noise is thus ambiguous.

The broadband noise is well calculated for the 79 and 95% rpm conditions. At 106% rpm, the high-frequency broadband is slightly overpredicted. At 116% rpm, the broadband is overpredicted by about 10 dB. It may be noted, however, that the measured noise levels for the 116% rpm condition are lower than those for the 106% rpm condition, and do not follow the trend shown by the 79, 95, and 106% rpm data. Noise prediction methodologies in general will show increasing noise levels with increasing tip speed and increasing power input. Thus, the large discrepancy between measured and calculated levels at the 116% rpm condition result from higher calculated levels due to high tip speed and power and measured levels which underwent a trend reversal.

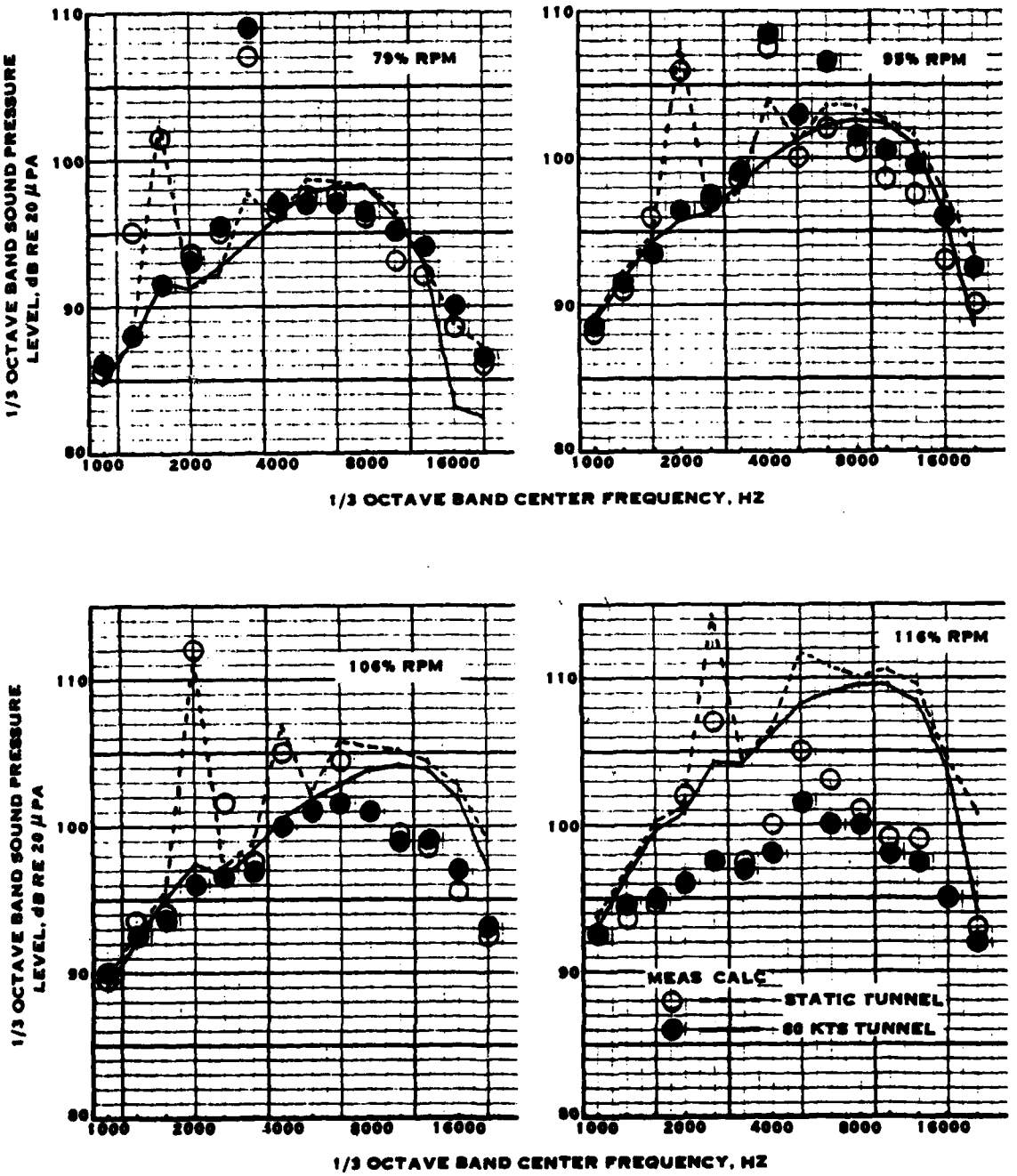

FIGURE 5-23. COMPARISON OF MEASURED AND CALCULATED FAN INLET NOISE AT 60 DEGREES AZIMUTH (FROM REFERENCE 11)

It is thus concluded from this correlation that for the three fan operating conditions from 79% of design tip speed to slightly above design tip speed the correlation between measurements and calculations is good and that the methodology properly accounts for changes in flight speed from static to 80 kts simulated flight.

Reference 12. - The data presented in these reports were acquired on a 1.5 ft diameter variable-pitch fan driven by an electric motor. The acoustic measurements were made under free-field conditions and include one-third octave band analyses at several azimuth angles. Figure 5-24 shows the comparison of measured and calculated one-third octave band sound power levels for several operating conditions spanning a tip speed range of 557 ft/sec to 811 ft/sec. The calculations were made for fan and jet noise and include rotor unsteady loading and broadband noise, stator tones and broadband noise, and fan discharge jet noise. The correlation between measured and calculated levels is seen to be good for the fundamental tone frequency and higher. The low frequency noise is consistently underestimated, by up to 10 dB. The origin of this low frequency noise is not fully understood, but may be due to high velocity fan air interacting with the drive rig. There is nothing in the methodology to calculate this noise, of course. The only source of low frequency noise shown by the calculations is jet noise, which peaks in the 250 Hz range and holds up the low frequencies. The tones and high frequency broadband noise level appear to be well predicted, although the measurements do not show the tones to be as dominant above the broadband noise as do the calculations.

Figure 5-25 shows the comparison between measured and calculated sideline PNL and PNLT. The calculations show a greater tone correction than do the measurements, consistent with a calculated stronger tone dominance as was seen in figure 5-24. In general, the correlation between measured and calculated levels is better for PNLT than PNL. The calculations generally agree with the measurements within ± 3 dB except for the 757 ft/sec tip speed condition which is underpredicted by about 5 dB at the peak sideline location. However, this condition shows a questionable directivity bulge at 100 degrees not shown by the other conditions.

Data Catalog Item 7. - This data was acquired on a full-scale fan driven by a turboshaft engine. Noise measurements were made under free-field conditions. Since the engine had inlet acoustic treatment, the calculations were made with engine compressor noise omitted. Also, a generalized engine was used, as the specific-engine operating parameters were not available. Figure 5-26 shows the comparison between measured and calculated one-third octave band sound power levels. Two calculations are shown: one with the fan and fan-jet noise only and one including the fan, engine combustor, engine turbine, and fan and engine jet noise. As seen, the engine noise improves the correlations at low and high frequencies. The very low frequencies are underpredicted, but these do not significantly contribute to the PNL's. Also, it can be seen that some very high frequency noise exists in the test test data, indicating that the engine inlet treatment was not totally effective. Over the frequency range 250 to 8000 Hz the low power condition, run AC-5, is well predicted assuming engine noise contribution. The high power condition, run AC-6, is well predicted over the frequency range 250 to 2000 Hz. The higher frequencies, which are calculated to be rotor broadband noise, are moderately overpredicted.

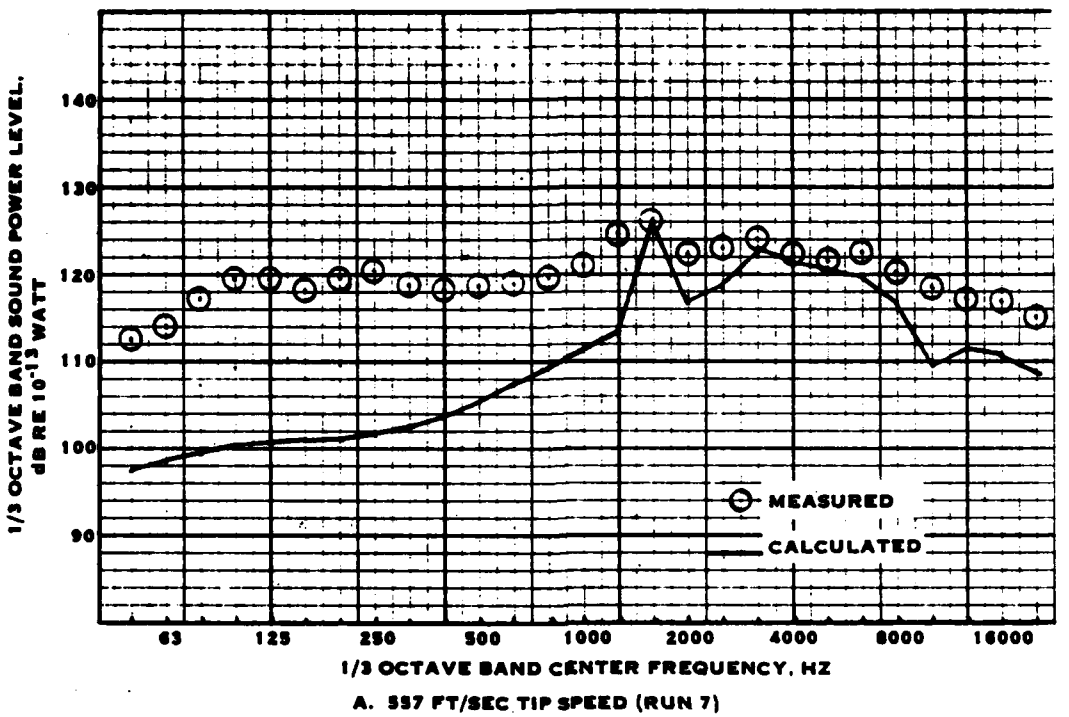

A. 557 FT/SEC TIP SPEED (RUN 7)

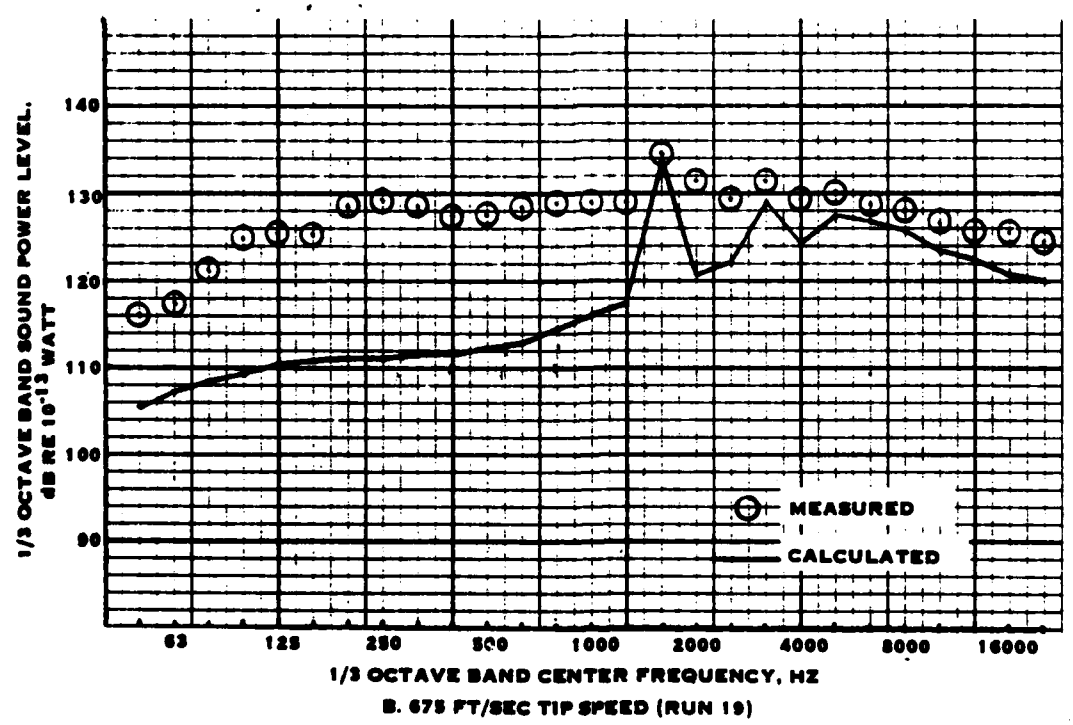

B. 675 FT/SEC TIP SPEED (RUN 19)

FIGURE 5-24. COMPARISON OF MEASURED AND CALCULATED 1/3 OCTAVE BAND SOUND POWER SPECTRA FOR THE 1.5 FT DIAMETER FAN

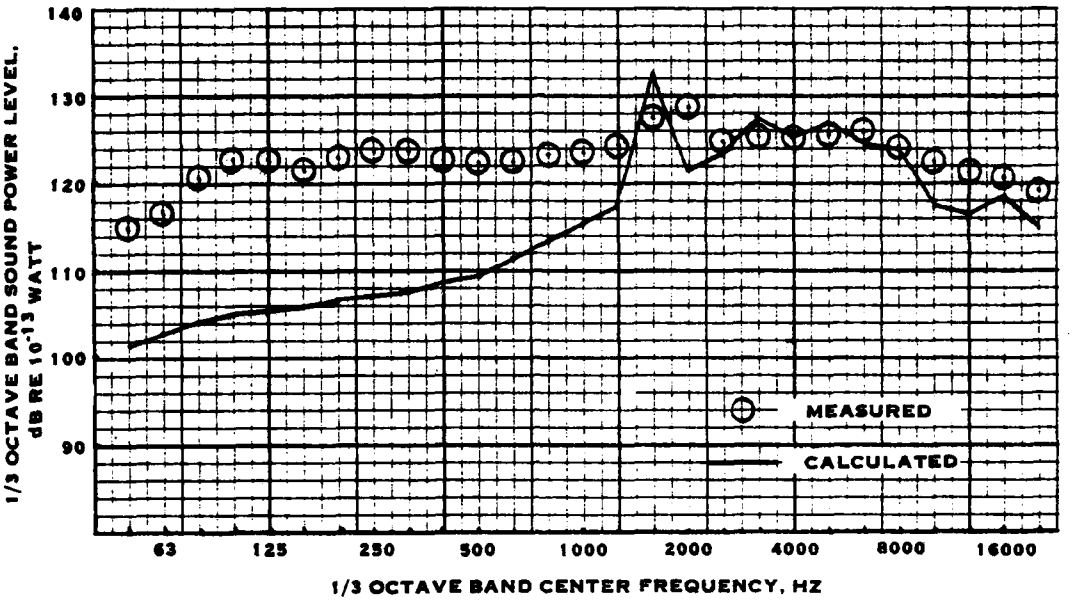

C. 697 FT/SEC TIP SPEED (RUN 11)

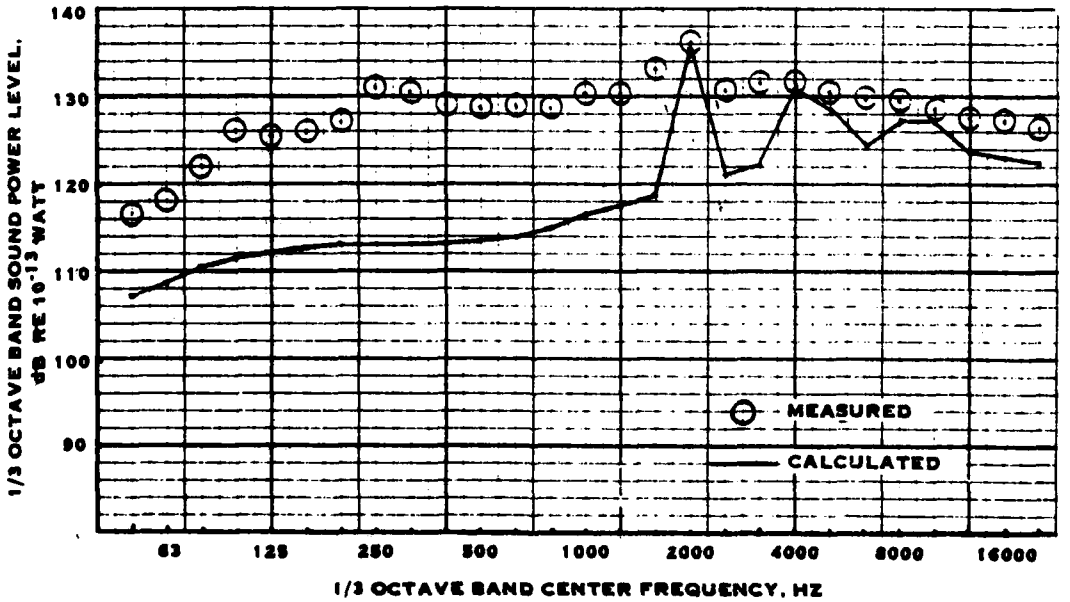

D. 703 FT/SEC TIP SPEED (RUN 20)

FIGURE 3-24. CONTINUED

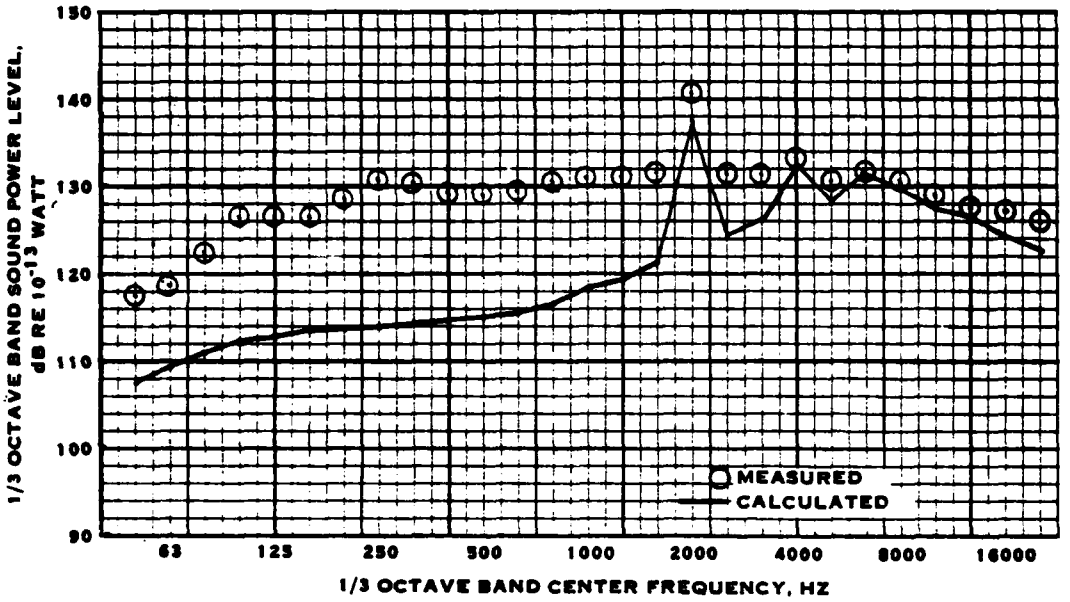

E. 757 FT/SEC TIP SPEED (RUN 22)

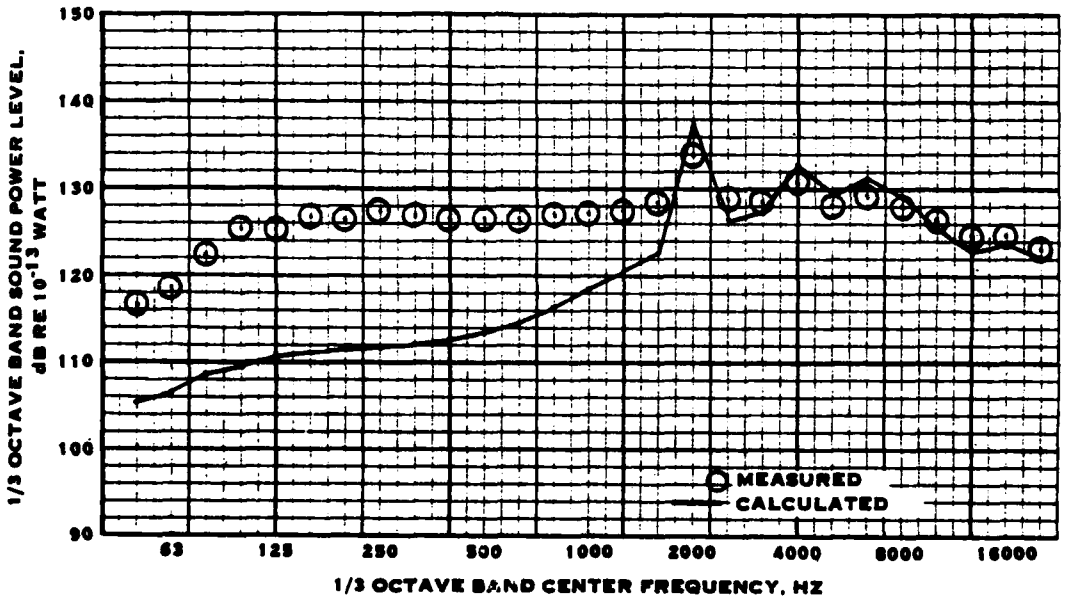

F. 811 FT/SEC TIP SPEED (RUN 18)

FIGURE 5-24. CONCLUDED

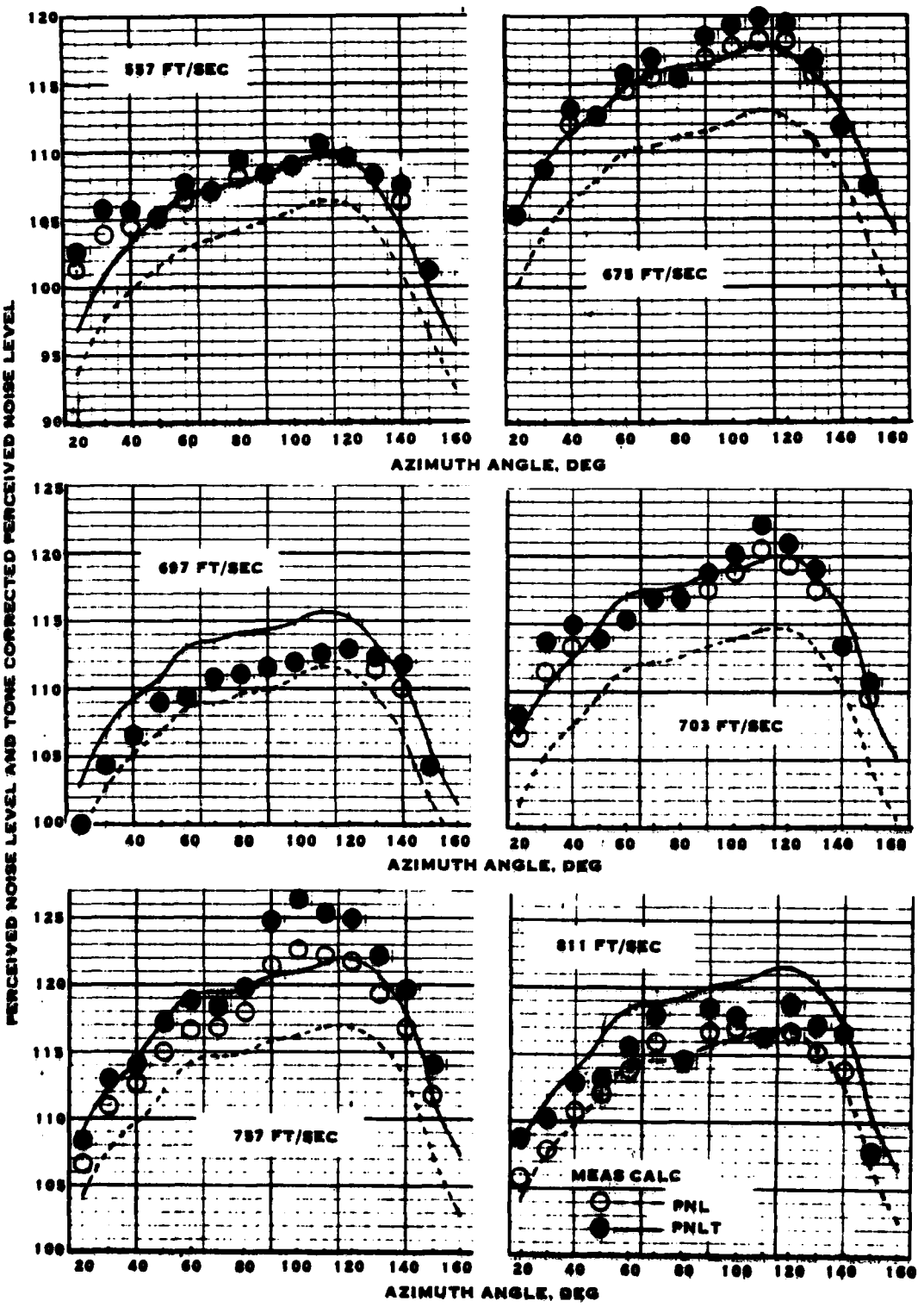

FIGURE 5-25. COMPARISON OF MEASURED AND CALCULATED PNL AND PNLT FOR THE 1.5 FT DIAMETER FAN

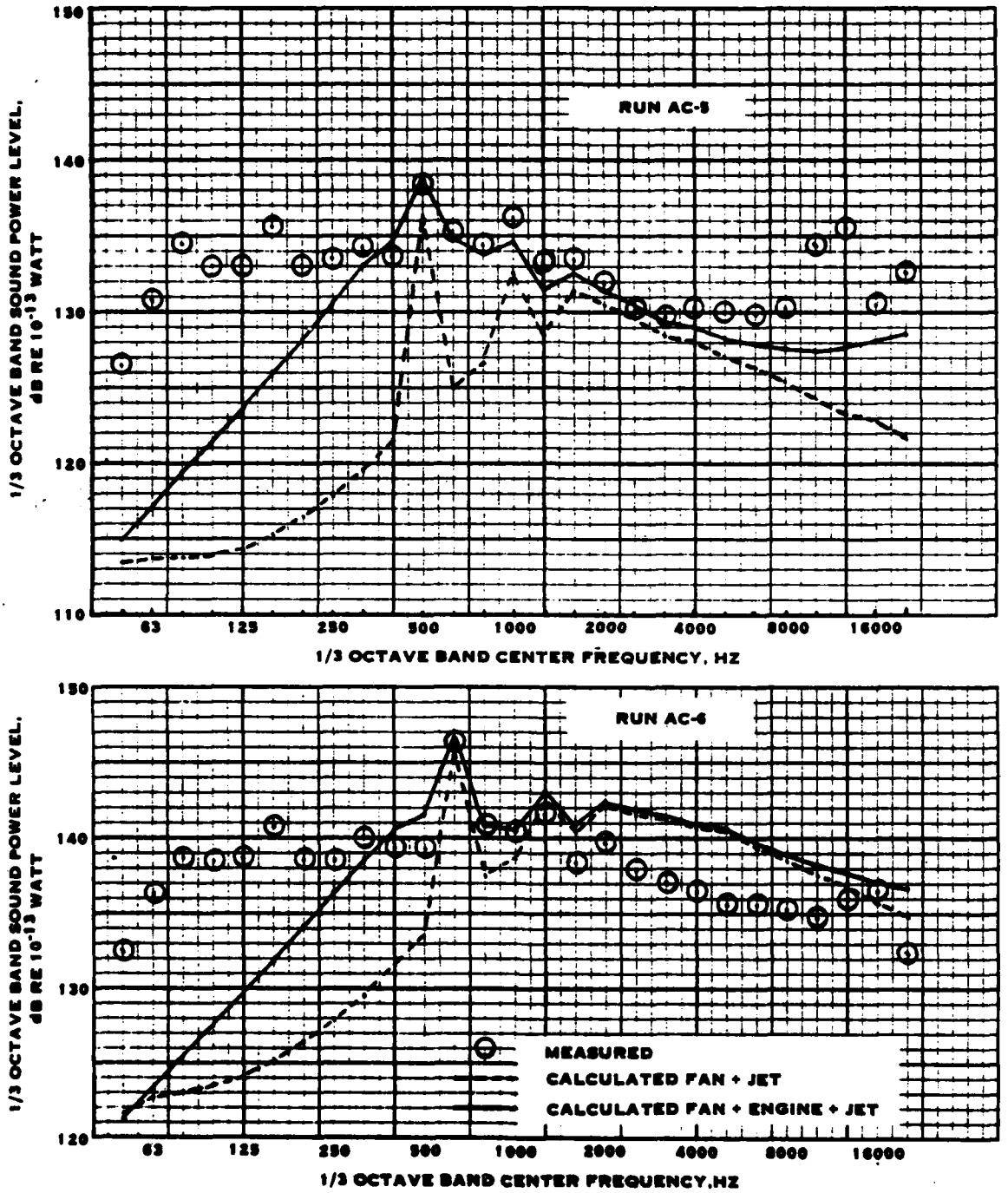

FIGURE 5-26. COMPARISON OF MEASURED AND CALCULATED 1/3 OCTAVE BAND SOUND POWER SPECTRA FOR THE 4.6 FT DIA FAN

Figure 5-27 shows the comparison of measured and calculated sideline PNL and PNLT. For both conditions, the test data and calculated tone corrections are about the same. Run AC-5 shows excellent agreement between measurements and calculations, especially near the peak in the region 100 to 120 degrees. Run AC-6 is well predicted in the front quadrant, but slightly overpredicted in the aft quadrant. The measurements indicate a peak PNL of 119.9 PNdB and peak PNLT of 121.3 PNdB, whereas the calculated peak PNL is 123.1 PNdB and peak PNLT is 124.5 PNdB for an overprediction of run AC-6 of about 3 dB.

Summary for Variable-Pitch Fans

The calculations show generally good agreement with the available data. Both fan tones and broadband noise are well predicted. Limited data on a fan tested in a wind tunnel showed good correlation with calculations of forward-flight effects. Data acquired on two fans, one driven by an electric motor and one driven by a turboshaft engine, show high levels of low-frequency noise which are not well predicted. However, this does not appreciably influence the perceived noise levels of the fans. The correlation between measured and calculated sideline PNL and PNLT is generally within about ± 3 dB, with good agreement in directivity.

EVALUATION OF FIXED-PITCH FAN NOISE PREDICTION

Introduction

Much of the available data on fixed-pitch fans were acquired on total engines either installed on test stands or installed on airplanes and tested in flyover. As such, these data include noise contributions from core engines. Also, the data from real installations contain installation effects, such as shielding from wings and fuselages, propagation through wing wakes, ingestion of fuselage and wing vortices, etc. These effects were previously described under the discussion of forward-flight effects. Low-bypass-ratio fans generate significant jet noise in addition to fan and core engine noise. Finally, much data has been obtained from configurations which have some acoustic treatment in the fan and core engine flow ducts.

Thus, it is not possible to directly evaluate the fan noise prediction methodology, with the possible exception of fan tones, from real engine data as those include many other sources of noise which may be as significant as the fan noise. However, a series of fans driven by electric motors has been tested at NASA-Lewis. These fans were tested statically, and the noise measurements are fairly representative of noise from isolated fans, except for fan discharge jet noise (which due to relatively low velocity is not generally dominant). Several fan configurations were also tested with inlet and outlet noise suppressors. It is thus possible to evaluate the fan noise prediction methodology using the data from these fans, and also evaluate the effects of acoustic treatment.

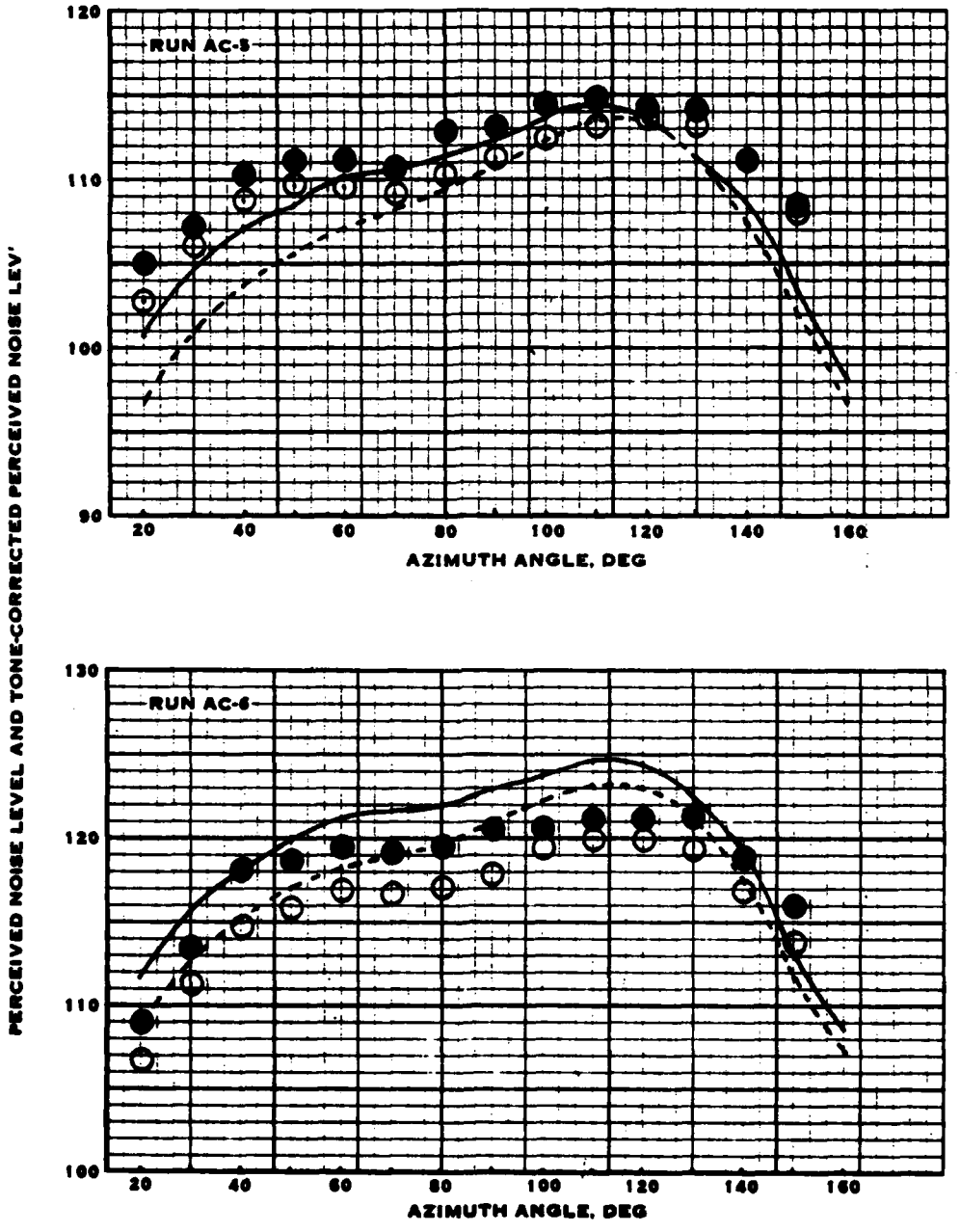

FIGURE 5-27. COMPARISON OF MEASURED AND CALCULATED PERCEIVED AND TONE-CORRECTED PERCEIVED NOISE ON A SIDELINE FOR THE 4.6 FT DIAMETER VARIABLE PITCH FAN

In this section, the fan noise prediction methodology will first be evaluated using isolated static fan noise data including the effects of acoustic treatment. Then, the noise of fans driven by core engines will be evaluated. Finally, the fan noise prediction methodology will be evaluated using airplane flyover data.

Methodology Evaluation Using Isolated Static Fan Data

Data Catalog Item 21. - This data was acquired on a six-foot diameter fixed-pitch fan with a design pressure ratio of 1.5 at a tip speed of 1107 ft/sec. Data is presented for the fan operating at 60, 70, 80, and 90% of design tip speed. Although the data was acquired with microphones installed at the fan centerline height with noise propagation over hard ground, the sound power levels were calculated assuming radiation over a hemisphere, which essentially assumes a 3 dB correction for ground reflections. This appears to provide a fair estimate of free-field levels for frequencies above a few hundred Hertz.

Figure 5-28 shows the comparison of calculated and measured fan noise sound power level spectra for 60, 70, 80, and 90% of design tip speed. The correlation is seen to be quite good over the entire frequency range. At 90% of design tip speed condition, the low frequency noise below 500 Hz is calculated to be jet noise. This appears to be confirmed by the measurements.

Figure 5-29 shows the comparison between measured and calculated PNL's on a 1000 ft sideline. The measured levels are based on the test data extrapolated from a 100 ft radius to a 1000 ft sideline. The data was also reduced by 3 dB to correct it to equivalent free-field conditions. The data shows a pronounced depression in the directivity at 60 to 70 degrees which is not reflected in the calculations. However, the peak sideline is calculated to within 3 dB at 60% of design speed and within 2 dB at the three other speeds. At 80 and 90% of design speed, the agreement is good over the entire range of angles, except for the peak in the measurements shown at 50 degrees.

Data From Reference 13. - A fan very similar to the one described above was tested earlier with noise suppressors in the inlet and exhaust. Since installed fans typically utilize acoustic treatment, the evaluation of the noise prediction methodology for fixed-pitch fans for those installations requires a performance assessment of the duct treatment methodology. Reference 13 presents noise measurements made on an isolated fixed-pitch fan which was tested statically with and without noise suppressors. Since the fan was driven by an electric motor, the only noise sources are the fan and the fan jet.

In defining the acoustic treatment, it should be noted that the existing methodology does not recognize subtleties in fan geometry. For instance, the fan described in reference 13 changes diameter through the fan rotor stage. Thus, the rotor tip diameter is 71.81 inches, while the stator tip diameter is 67.94 inches and the discharge duct diameter is 68.06 inches. Similarly, the rotor hub-to-tip ratio (at the inflow face) is 0.50, while the discharge duct has a "hub-to-tip" ratio of 0.58.

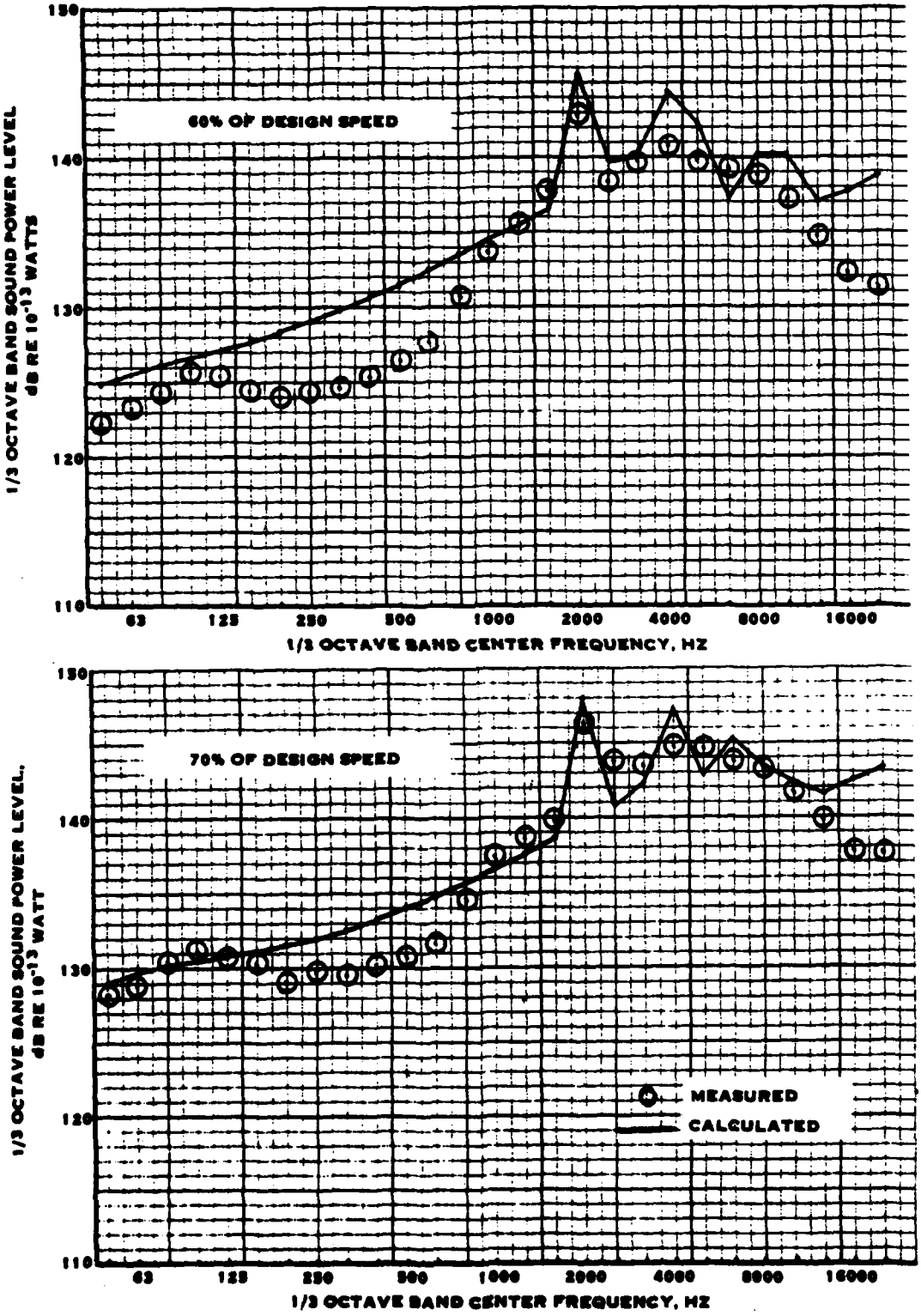

FIGURE 5-28. COMPARISON OF MEASURED AND CALCULATED QF-2 FAN NOISE LEVEL (FROM DATA CATALOG ITEM 21)

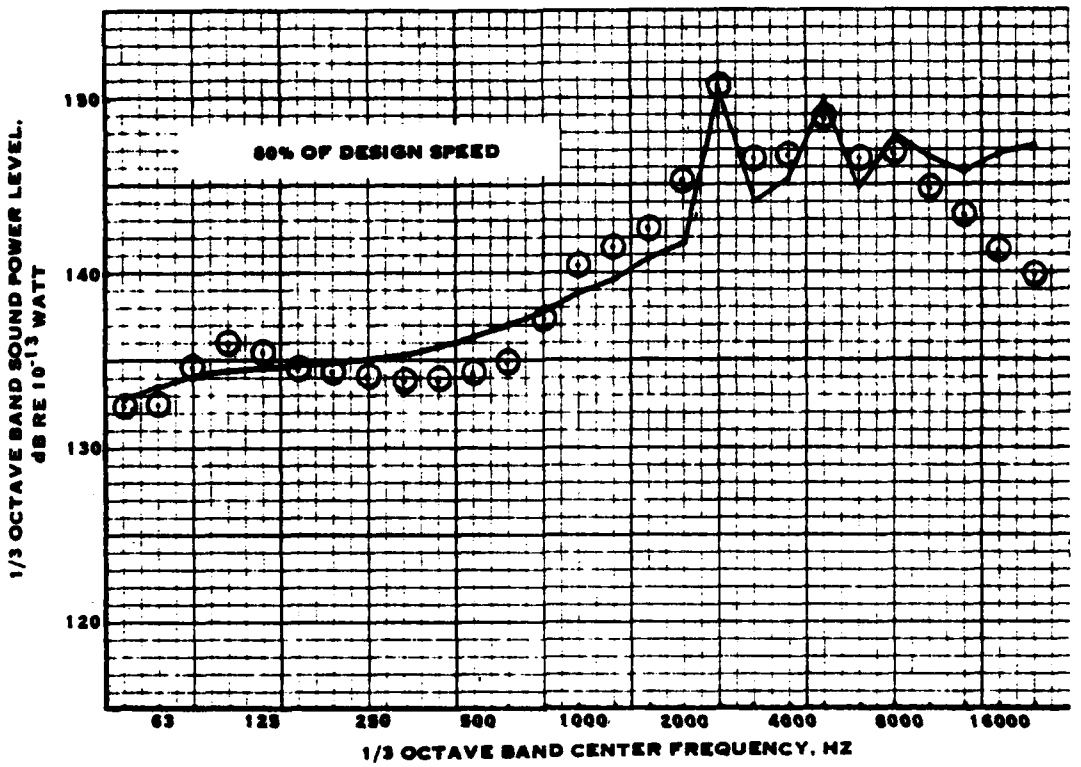

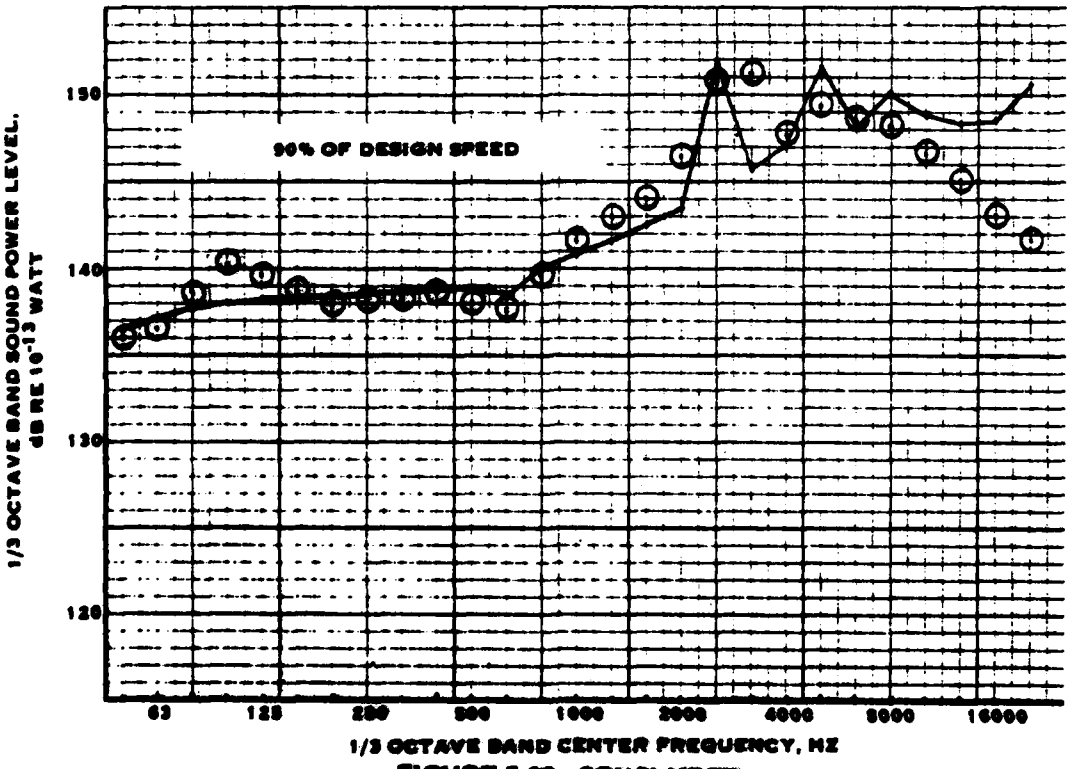

FIGURE 5-28. CONCLUDED

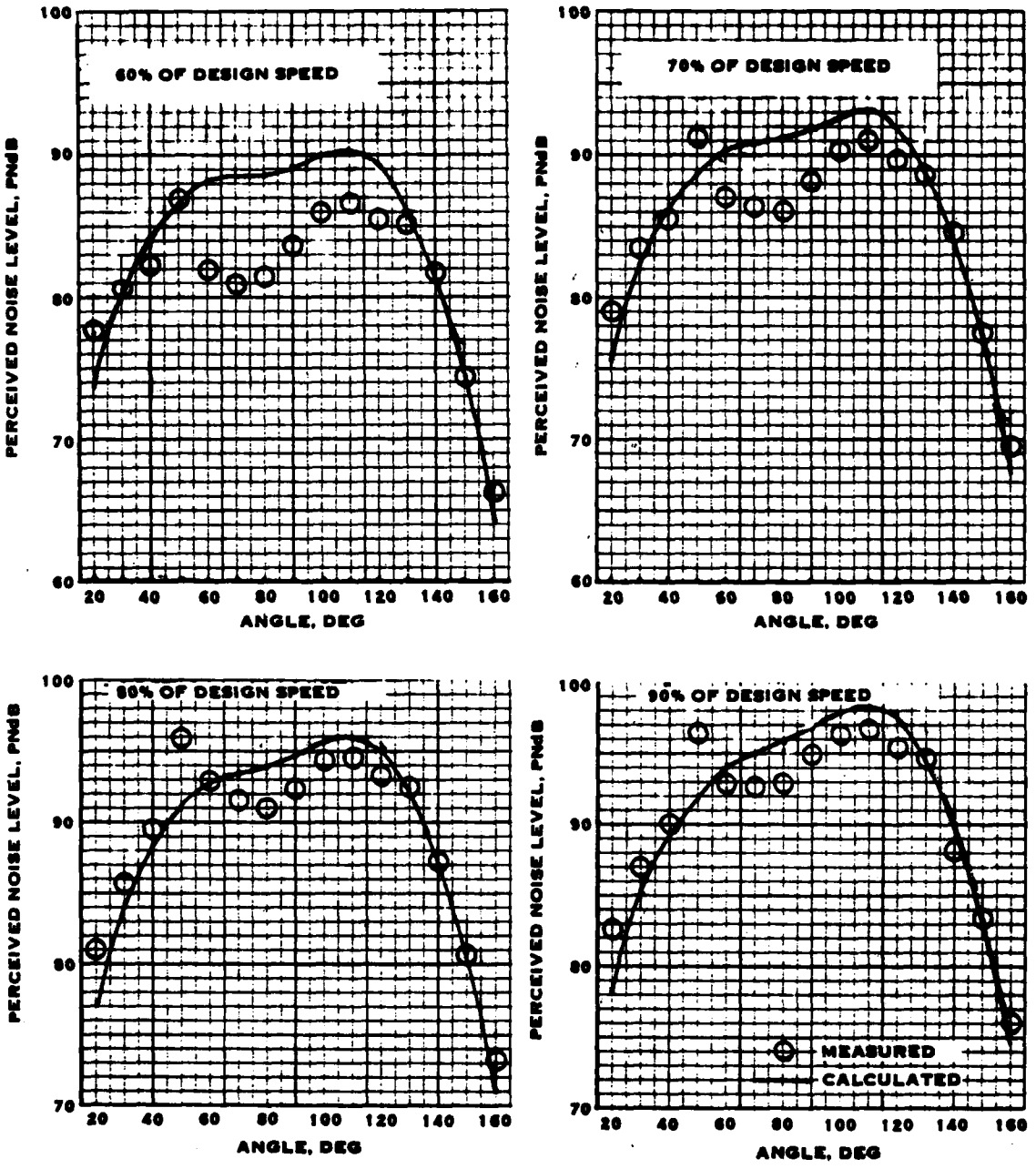

FIGURE 5-29. COMPARISON OF MEASURED AND CALCULATED SIDELINE PERCEIVED NOISE LEVELS FOR THE QF2 FAN

The only inputs to the noise prediction methodology are the fan rotor diameter (location 78) and the fan rotor hub-to-tip ratio (location 82). These are assumed constant throughout the fan. The acoustic treatment attenuation is calculated primarily from the length-to-height ratio of the treated flow (acoustic) channel. It is thus necessary to adjust the treatment definition inputs to match the actual treatment length-to-height ratio. The recommended procedure for making predictions for such a fan stage is shown in the following example.

The noise suppression used on this fan is defined in figure 5-30. This consists of a 3-ring inlet and a straight exhaust duct with no flow splitter. First, the approximate treatment length-to-flow channel height of the inlet is calculated. The graphical procedure, in volume II of reference 1, may be referred to for clarification of the following discussion. The innermost flow channel has a height of 3.56 inches. Since it is treated on one side only, the height will be assumed to be twice that, or 7.12 inches. The treatment length is 25 inches for a length-to-height ratio of 3.51. The next passage has a height of 7.12 inches between treatment surfaces. The two-side treatment length is 25 inches (again length-to-height ratio of 3.51) with a one-side treatment length of 2 inches. Thus, the total effective length-to-height ratio for this passage is 3.51 + 0.14 = 3.65. The third flow passage has a height of 7.62 inches for a length of 27 inches, then an effective height of 15.24 inches for a length of 3 inches, then an effective height of 40.12 inches for a length of 4 inches for a total length-to-height ratio of 3.54 + 0.20 + 0.10 = 3.84. Finally, the outer duct has a passage height of 7.96 inches for a length of 34 inches, an effective height of 15.92 inches for a length of 3 inches, and an estimated effective height of 45.8 inches for a length of 21 inches for a total length-to-height ratio of 4.27 + 0.19 + 0.46 = 4.92. Since these passages are in parallel, the total length-to-height ratio is the treatment area weighted average of the length-to-height ratios of the four passages, or about 4.37. With an input fan diameter of 6 ft and a hub-to-tip ratio of 0.50, the passage height will be calculated to be 18 inches. Thus, for a length-to-height ratio of 4.92, the treatment length will be 78.66 inches. This could be input as such with no splitters, or the treatment can be defined to have 3 splitters. In the latter case, the passage height is reduced by a factor of 4, so that to maintain the desired length-to-height ratio of 4.37, the length required is 19.67 inches, or 27% of the fan diameter. The inlet treatment definition to be used in the calculations is then a length of 27% of the diameter, 2 degrees-of-freedom, and 3 flow splitters.

The exhaust treatment is simpler. The treatment length is 88 inches, with a passage height of 14.28 inches for a length-to-height ratio of 6.16. Since the passage height will be assumed to be 18 inches instead of the actual 14.28 inches, the treatment length must be input as 110.92 inches, or 154% of the fan diameter, to obtain the desired length-to-height ratio of 6.16. The inputs for the exhaust treatment are then a length of 154% of the diameter with no flow splitters.

The results of the calculations are compared to the measurements in figure 5-31 for two fan speeds. Although the comparison between measured and calculated fan noise levels is not very good (which is suprising, as excellent correlation was obtained in

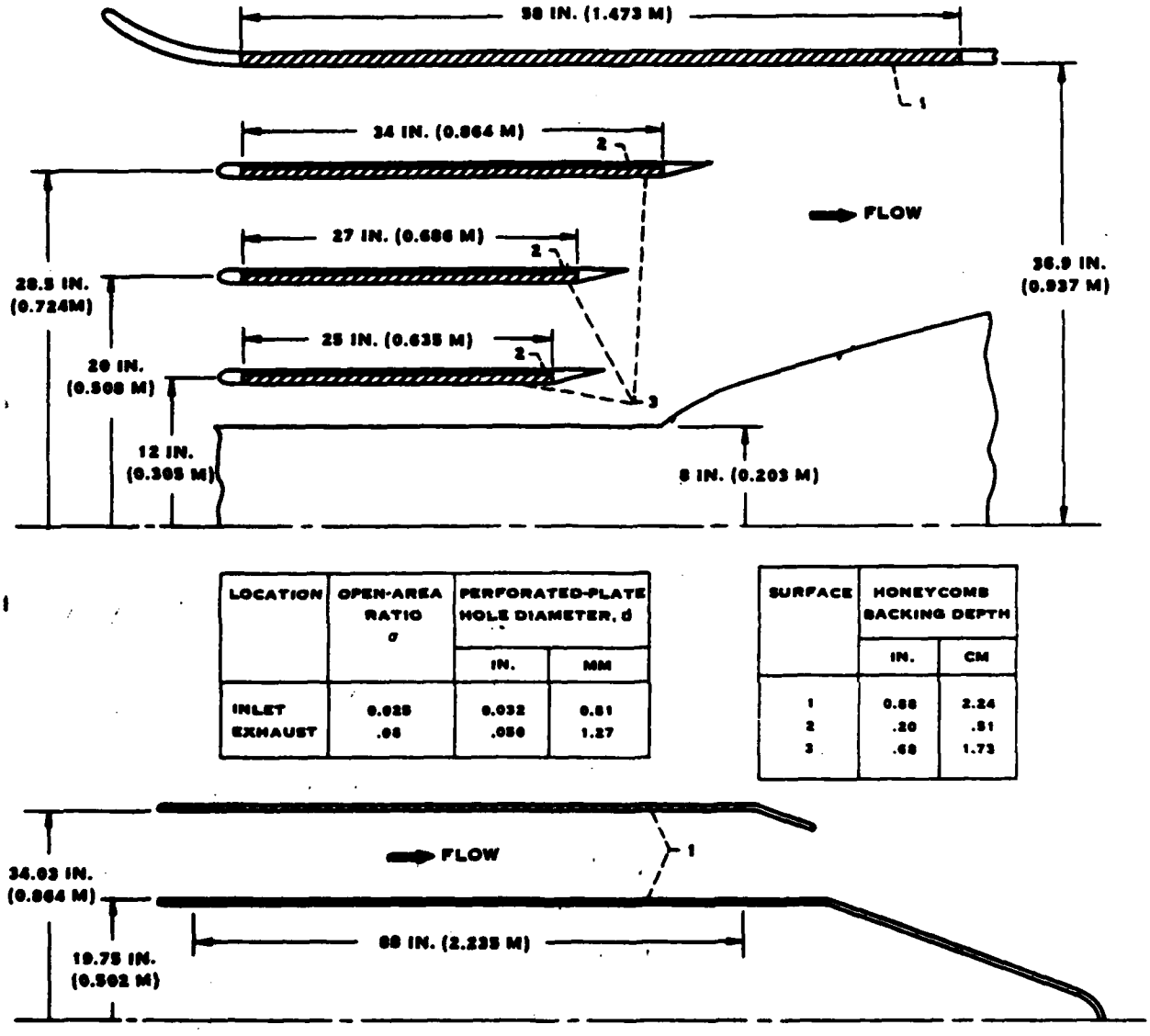

LOCATION	OPEN-AREA RATIO σ	PERFORATED-PLATE HOLE DIAMETER, d	
		IN.	MM
INLET	0.025	0.032	0.81
EXHAUST	.05	.050	1.27

SURFACE	HONEYCOMB BACKING DEPTH	
	IN.	CM
1	0.88	2.24
2	.20	.51
3	.68	1.73

FIGURE 5-30. DEFINITION OF FAN NOISE SUPPRESSORS (FROM REFERENCE 13).

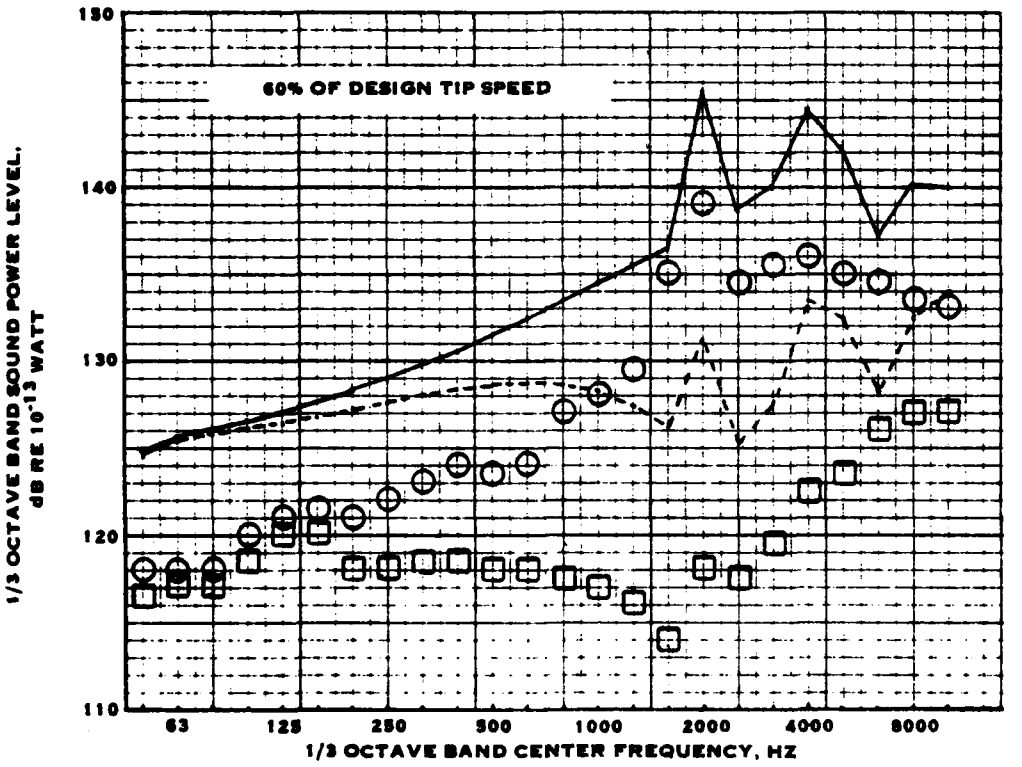

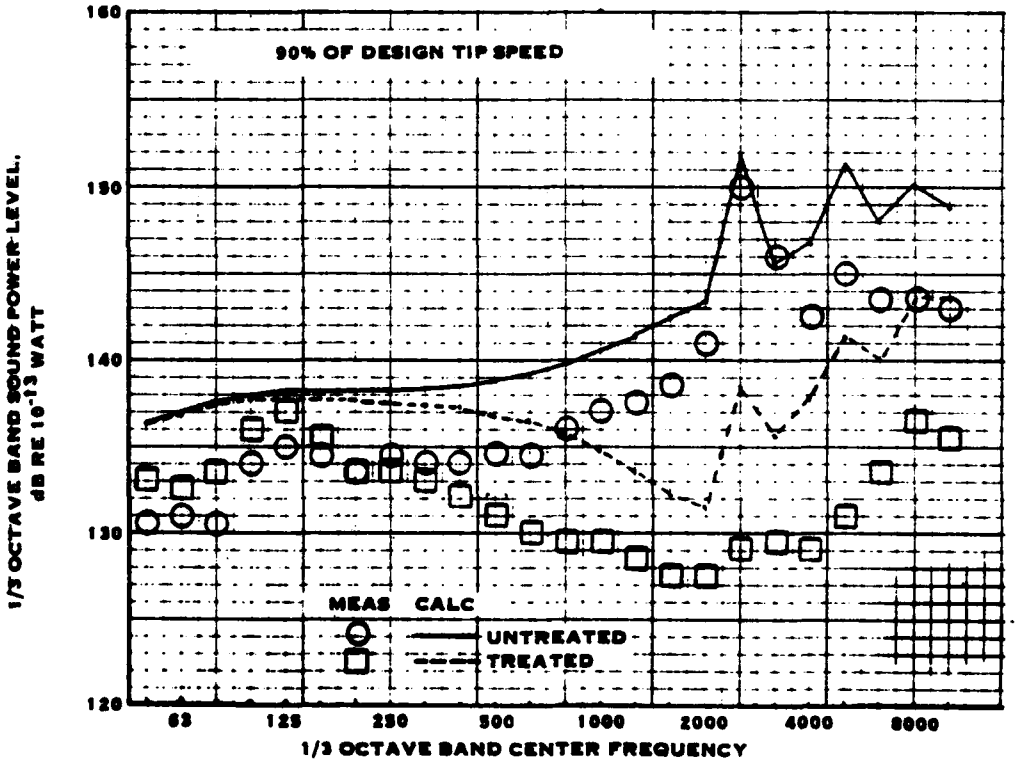

FIGURE 5-31. COMPARISON OF MEASURED AND CALCULATED FAN NOISE FROM REFERENCE 13 SHOWING THE EFFECTS OF NOISE SUPPRESSORS

the previous comparison for a similar fan), the trends between untreated and treated levels are similar for calculation and measurement.

Figure 5-32 shows the effect of the treatment on sideline noise. To account for ground reflection, the measured levels were reduced by 3 dB to adjust the test data to free-field noise levels. As had been observed earlier, the measured levels show a stronger lobe in the forward directivity than is calculated. However, the calculations show a reduction of about 8.5 PNdB in peak sideline noise which compares fairly well with measured reductions of 14 and 12 PNdB for approach and takeoff conditions, respectively. The reason for the better-than-predicted performance of the suppressors can be seen in figure 5-33, which shows a comparison of measured and calculated noise suppressor acoustic performance based on the sound power levels from figure 5-31. The correlation is good, especially for the 90% rpm condition, except for the peak attenuation. The peak value of 21 dB measured exceeds the peak of 14 dB calculated. It may be noted that this occurs in the bands containing the fan fundamental tone. This implies that the treatment is more effective in attenuating tones than in attenuating broadband noise. It can be seen in figure 5-31 that the measured spectra with suppressors show full elimination of the fan fundamental tone, thus showing better acoustic performance for the tones than for the broadband noise adjacent bands. An alternative explanation is that the acoustic treatment generates noise due to grazing air flow on the material. The noise generated is broadband and equilibrium is reached when the generated noise is attenuated to the observed noise level. This is typically results in a noise "floor" which limits the attenuation which can be obtained, i.e. increasing the amount of acoustic treatment does not result in additional attenuation. The attenuation of tones which exceed the broadband noise in level will be greater, as they will be attenuated to the full capability of the treatment. Thus, the higher than calculated sideline perceived noise attenuation is largely due to the better performance of the noise suppressors on the fan fundamental tone.

Since the general case is for attenuation of broadband noise and the self-generated noise of the treatment is not readily calculated, revisions to the methodology are not warranted on the basis of these data.

Data Catalog Item 25. - This fan is similar to the one described previously, i.e. six feet in diameter with the design pressure ratio of 1.5 being achieved at transonic tip speed. This fan was also tested with and without noise suppressors. Figure 5-34 shows the comparison between measured and calculated one-third octave band sound power level spectra for 60, 70, 80, and 90% of design tip speed and with and without noise suppressors. The bare fan at 60% of design speed is overpredicted, but the agreement is better at the higher fan speed conditions. The fan noise data for the configuration with noise suppressors is fairly well predicted for the four conditions.

Figure 5-35 shows the comparison of measured and calculated perceived noise on a sideline. As expected from figure 5-34, the levels for the bare fan are overpredicted. The levels for the configurations with noise suppressors are better predicted. Finally, figure 5-36 shows the comparison between measured and calculated noise suppressor

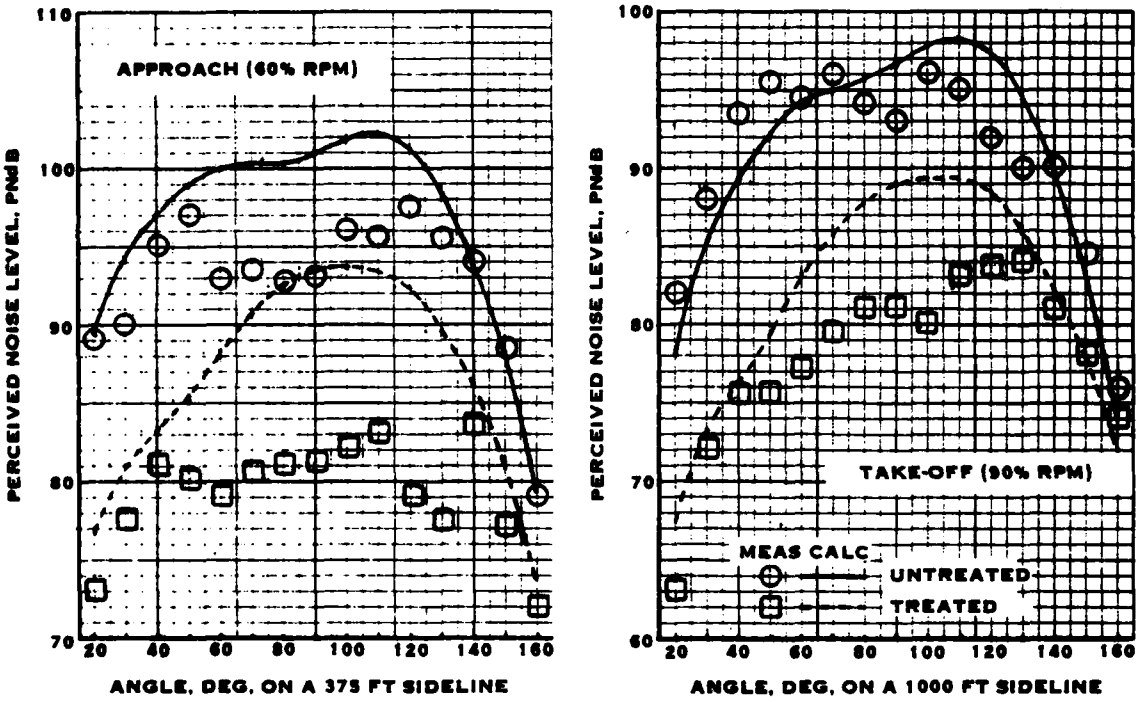

FIGURE 5-32. COMPARISON OF MEASURED AND CALCULATED SIDELINE PERCEIVED NOISE FOR THE FAN OF REFERENCE 13

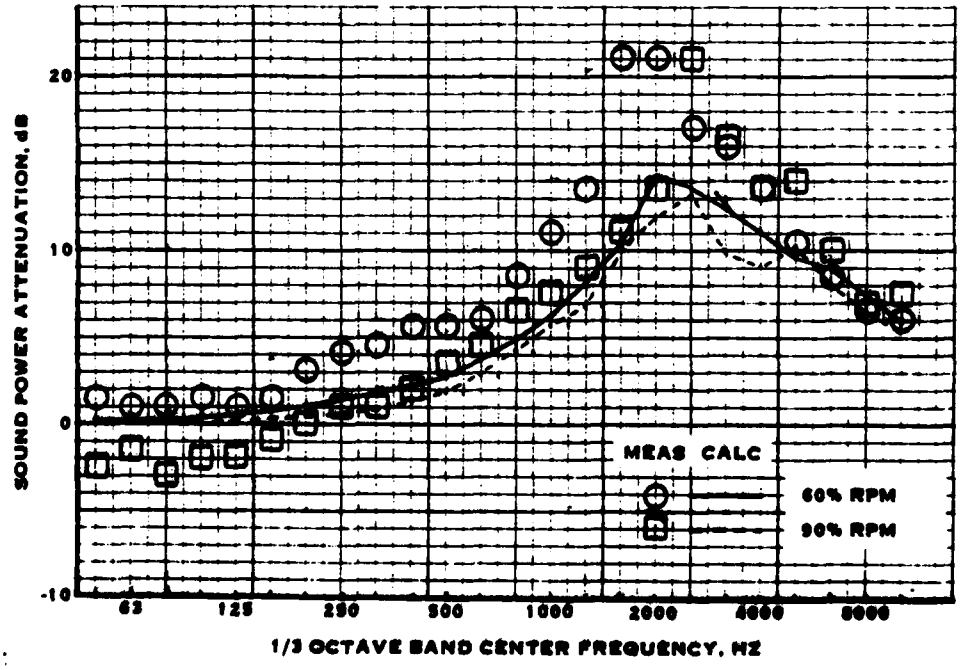

FIGURE 5-33. NOISE SUPPRESSOR ACOUSTIC PERFORMANCE

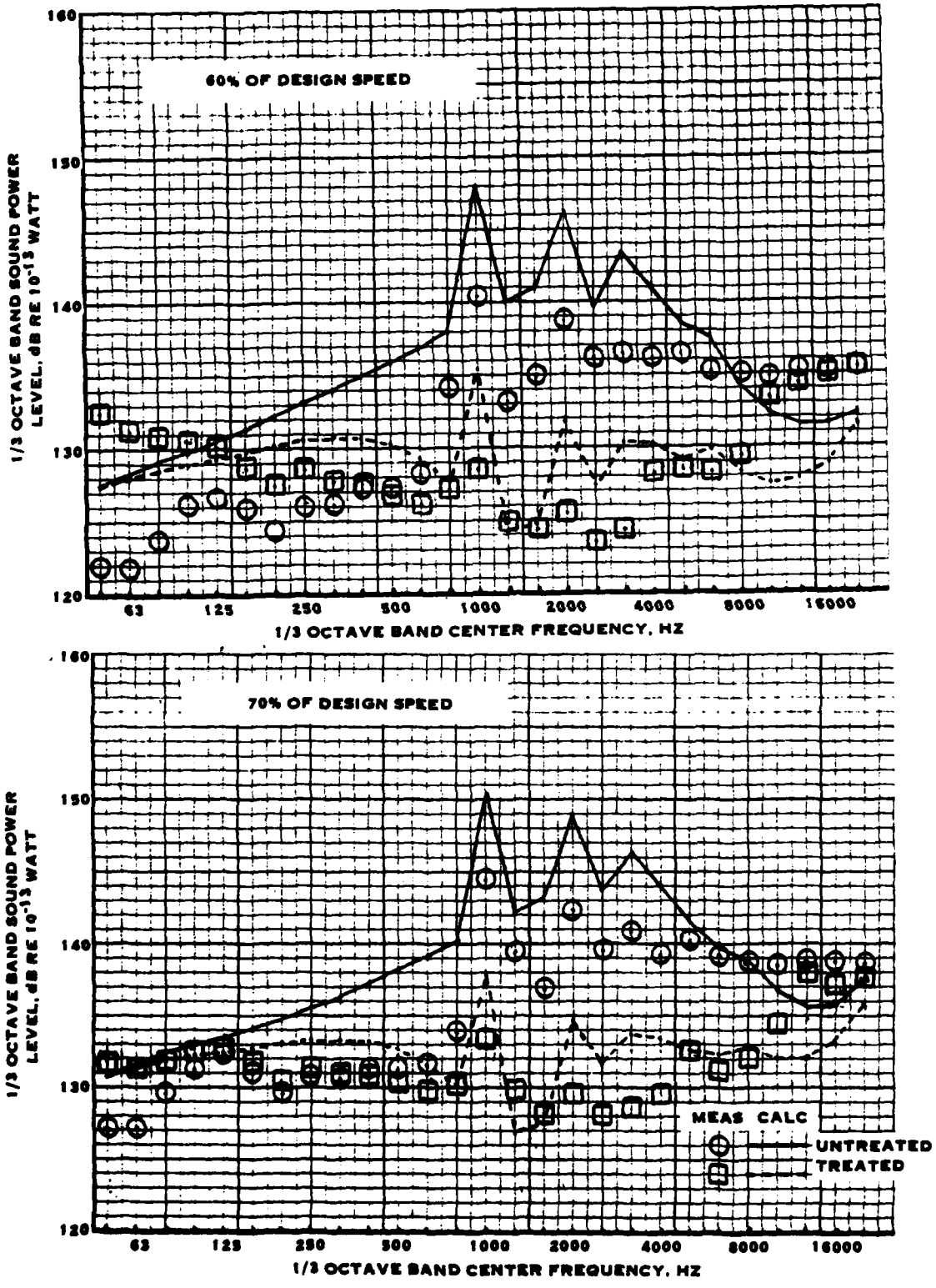

FIGURE 5-34. COMPARISON OF MEASURED AND CALCULATED FAN NOISE FROM DATA BASE ITEM 25.

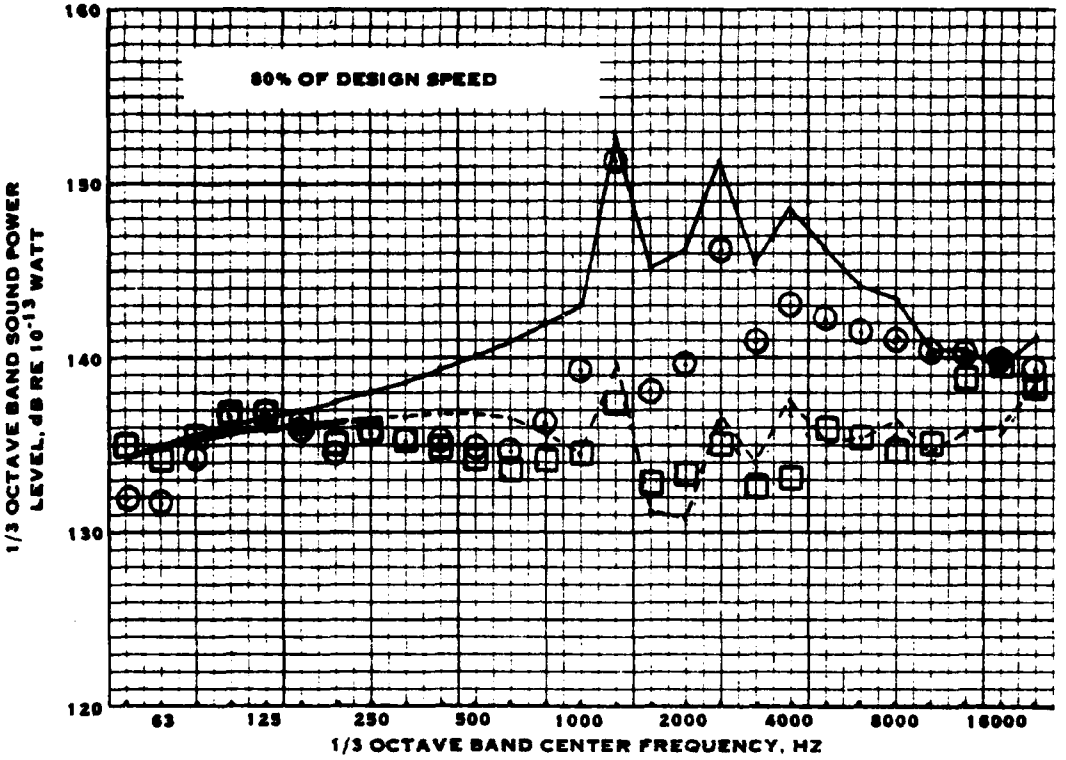

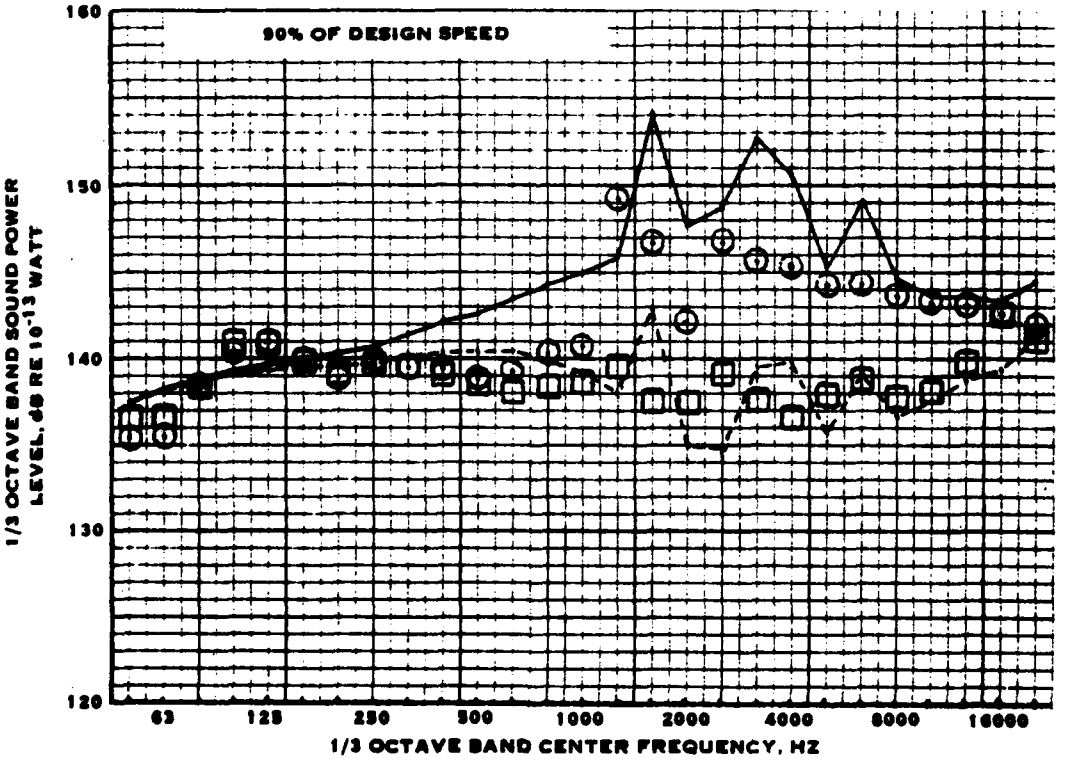

FIGURE 5-34. CONCLUDED

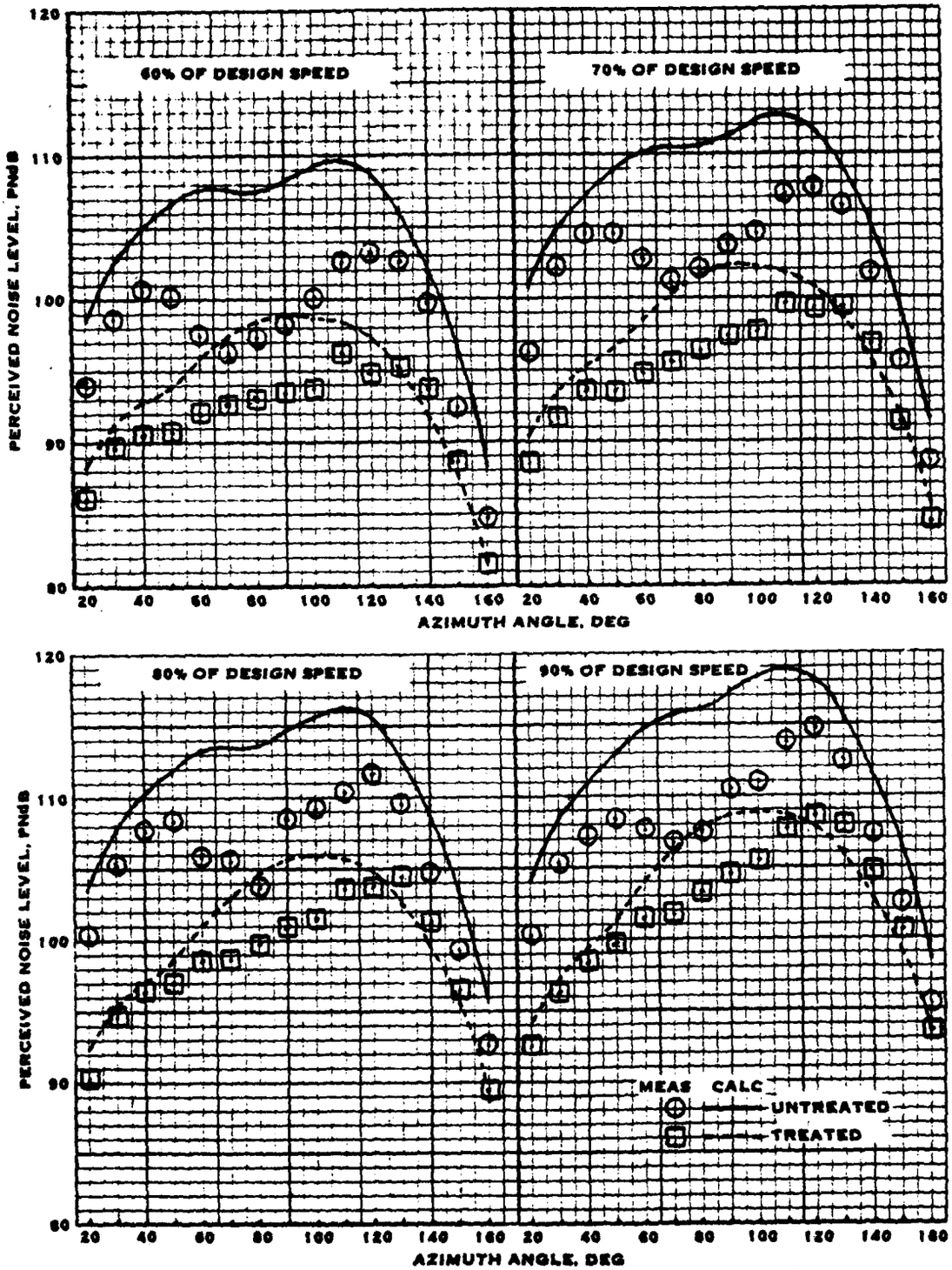

FIGURE 5-35. COMPARISON OF MEASURED AND CALCULATED SIDELINE PERCEIVED NOISE FOR THE DATA FROM DATA BASE ITEM 25

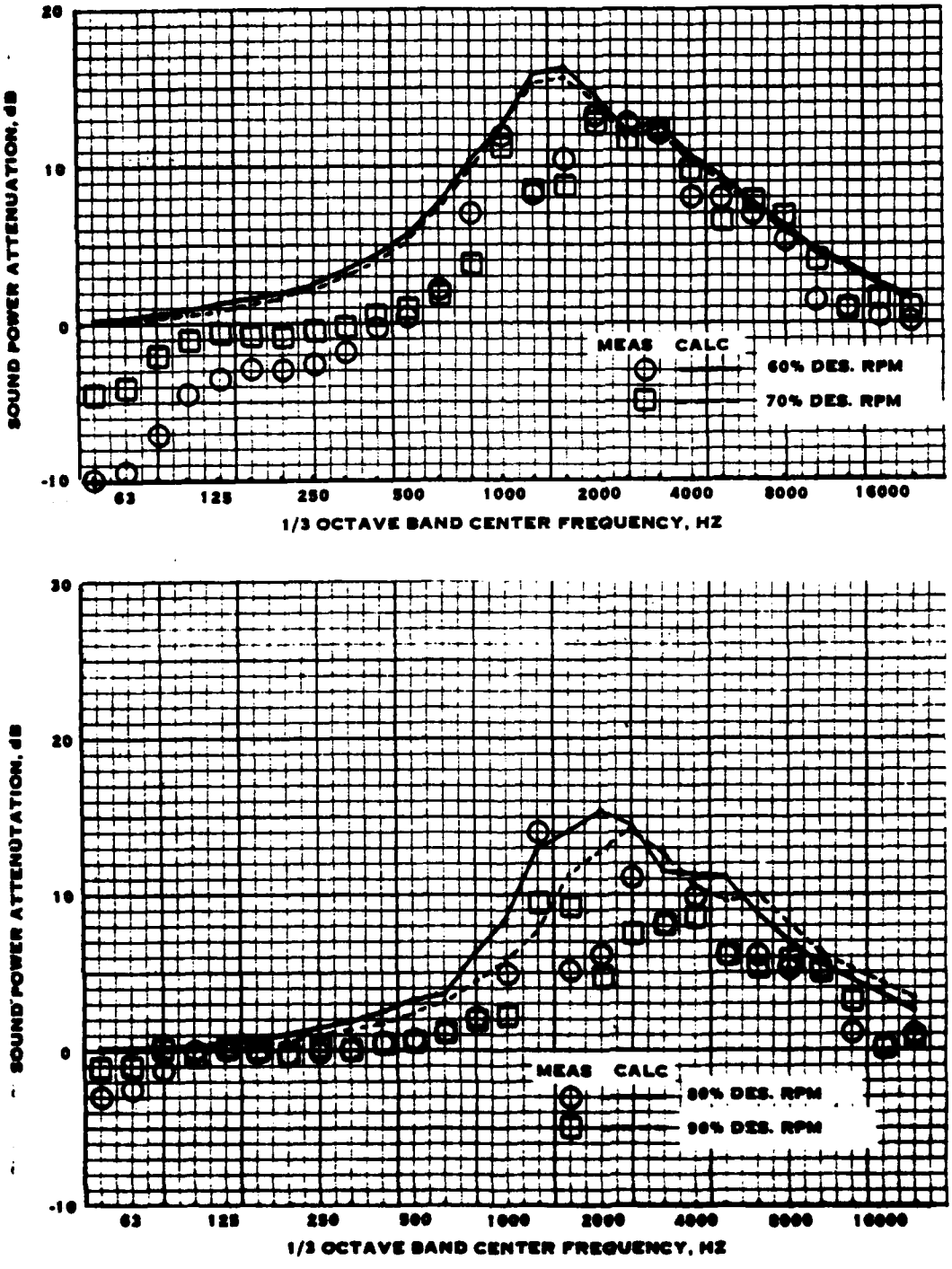

FIGURE 5-36. COMPARISON OF MEASURED AND CALCULATED NOISE SUPPRESSOR PERFORMANCE FROM DATA BASE ITEM 25

acoustic performance. These were derived from the data plotted in figure 5-34. The negative values for the measured attenuation indicate that the noise levels with the suppressors installed were higher than those for the bare fan, which could be caused by self-generated noise. In spite of scatter in the measurements, the agreement between calculated and measured noise suppressor acoustic performance is good.

Methodology Evaluation Using Real-Engine Data

Data Catalog Item 20. - This data was acquired on a JT8D engine operating statically on a test stand. The data was acquired using ground level microphones. The noise measurements were thus adjusted to equivalent free-field conditions by subtracting 6 dB. Figure 5-37 shows the comparison of measured and calculated one-third octave band sound power level spectra for three operating conditions: take-off, cut-back at low gross weight, and low power. Since this is a complete engine, the noise contains contributions from sources other than the fan. The noise below 2000 Hz is calculated to be primarily jet noise with some contributions from the core engine. The peaks at 4000, 3150, and 2500 Hz for take-off, cut-back, and low power conditions, respectively, are the fundamental tones of the first fan stage. The higher bands contain combinations of first stage fan harmonics, tones from the second fan stage, and fan broadband noise. The jet noise is somewhat overpredicted, probably due to the retracted (enclosed) primary exhaust configuration of the JT8D engine. The fan noise is well predicted for the take-off and cut-back conditions, but is underpredicted at the low power condition. The underprediction at the low power condition may be due to high levels of fan tone noise due to ingestion of inflow turbulence, possibly ground vortices, as discussed earlier for the evaluation of forward flight effects.

Figure 5-38 shows the comparison of measured and calculated perceived noise levels on a 100-foot sideline. The measured directivity shows a substantial peak on a 100-foot sideline. The measured directivity shows a substantial peak at 90 degrees, which is not calculated. The other three points define a directivity which is in fair agreement with the calculations, although lower in level. Both the data and the calculations show a peak in the directivity at about 140 degrees for the take-off condition which shifts forward for the lower power conditions. This is indicative of jet noise dominance at take-off power with a shift to fan noise dominance at low power. It is apparent that the agreement in peak sideline noise (without including the 90 degree data) improves as engine power is decreased. This is in agreement with the data from figure 5-37.

Hamilton Standard Data Bank; DC9. - This data was acquired during airplane take-off and landing. Although no special precautions were taken to acquire free-field data, the microphone was located at about 12 feet above the ground plane (sand covered with tall grass). It was assumed that the ground reflection effects were negligible at mid- and high-frequencies.

Figure 5-39 shows the comparison between measured and calculated PNLT time histories for the airplane on take-off. Although the peak noise levels are in fair agreement, the measurements show a much shorter duration than the calculations. The

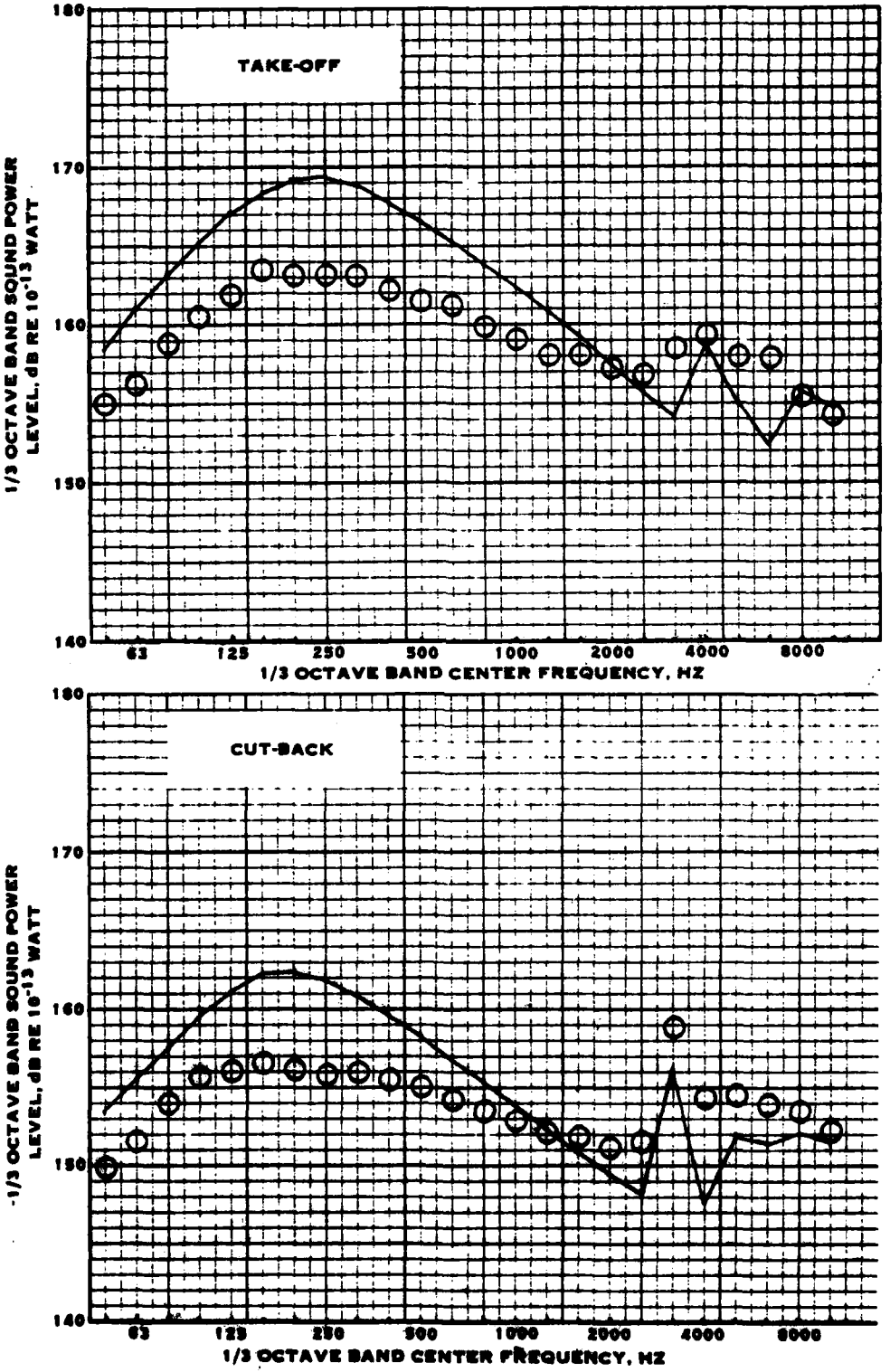

FIGURE 5-37. COMPARISON OF MEASURED AND CALCULATED 1/3 OCTAVE BAND LEVELS FOR THE JT8D FROM DATA BASE ITEM 20

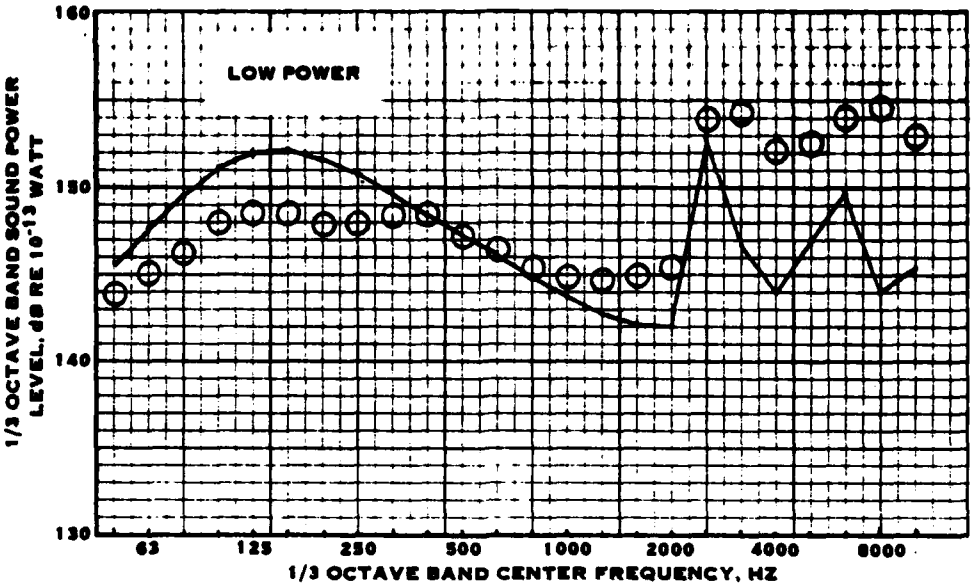

FIGURE 5-37. CONCLUDED

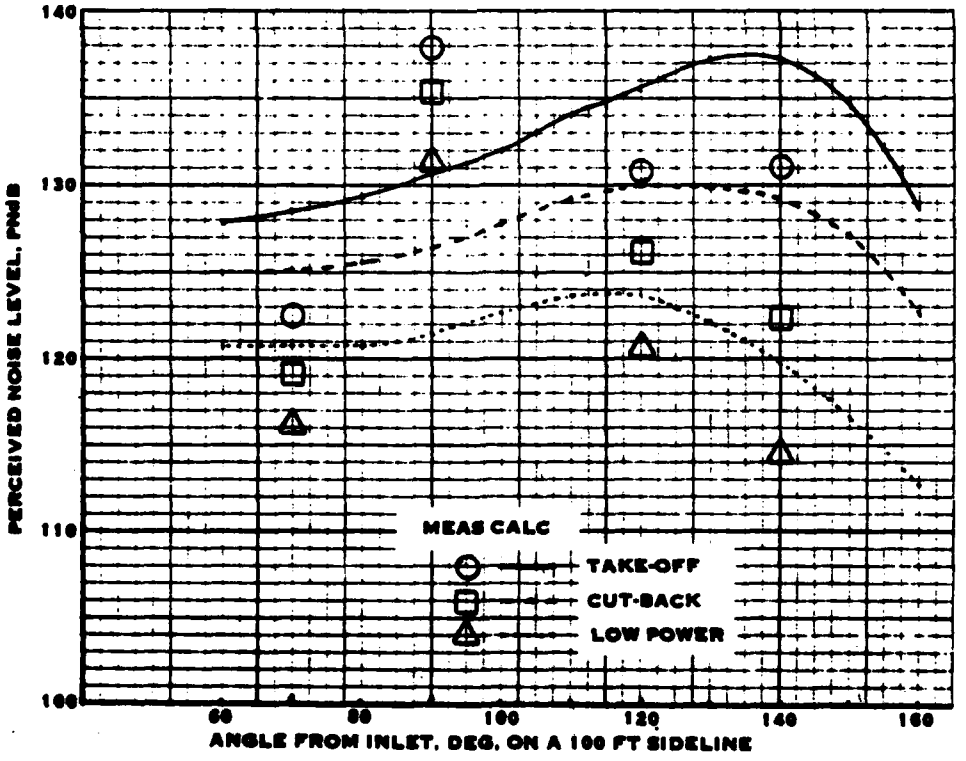

FIGURE 5-38. COMPARISON OF MEASURED AND CALCULATED SIDELINE PERCEIVED NOISE LEVEL FOR DATA BASE ITEM 20

more rapid drop in level in the aft quadrant could be due to a difference in calculated versus actual noise source contribution, while the more rapid drop in level in the front could be an installation effect, such as shielding from the wings.

Figure 5-40 shows a comparison of measured and calculated spectra for the maximum PNLT. As for the previous data on the JT8D engine, the calculations indicate higher jet noise than do the measurements. This may explain the longer calculated time duration after the peak noted in figure 5-39, as jet noise peaks near 140 degrees, well past the peak PNLT point and where directivity is not changing rapidly with time. While the jet noise appears overpredicted, the higher fan noise frequencies appear underpredicted. These effects tend to offset one another so that the correlation in peak PNLT, 117.4 calculated versus 115.1 measured, is close. For the total flyover, the calculated EPNL is 115.4 EPNdB versus 109.8 EPNdB measured. The larger difference between measured and calculated EPNL versus measured and calculated peak PNLT is, of course, due to the calculated longer time duration.

Figure 5-41 shows the PNLT time history during approach. For this condition, the agreement in the aft quadrant is better, because the jet noise is lower than it is for the take-off condition. The level of noise in the front quadrant still drops faster than shown by the calculations, again possibly due to shielding by the wings. The peak PNLT is calculated to be 116.0 PNdB versus 112.7 PNdB measured. The comparison in EPNL is 112.5 and 107.4 EPNdB for calculated and measured values, respectively.

Figure 5-42 shows the comparison of calculated and measured spectra at the peak PNLT point. The agreement in jet noise is better than it is for the take-off condition, although the high frequency fan noise is underpredicted.

Data Catalog Item 14. - In this program airplane flyover noise data were acquired during the evaluation of the refanned JT8D engines. The noise levels were measured using a four-foot high microphone at FAR Part 36 locations. The spectra were thus corrected to equivalent free-field conditions. This resulted in adjustments of up to 8.5 dB at 63 Hz and -3 dB for frequencies above 200 Hz. Engine data for two conditions, take-off with cut-back and 50 degree flap approach, were obtained for the calculations. Although the noise for the take-off condition was measured at ambient conditions of 52.5°F and 35% relative humidity, these could not be run on the computer because the very large values of atmospheric attenuation at 20,000 Hz for these ambient conditions cause underflow at the extremes of the directivity angles. Instead, the calculations were made assuming 70% relative humidity.

Figure 5-43 shows the comparison of measured and calculated PNLT time histories for the take-off condition. Both the calculations and the measurements show a fairly long duration. The calculations span about 26 seconds between the 10 dB-down points, while the measurements span about 20 seconds. The calculated peak PNLT is 90.0 PNdB, compared to 85.6 PNdB measured (but adjusted for ground reflections effects). The EPNL comparison is 90.7 EPNdB verus 85.2 EPNdB calculated and measured, respectively.

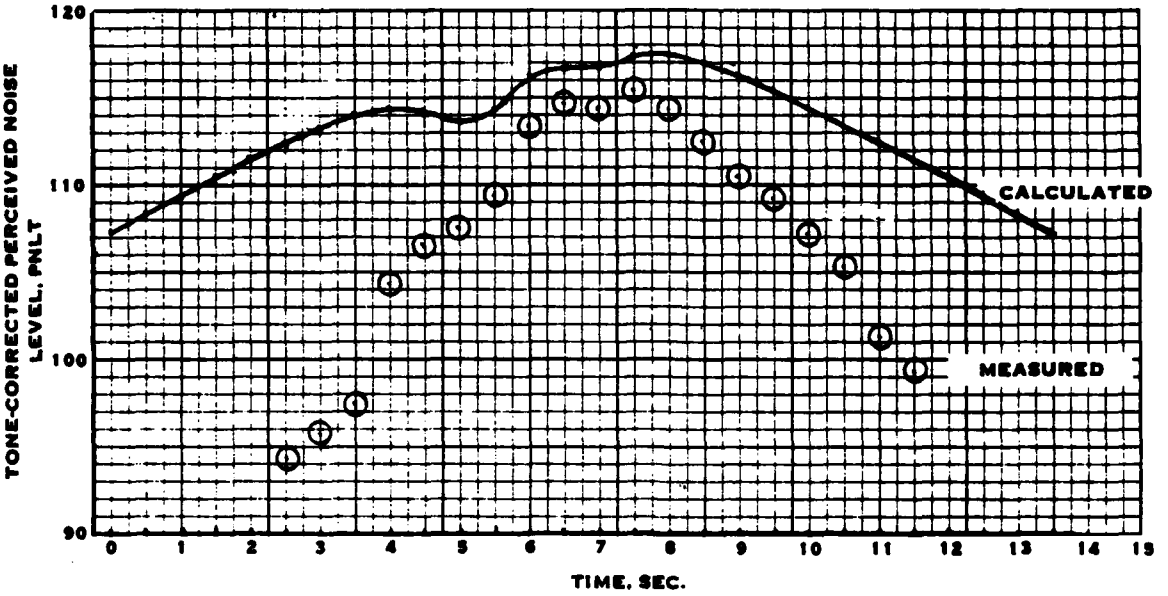

FIGURE 5-39. FLYOVER TIME HISTORY FOR THE DC9 AIRPLANE ON TAKE-OFF

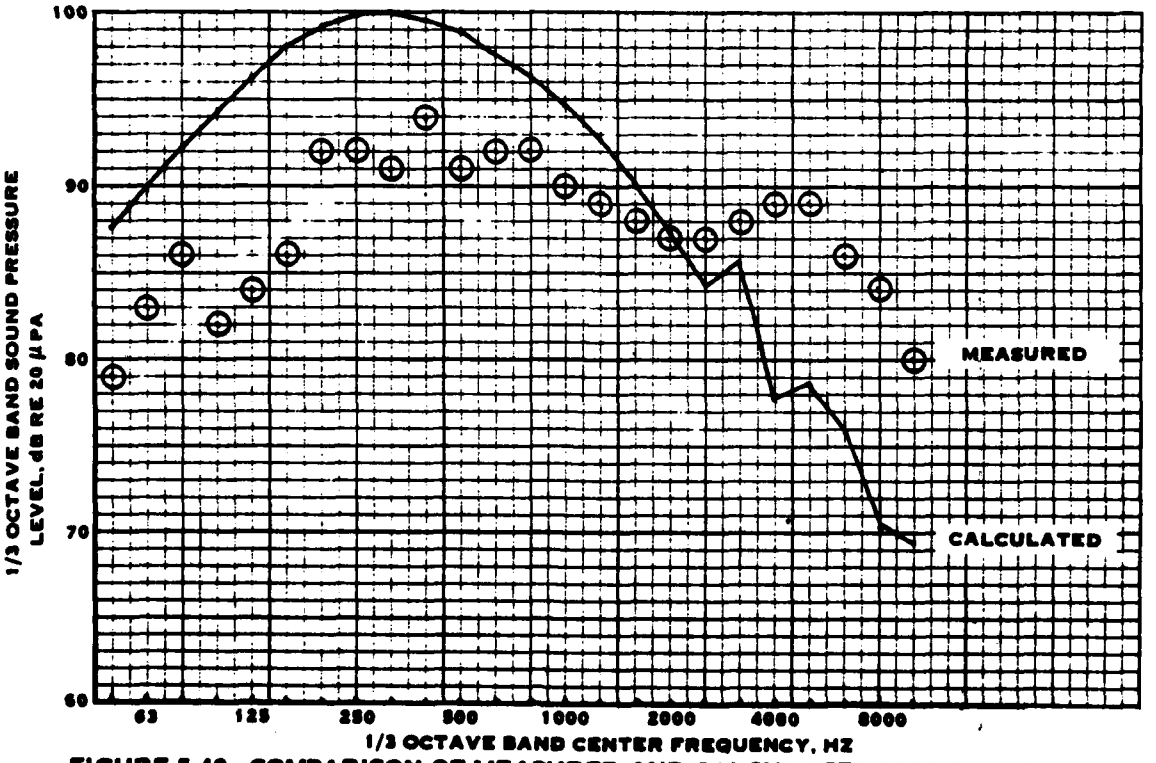

FIGURE 5-40. COMPARISON OF MEASURED AND CALCULATED SPECTRA FOR THE DC9 ON TAKE-OFF AT THE PEAK PNLT POINTS

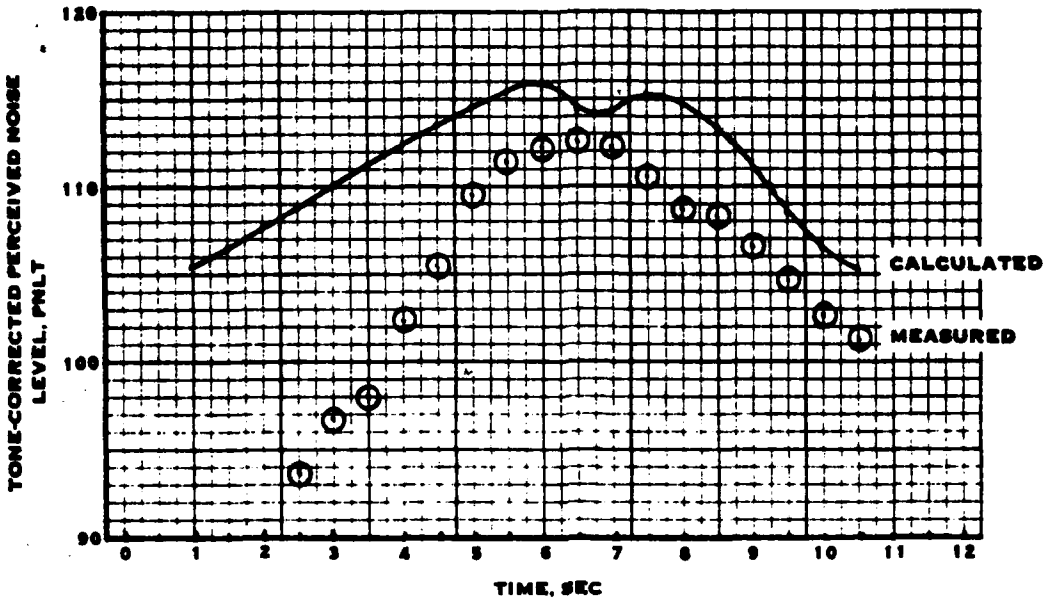

FIGURE 5-41. FLYOVER TIME HISTORY FOR THE DC9 AIRPLANE ON APPROACH

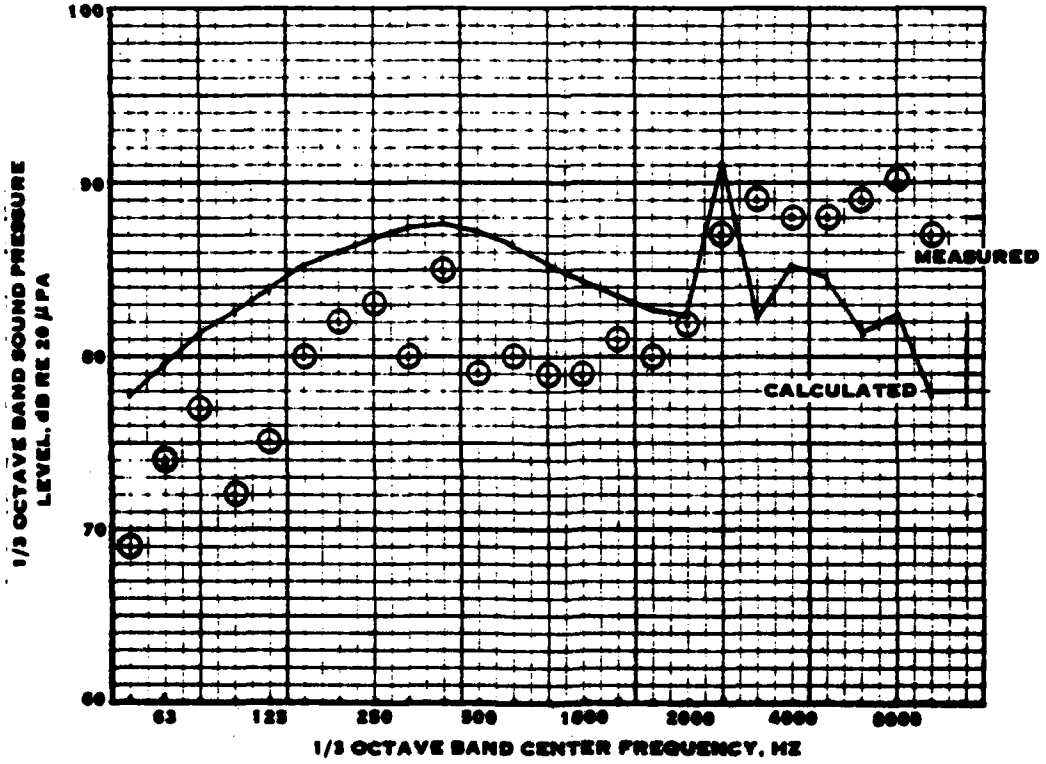

FIGURE 5-42. COMPARISON OF MEASURED AND CALCULATED SPECTRA FOR THE DC9 ON APPROACH AT THE PEAK PNL POINTS

Figure 5-44 shows the comparison of measured and calculated spectra for the maximum PNLT point. The ground reflection corrections give rise to several peaks in the adjusted spectrum, notably at 63, 200, and 315 Hz. Otherwise, the low frequency jet noise is fairly well predicted. The levels of the high frequencies drop faster than calculated, primarily due to higher atmospheric attenuation than could be used for the calculations. Both the calculations and the measurements show that the combination of atmospheric attenuation and fan duct acoustic treatment reduce the fan noise to insignificant levels.

Figure 5-45 shows the comparison of calculated and measured PNLT time histories. The duration is well predicted, although about 5 dB higher in level than measured. The peak PNLT is 105.9 PNdB calculated versus 100.7 PNdB measured. The calculated EPNL is 101.2 EPNdB compared to a measured value of 94.5 EPNdB.

Figure 5-46 shows the comparison of measured and calculated spectra at the peak PNLT point. As before, the ground reflection correction assuming a microphone height of 4 ft (resulting in a first cancellation frequency of 69 Hz for the source directly over head) produces extraneous peaks in the measured spectrum. The calculations show that the peak PNLT occurs well ahead of the airplane. Locating the peak ahead of the airplane reduces the path length difference and raises the frequency of the first cancellation. An examination of the data shows the apparent first cancellation to be closer to 90 Hz than to 69 Hz. Thus, the ground reflection corrections were recomputed assuming a first ground cancellation of 90 Hz (effective path length difference of 6.2 ft). Except at 80 and 100 Hz, the adjusted spectrum looks better and more characteristic of jet noise. It can be seen that although this refined adjustment is more consistent with the expected noise spectrum, it really has but a minor effect on the perceived noise. The PNLT of the original adjusted spectrum was 101.4 PNdB while the PNLT of the refined spectrum is 100.7 PNdB, compared to an unadjusted value of 103.6 PNdB. In figure 5-46 it can be seen that the low-frequency jet noise is underpredicted while fan noise is overpredicted.

In support of the estimated levels, it should be stated that the ground reflection corrections were assumed to be 3 dB at high frequencies. This assumption resulted in a PNLT correction of about 3 dB. The 3 dB adjustment, however, is idealized in that it assumes a perfect reflecting ground plane. In actuality, the measurements were made over sandy ground, which could produce relatively high absorption at high frequencies. The ground reflection corrections could actually be considerably less than 3 dB.

Noise Certification Levels. - Engine data were acquired for the JT15D and JT9D-59A for estimation of the noise on take-off and landing (approach) for the Cessna Citation and Douglas DC-10-40 airplanes.

The Citation measured noise levels are 77.7 EPNdB on take-off and 87.7 EPNdB on landing at the FAR Part 36 locations. The calculated levels are 82.1 EPNdB and 99.9 EPNdB for take-off and landing, respectively. Since these calculations are for

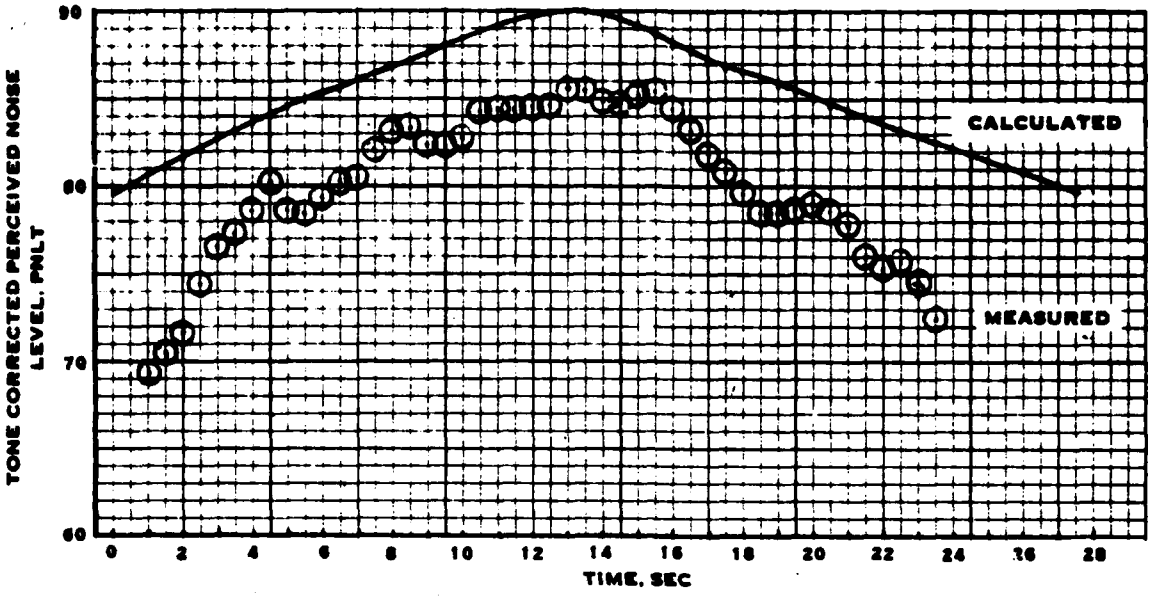

FIGURE 5-43. FLYOVER TIME HISTORY FOR THE JT8D-109 ON TAKE-OFF

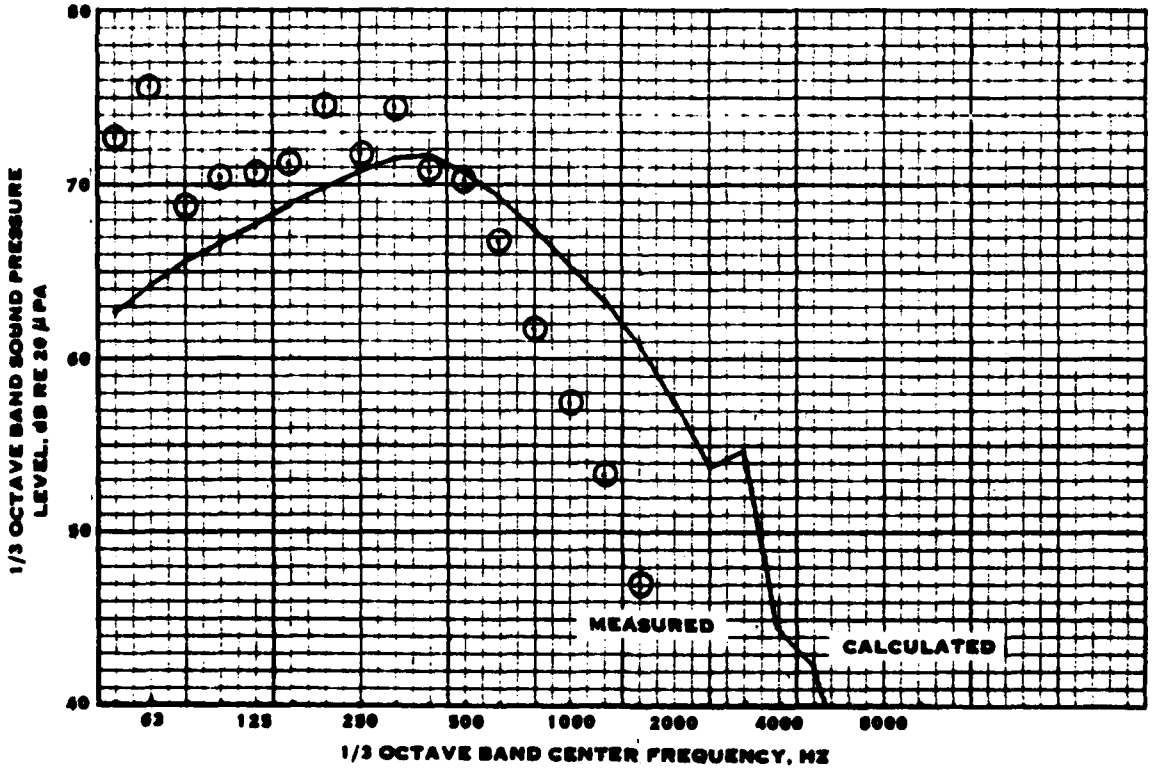

FIGURE 5-44. COMPARISON OF MEASURED AND CALCULATED SPECTRA FOR THE JT8D-109 ON TAKE-OFF AT THE PEAK PNL POINT

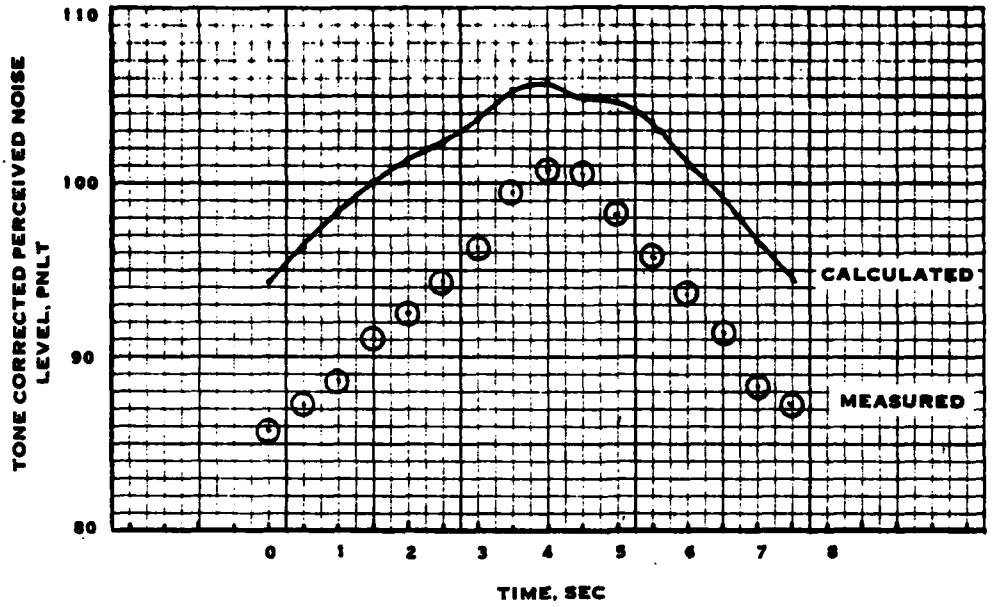

FIGURE 5-45. FLYOVER TIME HISTORY FOR THE JT8D-109 ON APPROACH

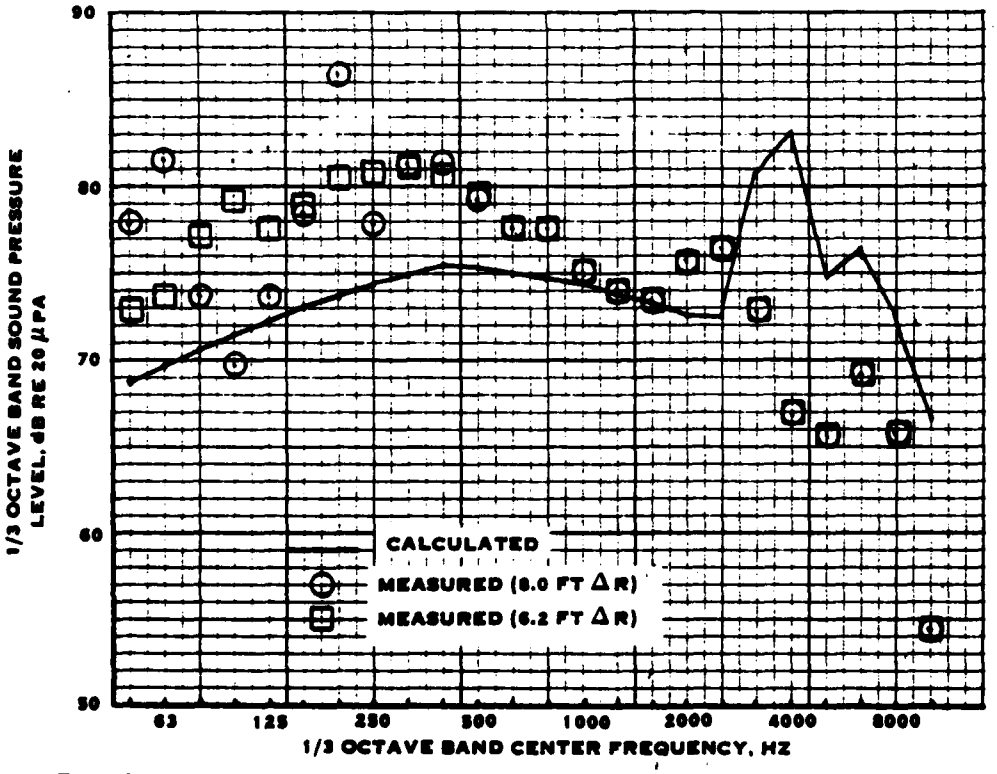

FIGURE 5-46. COMPARISON OF MEASURED AND CALCULATED SPECTRA FOR THE JT8D-109 ON APPROACH AT THE PEAK PNLT POINT

free-field conditions, they must be adjusted by 0 to 3 dB to correct them to equivalent measurements made using a microphone located at four feet above a ground plane. The calculated levels are thus 82.1 to 85.1 EPNdB compared to measured levels of 77.7 EPNdB on take-off. For landing, the calculated levels are 99.9 to 102.9 EPNdB compared to measured levels of 87.7 EPNdB. Although the take-off noise levels are in fair agreement, the approach noise levels are significantly overpredicted. It should be recalled that the Citation engine inlets are over the wings (as described under the forward-flight effects evaluation) and thus shielded from below. This would be expected to produce low fan noise levels, and thus lower engine noise levels, especially during approach when fan noise levels dominate. Thus, the discrepancy between measured and calculated noise levels can be explained by installation effects — namely the shielding of the engine inlets by the wings.

The Douglas DC-10-40 measured noise levels are 102.6 EPNdB on take-off and 106.6 EPNdB on landing. The calculated free-field levels are 105.4 EPNdB on take-off and 108.6 EPNdB on landing. Adjusting for measurements above a ground plane would place the estimated levels at 105.4 to 108.4 EPNdB on take-off and 108.6 to 111.6 EPNdB on landing. These are slight overpredictions, but again the DC-10 airplane configuration has installation effects which also tend to lower the noise. For instance, the center engine inlet is shielded by the fuselage, which could account for about 1 dB in total noise.

Methodology Evaluation Using the Generalized Engine

The primary reason for developing the noise calculation procedure discussed in this report is the evaluation of the noise from various propulsor configurations on a preliminary design basis. This was addressed in the development of the methodology by including a generalized core engine. This "canned" engine would be scaled to the required size and provide the inputs to the core engine noise calculation procedures. As this is a universal engine, it serves as both a turboshaft and a turbofan core engine and is intended to be used for turboprops, variable-pitch fans, lift-fans, and helicopters as well as for fixed-pitch fans.

To evaluate the performance of the generalized engine in calculating fixed-pitch fan noise, the four flyovers previously described were recalculated using generalized core engines instead of the actual engine parameters. The results of these calculations are summarized in table 5-I. These levels have not been adjusted for installation effects, for propagation effects other than spherical spreading and atmospheric attenuation, or for ground reflections. As can be seen, the noise levels calculated using the generalized engine are higher than those using the fully defined core engine parameters, except for the JT15D-1 engine on landing. This is due to the generalized engine producing generally higher levels of jet noise. Also, for the JT8D-9 and JT8D-109 engines, the generalized core engine uses less air than the actual engine, resulting in a higher bypass ratio. The fan noise prediction methodology calculates higher fan discharge noise for higher bypass ratios. The generalized core engine for the JT9D-59A results

TABLE 5-I

COMPARISON OF MEASURED FLYOVER NOISE LEVELS WITH THOSE CALCULATED USING THE GENERALIZED ENGINE

AIRPLANE	ENGINES	FLIGHT CONDITION	MEASURED EPNL	CALCULATED* EPNL	CALCULATED+ EPNL
Douglas DC-9	JT8D-9	Take-off	109.8	115.4	116.8
		Approach	107.4	112.5	114.3
Douglas DC-9	JT8D-109	Take-off	85.2	90.7	95.5
		Approach	94.5	101.2	104.6
Cessna Citation	JT15D-1	Take-off	77.7	82.1	83.7
		Approach	87.7	99.9	95.6
Douglas DC-10-40	JT9D-59A	Take-off	102.6	105.4	113.2
		Approach	106.6	108.6	113.5

* Calculated with defined core engine parameters
\+ Calculated with generalized engine parameters

in higher levels of core engine noise, expecially that of the compressor and turbine, and much higher levels of jet noise although the fan noise levels remain about the same. The noise of the JT15D-1 on landing decreases because the generalized core engine compressor noise is lower.

It is thus concluded that using the generalized core engine for fixed-pitch fan noise calculations will result in some overpredictions. Based on the comparison of calculated and measured EPNL for take-off and landing for the four engines (8 data points), the calculations with the generalized core engine overpredicts by an average of 8.2 EPNdB, compared to an average overprediction of 5.5 EPNdB for the calculations done using the actual core engine parameters. As a first approximation, the noise estimates made using the generalized core engine can be reduced by 8.2 EPNdB for a better estimate. Alternately, a more sophisticated approach to the generalized core engine, i.e. one specifically tailored to a particular class of turbofans, can be used. This, however, is beyond the scope of the current effort. In any case, it should be noted that the correlation is based on a limited number of engines, all Pratt and Whitney designs. Other engines may show different correlations.

Summary for Fixed-Pitch Fans

The correlation between calculated and measured isolated, static fan noise levels are in reasonable agreement, although the calculations tend to overpredict at high frequencies. Based on evaluation of calculated noise suppressor performance, it appears that the broadband noise attenuation is good for moderate levels of treatment.

It is more difficult to assess the performance of the fan noise prediction methodology for complete engines as other sources of noise, such as those of the jet and core engine are significant contributors. Also, for the cases of airplane flyovers, installation effects appear important. In general, the calculated levels exceed the measurements, particularly if the measurements are assumed to include significant ground reflection effects. If it is assumed that the measurements are representative of free-field conditions, as might be the case for measurements made over grass-covered sand, the correlation between measured and calculated EPNL is about 5 dB for the JT8D-9 engine, 6 dB for the JT8D-109 engine, 4.5 dB on take-off and 12 dB on approach for the JT15D-1 engine, and 3 dB for the JT9D-59A engine: an average of 5.5 EPNdB. The agreement is typically better on the basis of peak sideline PNL and PNLT. Some of the differences are due to installation effects. For instance, the JT15D-1 engines installed on the Cessna Citation have their inlets over the wing and thus the engine inlet noise is shielded from below. This is especially significant for the approach condition where fan noise dominates. The center JT9D-59A engine inlet on the DC-10-40 airplane is shielded by the fuselage.

The noise calculation procedure using the generalized core engine was also evaluated. This typically showed higher noise levels than those calculated using the defined core engine parameters. This occurred because the generalized core engine resulted in higher compressor and jet noise levels.

Using the generalized engine, the calculated noise levels exceed the measurements by 6 EPNdB for the JT15D-1 on take-off to 10.6 EPNdB for the JT9D-59A on take-off, with an average of 8.2 EPNdB. Eliminating the JT15D-1 on approach as a special case, the average was 4.6 EPNdB with a standard deviation of 1.7 dB for the calculations using the defined engine parameters. As the standard deviations are small, good approximations can be achieved by adjusting the calculated EPNL downward by 4.6 dB for the calculations done using the defined engine parameters and by 8.2 dB for the calculations done using the generalized core engine. However, the user is cautioned that this is based on a limited number of calculations, all of which were done for engines designed by Pratt and Whitney. Other engines, of different manufacture, might show other results.

EVALUATION OF HELICOPTER NOISE PREDICTION

Introduction

The major problem in evaluating the noise prediction methodology for helicopters is the lack of suitable data. All the data identified were acquired with microphones located typically at four feet above a ground plane, with one exception. Data acquired at NASA-Langley utilized a ground-level microphone, but this was at a 4200 ft sideline for a low altitude flyover. Apart from resulting in only a small directivity change, this shallow a viewing angle generally results in excess attenuation due, in part, to grazing propagation along the ground. Thus, this data was not used, as it traded-off ground reflection effects for ground-to-ground propagation effects. Although it is generally possible to correct broadband noise with a relatively smooth spectrum (e.g. jet noise) for ground reflection effects, it is extremely difficult for sources containing low frequency tones, except when the microphone is located directly on a hard surface. As an example, the measured spectrum from a Sikorsky S-61 helicopter (from Data Base Item 3) was adjusted for ground reflection effects for the four-foot microphone height used in the measurements. Figure 5-47 shows the as-measured and adjusted spectra for the aircraft at 500 feet overhead. As can be seen, the spectrum shows a first cancellation in the 63 to 80 Hz range. The first reinforcement would then occur at 125 to 160 Hz, the second cancellation at 200 to 250 Hz, etc. These are not in perfect agreement with calculations. The calculated ground reflection corrections for the first 10 main rotor harmonics (16.92 Hz blade passing frequency) are -5.4, -3.2, 1.7, 21.8, 3.5, -2.4, -5.1, -6.0, -5.6, and -3.8 dB. It can be seen that the fourth harmonic is calculated to be very close to the first cancellation frequency, while the eighth harmonic is near the first reinforcement frequency. Since the low frequency noise is calculated to be due to the main rotor tones, the above corrections should be applied to the one-third octave bands which contain the particular tones. The resulting "corrected" spectrum (to 160 Hz) is shown in figure 5-47. As can easily be seen, the

corrected spectrum is no better than the measured spectrum. In fact, its appearance may be considered to be worse. Apparently, the measurements do not justify a 21.8 dB correction for the 63 Hz band, and the correction of -5.6 dB for the 160 Hz band appears excessive. The corrections for the 100 and 125 Hz bands appear reasonable, if that part of the spectrum is indeed a reinforcement. It is thus apparent that correcting the data to equivalent free-field conditions is not feasible, especially at those frequencies where cancellations are believed to occur. This is because the cancellation pattern for pure tones is very sharp. Small discrepancies in frequency can result in significant changes in the correction value. The discrepancies in the frequencies can come about due to uncertainties in the rotor speed and the Doppler frequency shift. The discrepancies in the cancellation frequencies occur due to uncertainties in exact microphone height, propagation path lengths, temperature gradients, wind, impedance of the ground, etc. Another consideration is that the composition of the source is not precisely known - it cannot be determined from the one-third octave band spectra if the noise is broadband, tones from the main rotor, or tones from the tail rotor. Due to differences in frequencies, the corrections for each of those sources are different.

It is thus apparent that one-third octave band analyses for noise sources containing significant low frequency tones are very difficult to correct for ground reflection effects. A more reasonable approach is to adjust the calculated levels for ground reflection effects. This offers several advantages. First, this can be done on a component basis, i.e., the main rotor tones can be adjusted separately from the tail rotor tones which are adjusted separately from the broadband noise sources, with the total noise then being the sum of the adjusted sources. Second, the adjustments for ground reflections are limited to the range $-\infty$ to +6 dB (full cancellation to full reinforcement), so that large positive increments, as, for example, the 21.8 dB correction to the 63 Hz band for the case shown in figure 5-47, are avoided. Third, this would be done in the computer program, which would save many man-hours of effort working with measured levels. At the time the noise prediction procedure was developed, the requirement was for estimates of free-field noise. Also, there were no defined procedures for calculating ground reflection effects. Although it is beyond the scope of the current effort to implement ground reflection effects into the existing computer program, existing procedures, such as that of reference 8, should be added in a future update. An alternative, which is likely to be more successful, is to acquire additional data using microphones which are flush with the ground. This results in constant low frequency pressure doubling yielding an adjustment to free-field of -6 dB which is independent of the source distribution and source location.

Due to the difficulty and generally poor results of correcting the helicopter noise measurements for ground reflection effects, this effort was discontinued. The correlations shown in the following discussion were made using the as-measured levels, uncorrected to equivalent free-field conditions, compared to calculation made for free-field conditions. The low frequency tones may be affected by up to $-\infty$ dB at full cancellation and up to +6 dB at full reinforcement. At higher frequencies, reflections from a perfect reflecting surface would be expected to result in levels which are +3 dB above those

under free-field conditions. In actual practice, low frequency corrections are probably in the -15 to +6 dB range, while the high frequency correction may not be as high as 3 dB. Measurements made over soft ground or grass may be fairly representative of free-field levels at high frequencies, as indicated in figure 5-48. On the basis of the results shown in figure 5-48, measurements made over grass are only about 1.5 PNdB higher than free-field noise levels.

Comparison of Measured and Calculated Helicopter Noise

Bell 212 From Data Base Items 3 and 4. - The noise from this helicopter was measured using a microphone located at four feet above the ground at a "soft" site. Data was acquired during hover and flyover at flight speeds of 60, 99, 110, and 114 kts.

Figure 5-49 shows the comparison of measured and calculated helicopter noise for the hover condition. The measured spectrum for the helicopter directly overhead shows several valleys and peaks, notably at 80, 160, 315, and 500 Hz. The first ground cancellation is calculated to occur in the 80 Hz band. The adjustment to free-field condition, assuming broadband noise, is calculated to be about 9 dB. The second ground cancellation would then be expected to occur in the 250 Hz band, although it appears in the 315 Hz band. The peak in the 160 Hz band could then be the first ground reflection reinforcement, justifying a correction to free-field conditions of -5.5 dB. The next reinforcement would be expected to occur in the 315 Hz band with an adjustment of about -4.5 dB, but appears in the 500 Hz band. The level of ground reflection corrections to be applied to the measured spectrum to adjust it to equivalent free-field conditions thus appears reasonable, but the frequencies are in disagreement. At higher frequencies the comparison between calculated and measured levels is quite good. As the data was acquired at a "soft" site, high frequency ground reflection effects are presumably small.

At the 500 ft sideline location, ground reflection effects are also apparent in the measured noise spectrum, although not as extreme as those seen at the overhead location. Again the agreement between measured and calculated levels is quite good at high frequencies. The comparison between measured and calculated PNLT values is 97.6 verus 95.0 PNdB and 92.2 verus 91.7 PNdB for the directly-overhead and 500 ft-sideline positions, respectively. The agreement between measured and calculated PNLT would be improved, particularly at the overhead location, if the ground reflection corrections were applied at low frequencies on the basis of level and not frequency (i.e. applying the correction to the band which is indicated by measurement rather than to the one calculated on the basis of microphone height). This results in the adjusted spectrum shown by the squares in figure 5-49. This adjusted spectrum provides a PNLT value of 95.6 PNdB, in close agreement with the calculated value of 95.0 PNdB.

Figure 5-50 shows the comparison between measured and calculated helicopter noise levels during flyover at the time of maximum PNLT. As for the hover data, ground reflection effects are apparent in these spectra. At 60 kts, the mid- and high-frequency

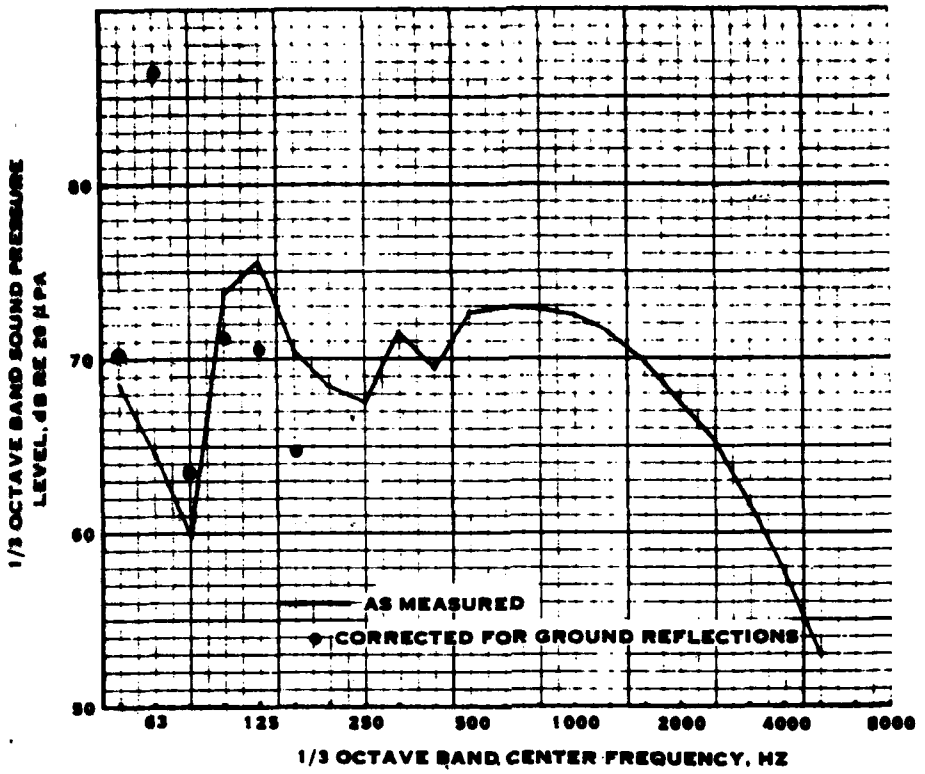

FIGURE 5-47. GROUND REFLECTION CORRECTIONS FOR HELICOPTER NOISE

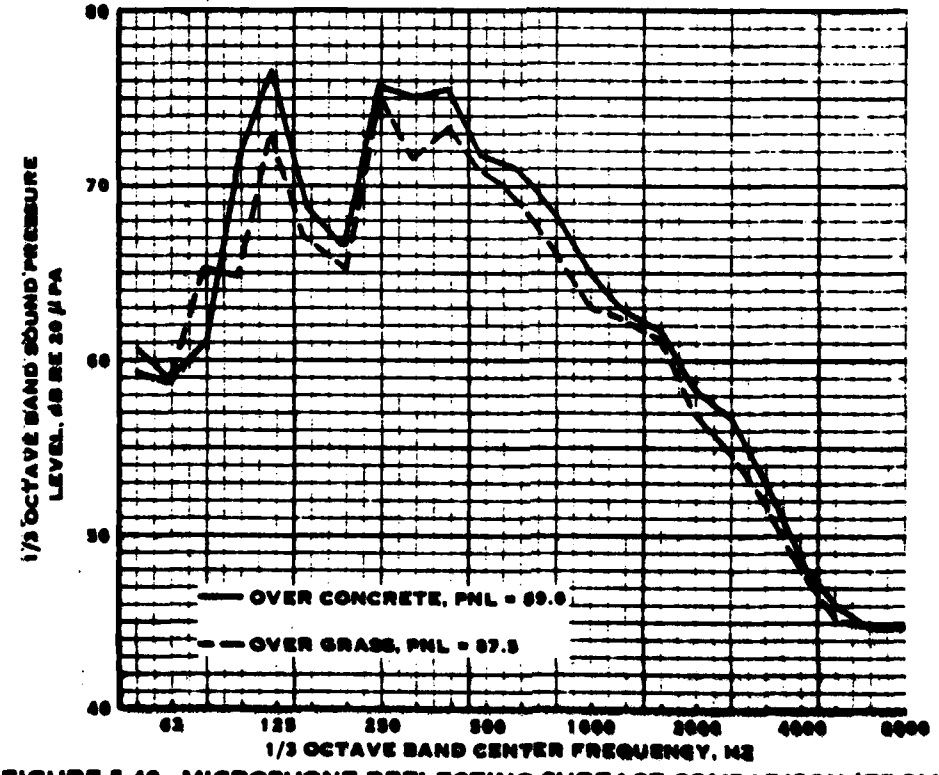

FIGURE 5-48. MICROPHONE REFLECTING SURFACE COMPARISON (FROM DATA BASE ITEM 3)

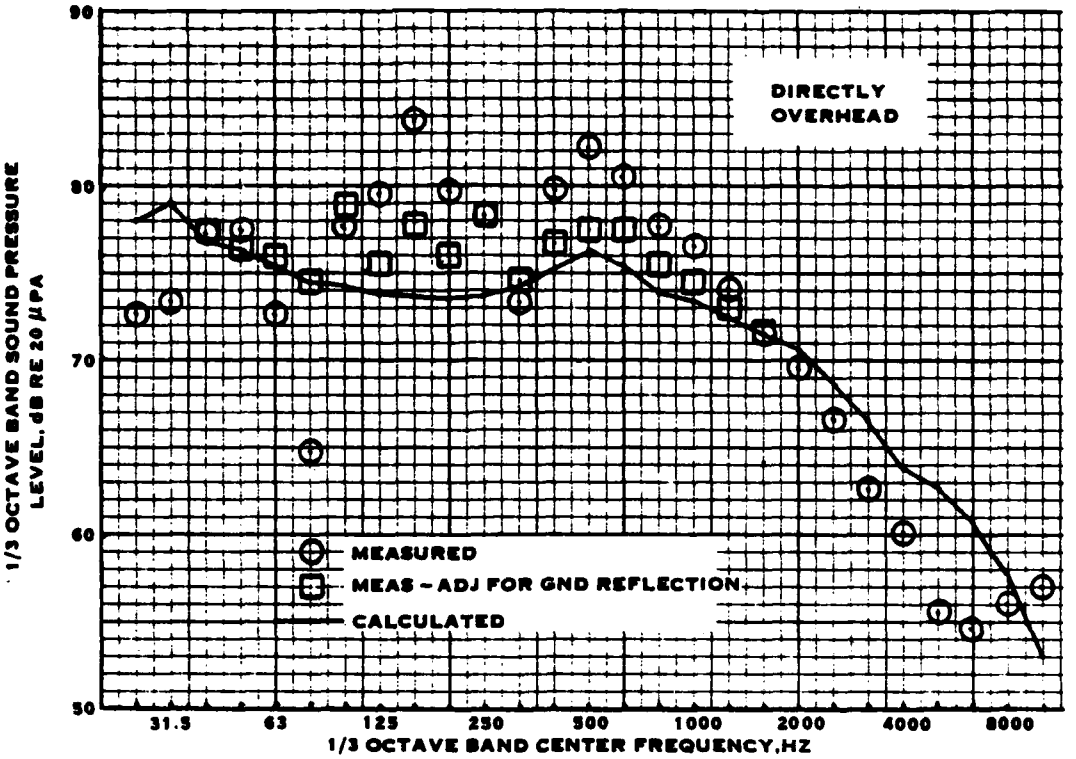

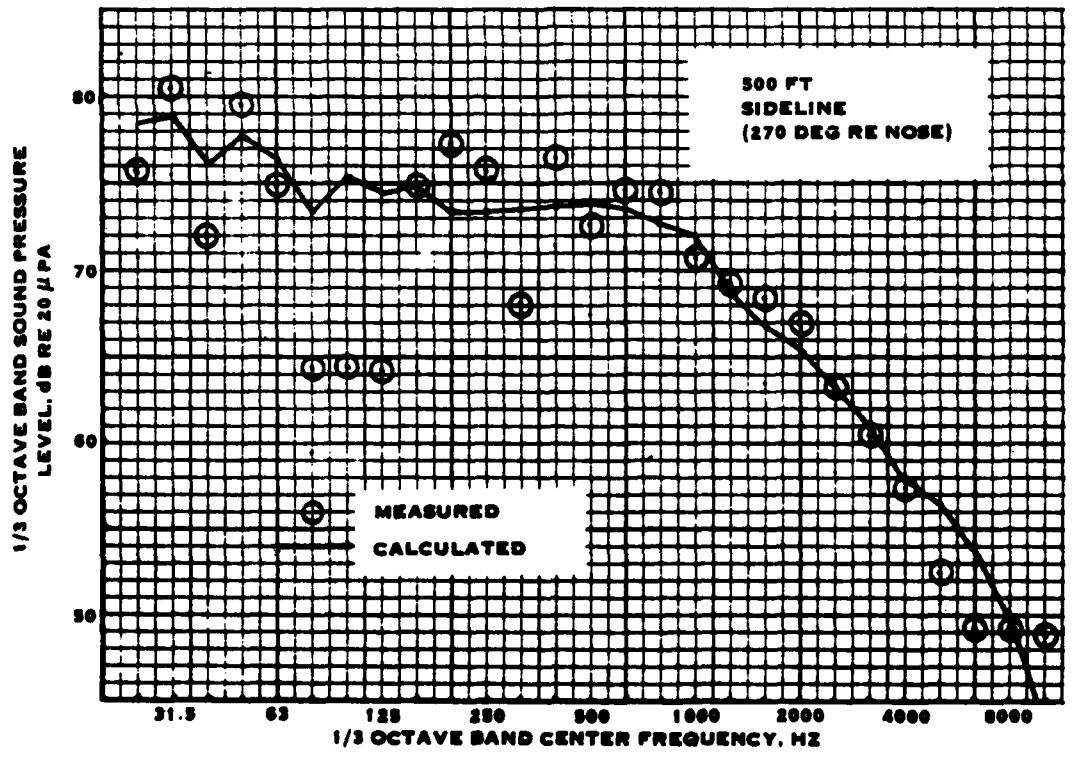

FIGURE 5-49. COMPARISON OF MEASURED AND CALCULATED BELL 212 HELICOPTER NOISE DURING HOVER-DATA BASE ITEM 4

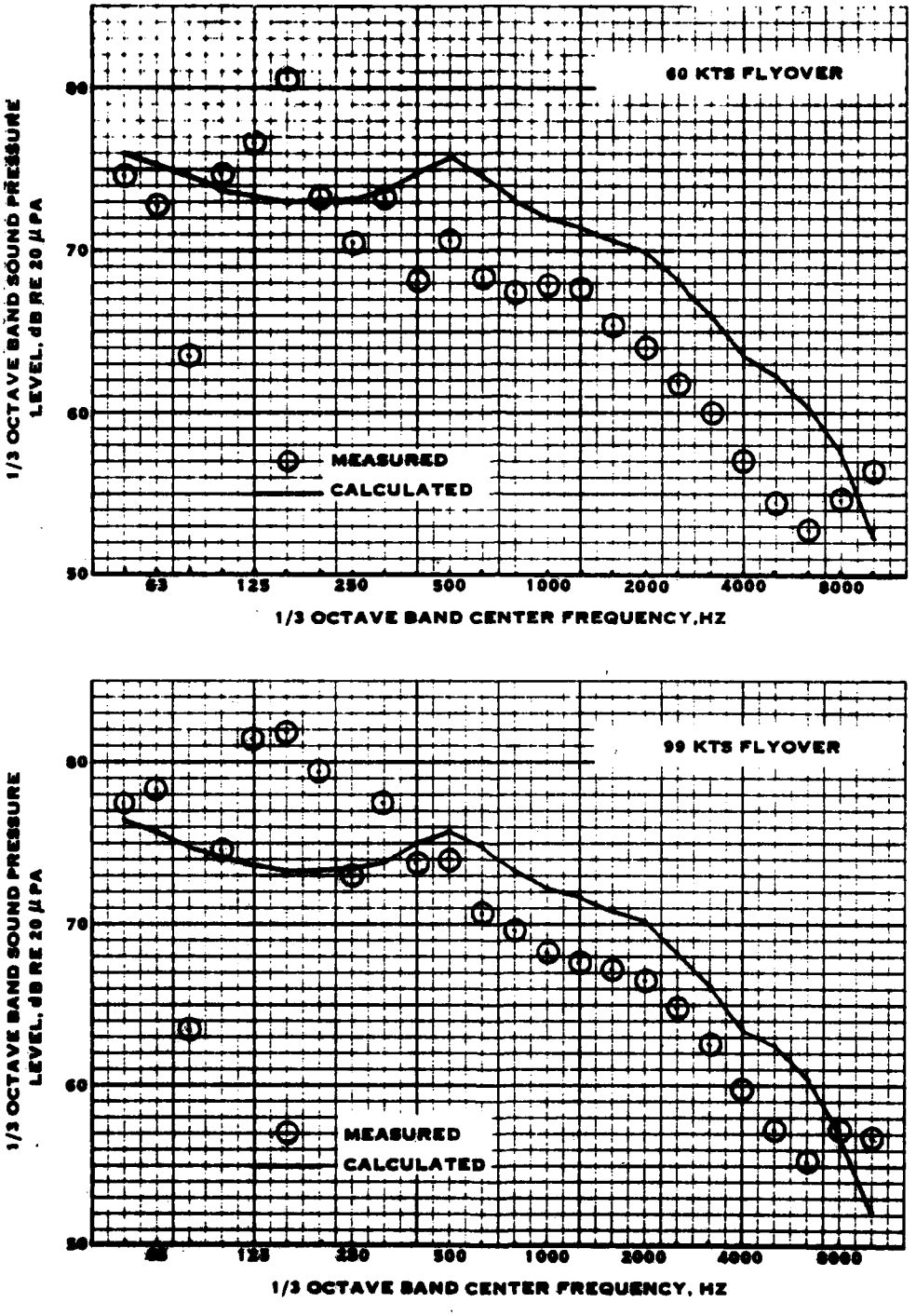

FIGURE 5-50. COMPARISON OF MEASURED AND CALCULATED BELL 212 HELICOPTER NOISE DURING FLYOVER - DATA BASE ITEM 4

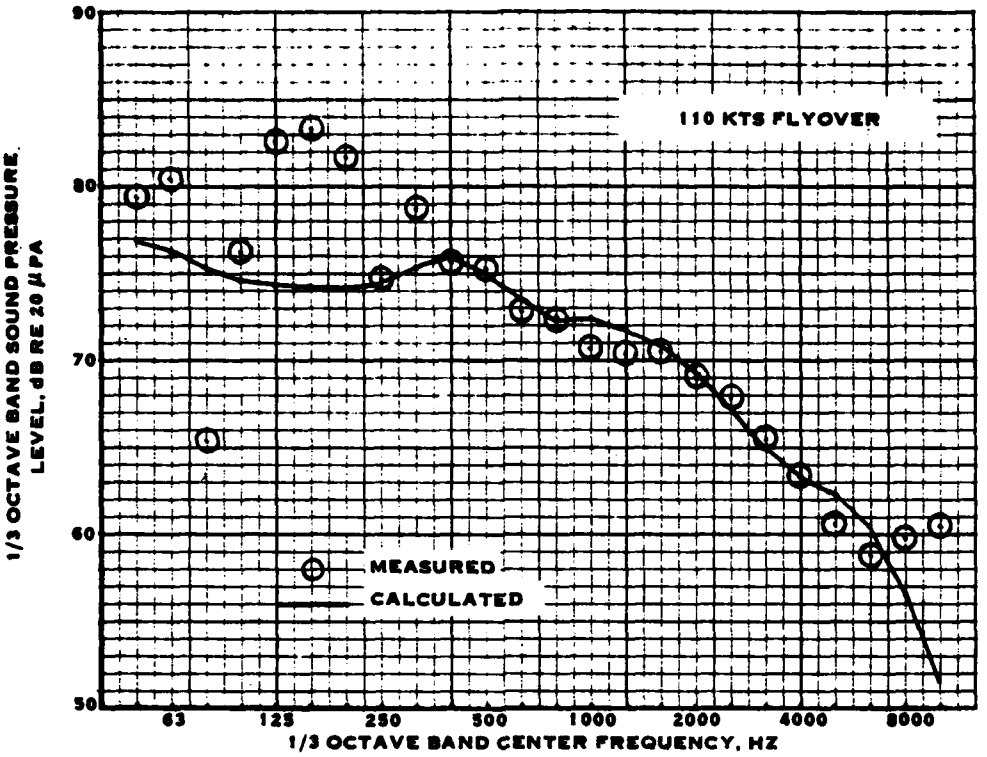

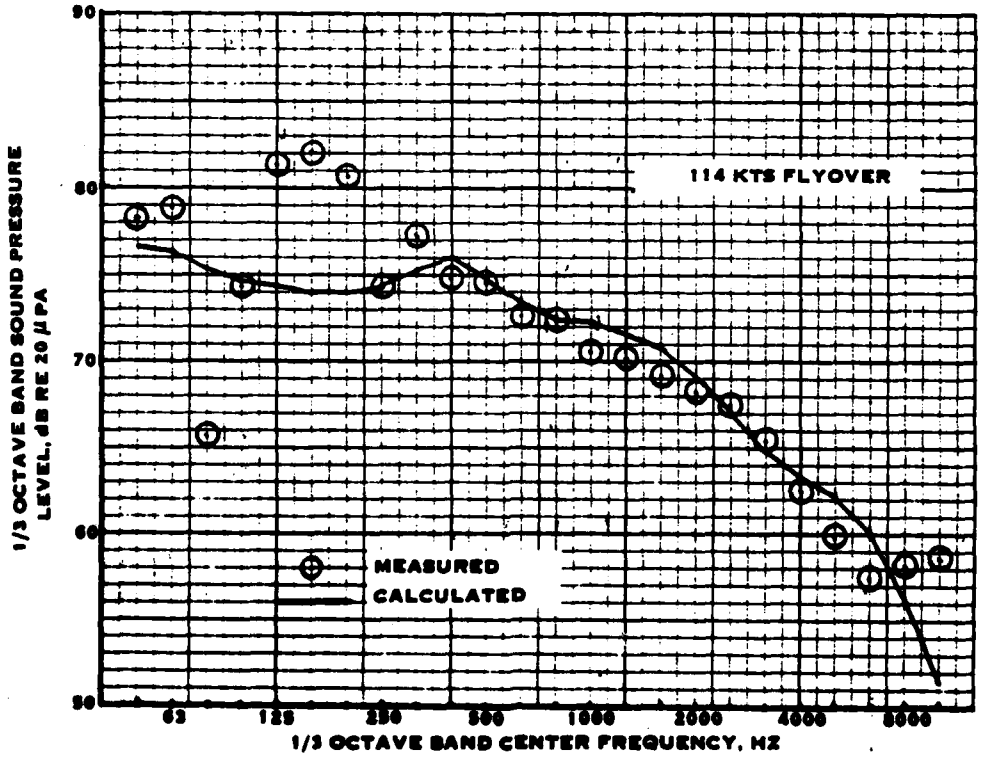

FIGURE 5-50. CONCLUDED

noise is overpredicted by about 5 dB. This provides a comparison between measured and calculated PNLT of 91.6 PNdB versus 94.6 PNdB, and over prediction of 3 PNdB. At 99 kts, the mid- to high-frequency spectrum overprediction is only about 3 dB and provides a comparison in PNLT of 94.0 PNdB measured versus 94.8 PNdB calculated. At 110 and 114 kts, the agreement at mid- and high frequencies is excellent. The comparison between measured and calculated PNLT is 95.2 PNdB versus 94.2 PNdB at 110 kts and 95.7 PNdB versus 94.3 PNdB at 114 kts. The higher-than-calculated levels at 110 and 114 kts flight are due, in part, to the ground reflection effects seen in the 125, 160, and 200 Hz bands. Nevertheless, the agreement between measured and calculated PNLT values at the overhead location during flyover is good, showing an overprediction of 3.0 PNdB at 60 kts to an underprediction of 1.4 PNdB at 114 kts.

Figure 5-51 shows the comparison between measured and calculated PNLT time histories during flyover at 60, 99, 110, and 114 kts. It should be noted that the measured and calculated time histories are related only to the time of occurrence of the maximum PNLT value, and not the physical location of the helicopter (i.e. time of overhead location). In all cases, the measured PNLT time histories are considerably longer than the calculated PNLT time histories. This occurs primarily because the Bell 212 helicopter produces impulsive main rotor noise (blade slap) which is apparent ahead of the helicopter. Thus, the signature of the helicopter is strong in impulsive noise as it is approaching, which results in a long duration. This is particularly apparent for the 114 kts flyover condition which show a nearly constant PNLT from 11 seconds before the peak to 2 seconds before the peak. Impulsive noise does not radiate directly below or to the rear, so that the PNLT would be expected to decrease more rapidly past the peak. The helicopter noise calculation procedure does not include impulsive noise, so that the PNLT time history on approach is underpredicted. However, past the peak, the agreement is fairly good. Thus, the measured duration correction is greater than that calculated. This results in measured EPNLT values of 96.3, 96.7, 98.6, and 99.3 EPNdB vs calculated values of 93.6, 91.9, 91.4, and 91.3 EPNdB for 60, 99, 110, and 114 kts, respectively.

Sikorsky S-61 from Data Base Items 3 and 4. - Sikorsky S-61 helicopter noise was measured during hover and flyover at 60, 100, and 115 kts flight speed. Measurements were made with a microphone located four feet above a ground plane at a "hard" site. The 115 kts flyover noise was also measured at a "soft" site.

Figure 5-52 shows the comparison between measured and calculated noise during helicopter hover directly overhead. Ground reflection effects are apparent at 63 and 200 Hz and probably contribute to the peaks at 160 and 250 Hz. At higher frequencies, the ground reflection effects would be expected to increase the measured levels by 3 dB over free-field conditions. It is apparent that correcting for ground reflection effects would improve the correlation between measurements and calculations at low frequencies, but the mid-frequencies will remain underpredicted by about 7 dB. At high frequency, the agreement is again good. The reason for the peak at 100 to 800 Hz in the measured spectrum cannot be established from the 1/3 octave band analysis. However, the main rotor has a blade passing frequency of 16.9 Hz, so that it would

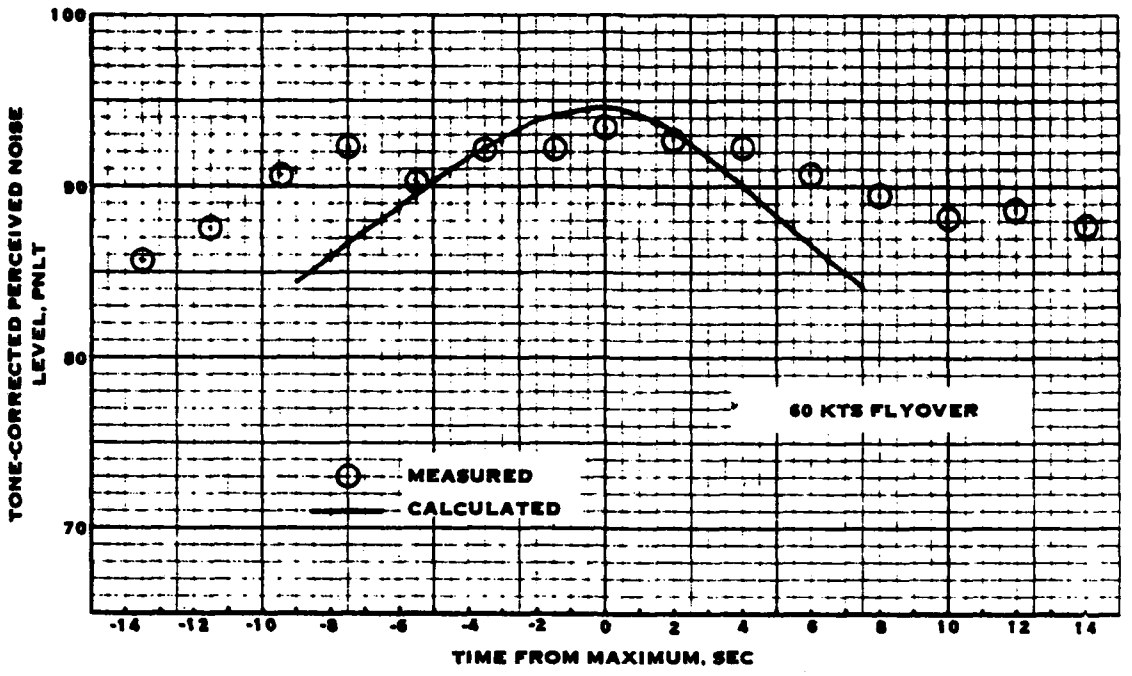

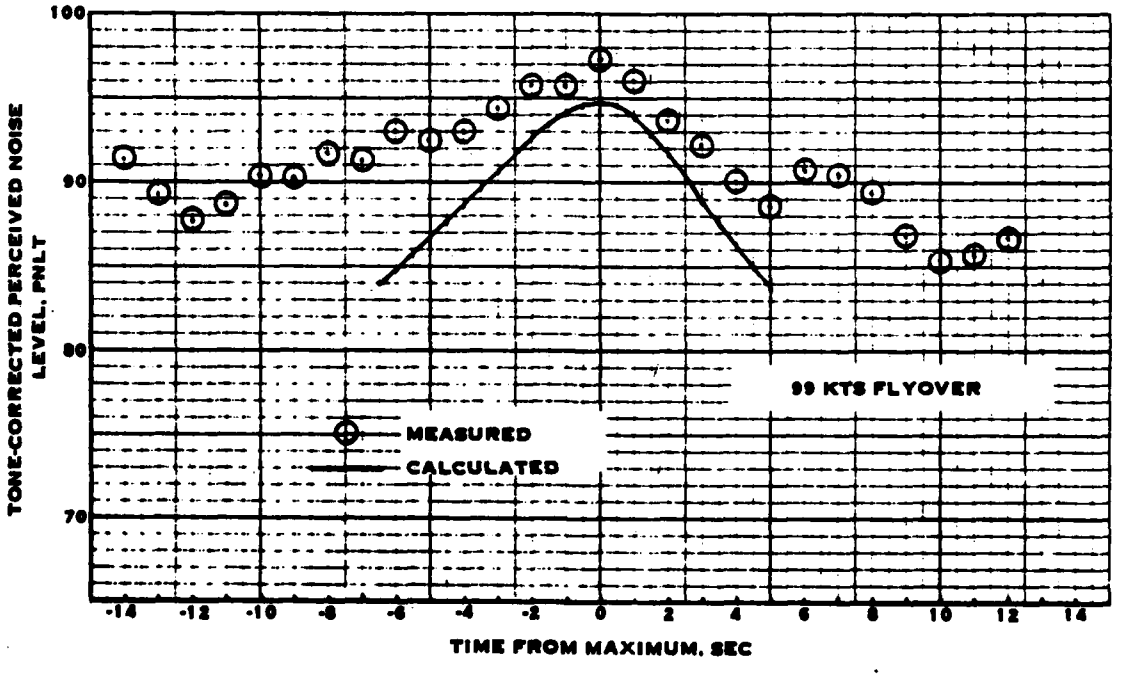

FIGURE 5-51. COMPARISON OF CALCULATED AND MEASURED BELL 212 HELICOPTER PNLT TIME HISTORIES

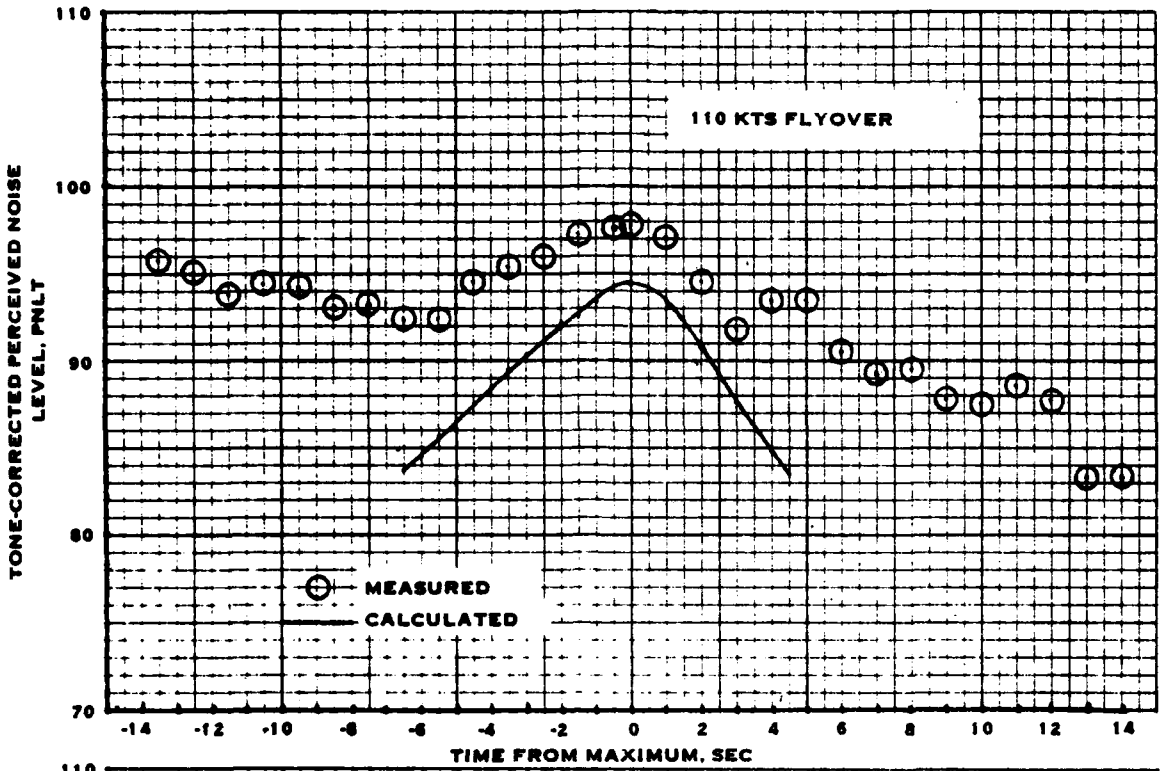

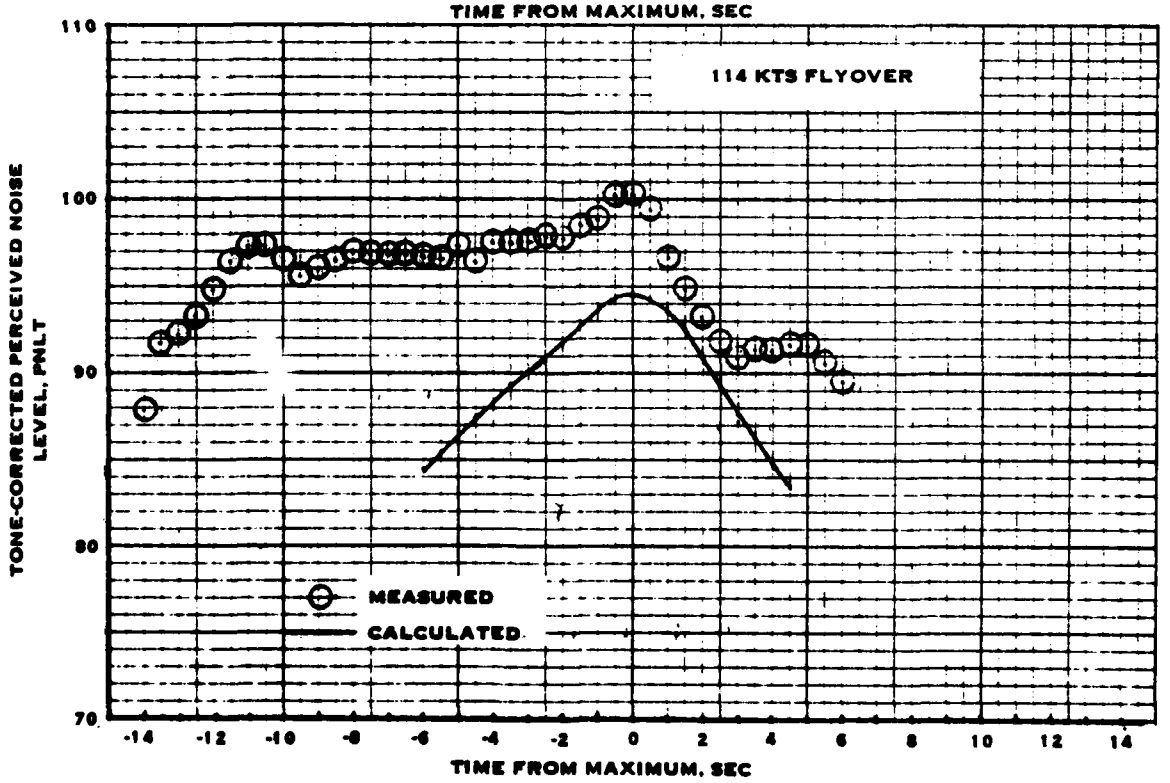

FIGURE 5-51. CONCLUDED

require more than 50 harmonics to contribute to the frequency range extending to the 800 Hz band. This does not appear plausible. The tail rotor has a blade passing frequency of 94.7 Hz, in a more reasonable range to contribute to the peak. In fact, it is observed in the data report that the helicopter noise sounds propeller-like when overhead. This indicates that the tail rotor tone noise is a dominant source. The calculations place the tail rotor noise at more than 10 dB below that of the main rotor in the 400 Hz band. This is consistent with the main rotor having a power input about 7 times that of the tail rotor. However, the noise calculations are for isolated rotors under uniform inflow. It is well known that inflow distortion will significantly raise the noise generated by a low to moderate tip speed rotor. Thus, the high levels of measured tail rotor noise are believed to be due to installation effects. The tail rotor is installed on the vertical tail with the thrust direction toward the tail. This results in significant blockage of the tail rotor inflow. The result is the generation of strong harmonics of blade passing frequency which extend well into the mid-frequencies. In flight, the wake from the vertical tail is blown downstream, so that the tail rotor inflow distortion is less and the noise would be expected to be significantly lower than during hover. This indeed appears to be the case, as shown in figure 5-53 for the helicopter noise during flyover. At 60 kts, the 100 to 800 Hz peak is not evident. The level of the 400 Hz band is 10 dB lower than during hover. It is thus concluded that the high levels of mid-frequency noise during hover are due to high levels of tail rotor noise caused by inflow distortion. This was also discussed earlier under the evaluation of forward-flight effects and offered as the explanation for the observed significant reduction in noise between hover and flight for conventional helicopters. As a point of interest, it may be recalled that the Bell 212 helicopter did not have apparent high levels of tail rotor noise as are shown by the Sikorsly S-61 helicopter. Although tail rotor noise could be contributing to the peaks attributed to ground reflection effects, it would be expected that the tail rotor noise in the Bell 212 is not as dominant during hover. This is because the tail rotor blade passing frequency is only 55.4 Hz, thus requiring many more harmonics to extend into the mid-frequencies, and the tail rotor thrust direction is away from the vertical tail so that the rotor wake interacts with the vertical tail rather than the tail producing inflow distortion. Although this configuration probably also produces interaction noise, it is not as intense as that produced by inflow distortion into the rotor.

As would be expected, the hover noise is underpredicted. The calculated PNLT is 94.9 PNdB, compared to a measured level of 99.7 PNdB. In flight, the agreement is better, as shown in figure 5-53. Ground reflections are apparent up to about 500 Hz, but the calculated levels fill in quite well between the peaks and valleys at low frequencies. The 115 kts flyover condition was measured at both the "hard" site and the "soft" site. As may be seen, the major effect is that levels at the "soft" site are about 2 dB lower than levels at the "hard" site at high frequencies. The comparison between measured and calculated PNLT values is 93.0, 93.9, and 92.3 PNdB verus 93.7, 93.7, and 93.5 PNdB for 60, 100, and 115 kts ("hard" site), respectively. The "soft" site PNLT value is 89.0 PNdB, or 3.3 PNdB lower than for the "hard" site measurement. It is apparent that the calculations are in better agreement with uncorrected measurements made at the "hard" site rather than those made at the "soft" site.

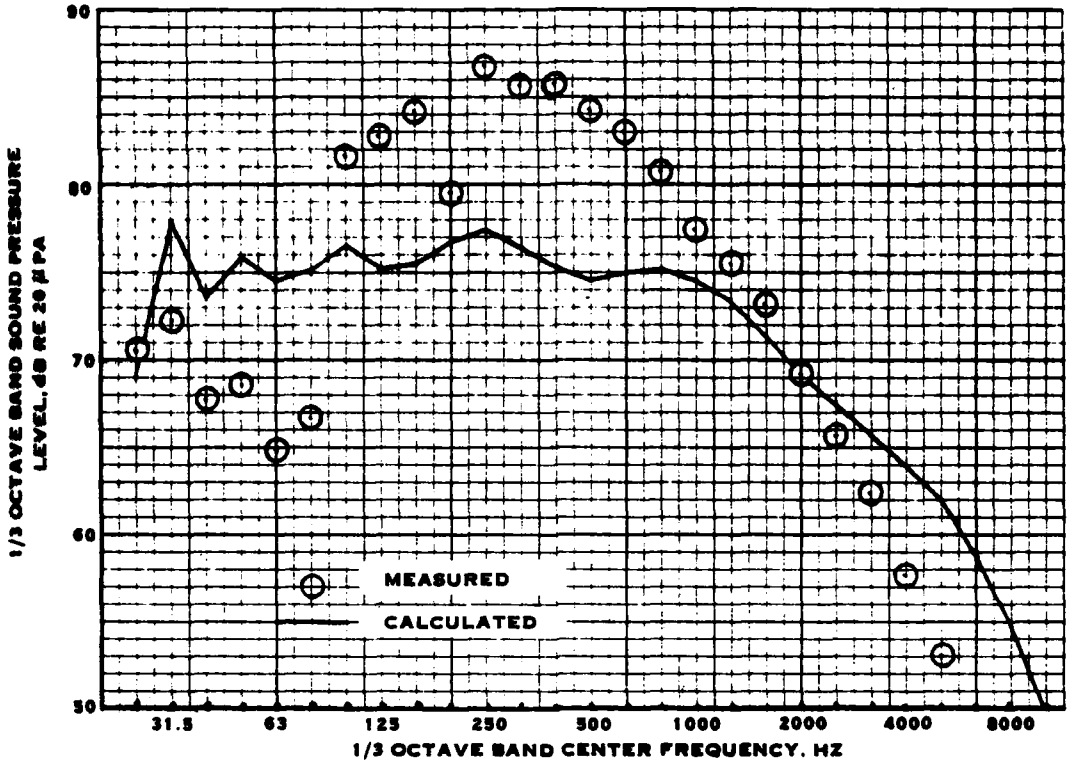

FIGURE 5-52. COMPARISON OF MEASURED AND CALCULATED SIKORSKY S-61 HELICOPTER NOISE DURING HOVER - DATA BASE ITEM 4

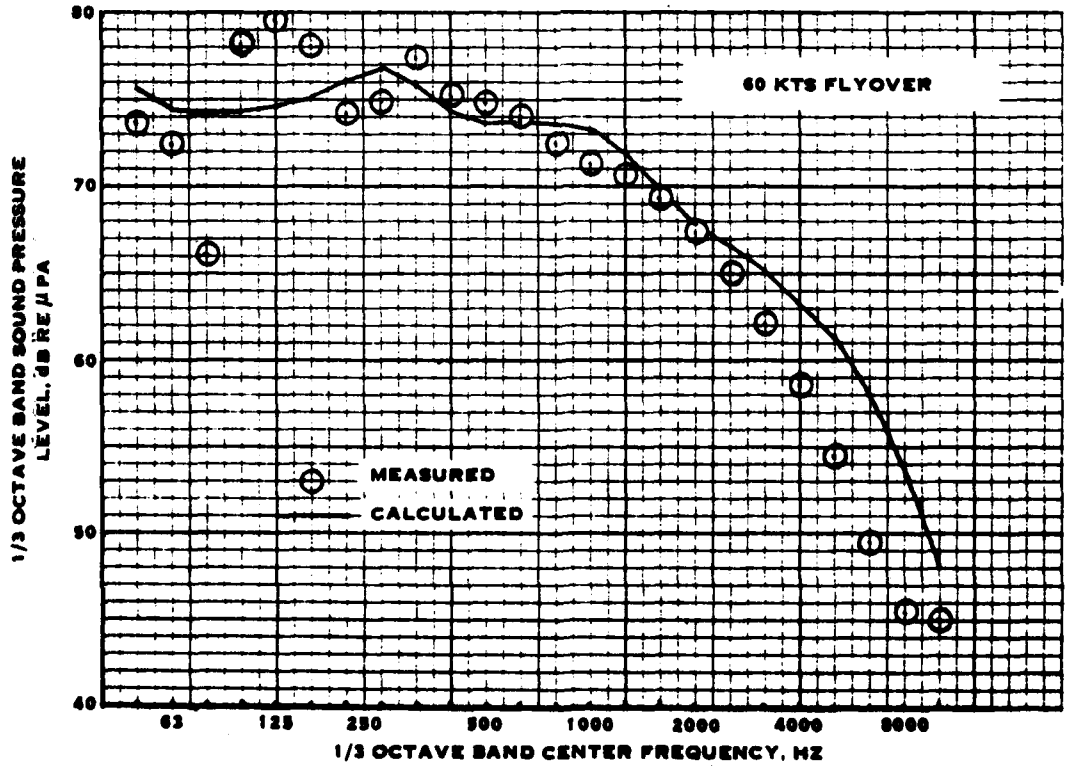

FIGURE 5-53. COMPARISON OF MEASURED AND CALCULATED SIKORSKY S-61 HELICOPTER NOISE DURING FLYOVER - DATA BASE ITEM 4

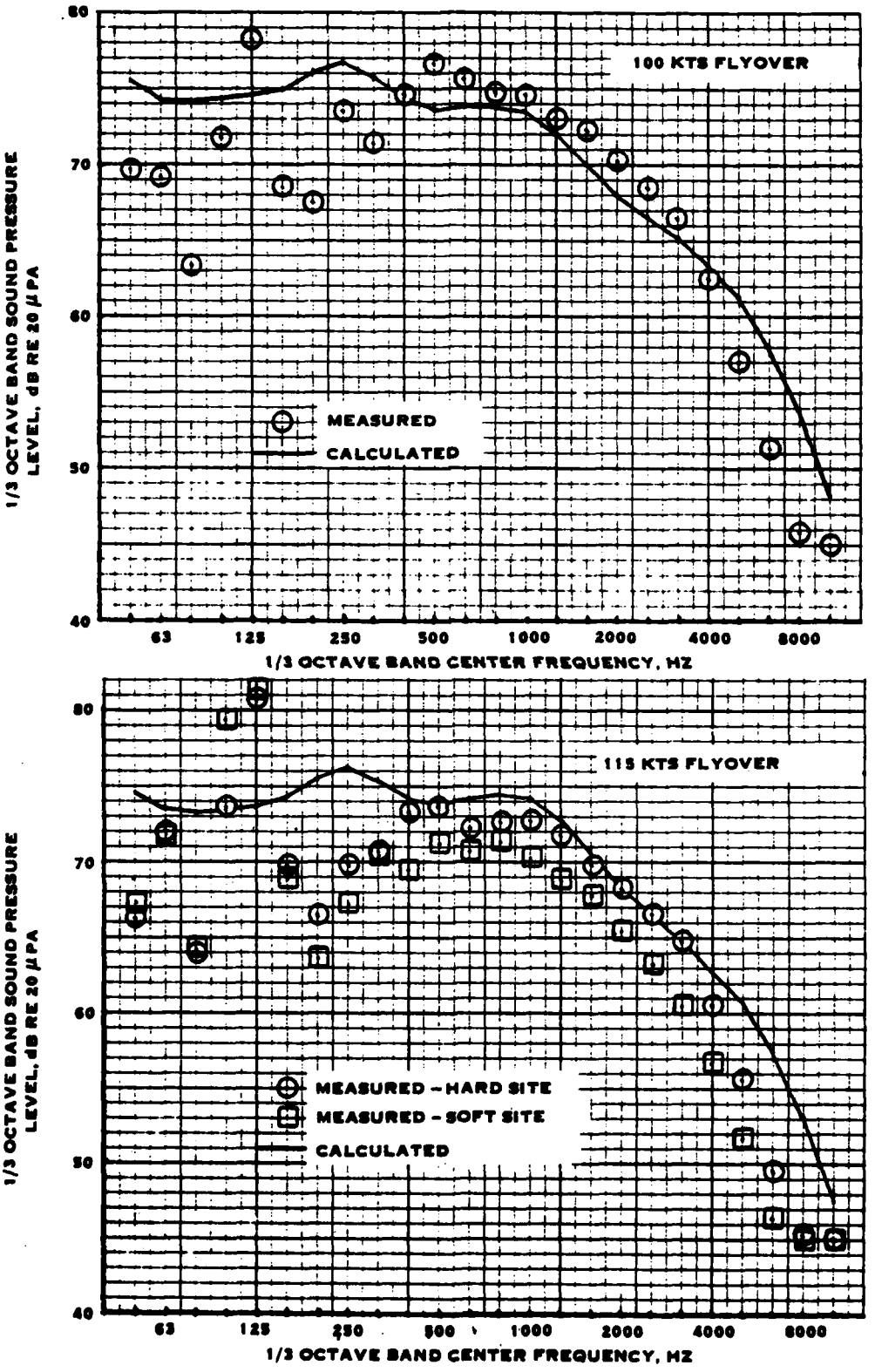

FIGURE 5-53. CONCLUDED

Figure 5-54 shows the comparison of measured and calculated PNLT time histories for the three flight speeds. The agreement is quite good. In contrast to the Bell 212 helicopter, the Sikorsky S-61 helicopter does not produce blade slap and thus does not produce high levels on approach. The calculated EPNL values are 92.8, 90.8, and 90.3 EPNdB at 60, 100, and 115 kts, respectively, compared to measured values of 91.5, 91.1, and 90.4 EPNdB. The "soft" site measurement is 88.0 EPNdB, or 2.4 EPNdB below that of the "hard" site.

It is thus concluded that the Sikorsky S-61 helicopter noise is underpredicted significantly during hover, due primarily to installation effects associated with tail rotor noise. For the flyover conditions, the calculations show excellent agreement with unadjusted (to free-field) measurements made over hard ground.

Sikorsky S-64 from Data Base Items 3 and 4. - The comparison between calculated and measured hover noise for the Sikorsky S-64 helicopter, acquired as part of the series which included the Bell 212 and Sikorsky S-61, is shown in figure 5-55. As for the S-61 helicopter, the hover data shows high levels of noise in the mid-frequencies. This again is believed due to the tail rotor caused by inflow distortion from the vertical tail. The calculated PNLT is 97.5 PNdB compared to a measured value of 104.8 PNdB.

Figure 5-56 shows the comparison of the overhead noise spectra for flyovers at 60 and 85 kts. In spite of ground reflection effects, the agreement between measured and calculated levels is good. The calculated PNLT values are 96.3 and 96.0 PNdB at 60 and 85 kts, respectively, compared to measured values of 95.8 and 96.5 PNdB. The measurements were made at the "hard" site.

Figure 5-57 shows the PNLT time histories. The agreement between measurements and calculations is generally good. The time duration agreement is good, except for the 60 kts flyover measurements which show the noise holding up beyond 7 seconds past the peak. The measured EPNLT values are 96.6 and 94.7 EPNdB compared to calculated values of 95.2 and 93.5 EPNdB for 60 and 85 kts, respectively.

Thus, the Sikorsky S-64 helicopter also shows high levels of noise during hover which are underpredicted. During flyover, the calculated levels are in good agreement with the unadjusted levels measured over hard ground.

Data Base Item 2. - This data report presents noise measurements made on a Hughes OH-6A helicopter which was modified for noise reduction. Data was acquired during flyover at 40, 60, and 85 kts. For comparison with calculations, the configuration with a four-bladed tail rotor, configuration B, was selected. This configuration was chosen because it had reduced tail rotor noise. In contrast to the Sikorsky S-64 helicopter, this is a small helicopter and thus represents the other extreme in helicopter size.

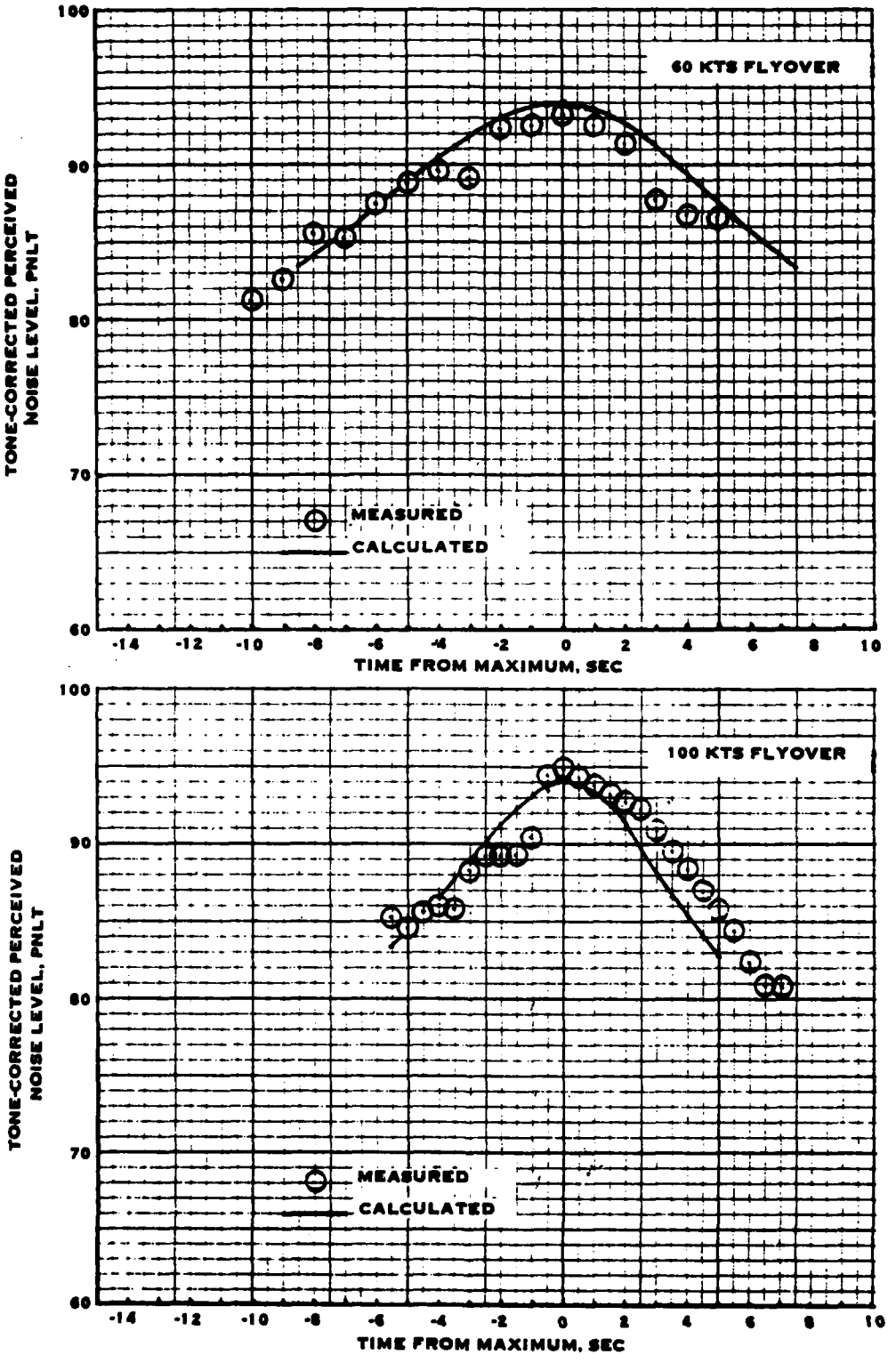

FIGURE 5-54. COMPARISON OF MEASURED AND CALCULATED SIKORSKY S-61 HELICOPTER PNLT TIME HISTORIES

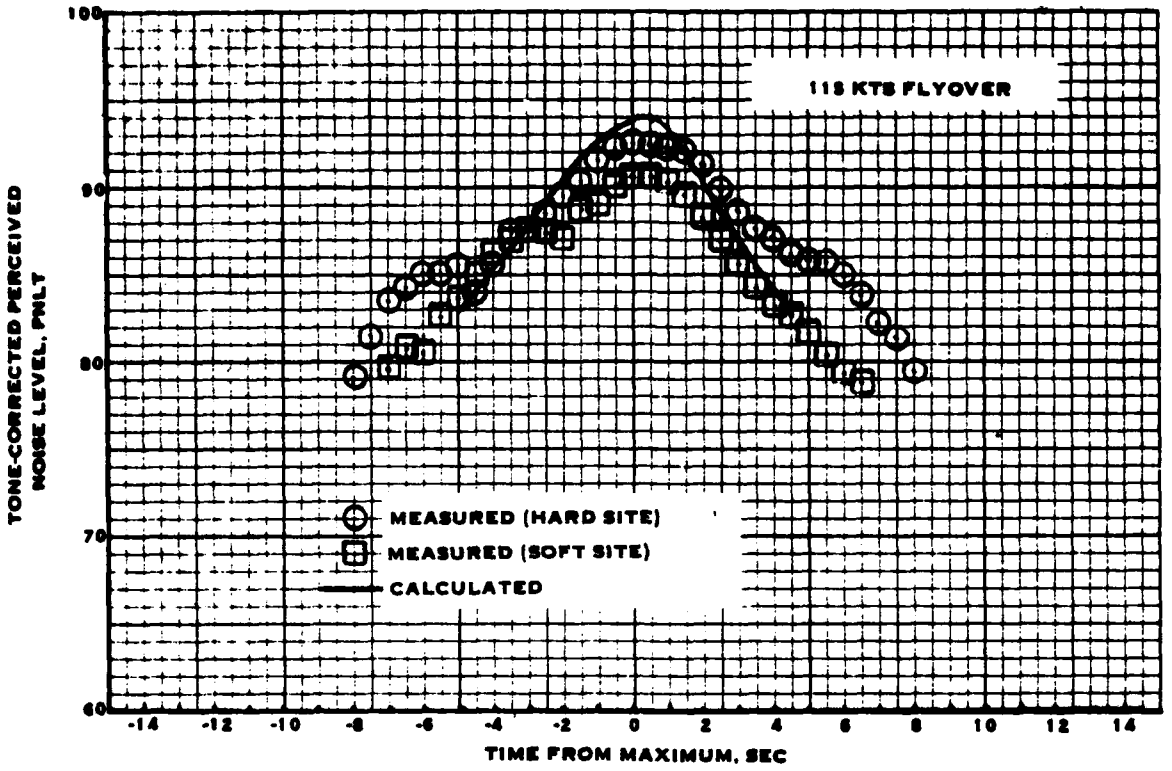

FIGURE 5-54. CONCLUDED

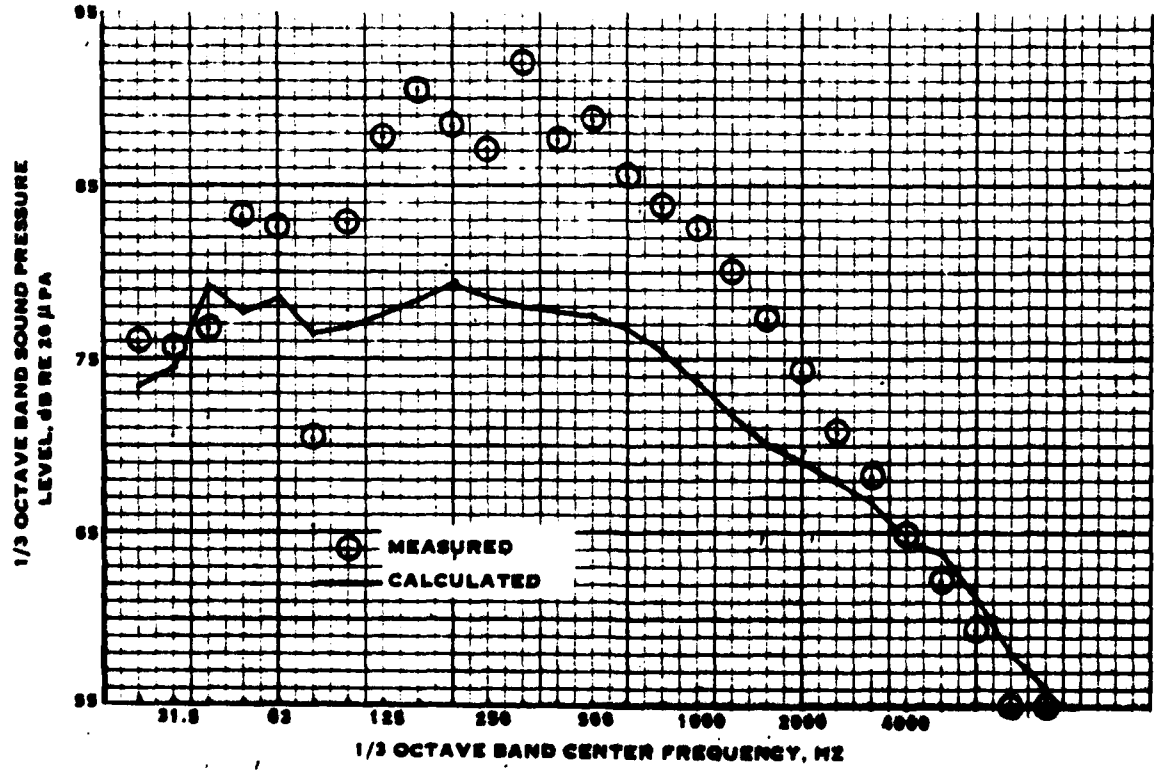

FIGURE 5-55. COMPARISON OF MEASURED AND CALCULATED SIKORSKY S-64 HELICOPTER NOISE DURING HOVER - DATA BASE ITEM 4

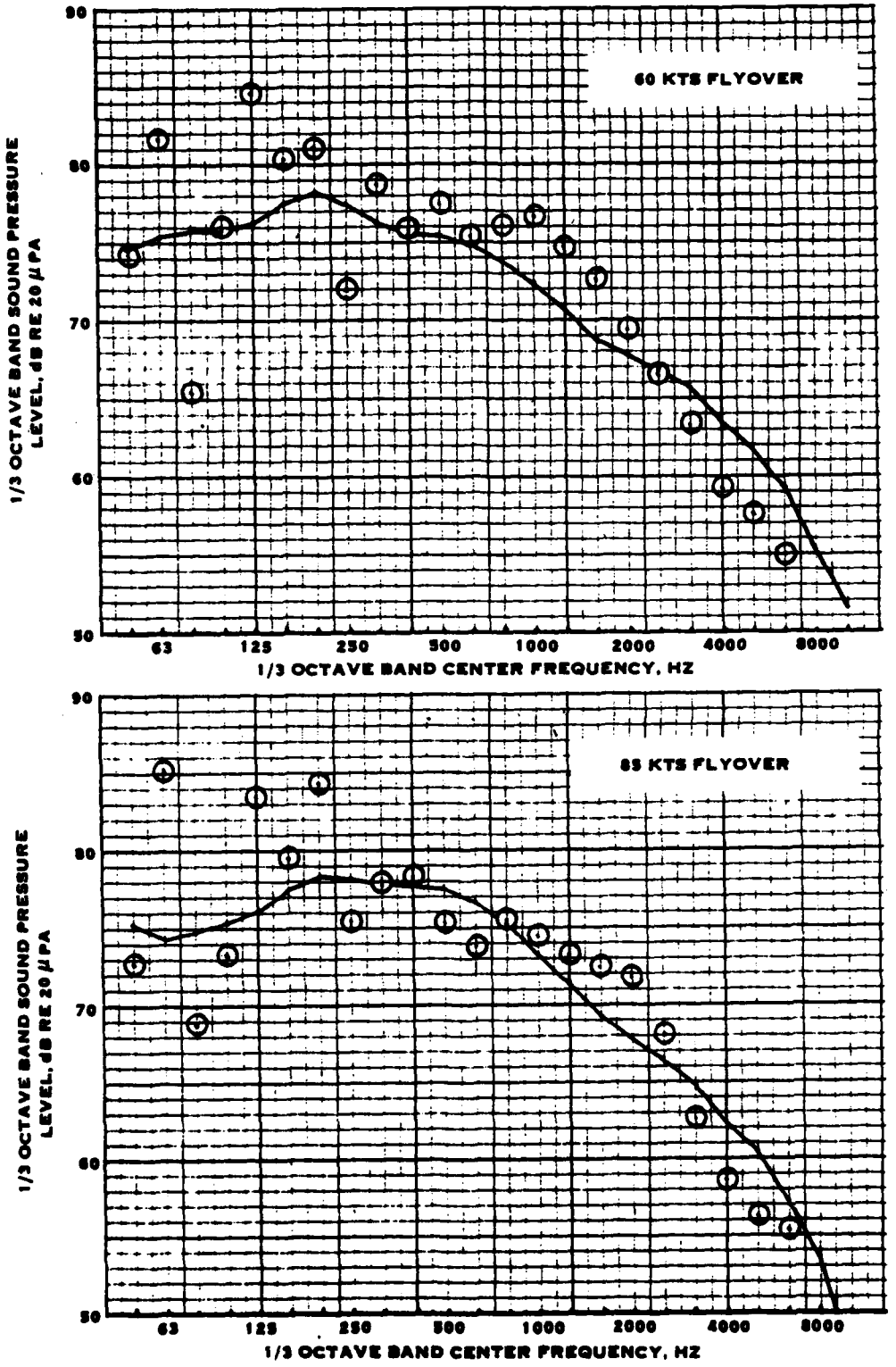

FIGURE 5-56. COMPARISON OF MEASURED AND CALCULATED SIKORSKY S-64 HELICOPTER NOISE DURING FLYOVER

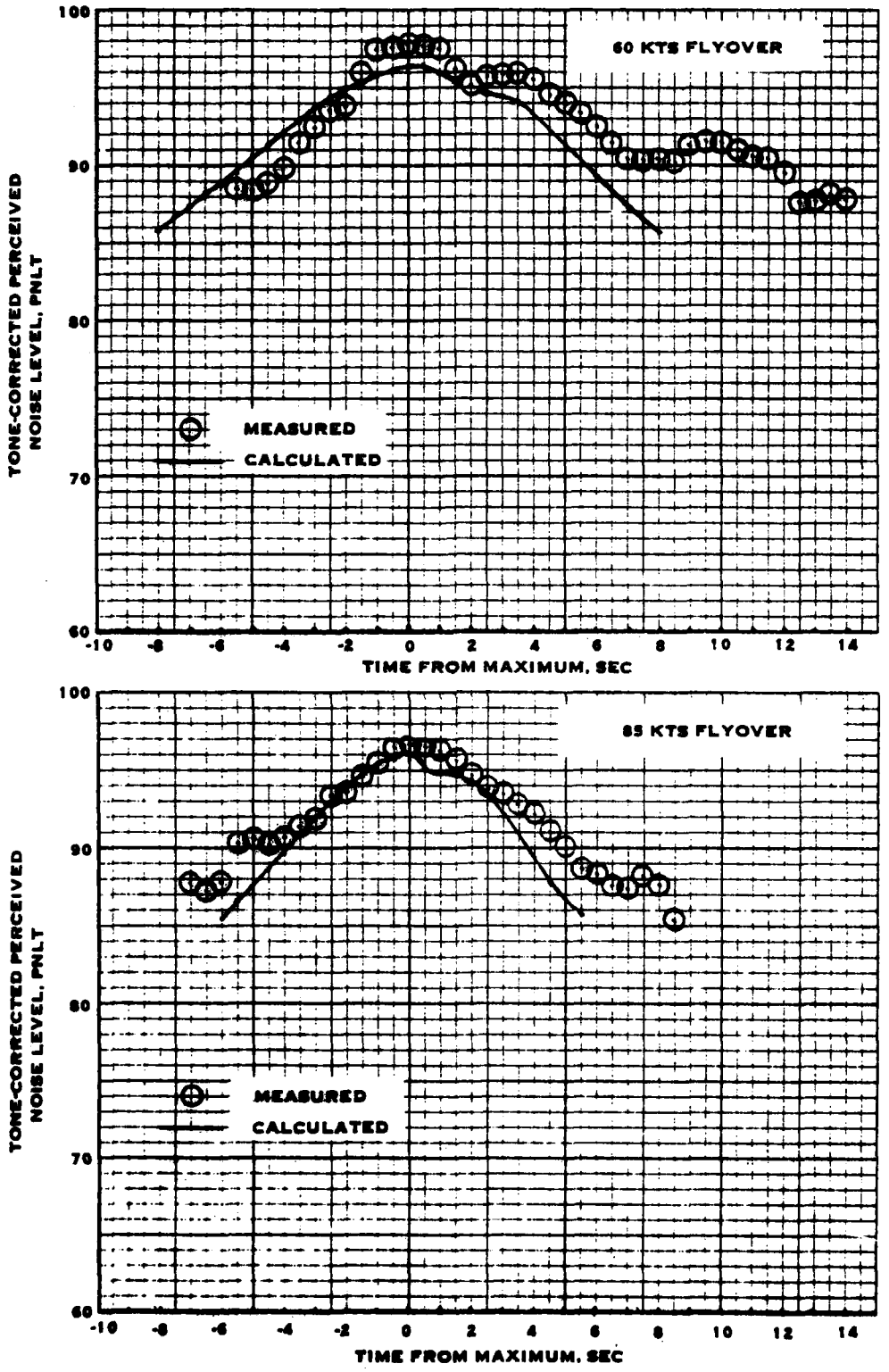

FIGURE 5-57. COMPARISON OF MEASURED AND CALCULATED SIKORSKY S-64 HELICOPTER PNLT TIME HISTORIES

Figure 5-58 shows the comparison between measurements and calculations for the maximum noise point during level flyover. Measurements were made with a microphone located at approximately four feet above a ground plane. As may be seen in figure 5-58, ground reflection effects are apparent. Also, the data shows a small amount of scatter. It is apparent that the high-frequency noise is overpredicted. The comparison of measured and calculated PNLT levels is 90.7, 92.0, and 93.1 PNdB versus 95.1, 95.1, and 95.0 PNdB for 40, 60, and 85 kts, respectively. The measured levels are the average of the data shown in figure 5-58. It is apparent that the Hughes OH-6A helicopter noise is slightly overpredicted.

Figure 5-59 shows the comparison of measured and calculated overall noise time histories for the 40 kt flyover. Although the calculated values are about 3 dB higher than the measured values, the calculated shape of the time history is in good agreement with that measured.

It is thus apparent that for the small helicopters represented by the Hughes OH-6A, the helicopter noise calculation procedure tends to overpredict by 3 to 5 PNdB.

Kaman HH-43B Helicopter from Reference 6. - This helicopter is of particular interest in the evaluation of the helicopter noise prediction methodology for hover conditions, as it does not have a tail rotor. Instead, is uses two side-by-side counter-rotating main rotors. Reference 6 represents noise measurements made during hover and during 85 kts flyover. As with previous data, the microphone was located four feet above a ground plane.

Figure 5-60 shows the comparison between measured and calculated levels during hover and 85 kts flight. It is apparent from figure 5-60 that the spectrum during hover is very similar to that during flight. In contrast to the data from conventional helicopters, there is no mid-frequency peak during hover which disappears in flight. This supports the assertion that the conventional helicopter noise signature contains significant tail rotor noise due to installation effects.

Figure 5-60 shows that the noise is slightly underpredicted at high-frequency. This could be due to higher rotor noise inflow distortion caused by the intermeshing main rotors. In hover, the measured PNL is 96 PNdB compared to a calculated value of 91 PNdB. In flight, the measured PNL is 91 PNdB compared to a calculated value of 87.5 PNdB.

Data Base Item 6. - This data was also acquired on a Kaman HH-43B helicopter during flyover at 40, 60, and 70 kts flight speed. Noise measurements were made using a microphone located at four feet above the ground plane.

Figure 5-61 shows the comparison between measured and calculated peak flyover noise levels for 40, 60, and 70 kts flight speed. It is apparent from figure 5-61 that the measurements have little scatter. The correlation between measurements and calculations is very good. The measured PNL values, based on the average of the three

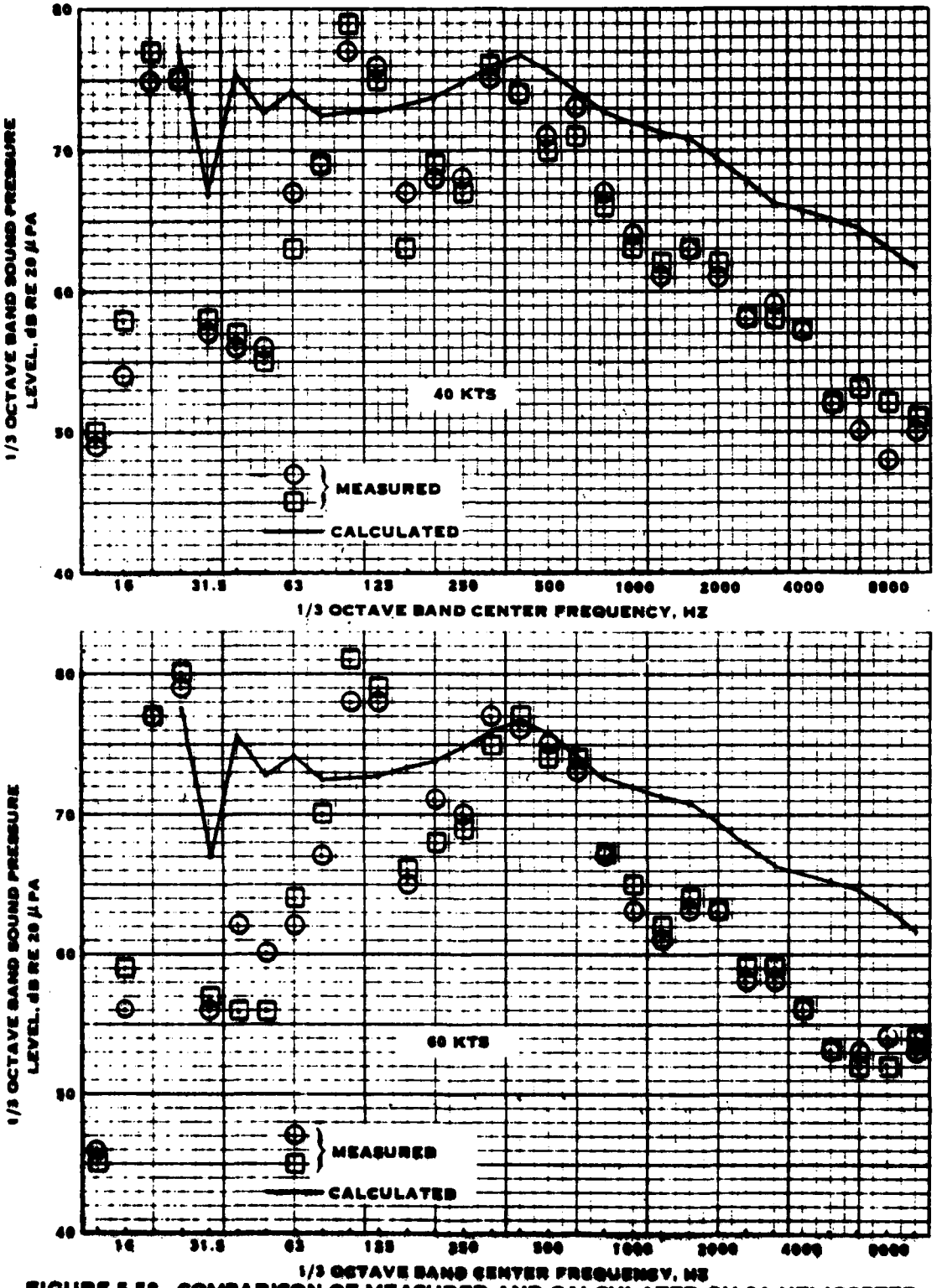

FIGURE 5-58. COMPARISON OF MEASURED AND CALCULATED OH-6A HELICOPTER NOISE SPECTRA FROM DATA BASE ITEM 2

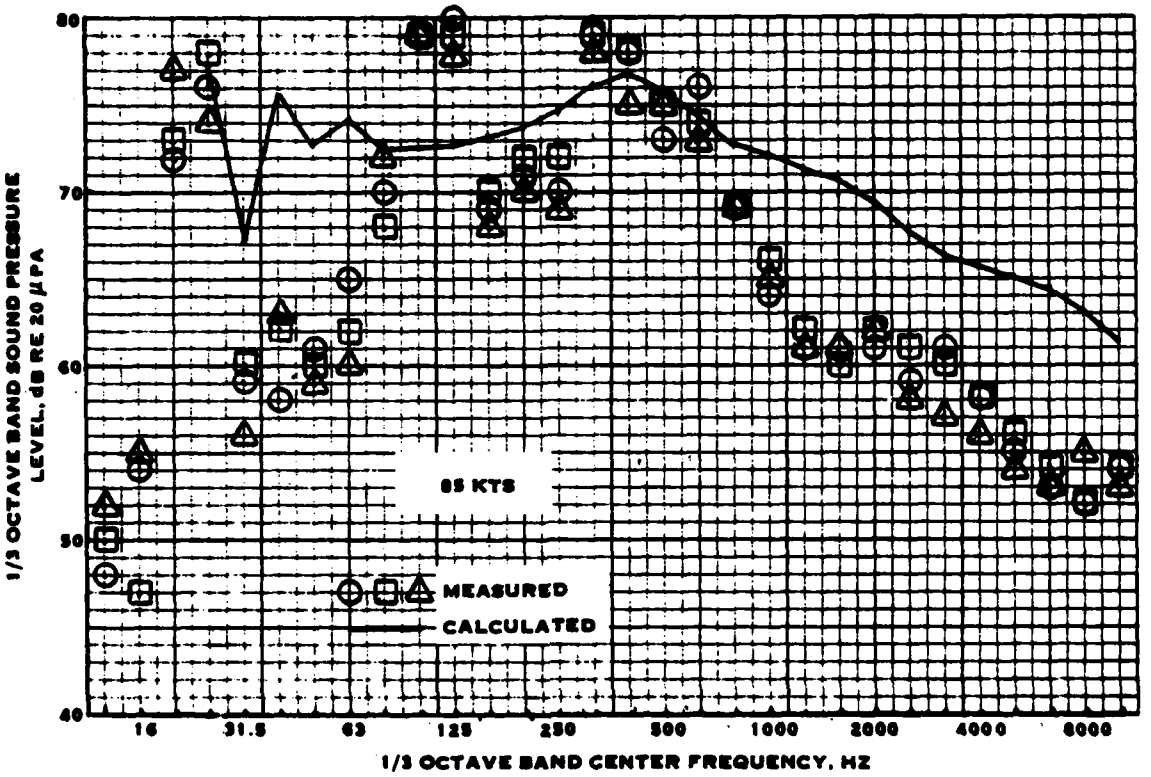

FIGURE 5-58 CONCLUDED

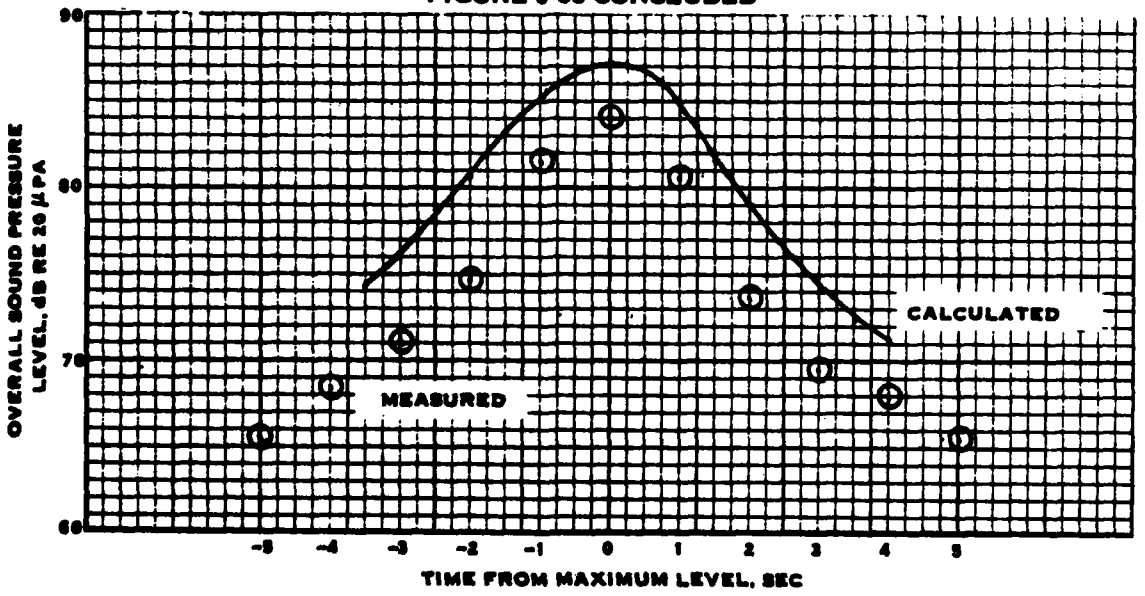

FIGURE 5-59. COMPARISON OF MEASURED AND CALCULATED OVERALL SOUND PRESSURE LEVEL FLYOVER TIME HISTORIES FOR THE OH-6A

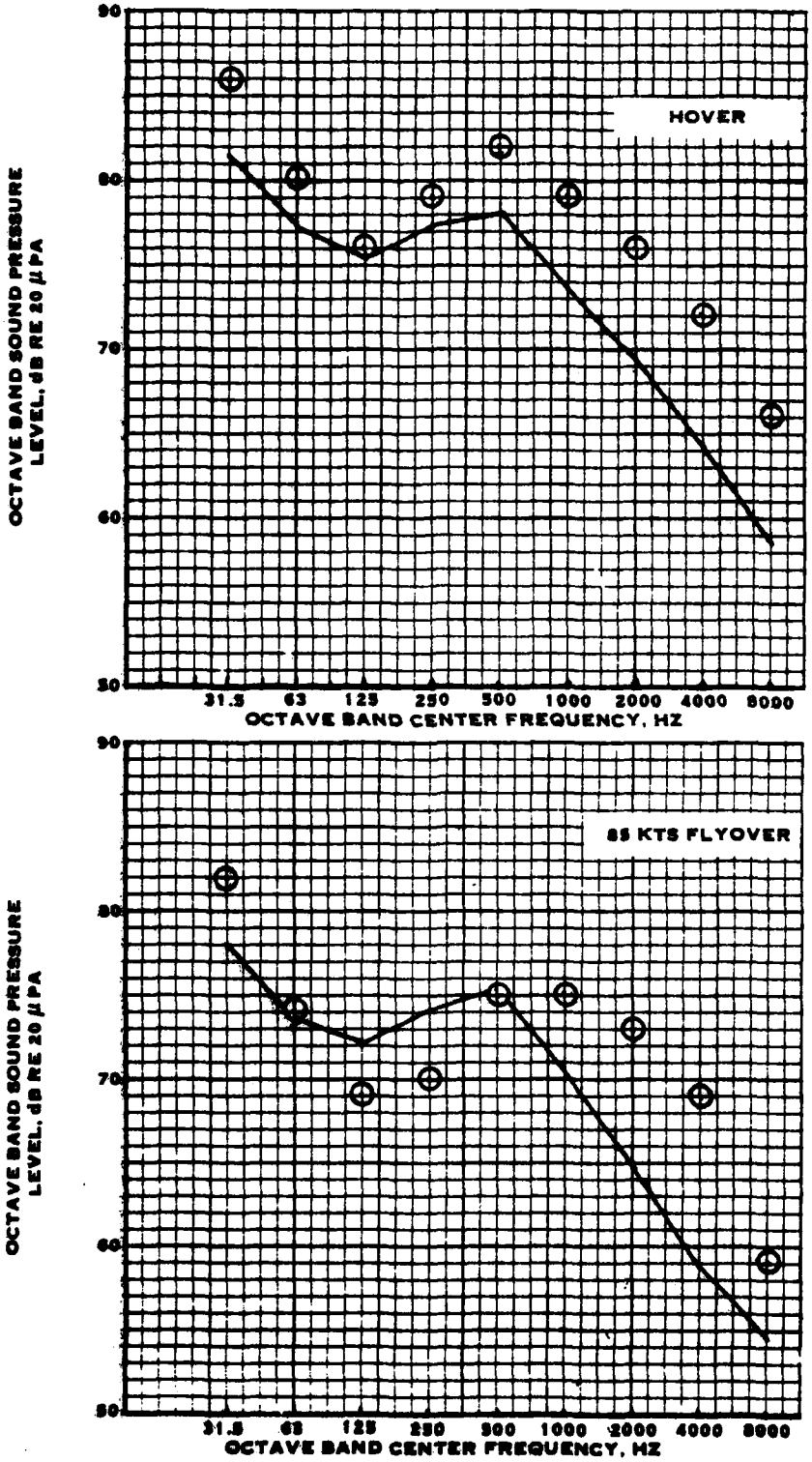

FIGURE 5-60. COMPARISON OF MEASURED AND CALCULATED HH-43B HELICOPTER NOISE SPECTRA FROM REFERENCE 6.

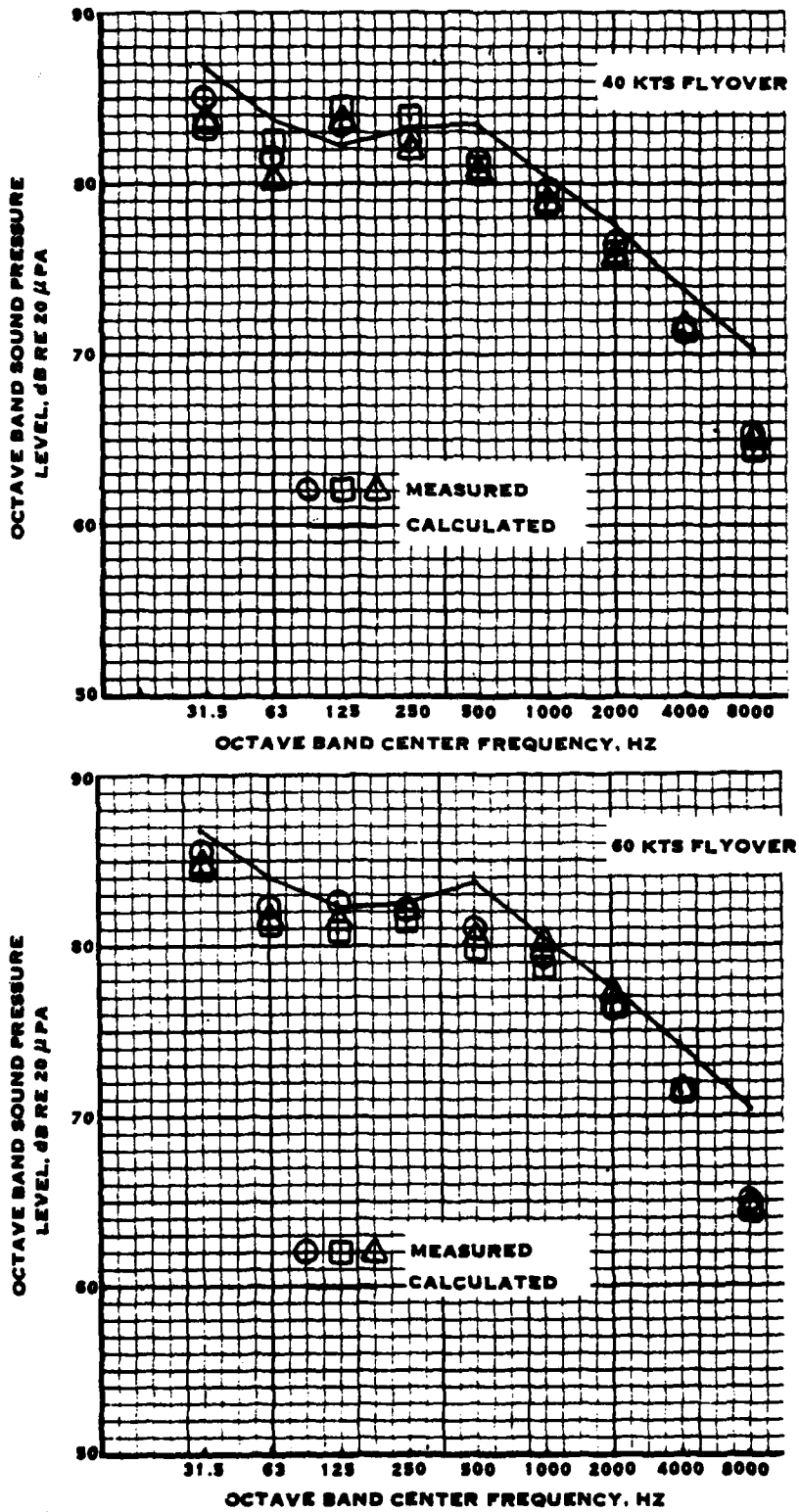

FIGURE 5-61. COMPARISON OF MEASURED AND CALCULATED HH43B HELICOPTER FLYOVER NOISE LEVELS FROM DATA BASE ITEM 6

sets of data indicated at each flight speed, are 96.6, 96.6, and 96.9 PNdB for 40, 60, and 70 kts flight speed, respectively. This compares to 98.6, 98.6, and 98.8 PNdB calculated, an overprediction of 2 PNdB.

Figure 5-62 shows the comparison between measured and calculated overall sound pressure level time histories for the helicopter at 60 kts. The calculated values appear to match the average of the measurements very well.

This data is slightly overpredicted, in contrast to that from reference 6 which was slightly underpredicted.

Summary for Helicopters

Since all the helicopter noise measurements were made using microphones located four feet above a ground plane, ground reflection effects were very apparent at frequencies below 500 Hz. Attempts to correct for ground reflection effects were not successful, primarily because the calculated frequencies of reinforcements and cancellations do not seem to match their apparent locations in the measured spectra. It was thus not possible to verify the agreement between measured and calculated one-third octave band spectra at low frequencies. Despite these limitations, the agreement between measured and calculated Perceived Noise Levels appears quite good.

It was found that conventional helicopters appear to produce high levels of tail rotor noise during hover, probably due to severe inflow distortion from the vertical tail. In flight, the inflow distortion is diminished and tail rotor noise decreases. Thus, these showed significantly higher noise levels during hover than were calculated. Only one helicopter, the HH-43B, showed similar noise levels during hover and flight. This was attributed to the fact that this helicopter does not have a tail rotor.

The PNLT time histories are quite well calculated for those helicopters which do not produce significant blade slap. The Bell 212 has blade slap, which prolongs the duration of the flyover significantly. Since the helicopter noise prediction method does not include impulsive noise, the duration correction is underpredicted for this helicopter.

Table 5-II presents the summary of comparison between measured and calculated helicopter noise levels. The measured levels are based on as-measured spectra and do not include any adjustments for ground reflections. For the hover conditions, the calculation procedure underpredicted by 0.5 PNdB (for the Bell 212 sideline condition) to 7.3 PNdB (for the Sikorsky S-64). The average measured-minus-calculated level is 4.0 PNdB with a standard deviation of 2.6 PNdB.

The agreement between measured and calculated peak PNLT and peak PNL (for the Kaman HH-43B) during flyover is seen to be better. For the flyovers the average measured-minus-calculated level is -0.9 PNdB with a standard deviation of 2.0 PNdB. The average measured-minus-calculated EPNL is 2.7 EPNdB with a standard deviation of 3.3 EPNdB. However, this includes the data from the Bell 212, which was shown

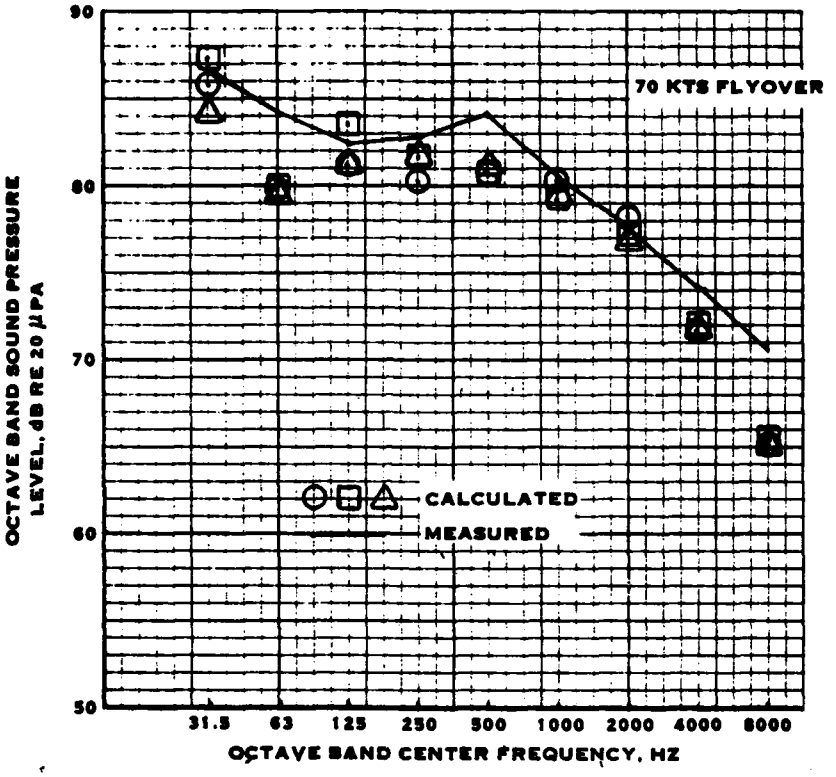

FIGURE 5-61. CONCLUDED

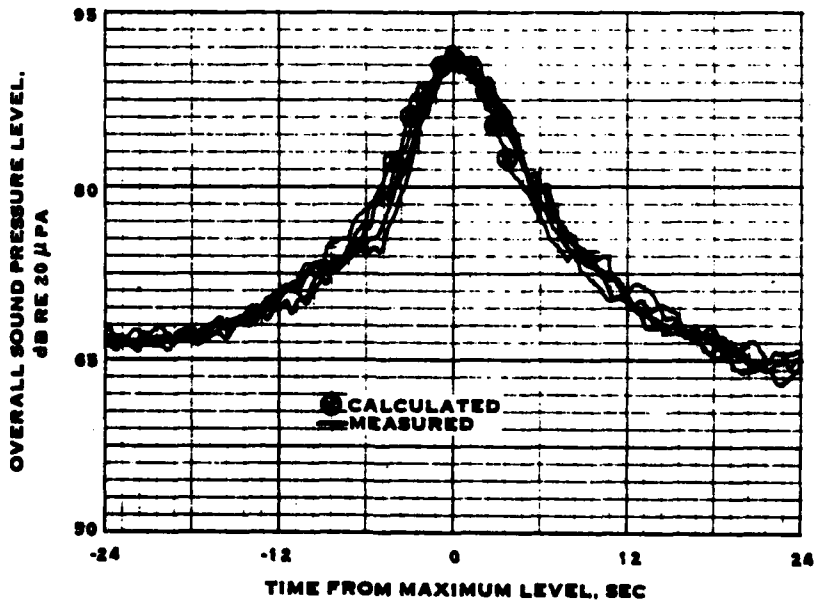

FIGURE 5-62. COMPARISON OF MEASURED AND CALCULATED TIME HISTORIES FOR THE HH-43B HELICOPTER AT 60 KTS AND 200 FT.

TABLE 5-II

SUMMARY OF THE COMPARISON BETWEEN MEASURED AND CALCULATED HELICOPTER NOISE LEVELS

BELL 212

Flight Condition	PNLT Meas	PNLT Calc	EPNL Meas	EPNL Calc
Hover-Overhead	97.6	95.0	-	-
Hover-Sideline	92.2	91.7	-	-
60 kts	91.6	94.6	96.3	93.6
99 kts	94.0	94.8	96.7	91.9
110 kts	95.2	94.2	98.6	91.4
114 kts	95.7	94.3	99.3	91.3

Sikorsky S-61

Flight Condition	PNLT Meas	PNLT Calc	EPNL Meas	EPNL Calc
Hover	99.7	94.9	-	-
60 kts	93.0	93.7	91.5	92.8
100 kts	93.9	93.7	91.1	90.8
115 kts	92.3	93.5	90.4	90.3

Sikorsky S-64

Flight Condition	PNLT Meas	PNLT Calc	EPNL Meas	EPNL Calc
Hover	104.8	97.5	-	-
60 kts	95.8	96.3	96.6	95.2
85 kts	96.5	96.0	94.7	93.5

Hughes OH-6A

Flight Condition	PNLT Meas	PNLT Calc
40 kts	90.7	95.1
60 kts	92.0	95.1
85 kts	93.1	95.0

Kaman HH-43B

Flight Condition	PNL Meas	PNL Calc
Hover	96.0	91.0
40 kts	96.6	98.6
60 kts	96.6	98.6
70 kts	96.9	98.8
85 kts	91.0	87.5

to have very long flyover time histories due to high levels of impulsive noise. Eliminating the Bell 212 data from the computation gives an average measured-minus-calculated EPNL of 0.3 EPNdB with a standard deviation of 1.1 EPNdB.

It is thus concluded that helicopter flyover noise levels calculated using the current methodology are in good agreement with flyover noise levels measured using a microphone located at four feet above a "soft" ground plane.

EVALUATION OF CORE ENGINE NOISE PREDICTION

Introduction

The data available for isolated core engine noise is very limited. Although some data exists on isolated components of engine noise, such as that from the combustor, the measurements are usually made on special test facilities and do not include the effects of propagation through the rest of the engine (such as through the turbine stages). The two cases selected for this study were chosen because the first is an uninstalled, isolated engine while the second is installed in an airplane nacelle and thus shows the effects of inlet and exhaust ducting.

Comparison of Measured and Calculated Core Engine Noise

T-56 Engine from the Hamilton Standard Data Base. - This engine was tested out-of-doors on an isolated test stand. As this is a single shaft engine, it can be (and was) tested without a load at idle. Although the engine power output is negligible, it was run at full output rpm and thus the turbine was developing power to keep the compressor running.

The measured levels were corrected for ground reflection effects using the procedure from reference 8 and extrapolated from a constant 43-foot measurement radius to a 43-foot sideline. Figure 5-63 shows the comparison between measured and calculated levels for five azimuth angles, from 45 degrees (with zero degrees along the inlet axis) to 135 degrees. Although the low-frequency (combustion) noise is underpredicted and the high-frequency compressor noise is overpredicted at the two forward locations, the agreement is fairly good for the 90, 112. and 135 degree locations, where the total propulsor noise normally peaks.

T-56 Engine from Reference 15. - This data was derived from Lockheed Electra turboprop flyover noise measurements. The comparison shown in figure 5-64 is for four engines for the peak PNLT point for a flyover at 584 ft at the take-off condition.

The agreement between measured and calculated levels at frequencies below 1600 Hz is good, missing at the peak by only 3.5 dB. Above 1600 Hz, the engine noise is overpredicted. The high-frequency noise is calculated to be that from the turbine. As uninstalled engine noise (figure 5-63) showed better agreement between measured and calculated levels in the aft quadrant, the apparent overprediction is believed to be an indication of installation effects, such as attenuation from the tailpipe or shielding by the wing (the T56 exhaust is above the wing).

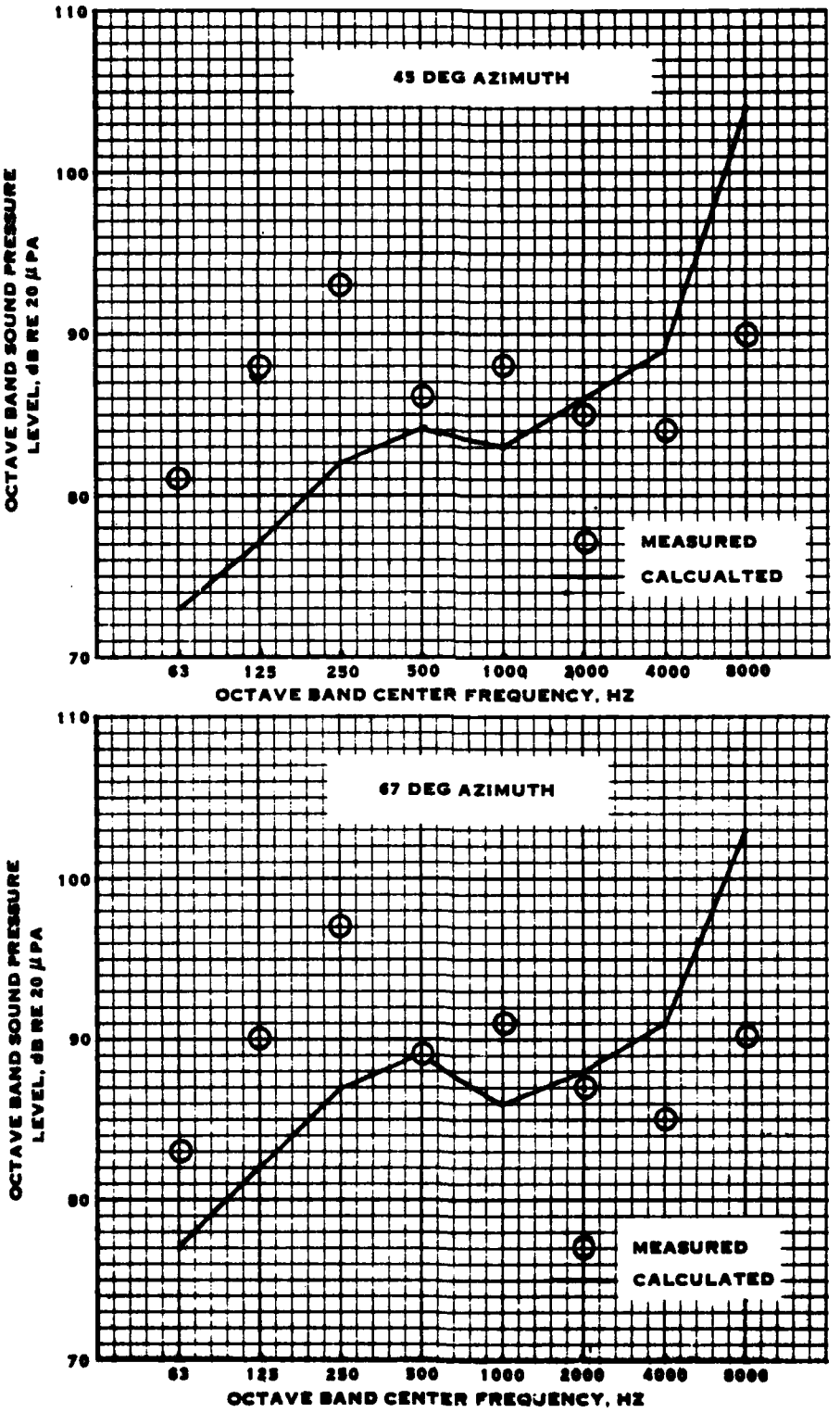

FIGURE 5-63. COMPARISON OF MEASURED AND CALCULATED ISOLATED T-56 ENGINE NOISE LEVELS

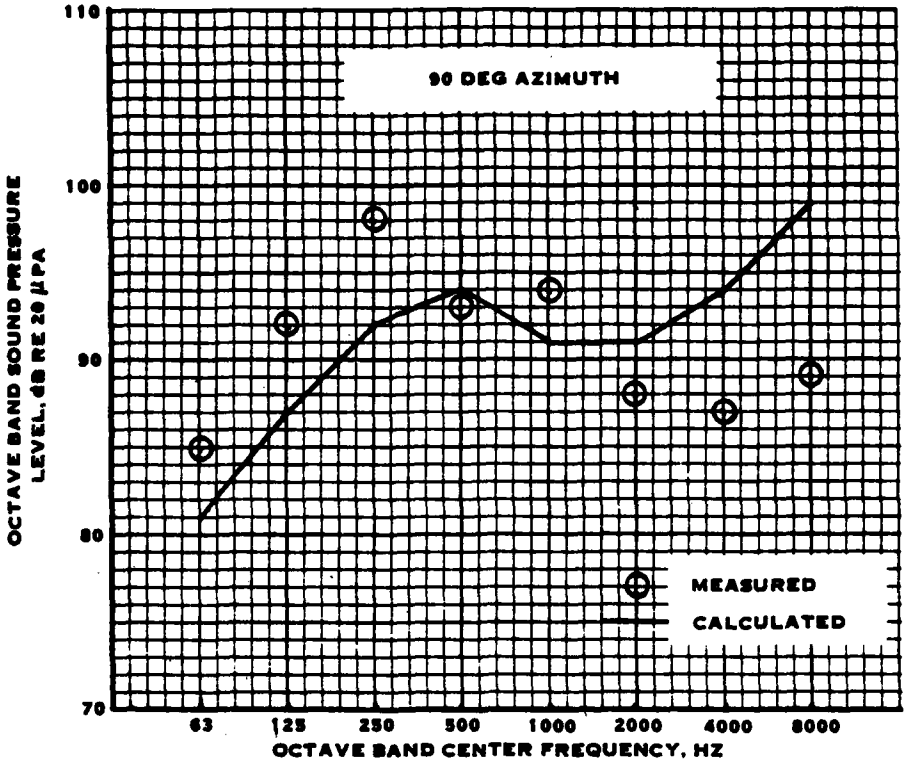

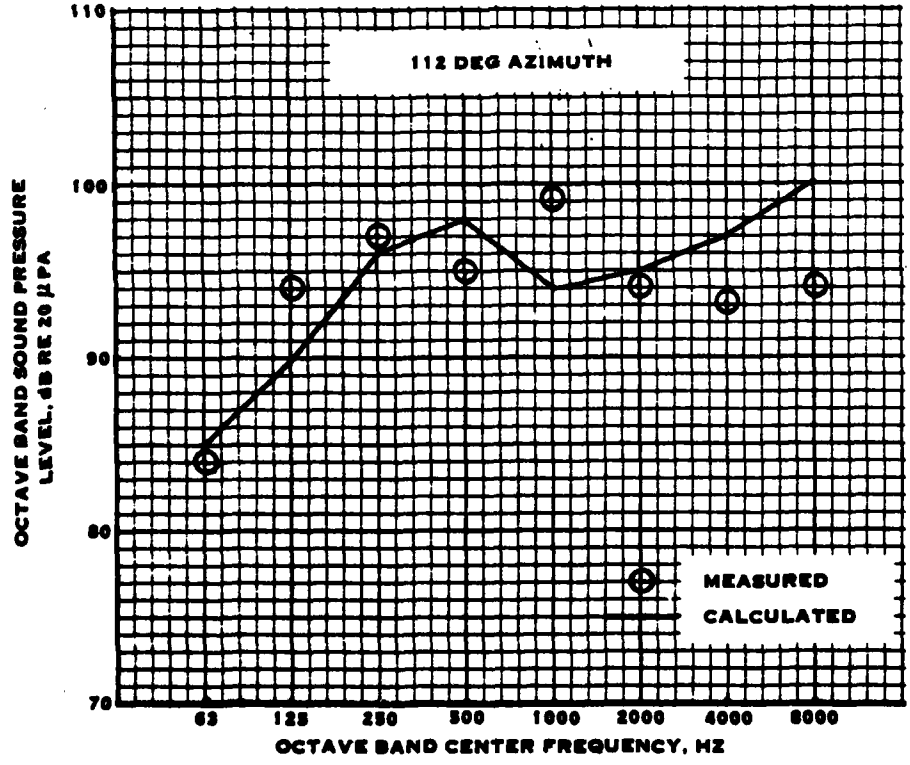

FIGURE 5-63. CONTINUED

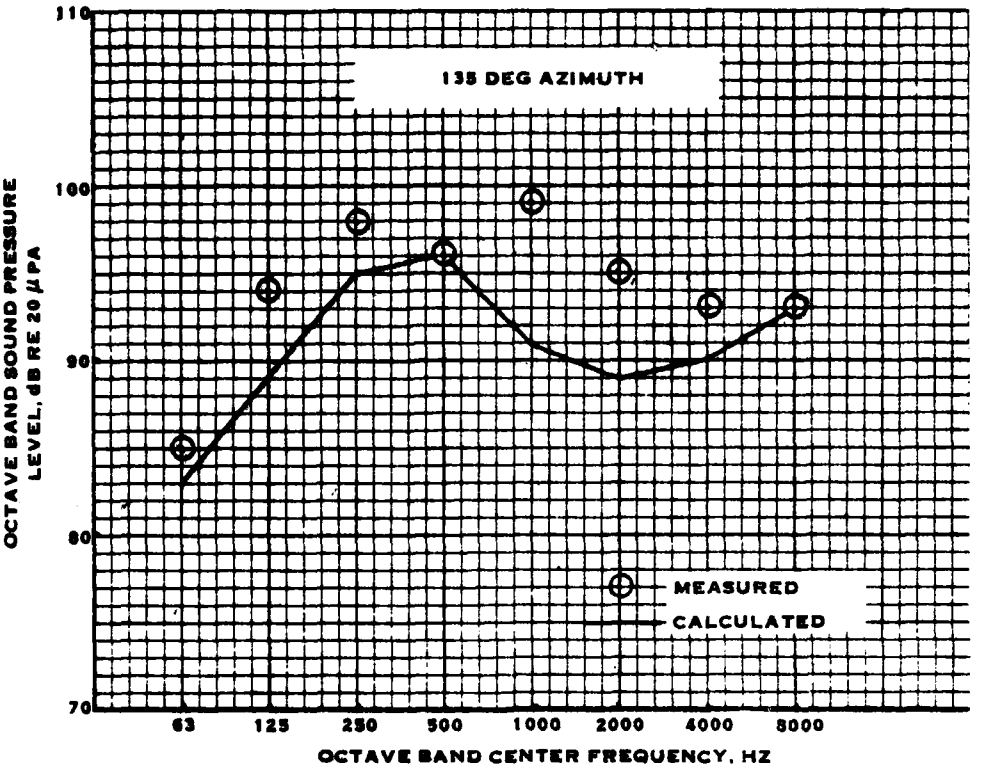

FIGURE 5-63. CONCLUDED

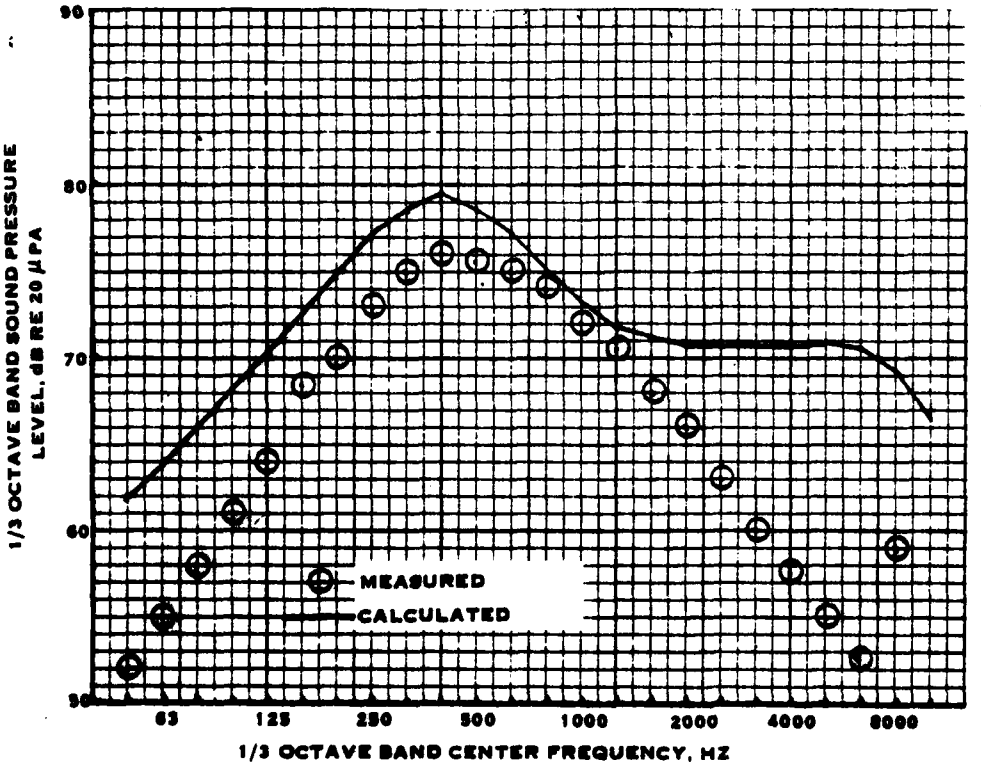

FIGURE 5-64. COMPARISON OF MEASURED AND CALCULATED T-56 ENGINE ON THE LOCKHEED ELECTRA AT TAKE-OFF CONDITION

Summary for Core Engines

Although the sample of engine noise data is small, the correlation between measured and calculated core engine noise showed encouraging results. The agreement in the aft quadrant was good for an isolated engine. For the installed engine, the low-frequency noise appeared well calculated while the high-frequency turbine noise was overpredicted. However, this could be due to installation effects, such as tailpipe attenuation or wing shielding.

EVALUATION OF JET NOISE PREDICTION

Introduction

Much of the jet noise data is from model jets and includes noise measurements made on cold and hot jets as well as single and coaxial jets. Some data includes flight effects by forward-flight simulation in a wind tunnel. Some data was also found in full-scale jets. These are measurements made of engine exhaust. Thus, the engine jet noise data could be contaminated by other noise sources, such as combustors and turbomachinery. This can be a significant problem at low jet velocities, as jet noise decreases rapidly with decreasing stream velocity. Model jets generally do not have other sources of noise, as the supply-air compressors are remote and well muffled. However, model jets have typical nozzle diameters of a few inches, compared to up to several feet for full scale engine exhaust nozzles, thus requiring large scaling functions to full-scale.

The data which was used for the evaluation of the jet noise prediction methodology was selected first because it was considered to be high quality data and second because the necessary information to perform the calculation was available. It should be noted that the jet noise calculation subroutine uses jet net thrust, weight-flow-rate, and nozzle area as inputs. The jet noise prediction method is based primarily on jet velocity with adjustments for jet density, frequency spectra adjusted for jet temperature, and forward-flight effects based on flight speed. The jet velocity, density, and temperature are calculated in the subroutine by applying aerodynamic relationships (perfect gas law, momentum equation, etc). In some cases, test reports indicate jet velocity, density, and temperature while others indicate jet thrust. In the first instance, the parameters given were used to calculate jet thrust and weight-flow-rate for input to the noise prediction method rather than using them directly in the jet noise calculation procedure. Although this could lead to greater errors due to the conversion from jet velocity, density, and temperature to jet thrust and weight-flow and back again, it is more representative of the way jet noise is normally calculated by the jet noise subroutine and thus gives a more realistic evaluation.

Comparison of Measured and Calculated Model Jet Noise

The comparisons between measurements and calculations presented in this section are for model jets. These include single stream jets and coaxial jets, hot jets and cold jets, and static jets and jets in simulated forward-flight. In all cases, measurements

were made under free-field conditions (although in one or two instances tunnel reverberation effects were marginal at some frequencies) so that comparisons between measurements and calculations could be made directly.

Data Base Item 9. - This report presents noise measurements made on a hot, single stream jet under static and forward-flight conditions. Two static jet conditions were calculated. The first conditions was for a jet velocity of 1325 ft/sec (jet thrust of 306.5 lbs and weight-flow-rate of 7.45 lb/sec). The comparison between calculations and measurements is shown in figure 5-65. This figure shows the comparison between measured and calculated noise directives for the one-third octave band levels at octave band center frequencies. The comparison is seen to be very good, particularly in the frequency range 1000 to 8000 Hz. Both the levels and the directivity are seen to be well predicted.

Figure 5-66 shows the comparison between measurements and calculations for the second condition, a jet velocity of 1640 ft/sec (jet thrust of 488.5 lbs and weight-flow-rate of 9.59 lb/sec). Although this condition is not as well predicted as the previous one, the correlation is still quite good. The location of the peak directivity is well predicted at all frequencies except 2000 Hz which misses by about 10 degrees. In all cases, the calculated levels are within about ± 3 dB of the average of the measurements.

Figure 5-67 shows the comparison between measured and calculated jet noise levels for a simulated forward-flight condition. This condition is for jet velocity of 1641 ft/sec (jet thrust of 442.5 lbs and weight-flow-rate of 9.59 lb/sec) and simulated flight speed of 151 ft/sec. As for the static conditions, the 250, 500, and 16000 Hz band levels are slightly underpredicted at the directivity peak. At all other bands, the agreement is excellent at all azimuth angles.

On the basis of comparison between measured and calculated jet noise levels for this model jet, the jet noise prediction method appears to do well, showing excellent agreement in level, directivity, and forward-flight effects.

Data Base Item 13. - The single jet noise measurements presented in this paper were obtained in an open-jet wind tunnel and thus include the effects of simulated forward-flight. The data used for comparison with the calculations were adjusted for propagation through the moving medium and through the shear layer. Figure 5-68 shows the comparison of measured and calculated jet noise 1/3 octave band spectra for three jet velocities, all at an angle of 130 degrees and a tunnel speed of 200 ft/sec. The correlation is very good for all three jet velocities. Both the peak levels and the spectrum shapes are well predicted. The lowest jet velocity condition is slightly underpredicted and the highest jet velocity condition is slightly overpredicted, indicating that the variation of jet noise with jet velocity is calculated to be more than that shown by measurements. However, the disagreement is only about 1 dB at the 800 ft/sec condition and about 2 dB at the 1670 ft/sec condition.

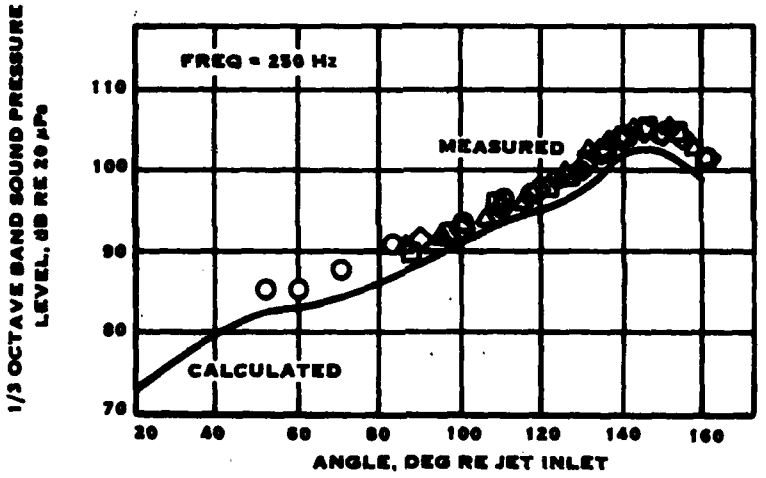

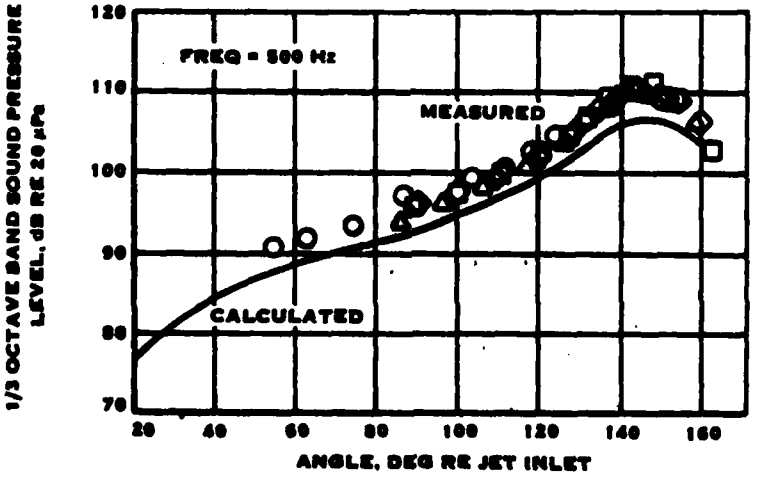

FIGURE 5-65. COMPARISON OF MEASURED AND CALCULATED JET NOISE FROM DATA BASE ITEM 9 - STATIC CONDITION, 1325 FT/SEC JET VELOCITY

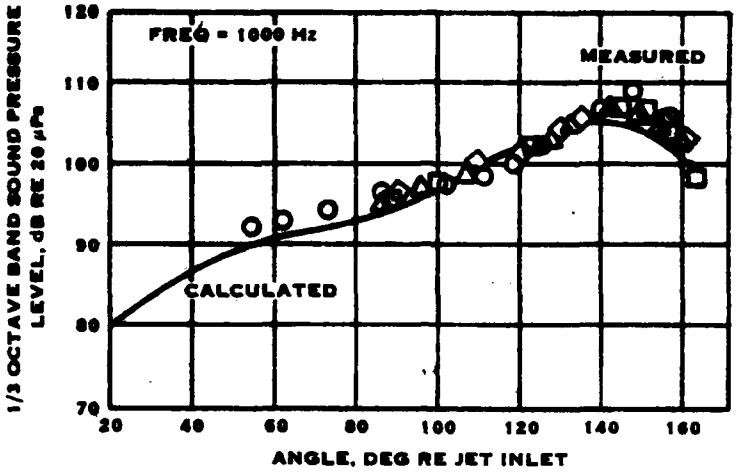

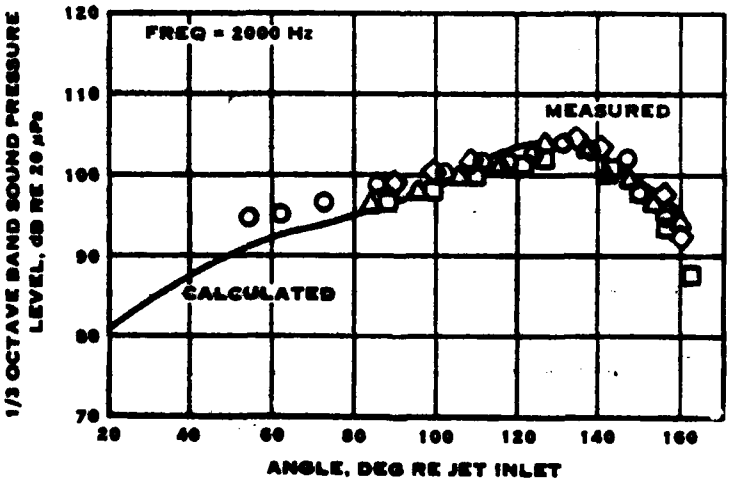

FIGURE 3-65. CONTINUED

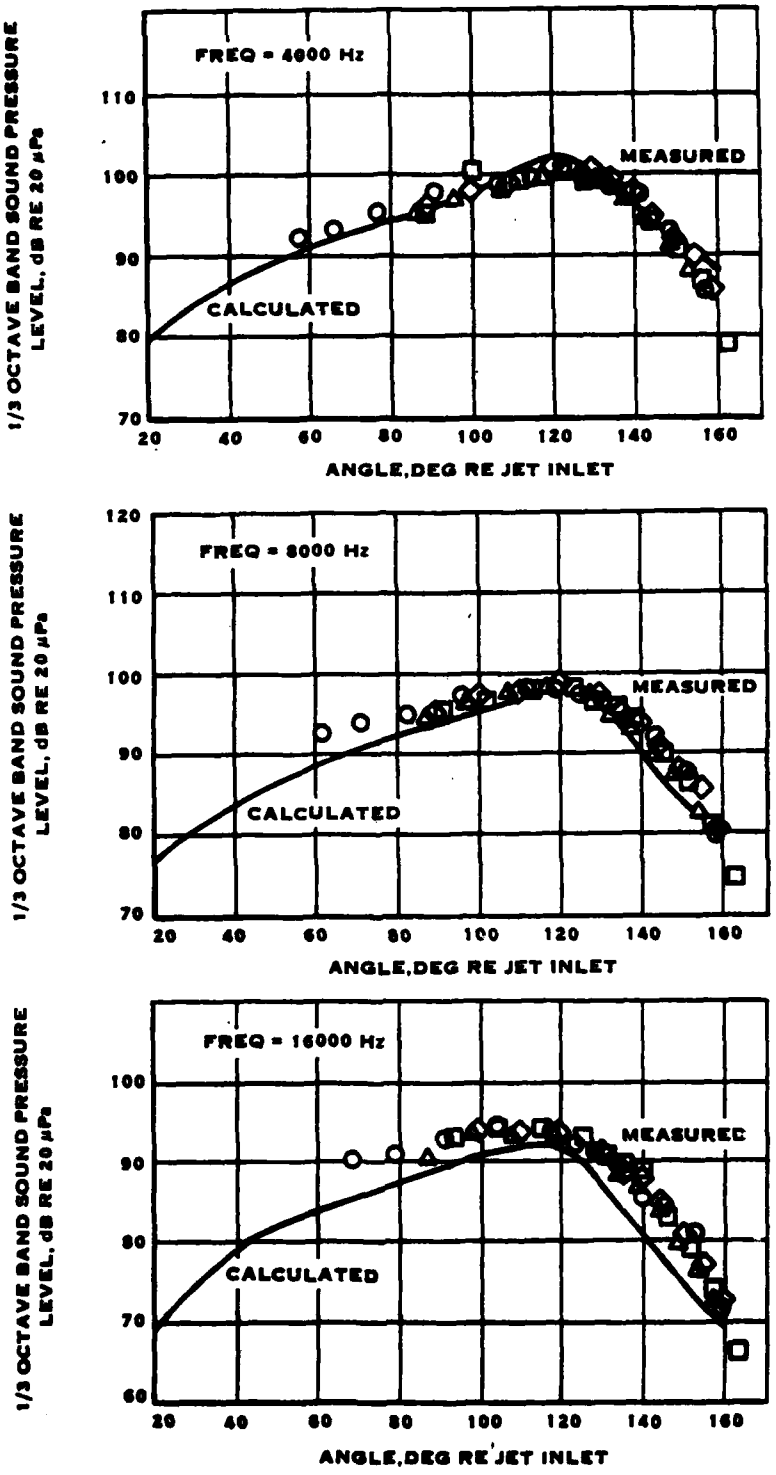

FIGURE 5-65. CONCLUDED

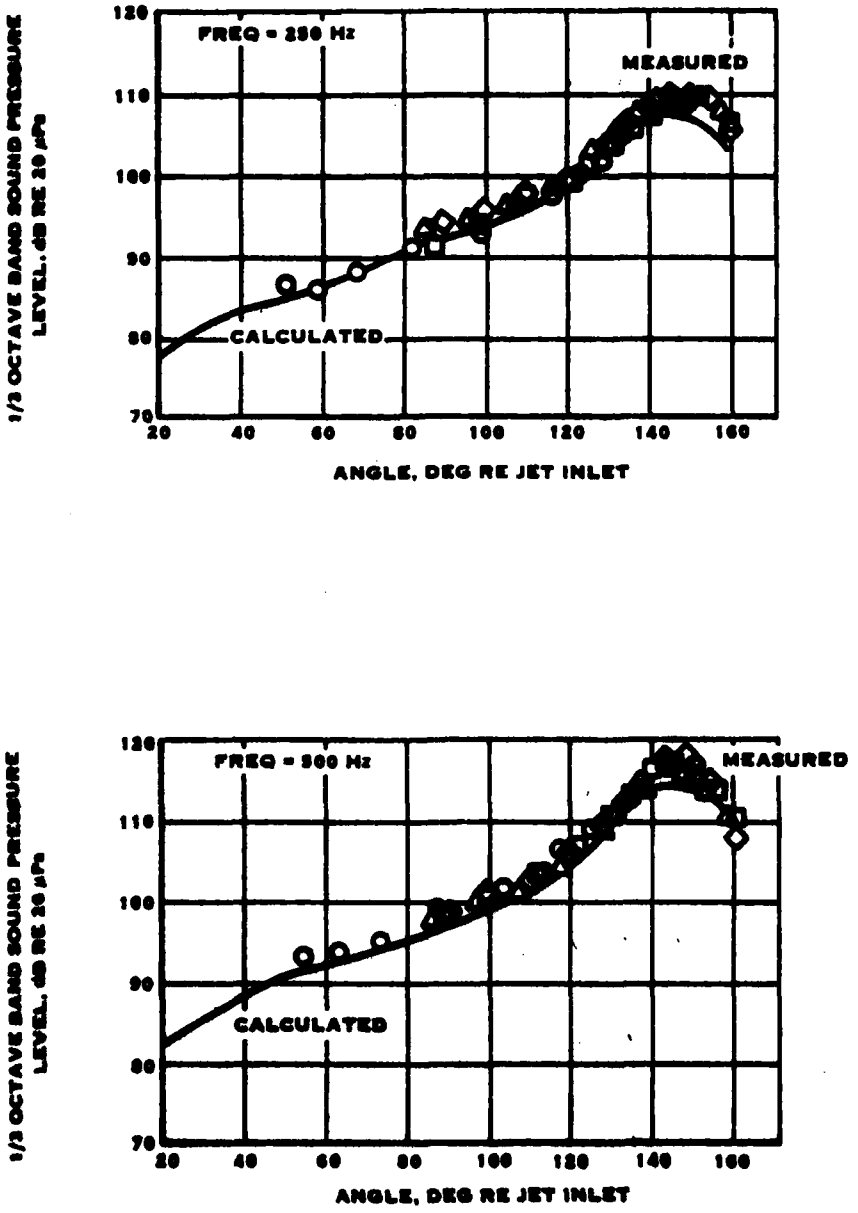

FIGURE 5-66. COMPARISON OF MEASURED AND CALCULATED JET NOISE FROM DATA BASE ITEM 9 - STATIC CONDITION 1640 FT/SEC JET VELOCITY

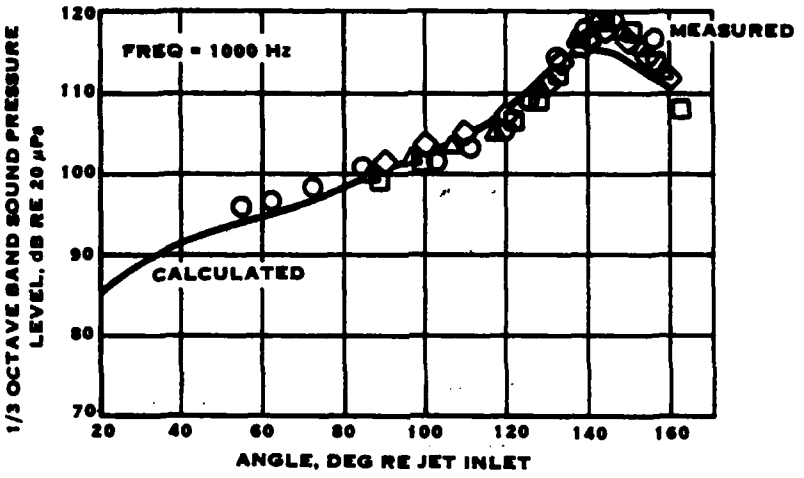

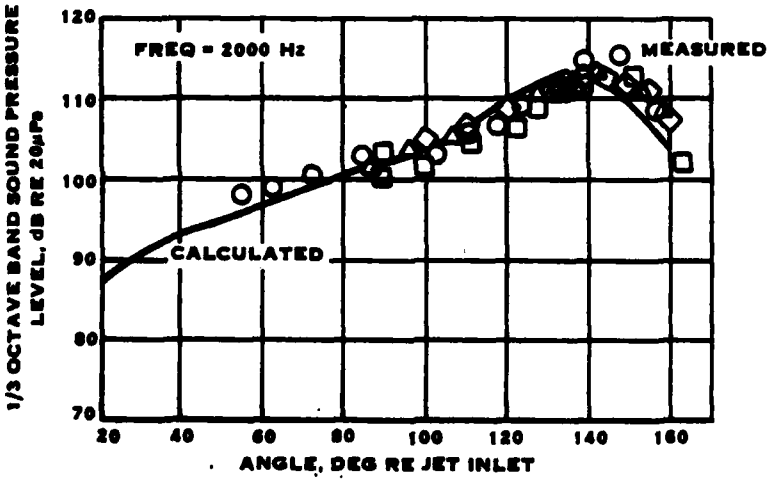

FIGURE 5-66. CONTINUED

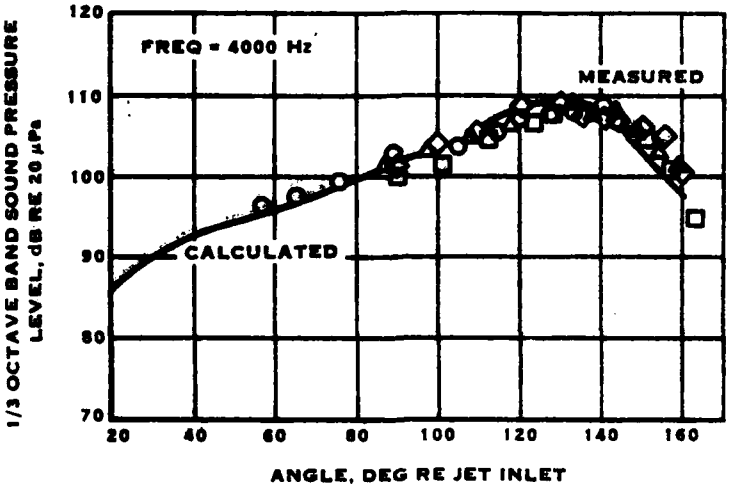

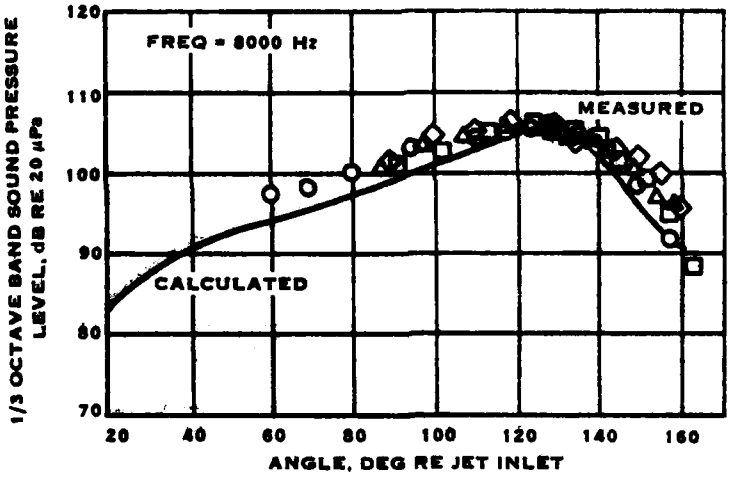

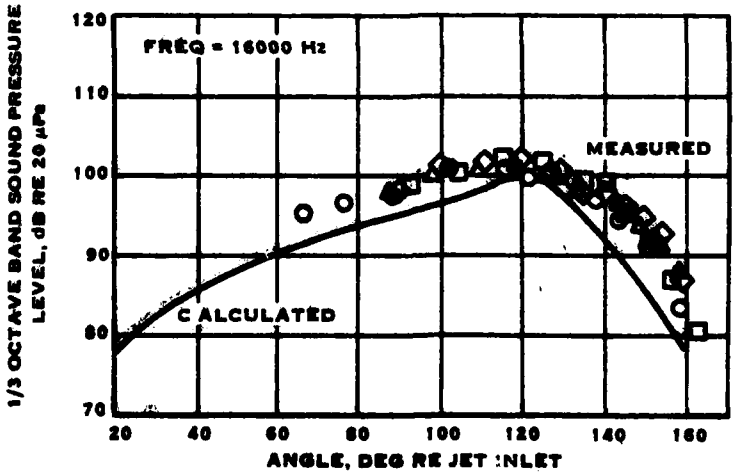

FIGURE 5-66. CONCLUDED

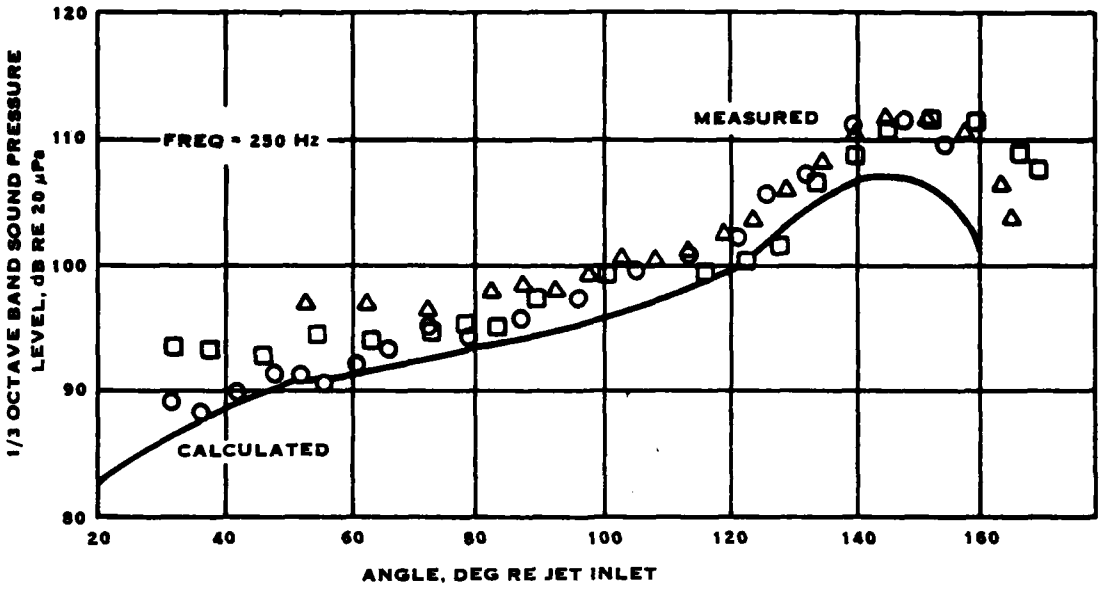

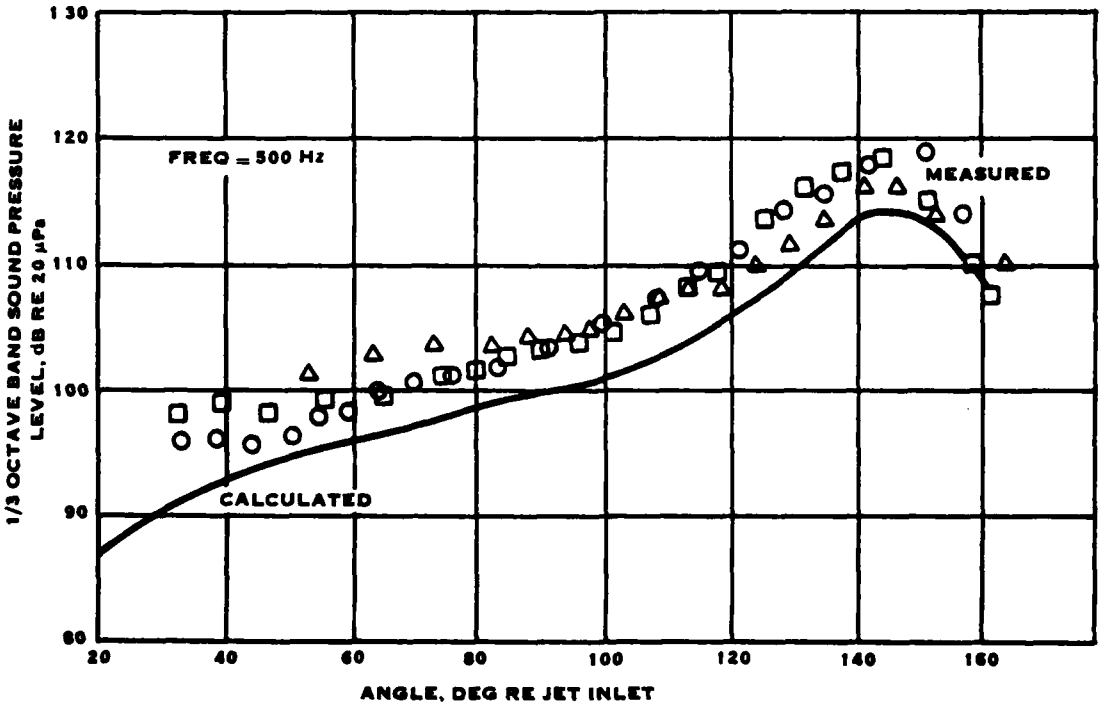

FIGURE 5-67 COMPARISON OF MEASURED AND CALCULATED JET NOISE FROM DATA BASE ITEM 9 - FLIGHT CONDITION

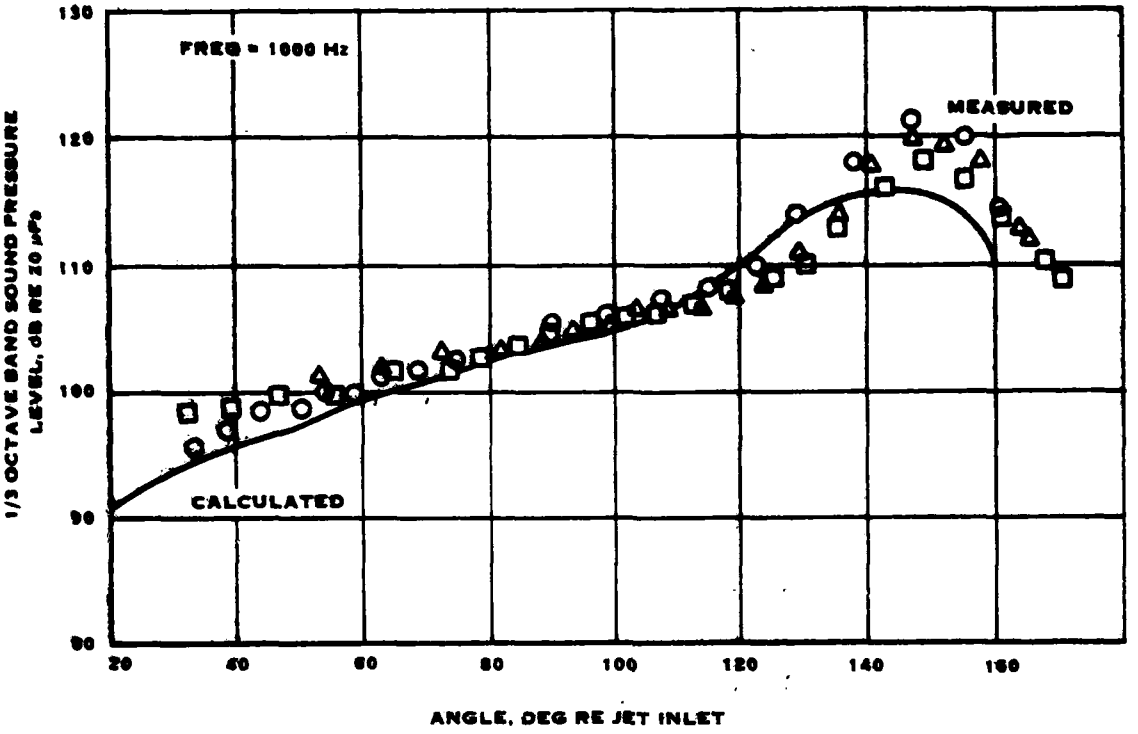

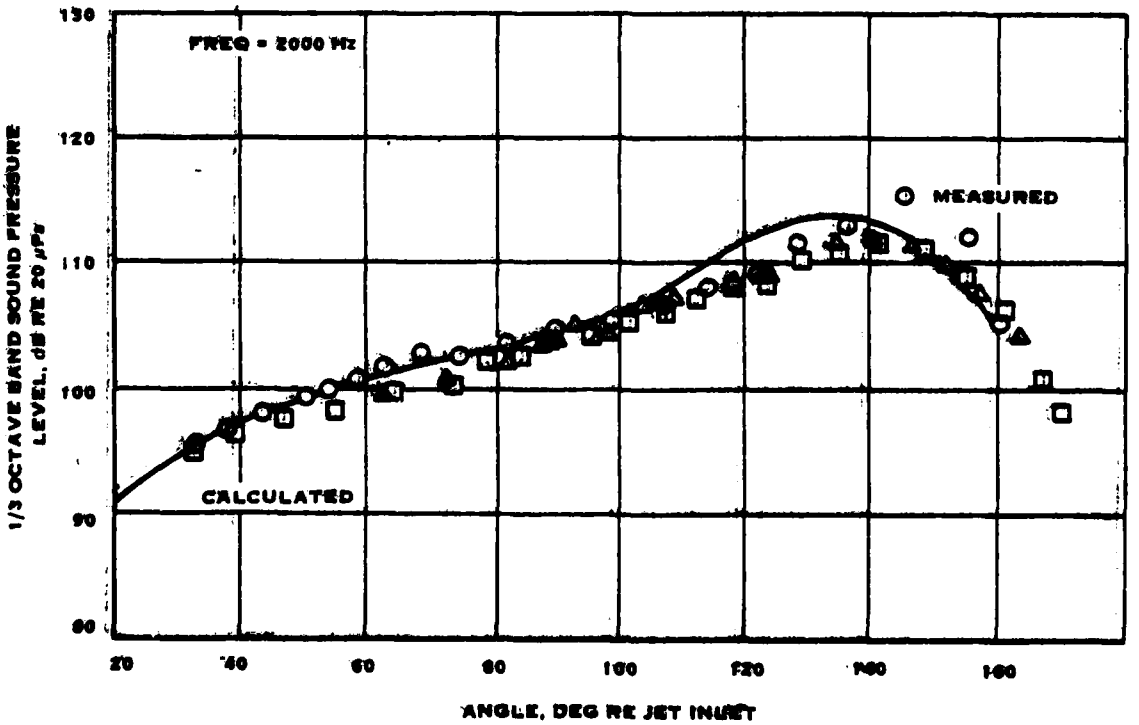

FIGURE 5-67 CONTINUED

AD-A082 616 UNITED TECHNOLOGIES CORP WINDSOR LOCKS CONN HAMILTON --ETC F/G 20/1
V/STOL ROTARY PROPULSOR NOISE PREDICTION MODEL UPDATE AND EVALU--ETC(U)
DEC 79 B MAGLIOZZI

UNCLASSIFIED FAA-RD-79-107 NL

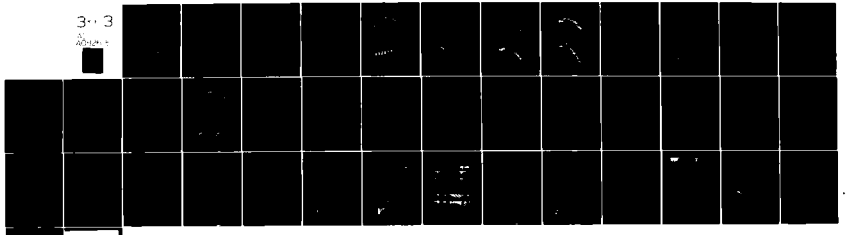

END
DATE FILMED
5-80
DTIC

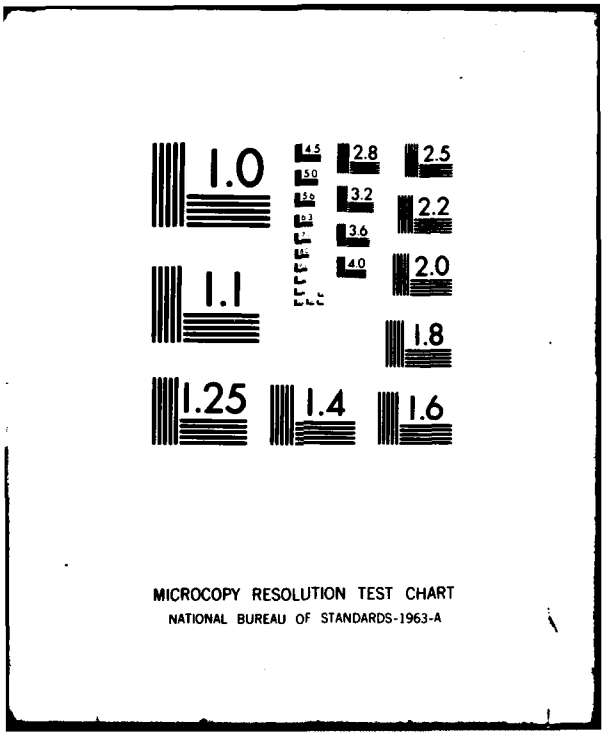
1.0
1.1
1.25
1.4
1.6
1.8
2.0
2.2
2.5
2.8
3.2
3.6
4.0
4.5
5.0
5.6
6.3
MICROCOPY RESOLUTION TEST CHART
NATIONAL BUREAU OF STANDARDS-1963-A

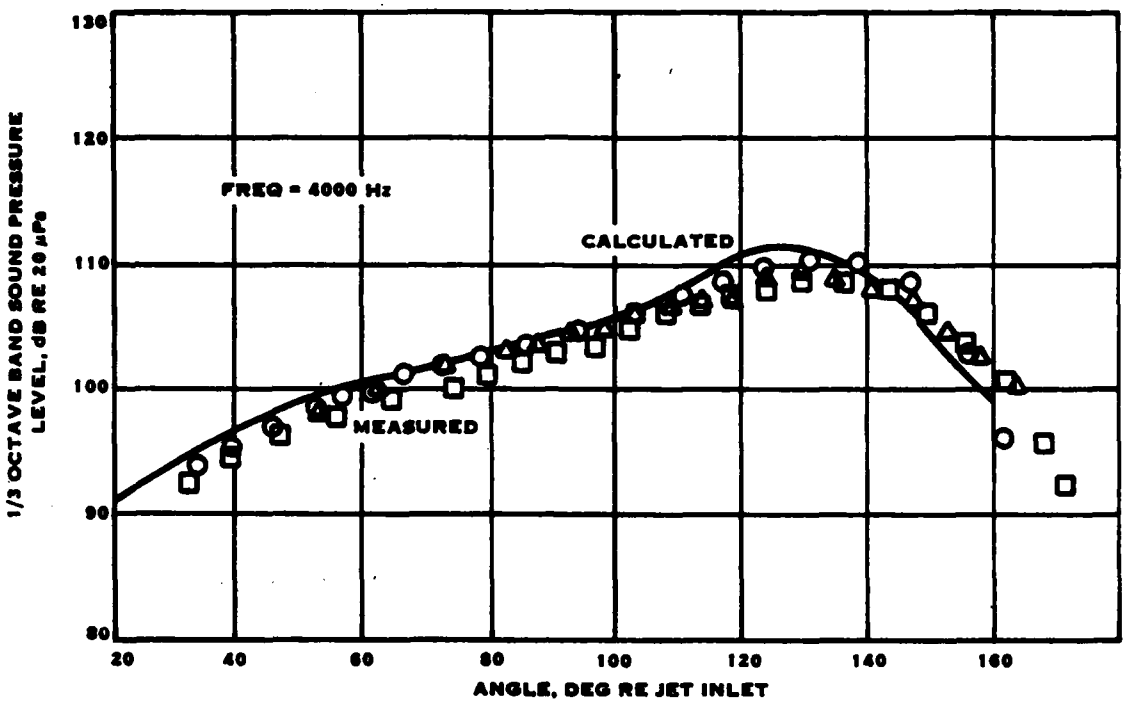

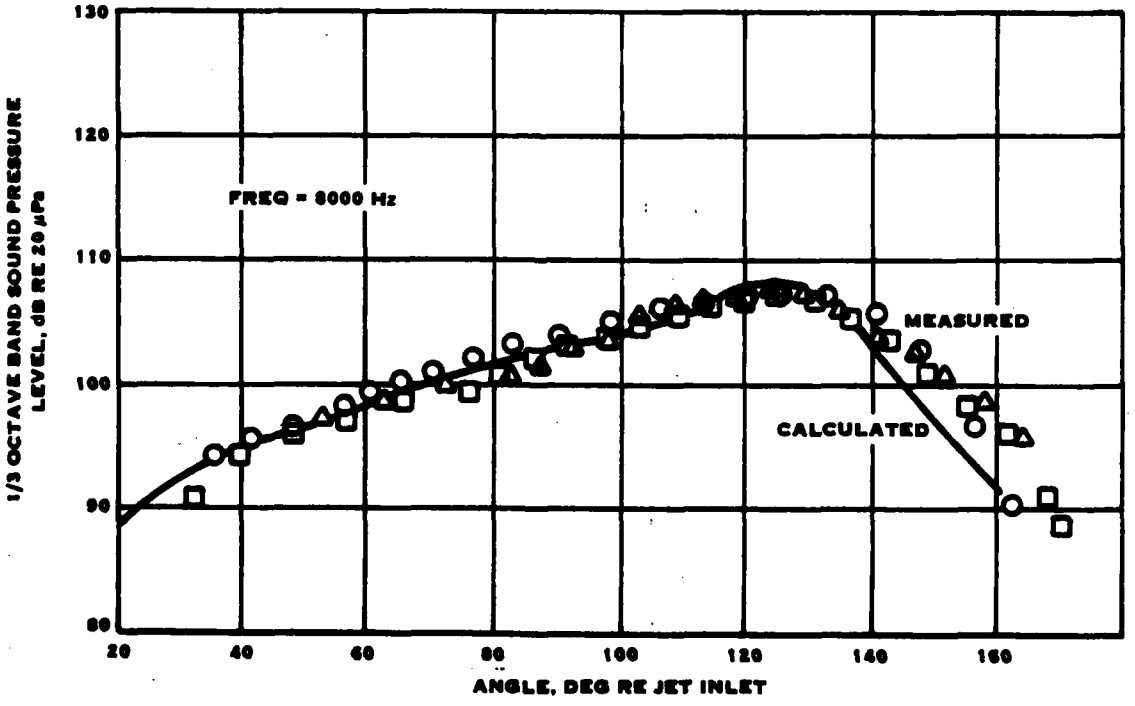

FIGURE 5-67 CONTINUED

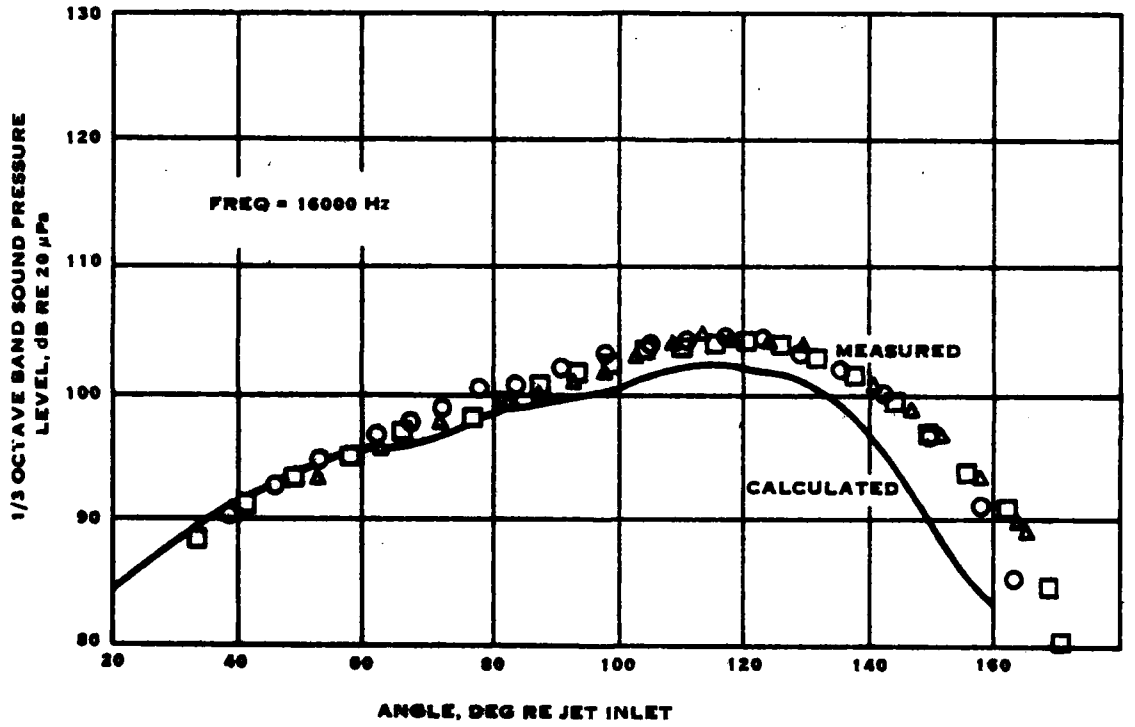

FIGURE 5-67 CONCLUDED

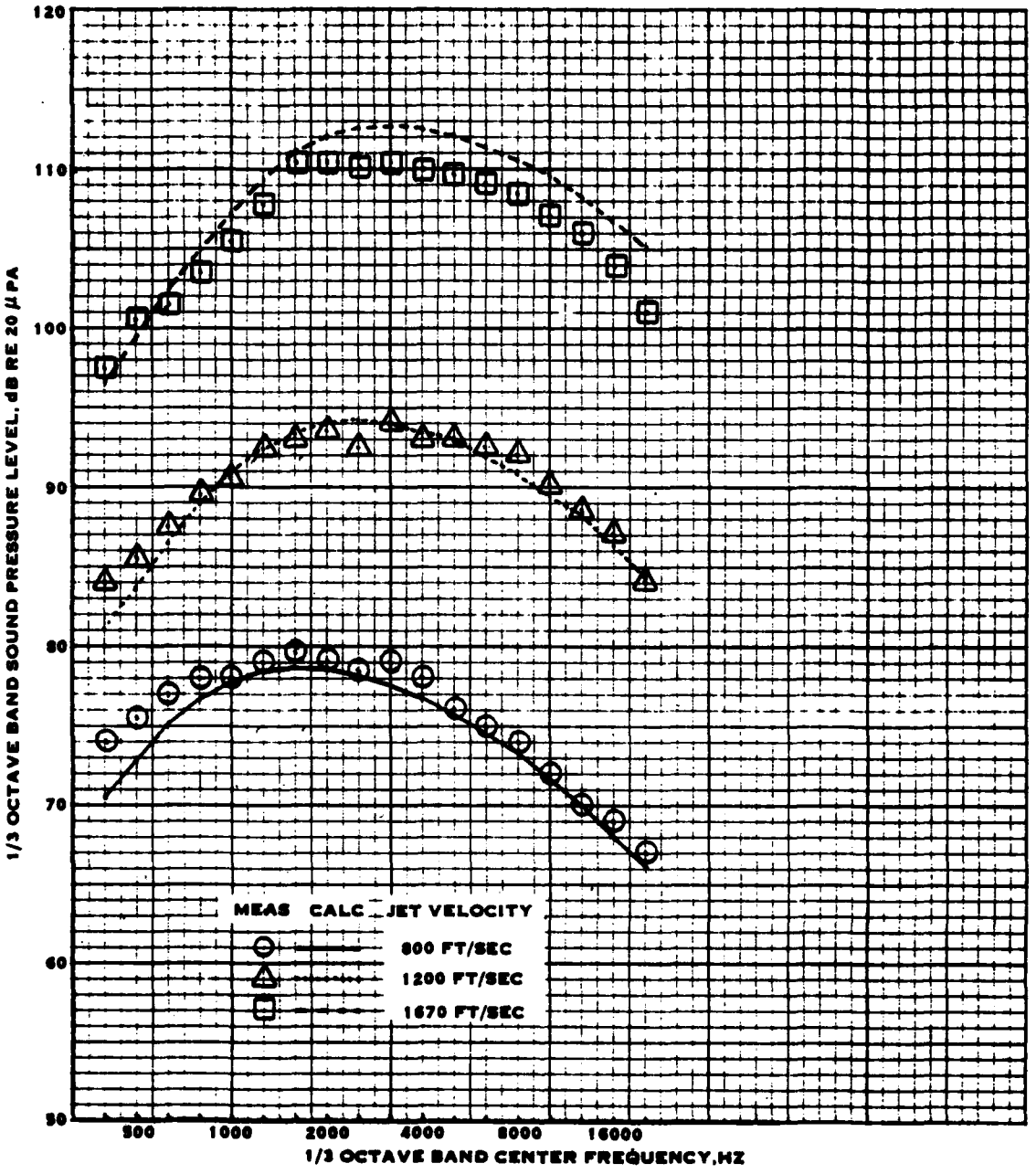

FIGURE 5-68. COMPARISON OF MEASURED AND CALCULATED JET NOISE AT 130 DEGREES AND FLIGHT SPEED OF 200 FT/SEC FOR THREE JET VELOCITIES - FROM DATA BASE ITEM 13.

Figure 5-69 shows the comparison between measured and calculated jet noise spectra at three tunnel speeds at 130 degrees azimuth and a jet velocity of 1670 ft/sec. The agreement in levels is fair, showing an overprediction of about 3 dB. The change in peak noise level is well calculated (8.5 dB calculated vs 9 dB measured) over the flight speed range 25 to 350 ft/sec.

Figure 5-70 shows the comparison between measured and calculated overall jet noise directivities at a jet velocity of 1670 ft/sec for tunnel speeds from 25 to 350 ft/sec. The shapes of the jet noise directivities are well calculated. At 25 ft/sec, the agreement between calculated and measured levels is quite good. Although the agreement is still good at 200 ft/sec, a slight overprediction is becoming apparent. At the two highest tunnel speeds, the overall jet noise levels are moderately overpredicted beyond 120 degrees. All-in-all, the agreement is very good in the range 70 to 120 degrees. Beyond 120 degrees, the levels are slightly overpredicted, by about 1 dB at 25 ft/sec to 3 dB at 350 ft/sec.

On the basis of the comparison with this data, the noise of a single jet is well predicted over the jet velocity range 800 to 1670 ft/sec. The spectrum shapes are particularly well predicted. Although the noise is slightly overpredicted at high jet velocities, the calculated forward-flight effects are in good agreement with those measured.

Data Base Item 24. - This paper presents results of noise measurements made in a wind tunnel on single-stream and coaxial cold jets. The single-stream jet was tested at 943 ft/sec jet velocity over the flight speed range 13 to 100 ft/sec (6.21 lb/sec weight-flow-rate and 179.6 to 162.8 lb jet thrust). The coaxial jet was tested at 1000 ft/sec primary jet velocity and a secondary-to-primary jet velocity ratio of 0.6 over the flight speed range 18 to 100 ft/sec (6.58 lb/sec primary weight-flow-rate, 8.54 lb/sec secondary weight-flow-rate, 201.0 to 184.2 lb primary jet thrust, and 154.6 to 132.8 lb secondary jet thrust).

Figure 5-71 shows the comparison between measured and calculated noise levels for the single-stream jet. At 90 degrees, the agreement between measurements and calculations is very good for the three tunnel speeds. At 120 degrees, the agreement between measurements and calculations is good at the lowest tunnel speed, but the calculations show a slight overprediction of about 1.5 dB at the peak for the 100 ft/sec tunnel speed. At 145 degrees, the peak levels are underpredicted by about 2 dB. The spectrum shapes are well predicted.

The comparison of measured and calculated noise levels for the coaxial jet is shown in figure 5-72. At 90 degrees the measurements show a flatter spectrum shape than that shown by the calculations, but both the peak levels and change in noise level with flight speed are fairly well predicted. At 120 degrees there is better agreement between measured and calculated spectrum shape, but the calculations show an overprediction of about 2 dB. At 145 degrees, the spectrum shape is well predicted. At the 18 ft/sec tunnel speed the peak level is underpredicted by about 1 dB, while at the 100 ft/sec tunnel speed the peak level is underpredicted by about 2 dB.

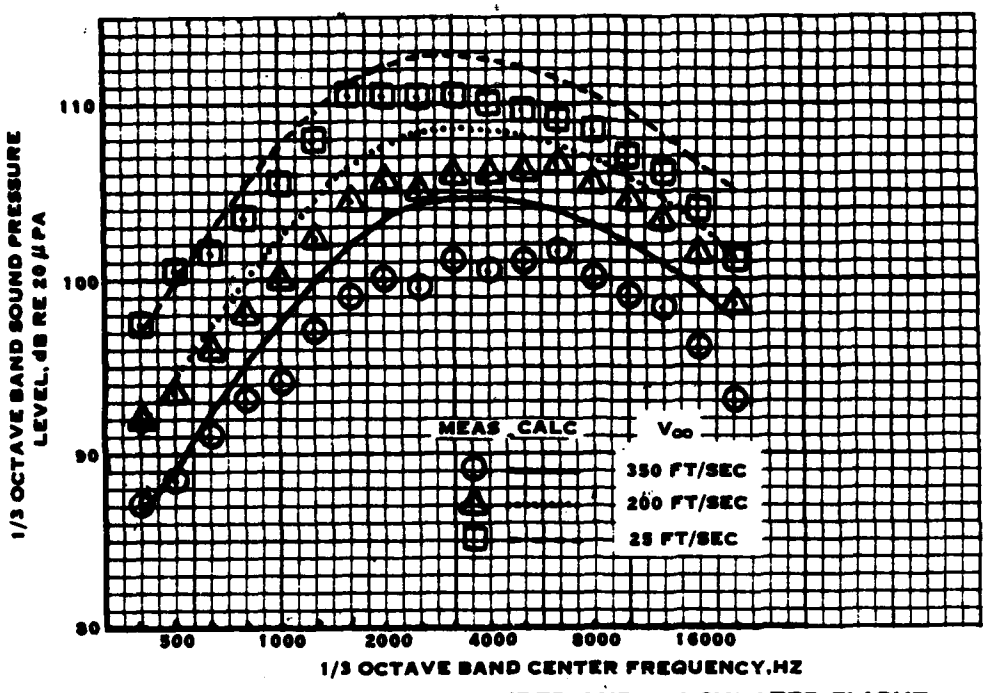

FIGURE 5-69. COMPARISON OF MEASURED AND CALCULATED FLIGHT SPEED ON JET NOISE AT 130 DEGREES AND 1670 FT/SEC JET VELOCITY

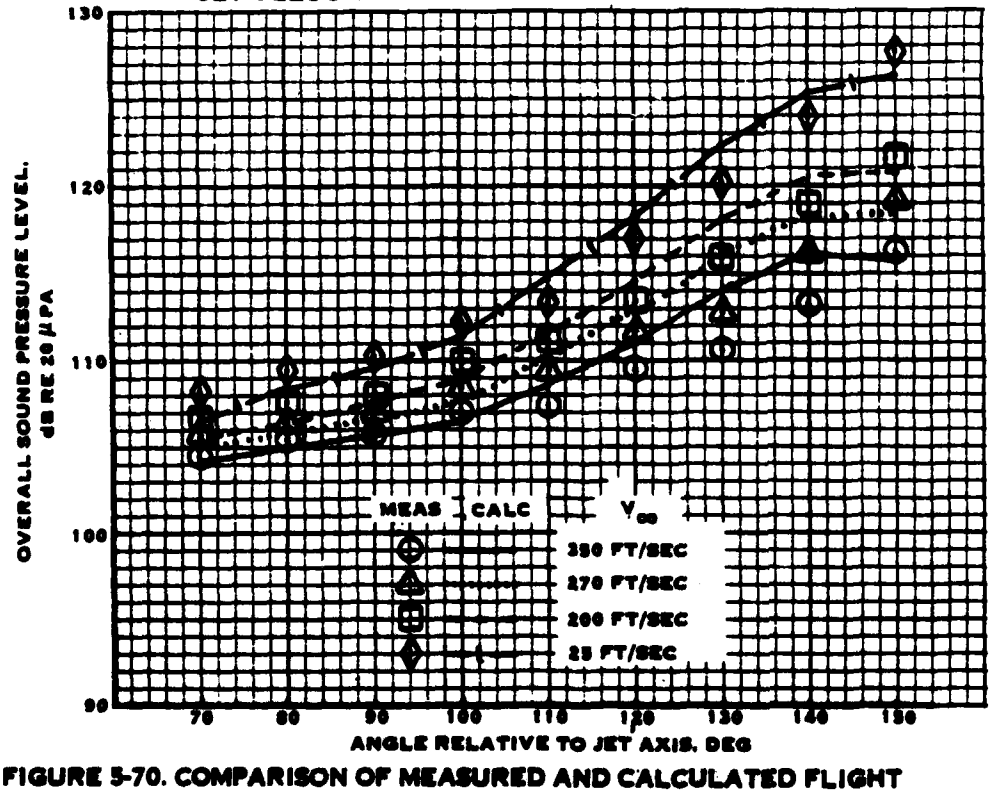

FIGURE 5-70. COMPARISON OF MEASURED AND CALCULATED FLIGHT SPEED ON JET OVERALL NOISE DIRECTIVITY AT 1670 FT/SEC JET VELOCITY

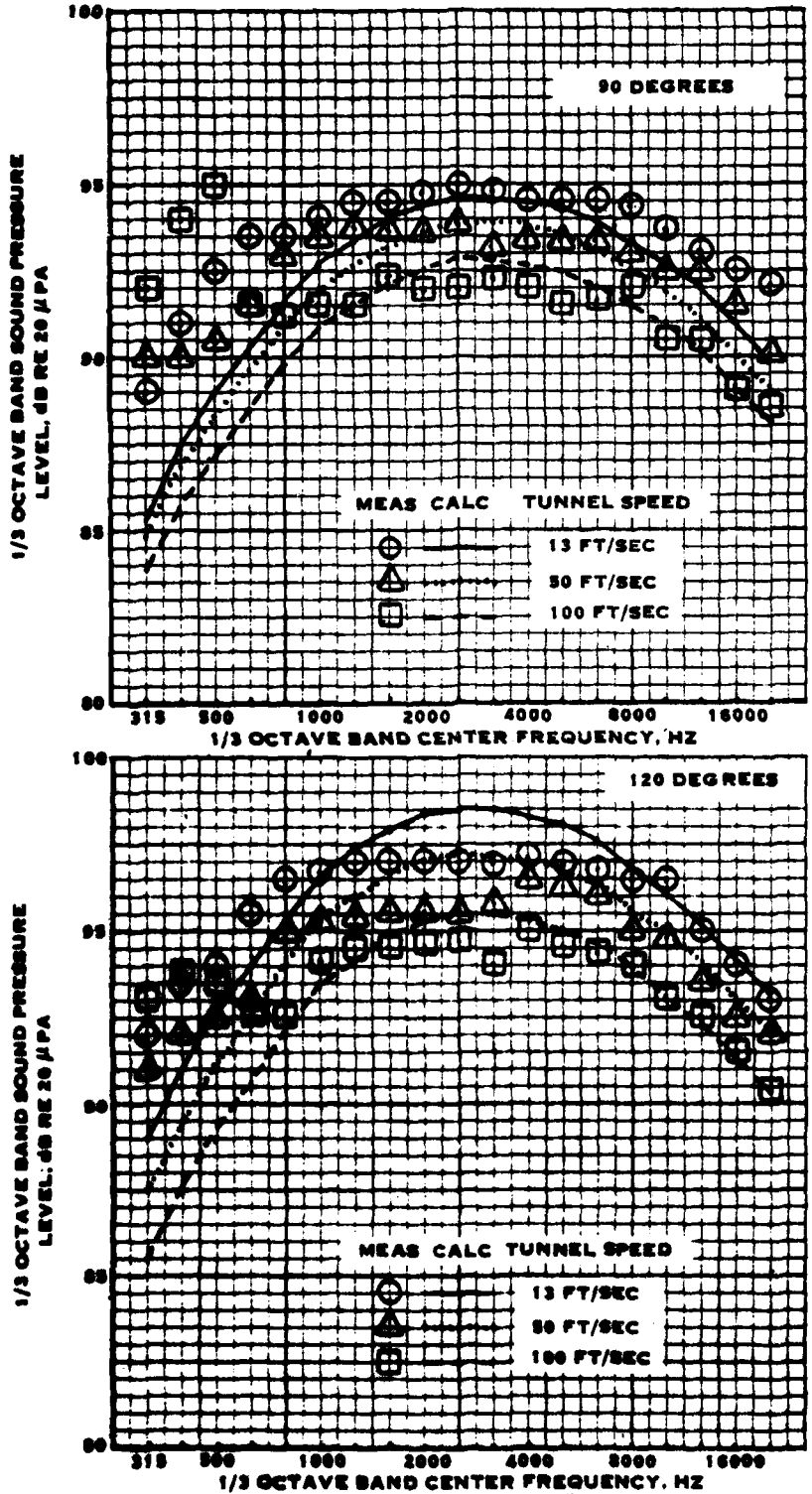

FIGURE 5-71. COMPARISON OF MEASURED AND CALCULATED SINGLE STREAM JET NOISE FROM DATA BASE ITEM 24

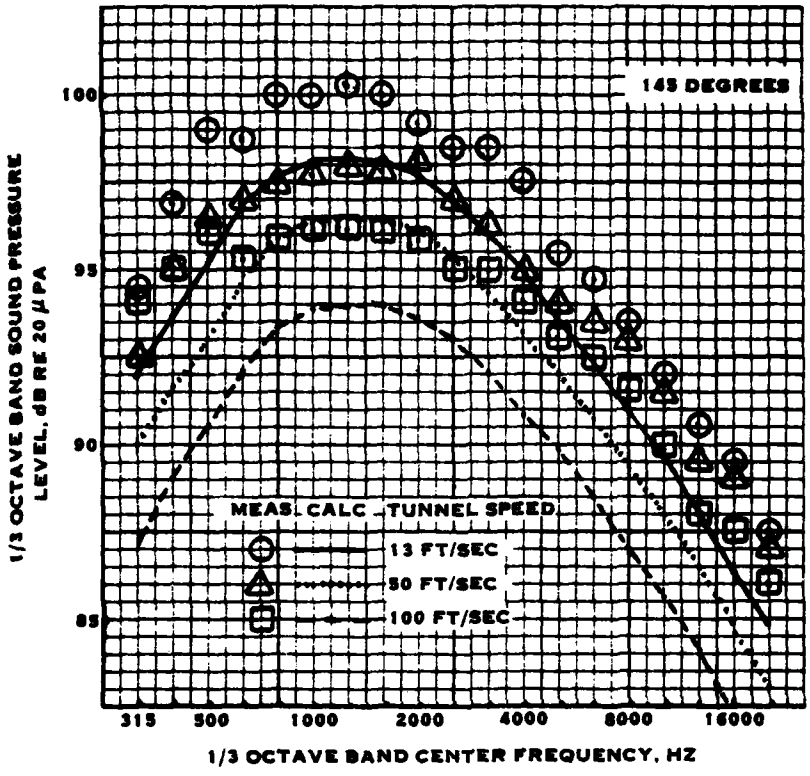

FIGURE 5-71. CONCLUDED

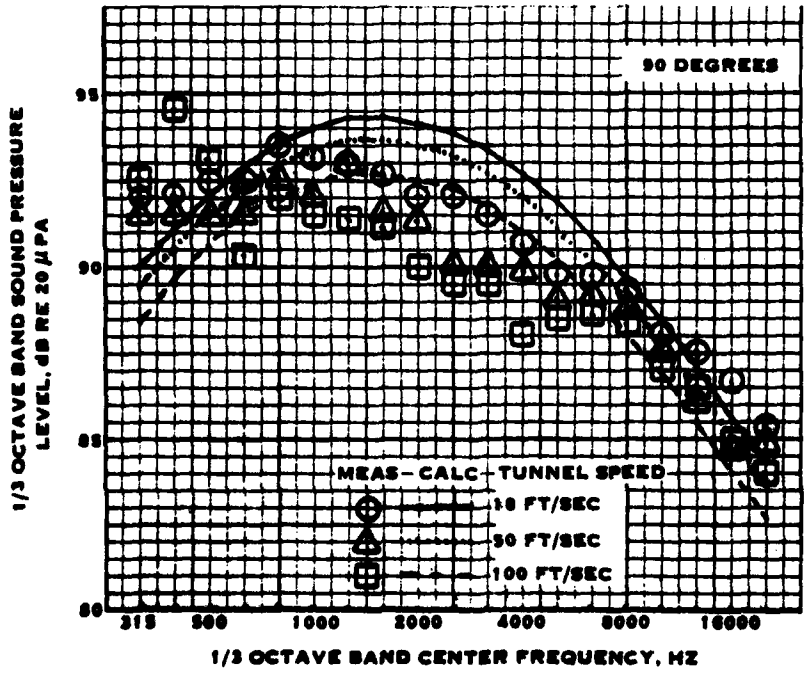

FIGURE 5-72. COMPARISON OF MEASURED AND CALCULATED COAXIAL JET NOISE FROM DATA BASE ITEM 24

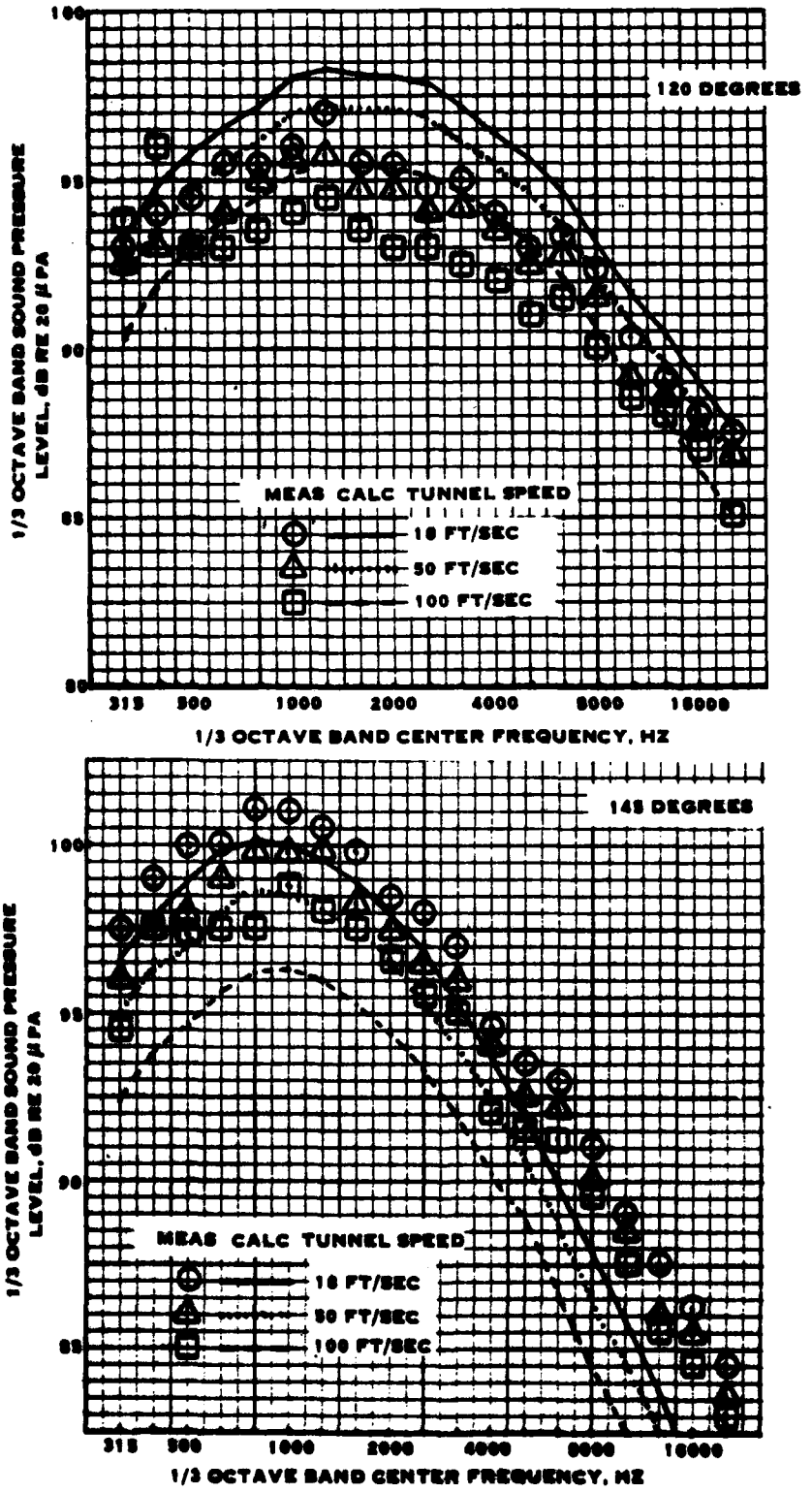

FIGURE 5-72. CONCLUDED

Data Base Item 25. - Although this report does not show absolute noise levels, this data was evaluated because it is one of the few found on model coaxial jets with hot primary flow. As the noise scale is indicated to be in 5 dB increments it was assumed that the scales were at integer multiples of 5 dB. Thus, the actual levels were estimated by selecting which multiple of 5 dB gave the best match to the calculations. Although this could lead to errors, the correlation between calculations and measurements had been quite good so far and the data was to be used primarily for evaluation of forward-flight effects. As the low and high tunnel speed data are shown on the same scale, the forward-flight effects can be precisely determined.

Figure 5-73 shows the correlation between measured and calculated noise levels for the single-stream jet at 1164 ft/sec for tunnel speeds of 20 to 98 ft/sec (39.6 and 37.0 lb of jet thrust and weight-flow-rate of 1.114 lb/sec). At 60 degrees, the agreement between measurements and calculations show the peak to occur at 5000 Hz whereas the measurements show a peak at 1250 Hz. Raising the measurements by 5 dB would improve the mid- and high-frequencies. The report does indicate the presence of spectral distortion at low and high frequencies. The low-frequency distortion is conjectured to be reverberation effects, but no explanation is given for the high-frequency distortion. In any case, the measurements indicate a reduction of about 2 dB due to forward-flight vs about 1 dB calculated. At 90 degrees the agreement between measured and calculated jet noise levels is seen to be better. Again the measurements show a change of about 2 dB and the calculations show a change of about 1 dB for flight effects. At 120 degrees the flight effects calculated are in good agreement with the measurements. At 145 degrees the calculated spectra are in good agreement with the measurements. The calculated levels indicate a flight effect of about 3 dB, which compares well with a measured flight effect of about 2.5 dB.

Figure 5-74 shows the comparison between measured and calculated coaxial jet noise levels. For this data the primary jet velocity was 1463 ft/sec and the bypass jet velocity was 878 ft/sec with the tunnel operating at 20 and 130 ft/sec. The jet noise calculations were done using a primary weight-flow-rate of 1.46 lb/sec and bypass weight-flow-rate of 6.875 lb/sec, primary jet thrust of 65.4 and 60.4 lbs at 20 and 130 ft/sec tunnel speed, respectively, and a bypass jet thrust of 179 and 155 lbs at 20 and 130 ft/sec tunnel speed, respectively. Similar problems to those for the single-stream jet can be seen at 60 degrees, although the agreement between measurements and calculations is better for the coaxial jet than for the single-stream jet. At 90 degrees, the levels appear to be overpredicted, but an adjustment in measurements of 5 dB would improve the mid- and high-frequency correlation. The flight effects are measured to be about 2 dB compared to a calculated value of about 1.5 dB. The comparison of calculated vs measured flight effects improves with increasing angle. At 120 degrees, the flight effects are in excellent agreement. At 145 degrees, the calculated spectra are in excellent agreement with the measured spectra.

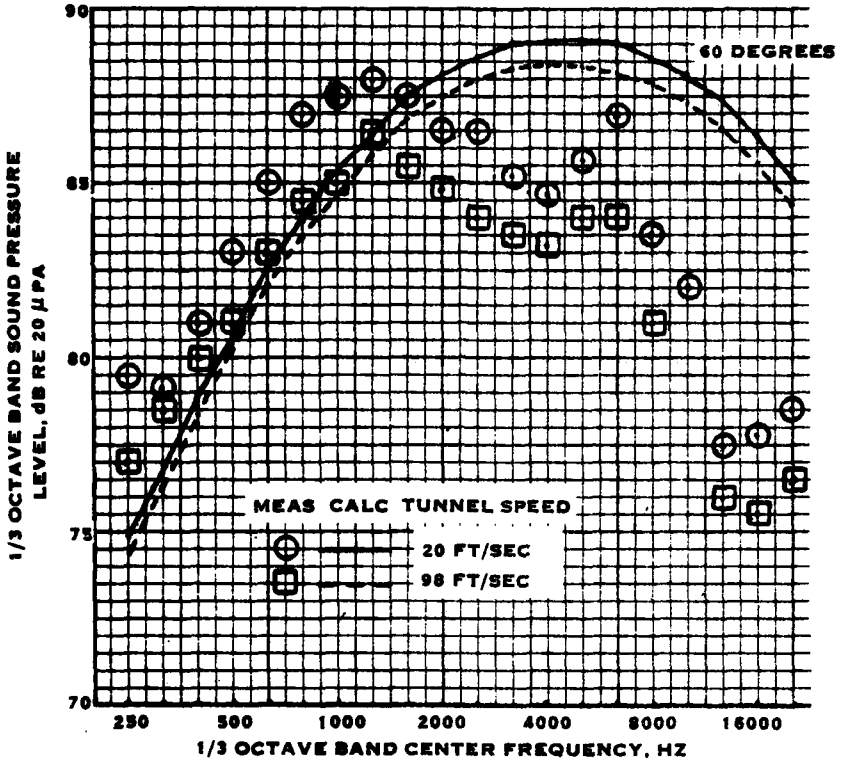

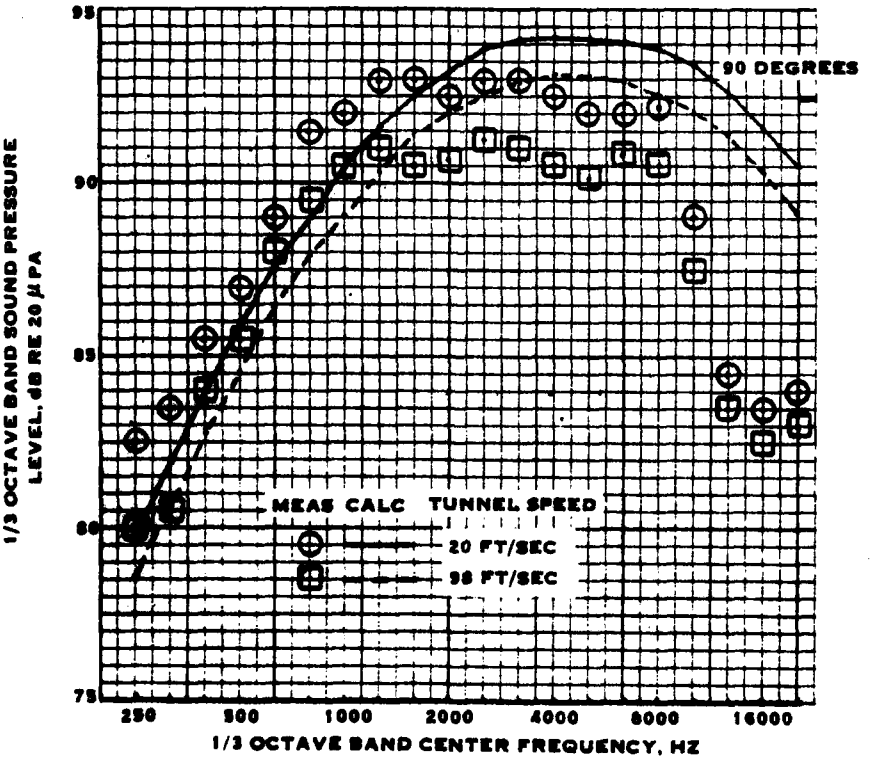

FIGURE 5-73. COMPARISON OF MEASURED AND CALCULATED SINGLE STREAM JET NOISE FROM DATA BASE ITEM 25

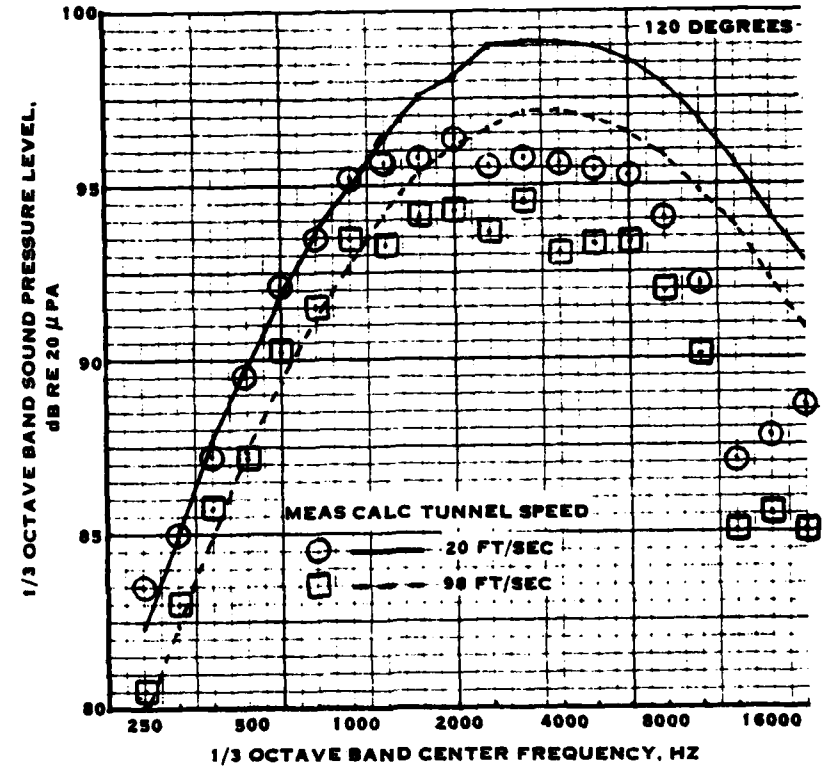

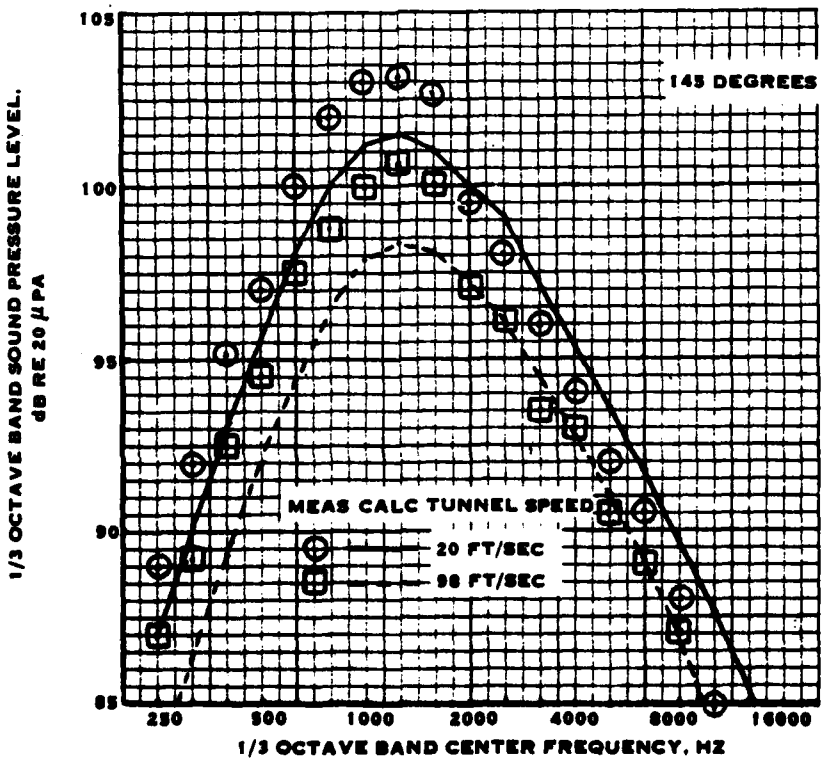

FIGURE 5-73. CONCLUDED

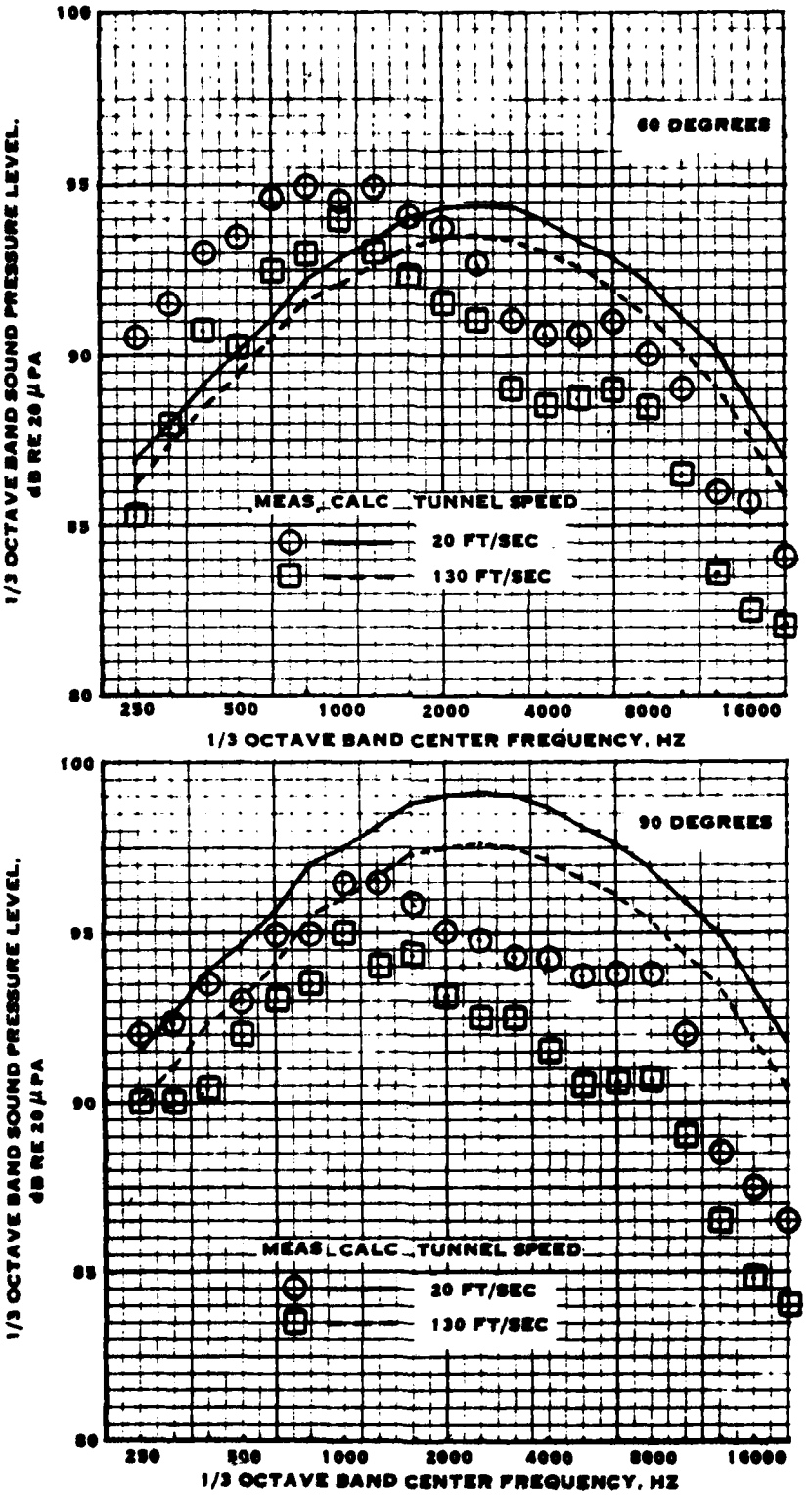

FIGURE 5-74. COMPARISON OF MEASURED AND CALCULATED COAXIAL JET NOISE FROM DATA BASE ITEM 25.

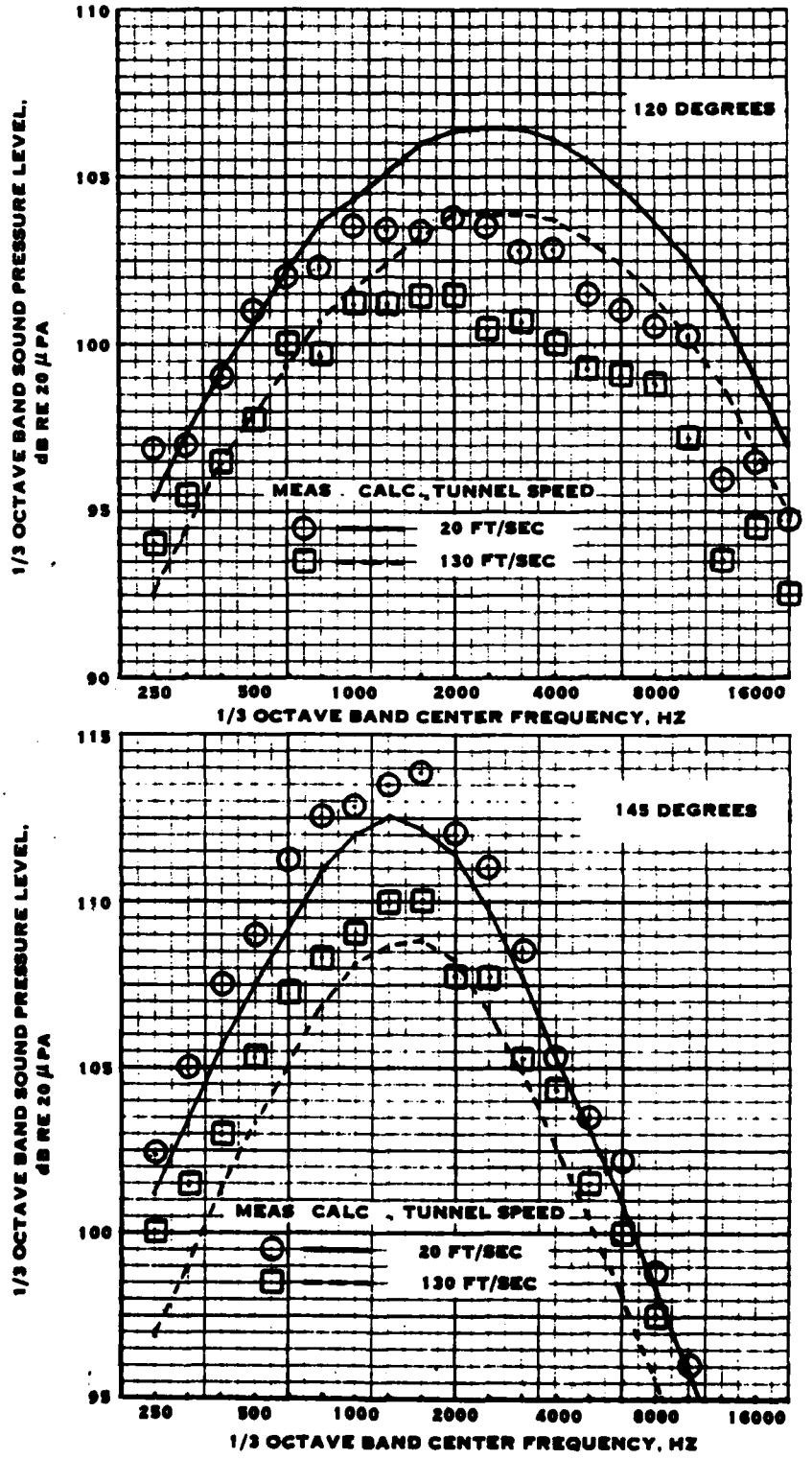

FIGURE 5-74. CONCLUDED

Thus, although the calculated jet noise spectra are not in very good agreement with the measurements due to low- and high-frequency distortions and due to uncertain amplitude scales, the calculated flight effects on jet noise are in excellent agreement with those measured.

Comparison of Measured and Calculated Full-Scale Jet Noise

Data Base Item 2. - This paper presents measurements made of the noise from a J85 engine installed on the Aerotrain. Data was acquired at static conditions and at a flight speed of 269 ft/sec. The data used for comparison is that taken using the convergent/divergent nozzle. Figure 5-75 shows the comparison between measured and calculated J85 engine jet noise spectra for the static and 269 ft/sec flight conditions. At 30 degrees, both the measurements and calculations show a small effect on noise due to flight. The agreement between measured and calculated peak noise levels is good, the levels being underpredicted by 1 to 2 dB. At 90 degrees, the shapes of the frequency spectra are well calculated and the calculated flight effects are in excellent agreement with the measurements. As for the 30 degree location, the levels at 90 degrees are underpredicted by about 2 dB. At 120 degrees the calculations are in perfect agreement with the measurements at frequencies above 1250 Hz. However, the data shows peaks in the spectra at 500 to 630 Hz which do not match the calculated peak frequency of 1250 to 1600 Hz. This results in an underprediction of the peak of about 3.5 dB. The origin of this peak is not known, but appears as a second component which extends from about 100 Hz to about 1250 Hz. The change in noise level with flight speed is, however, well predicted.

Figure 5-76 shows the comparison between measured and calculated jet noise directivities at 400 and 2000 Hz. At 400 Hz, the agreement between measured and calculated levels is good to about 90 degrees but underpredicted at the aft angles. This was apparent from figure 5-75 which showed a low-frequency peak in the measurements at the 120 degree location. The calculated peak (at 140 degrees) is about 3 dB lower than the measured peak (at 130 degrees). At 2000 Hz, the agreement between measurements and calculations is good from 30 to 120 degrees. The static condition peak is underpredicted by 3 dB while the 269 ft/sec flight condition peak is underpredicted by 2 dB.

Data Base Item 23. - The data presented in this paper was acquired on a Viper engine under static and flight conditions. The static data was acquired using several microphones at various heights above the ground plane so that fairly accurate ground reflection effect corrections could be derived. The flight data was taken during 2000 ft altitude level flyover using a single microphone located at four feet above grass, so that corrections to free-field conditions were less well-defined than for the static data. All data were corrected to standard day and free-field conditions.

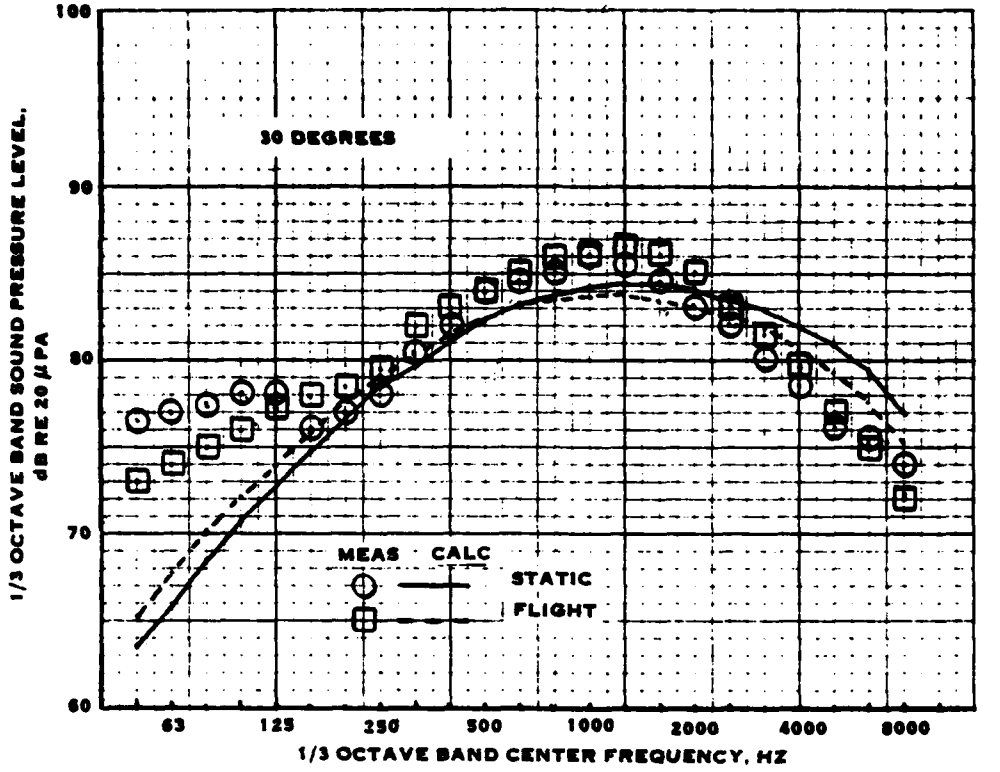

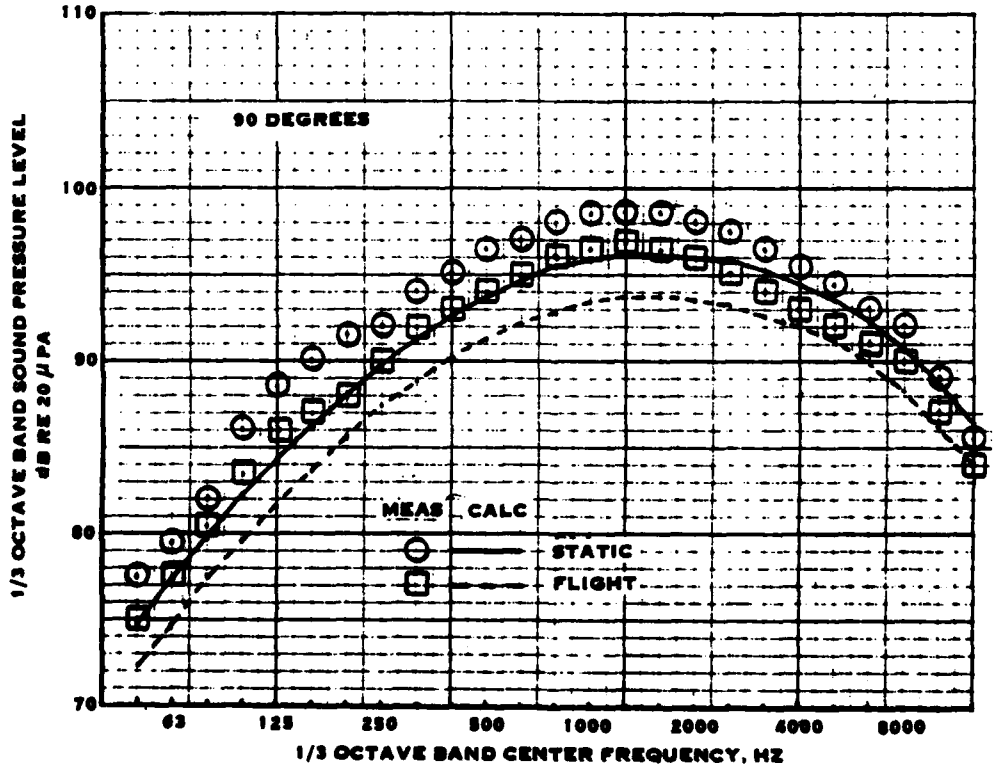

FIGURE 5-75. COMPARISON OF MEASURED AND CALCULATED J85 ENGINE JET NOISE SPECTRA FROM DATA BASE ITEM 2

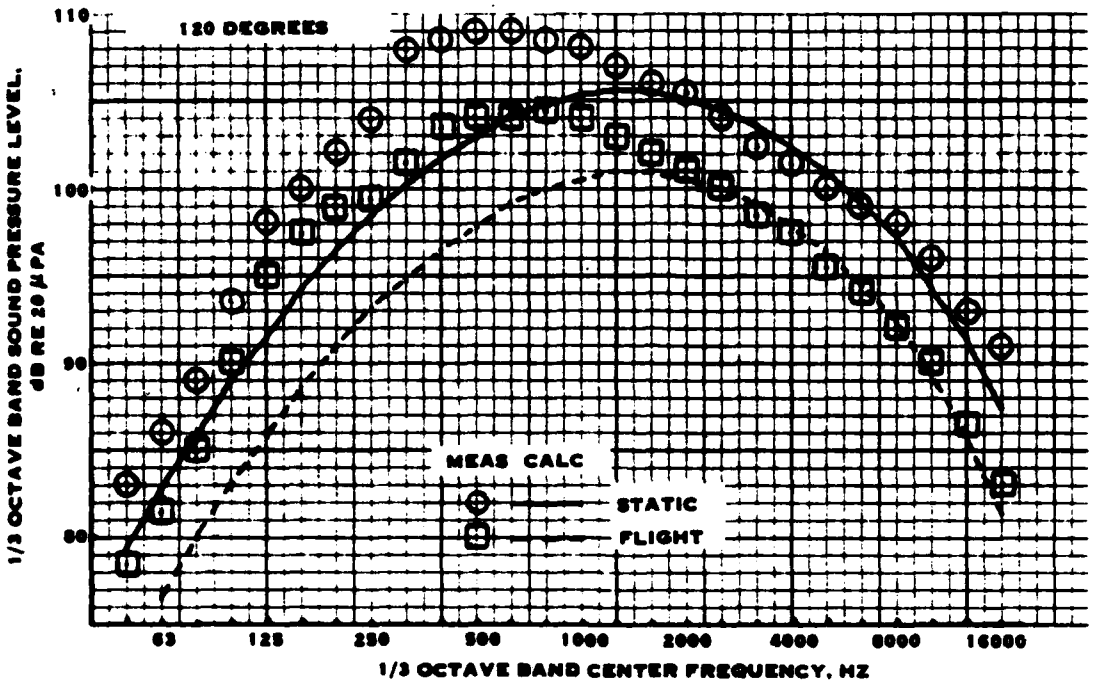

FIGURE 5-75. CONCLUDED

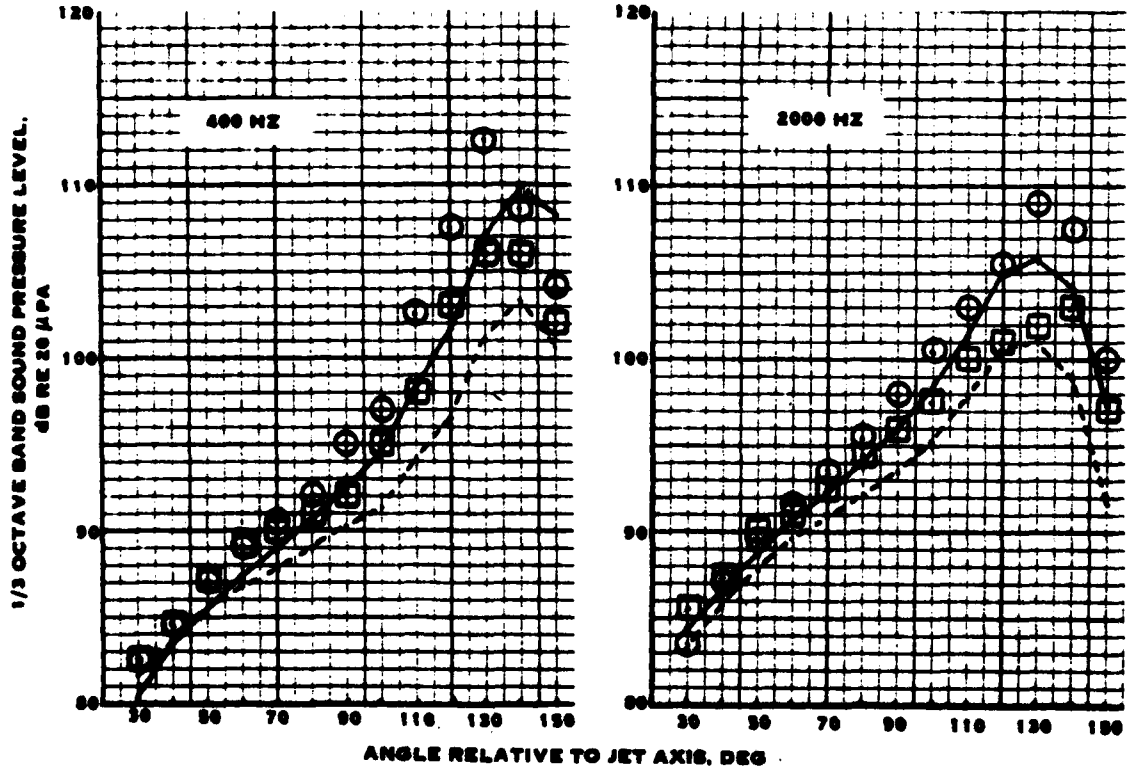

FIGURE 5-76. COMPARISON OF MEASURED AND CALCULATED JBS JET NOISE DIRECTIVITY FROM DATA BASE ITEM 2.

Figure 5-77 shows the comparison between measured and calculated Viper jet noise levels for a jet velocity of 2020 ft/sec. Spectra are shown for 90, 120, and 150 degree azimuths for static and 270 ft/sec flight conditions. The agreement between measured and calculated static jet noise levels is seen to be very good for the three azimuth locations, except at high frequency at 150 degrees. These are seen to remain high in level beyond 1600 Hz, rather than roll-off as indicated by the calculations and the earlier data on model jets. As this data was acquired using an unlined tailpipe, this high frequency noise is perhaps from engine internal sources. The flight noise is seen to be significantly underpredicted at all three azimuth angles. Actually, it is deduced in the paper that the static data extrapolated to flight data distance shows about the same noise levels as the flight data, i.e. the flight data does not show a reduction in noise level due to relative velocity effects. Although it would be expected that sources other than jet mixing noise could dominate at low jet velocities, it would not be expected to be the case at such a high jet velocity. In any case, this flight data is contrary to that presented for the model jets and the J85 engine.

Hamilton Standard Data Bank: DC9. - This data has been presented earlier under the evaluation of fixed-pitch fan noise prediction. It was concluded that under take-off condition, the low-frequency noise was dominated by that from the core engine jet. Figure 5-78 shows the comparison between measured and calculated JT8D engine noise on take-off. The measurements are for the total engine, while the calculations are for jet noise only. The first jet noise calculation was done assuming a coaxial jet, i.e., using the core engine parameters for the primary jet noise and the fan parameters for the bypass jet. As may be seen in figure 5-78, the jet noise is significantly overpredicted. However, the JT8D engine uses a retracted primary nozzle so that a certain amount of internal mixing of primary and bypass flows takes place before exiting. Thus, a second jet noise calculation was done assuming a single-stream jet with full internal mixing. As may be seen in figure 5-78, this results in underprediction. As the measured levels are between those calculated with the two assumptions, it is concluded that some internal mixing has taken place. Thus, the jet noise from engines with retracted primaries cannot be accurately calculated using the current jet noise calculation procedure.

Summary for Jets

The evaluation of the calculation procedure for jet noise indicated excellent agreement with measured noise levels of model jets. All aspects of the measurements (levels, spectrum shape, coaxial effects, flight effects) were well predicted. In general, the calculated levels agreed with the measured levels to within ± 2 dB on the basis of one-third octave band correlations. Of the three cases used for correlation of jet noise calculations for real engines, one showed agreement with calculations comparable to those obtained for the model jets, one showed good agreement statically but underprediction in flight, and the third showed relatively poor correlations. As these data are for complete engines, it is possible that engine internal noise sources are contributing to the measured noise levels and contaminating the jet noise. For example, the second engine jet noise used for correlation had an untreated tailpipe. Thus, other sources

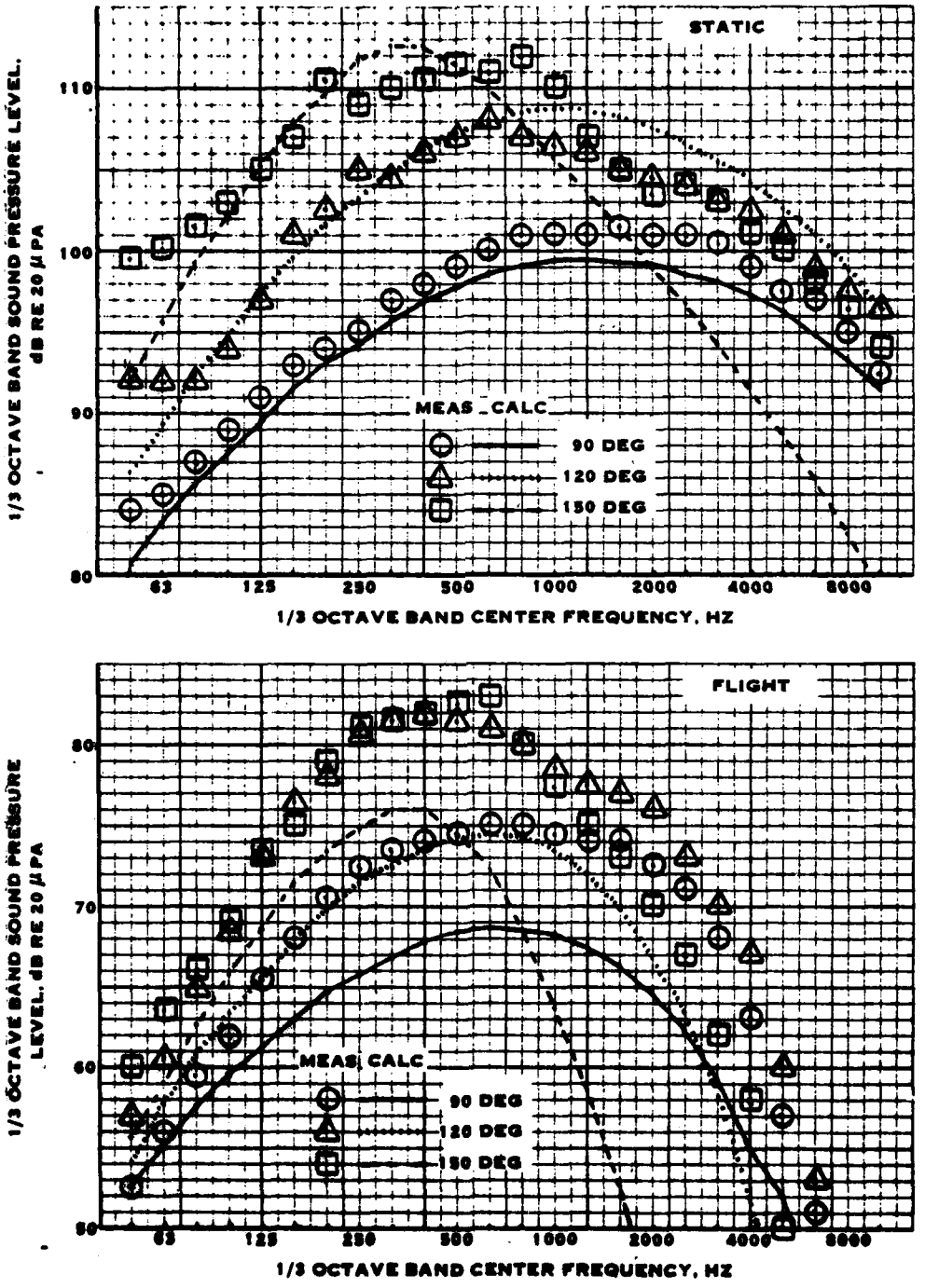

FIGURE 5-77. COMPARISON OF MEASURED AND CALCULATED VIPER ENGINE JET NOISE FROM DATA BASE ITEM 23

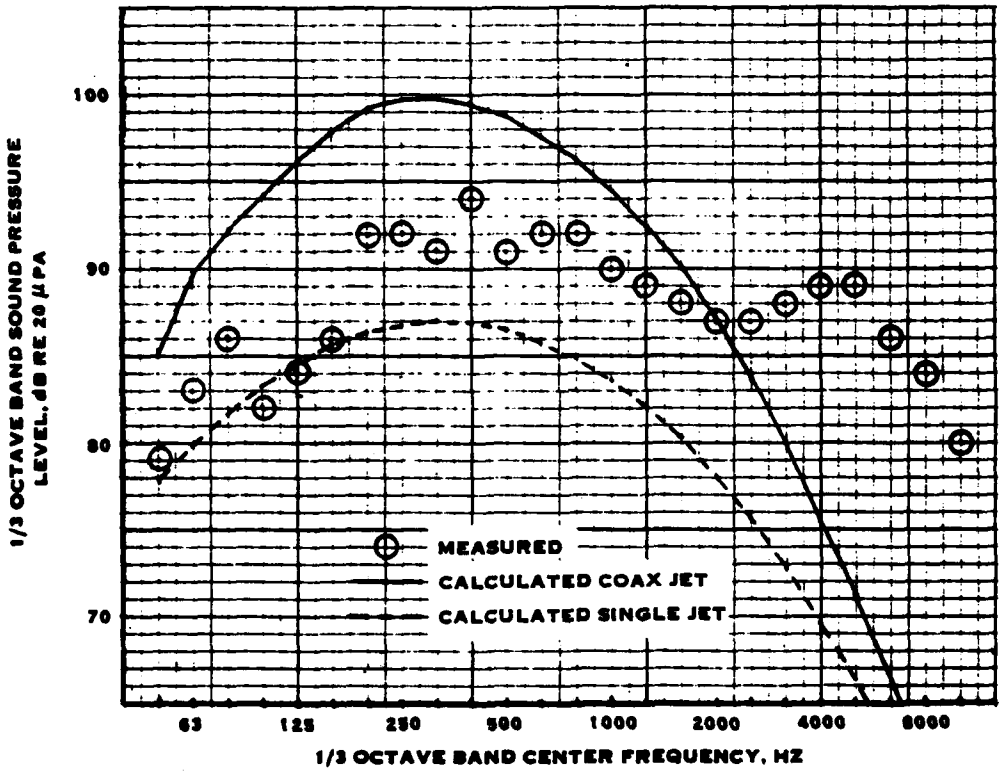

FIGURE 5-78. COMPARISON OF MEASURED AND CALCULATED JET NOISE FOR THE JT8D ENGINE

of noise such as those in the combustor and/or turbine could be contributing to the total noise. The third engine jet noise data used in the evaluation was that from a JT8D engine, which has a retracted primary nozzle. Calculations made assuming a coaxial jet (external mixing) showed overpredictions while those made assuming a single jet (full internal mixing) showed underpredictions. It was thus concluded that the current method is not appropriate for the calculation of jet noise for engines with retracted primary nozzles.

On the basis of the evaluation of the jet noise prediction method contained in the current noise prediction computer program it is concluded that good predictions of jet noise can be made for single-stream and coaxial jets which have full external mixing and which are not contaminated by engine internal noise sources. It may be deduced that the jet noise for engines with retracted primary nozzles (e.g. the JT8D) and those with jet noise suppression devices such as lobed nozzles, tube ejectors, and lined ejectors will be overpredicted by the current methodology as it does not have provisions for such configurations.

SUMMARY OF NOISE PREDICTION METHODOLOGY EVALUATION

The V/STOL Rotary Propulsor Noise Prediction Methodology has been evaluated for free-air propellers, variable-pitch fans, fixed-pitch fans, helicopters, core engines, and jets. The noise measurements used for correlation with calculations include those made for static and flight conditions and for isolated and installed propulsors. Although, in general, the results of this evaluation are encouraging, there are areas where significant discrepancies were found, particularly for installed propulsors. Also, ground reflection effects in the measurements were found to be significant. Generally, adequate corrections to free-field conditions could not be derived, particularly for those containing low-frequency tones.

The following paragraphs summarize the results of the noise prediction evaluation which was done using the updated version of the computer program.

Static uninstalled propeller noise is well predicted over the entire frequency spectrum. Static installed propeller noise is underpredicted at the mid-frequency harmonics, due to installation effects — specifically the ingestion of fuselage and/or ground vortices. In flight, low-to-moderate tip speed, lightly loaded propeller noise is underpredicted because this contains dominant thickness noise components which are not calculated by the current noise prediction methodology. In flight, the mid-to-high frequencies are due to engine noise. Within the range of validity of the propeller noise prediction methodology, the agreement between measured and calculated one-third octave band levels for the total propulsor is ± 5 dB. Agreement between calculated and measured overall, dB(A), PNL, PNLT, and EPNL was found to be about ± 3 dB.

Variable-pitch fan noise was found to be well predicted except for the very low-frequency one-third octave band levels. As these do not contribute significantly to perceived noise, the correlation between measured and calculated sideline PNL and PNLT was found to be within about ± 3 dB. Forward-flight effects, based on limited data acquired in a wind tunnel, are also fairly well predicted.

The correlation between calculated and measured isolated static fixed-pitch fan noise levels was found to be in reasonable agreement, although the high frequencies are slightly overpredicted. Acoustic suppressor performance for moderate levels of treatment was found to be well predicted. The noise of complete engines in flight is generally overpredicted by about 4.5 PNdB. Some of the differences are apparently due to installation effects such as shielding by wings and fuselages. Noise predictions utilizing the generalized core engine were also evaluated, as this engine would typically be used for preliminary design studies. These were found to exceed the measured levels by an average of about 8 PNdB, primarily because the use of the generalized engine resulted in higher compressor and jet noise levels. As the standard deviations in the calculated vs measured noise level comparison are small, adjustments of -4.5 PNdB for the calculations using defined core engine parameters and -8 PNdB for the calculations using the generalized core engine are recommended for improved installed fixed-pitch fan propulsor noise predictions.

The major problem in evaluating the performance of the noise prediction methodology for helicopters is in adjusting the measured noise levels to equivalent free-field conditions. Attempts to correct for ground reflection effects were not successful, primarily because the calculated frequencies of reinforcements and cancellations did not match the measurements. Also, it was not possible to apply the ground reflection adjustments to the measurements, as the contribution from each of the several sources (i.e. main rotor, tail rotor, engines, etc.) in a particular one-third octave band could not be determined. Significant underprediction was found for conventional helicopters in hover. It was concluded that this occurred because of high levels of tail rotor noise caused by severe inflow distortion due to the vertical tail. In flight, the inflow distortion is reduced and tail rotor noise decreases. One helicopter, the HH-43B, shows similar noise levels during hover and flight. This was attributed to the fact that this helicopter does not have a tail rotor. Although the measurements show evidence of significant low frequency ground reflection effects, the correlation between calculated and measured PNLT time histories was found to be quite good, thus giving good predictions of EPNL values. One exception was the Bell 212 helicopter, which is underpredicted due to its producing significant impulsive noise. During hover, the average measured-minus-calculated levels was found to be 4.0 PNdB with a standard deviation of 2.6 PNdB. During flyover, the correlation is much better. The peak PNLT measured-minus-calculated average is -0.9 PNdB, while the average measured-minus-calculated EPNL is 0.3 EPNdB (not including the Bell 212 helicopter).

Although only a small sample of core engine noise data was available for evaluation of the core engine noise prediction methodology, the correlation between measurements and calculations is encouraging. Good correlation was obtained for isolated engines. High-frequency turbine noise was overestimated for installed engines. However, these had over-the-wing exhausts so that the overprediction could be due to wing shielding.

The evaluation of the jet noise prediction method shows excellent agreement with measured noise of single stream and coaxial jets with both hot and cold primary jets and operating statically and in flight. Typical one-third octave band correlations are withing ± 2 dB. Real, full-scale engine jet noise correlations are not as good. Of the three full-size engine jet noise calculations one correlates well with measurements, one correlates well statically but not in flight, and one (which had a retracted primary nozzle) shows overpredictions. It was thus concluded that the current jet noise prediction method will give good estimates of noise from single-stream and coaxial jets which have full external mixing and which are not contaminated by engine internal noise sources, do not have retracted primary nozzles, and do not have jet noise suppression devices.

CONCLUSIONS

Based on the work performed under this study, the following conclusions have been reached:

1. Most of the data available from the open literature have many limitations, including unknown engine operating conditions, severe installation effects, and unknown ground reflection effects, which make the evaluation of forward-flight effects and methodology correlation very difficult using these data.

2. Except for some propeller noise data, the flyover noise data used for methodology correlation was acquired with microphones located above a ground plane. This made it impossible to establish forward-flight effects on low frequency noise, particularly those sources which have strong low-frequency tones such as propellers and helicopter rotors.

3. In general, flyover data suffers from ground reflection problems, while static data suffers from installation effects (ingestion of vortices, reflections from wings and fuselages, inflow distortion by fuselage and tail surfaces, etc.)

4. Based on careful interpretation of the best of the available data, the forward-flight effects included in the methodology could not be fully evaluated, as in many cases other effects (such as installation effects -- see Conclusion 3) result in noise level changes between static and flight conditions which are greater than those from the effects included in the methodology.

5. Noise measurements made in acoustic wind tunnels require further study before they can be fully accepted for evaluating forward-flight effects as the turbulence levels and length scales in the tunnels may not represent those encountered in the normal atmosphere.

6. A more accurate evaluation of the noise prediction methodology will require static data acquired for uninstalled propulsors tested on clean aerodynamic stands located well above the ground plane and in-flight data acquired on configurations relatively free of installation effects. Measurements are required which are not contaminated by unknown ground reflection effects, particularly in cases where the noise signature contains high levels of low frequency tones.

7. Although the noise prediction methodology evaluated appears suitable as a preliminary design tool, the presence of installation effects and the influence of ground reflections on noise (not included in the program) must be considered in using the method.

8. It is easier to apply ground reflection corrections to the calculated noise levels than to correct measurements to free-field conditions, although it does not appear to be readily feasible to correct for tones except on a statistical average basis for the duration of a flyover.

9. Although ground reflection effects are apparent in the measured data, better correlation between measured and calculated noise levels was obtained for fixed-pitch fans and helicopters by ignoring ground reflection effects.

RECOMMENDATIONS

In order to further refine the V/STOL Rotary Propulsor Systems Noise Prediction Methodology, the following are recommended:

1. Acquire a well documented data base to supplement the limited information available. This data should be free from installation effects and unknown ground reflection effects.

2. Incorporate ground reflection effects into the existing methodology, as it is easier to correct the calculations than to correct the measurements to free-field conditions.

3. Develop and incorporate into the methodology procedures for adjusting the source noise levels for installation effects.

APPENDIX A. - COMPUTER PROGRAM CHANGES

INTRODUCTION

As a result of the evaluation of the V/STOL Rotary Propulsor Noise Prediction Methodology, several changes were made in the computer program. These changes can be broadly classified into three categories: correction of programming errors, alteration of constants due to methodology revisions, and changes in the calculation procedure. In the first category, inevitable coding errors which were left undetected from the original programming of the methodology and several procedures allowed in IBM FORTRAN but not in other FORTRANs (such as for the CDC computers) were corrected and revised. In the second category, revisions resulting from the evaluation of the noise prediction methodology, such as a new set of forward-flight exponents in the jet noise calculation, were included in the new version of the computer program. Finally, in the third category, changes in the noise prediction methodology required to improve the correlation with measured data were also included in this revision. The revisions to the computer program resulting from the first two categories are essentially transparent to the user. Although the answers might be different, the inputs required to perform the calculations remain the same. The changes in the third category, however, did require a change in the list of inputs.

In the following sections, the changes made in the computer program will be described, the areas where new inputs are required will be identified, and the impact on the calculations will be explained.

PROGRAM CHANGES

The changes made to the computer program will be identified using the module number and name and the line numbers given in the Computer Program User's Manual, volume III of reference 1.

Program Corrections

In the course of the evaluation of the noise prediction methodology, several errors were found in the computer program. These were mostly coding errors, although a few were logic errors which were left over from the original formulation of the program.

Module H894, Main Program. - The area affected is in lines 8370 to 8540, inclusive. The flight distance increments resulting in one half-second intervals for the PNLT at the observer in the calculation of EPNL were incorrectly calculated.

Module H894D, JETN. - In the calculation of the bypass jet noise adjustment, the interpolation between area ratios of 2 and 4 was in error due to a mislabeled variable at line 1670.

Module H894F, ROTOR. - The helicopter rotor noise calculation procedure was originally formulated for a 200 ft sideline. This was unintentionally left in the computer program. The corrections are at lines 890 and 1050 and result in changing 200 to the input sideline distance. Also, the atmospheric attenuation adjustment at lines 4420, 4540, and 4550 was corrected to reflect the actual slant range.

Module H894H, FPFAN. - There was an inconsistency between the way the fan noise directivity factors were derived in this module and the way they are used in subroutine TREAT. The corrections are at lines 5060 to 5240.

Module H894I, FAPROP. - An error was found in summing in low frequency tones to the 1/3 octave band spectra. This was corrected by inserting an IF statement between lines 4130 and 4140.

Module H894K, RVINT. - There was an error in one of the terms in the calculation of stator noise for the OGV case. The correction was to delete line 590 and add the exponent part to the expression at line 1180.

Module H894R, GAAVPF, etc. - This module was originally H894Y. The error in the IF statement at line 1030 was corrected. The calculation of STLD1 at lines 2400, 2410, 2430, and 2440 was corrected.

Module H894T, TREAT. - Due to inconsistencies in the definition of the directivity indices, the conversion from PWL to SPL resulted in levels which were 3 dB too high. Thus, lines 1730, 1960, 2990, and 3610 were adjusted by -3 dB. The fixed-pitch fan treatment calculation had been omitted originally. The logic at lines 1710, 1720, 1730, 1910, and 1920 was changed, and lines after 2070, 2300, 2390, 2520, 2960, and 3580 were added. Finally, to make the treatment calculation for fixed-pitch fan compatible with that for variable-pitch fans, lines after 620 were added.

Module H894V, GAAFPF, etc. - The stage pressure ratio was incorrectly calculated. The proper factor was added after line 14900 and corrected at line 15100.

Methodology Changes

The following changes made to the computer program were a result of revisions to the methodology based on the evaluation performed under the current contract.

Module H894, Main Program. - PNLT values vs time will be printed if the print control is greater than zero.

Module H894D, JETN. - As a result of the evaluation of forward-flight effects, new values for the jet noise flight exponent were derived and incorporated into the jet noise caculation procedure.

Module H894H, FPFAN. - Several changes have been made to this module for convenience to the user. In order to allow a better match between calculated fan aerodynamic parameters and those which exist for an actual fan, it is now required that the fan design bypass ratio (fan-duct flow-rate/core flow-rate) be input. The fan thrust which is calculated and printed is the fan-duct thrust. The total engine thrust is then the sum of the fan-duct thrust and the core engine jet thrust.

Module H894I, FAPROP. - As a result of the methodology evaluation, it was determined that the original unsteady loading noise included installation effects. As a consequence, the empirically determined unsteady loading harmonics were rederived from static uninstalled propeller noise data. This resulted in revised coefficients, including a steeper harmonic level vs harmonic order roll-off. The revisions were made to lines 3490, 3510, 3920, 3940, and 4060.

Module H894K, RVINT. - A problem occurred here that prevented this module from compiling on certain machines. A branch was made from within a do-loop back to within the do-loop. This was corrected by moving the statements into the do-loop and eliminating the branch.

Module H894M, SHRP. - The printout of the thrust was changed to be only that from the fan. The total thrust is then the fan thrust plus the core engine thrust, if any. Also, the unsteady loading rotor noise calculation procedure was changed to match that for the free-air propeller, i.e., to calculate lower levels and a faster roll-off. Finally, a new input was generated. The original off-design tip speed was selected based on a generalization of tip speed schedule desired for approach conditions. However, for the evaluation study, test conditions did not generally follow this generalization. Thus, the operating tip speed can be specified. If it is not specified, the generalization is used.

Module H894N, VPFAN. - The same changes as described for the previous module, H894M, were made to this module. In addition, the rotor broadband noise level and spectrum shape were adjusted to give a better match with that from the measurements.

Module H894O, VPLFAN. - The changes made in this module are the same which were made for module H894M.

Module H894Q, SHTR. - Same changes as for H894M.

Module H894R, GAAVPF. - The module was changed to use the fan operating speed, if input. Also, the generalization of upstream blade drag coefficient, CD, vs pressure ratio and ratio of operating tip speed to optimum tip speed was changed as a result of the methodology evaluation.

Module H894V, GAAFPF, etc. - To give better estimates of fan flow-rates, the corrected weight-flow was changed to 41 lbs/sec/ft^2 for CTOL fixed-pitch fans and 36 lbs/sec/ft^2 for fixed-pitch lift fans. Variable-pitch fans use 40 lbs/sec/ft^2 throughout.

Module H894W, Utility. - This module was newly formed and contains the general usage subroutines: NOYS, TONE, BESJH, BIQUAD, LOAD, UNBAR, UNINT. BESJH, BIQUAD, and UNBAR were modified to allow them to compile on the CDC computer.

Changes in the Input List

The following changes were made to the input list. These resulted from the generation of additional inputs described previously. Thus, the following input data locations were added:

Location	Description of Input
93	Fixed-pitch fan design bypass ratio (Fan-duct flow-rate/core flow-rate).
352	Variable-pitch fan with IGV tip speed, ft/sec, if >0. If 0 uses generalization.
353	Variable-pitch fan with OGV tip speed, ft/sec, if >0. If 0 uses generalization.
354	Variable-pitch lift-fan tip speed, ft/sec, if >0. If 0 uses generalization.

It should be noted that the general usage locations are now in the range 355 to 400. These are available, as before, for input data used in gearbox noise calculations.

USER'S MANUAL REVISIONS

The following summarizes the revisions to the user's manual, volume III of reference 1. Only the text pertaining to the operation of the program will be addressed. Changes in the sample cases and to the program listing will not be indicated. The user is referred to the program itself for these changes.

Figure 3, page 10, should be revised to indicate that the fixed-pitch fan locations are 77 to 93 (from 77 to 92); location 352 is the operating tip speed for variable-pitch fans with IGVs; location 353 is the operating tip speed for variable-pitch fans with OGVs; location 354 is the tip speed for variable-pitch lift fans; and locations 355 to 400 (from 352 to 400) are not specifically allocated.

Page 13, first paragraph under "Variable-Pitch Fan with IGV," should be modified to include location 352 in the list of data locations. The second paragraph should

include location 352 as an input defining the operating conditions. The second paragraph should also have a sentence added to it stating that the operating tip speed (location 352) will be used if the input is greater than zero; otherwise a tip speed based on a generalization for approach conditions will be used.

Figure 7, page 14, should have location 352, "operating tip speed, ft/sec, if > 0. Else uses generalization" added to the input data list. Also, at locations 427 and 135, the word "net" should be changed to "bypass".

Page 15, the first sentence after "Variable-Pitch Fan with OGV" should have location 353 added to the data input list.

Page 15, the first sentence after "Fixed-Pitch Fan" should be revised to include location 93 (i.e., change 77-92 to 77-93). The second paragraph should have the sentence "The design bypass ratio (fan-duct flow-rate/core flow-rate) is loaded into location 93." added to it.

Figure 8, page 16, should have location 353, "operating tip speed, ft/sec, if > 0. Else uses generalization" added to the input data list. Also, at locations 155 and 163, the word "net" should be replaced by "bypass".

Figure 9, page 17, should have location 93, "BYPDS design bypass ratio (fan-duct flow-rate/core flow-rate)" added to the input data list. Also, for clarification, at location 229, after " . . . turbine rotor, fps" add "(or 0.7 UTIP)" and at location 230, after " . . . turbine exit, fps" add "or 48.5 SQRT (T_{T7})".

Figure 11, page 20, should have location 354, "operating tip speed, ft/sec, if > 0. Else uses generalization" added to the input data list. Also, at locations 277 and 285, the word "net" should be changed to "bypass".

APPENDIX B. - GRAPHICAL PROCEDURE CHANGES

INTRODUCTION

As a result of changes in the noise prediction methodology, the graphical procedures were changed to parallel the changes made in the computer program. The new charts described in this section are to replace their counterparts in volume II of reference 1.

REVISED CHARTS

Free-Air Propellers

The change in the free-air propeller noise calculation was in reducing the level of the unsteady loading noise to better match the data from uninstalled propellers. Figure B-1 gives the revised curve which provides partial level PRP7. This replaces figure PRP11, page 27.

Variable-Pitch Fans with IGVs

The unsteady blade loading noise for variable-pitch fans with IGVs was reduced based on the adjustments derived from the free-air propeller noise correlations. Figure B-2 is the replacement for figure IGV17, page 77.

Variable-Pitch Fans with OGVs

Two revisions were made to the procedure for calculating the noise of variable-pitch fans with OGVs. The first revision was to the broadband noise calculation procedure. This revision resulted in lower levels and a change in the spectrum. Figure B-3 replaces figure OGV13 on page 102. The use of this figure is different from the use of the figure it replaces. To calculate the partial level, figure B-3 is entered with the total blade area in ft^2 and the rotor tip Mach number to obtain partial level OGV12'. The partial level OGV12 is then computed to be partial level OGV12' (from figure B-3) times the rotor thrust. Thus, the instructions for step 3 on page 84 are now as follows:

Step 3. Obtain partial level OGV12' from figure OGV13 by entering with the total blade area in ft^2 and moving up to the tip Mach number. Calculate partial level OGV12 by multiplying OGV12' by the rotor thrust.

Figure B-4 is the revised rotor broadband noise spectrum and replaces figure OGV15, page 104. The second revision is to the rotor unsteady blade loading noise and is the same as was described for the variable pitch fan with IGVs. Figure B-5 is the revised figure OGV18, page 107.

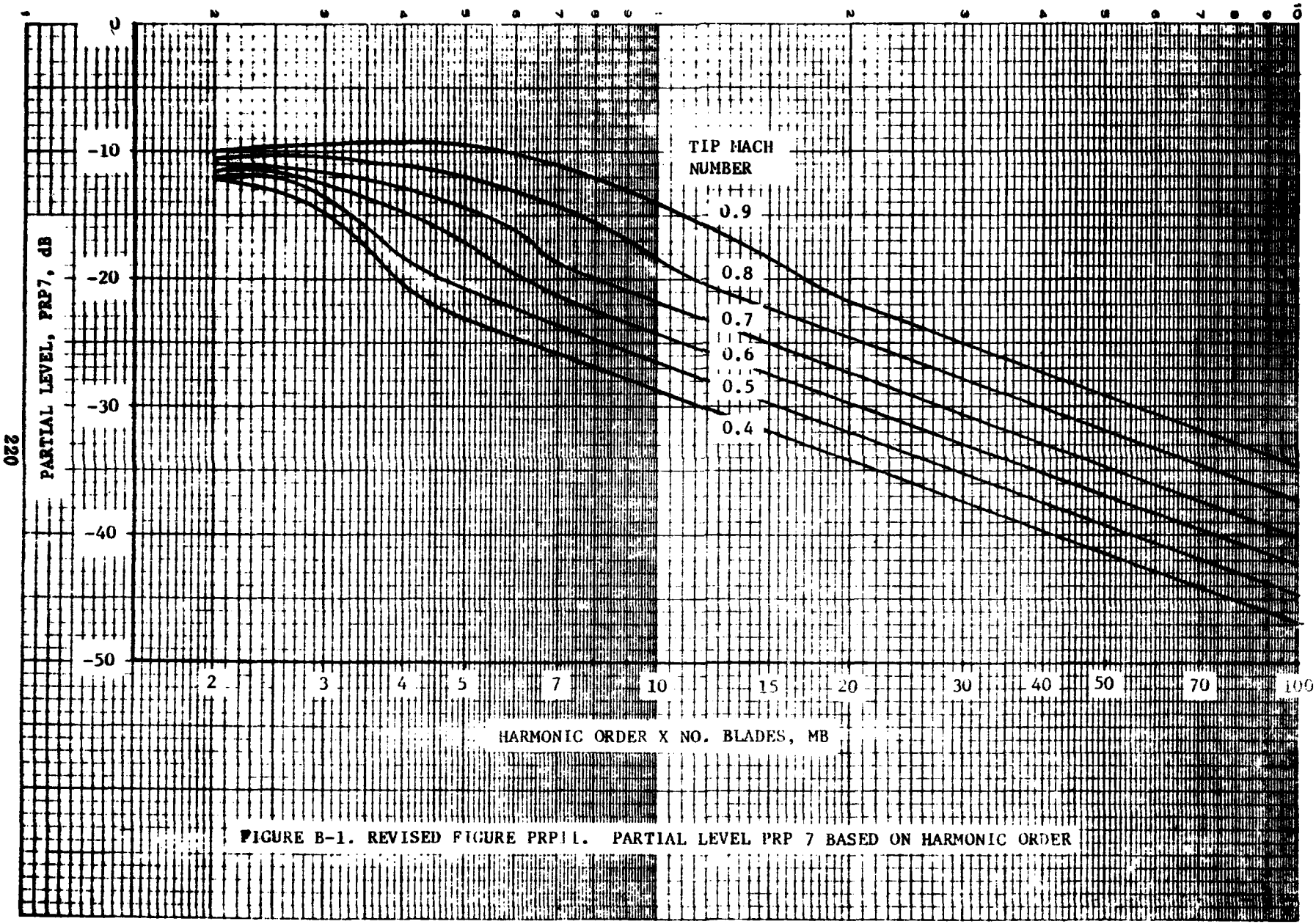

FIGURE B-1. REVISED FIGURE PRP11. PARTIAL LEVEL PRP 7 BASED ON HARMONIC ORDER

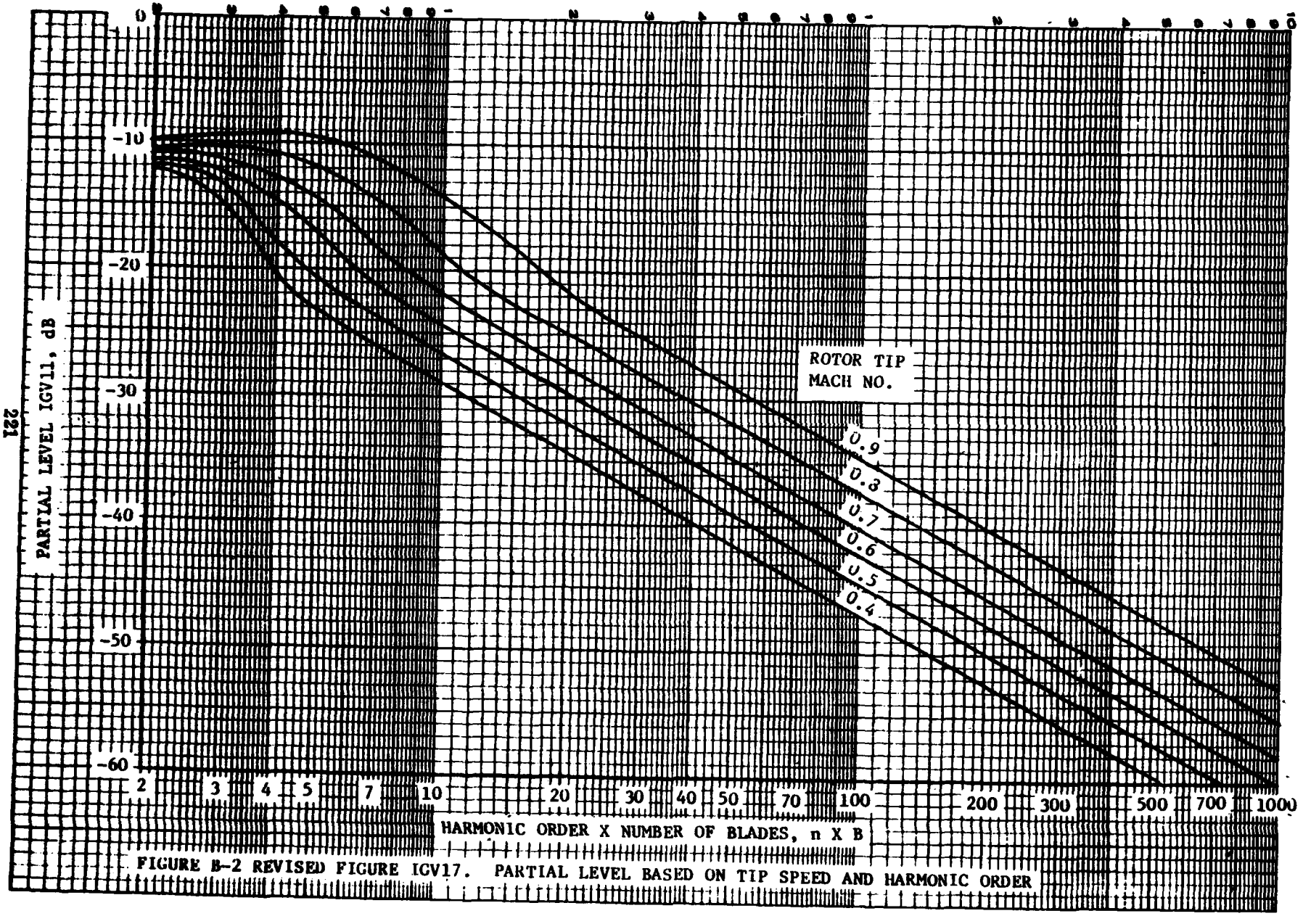

FIGURE B-2 REVISED FIGURE IGV17. PARTIAL LEVEL BASED ON TIP SPEED AND HARMONIC ORDER

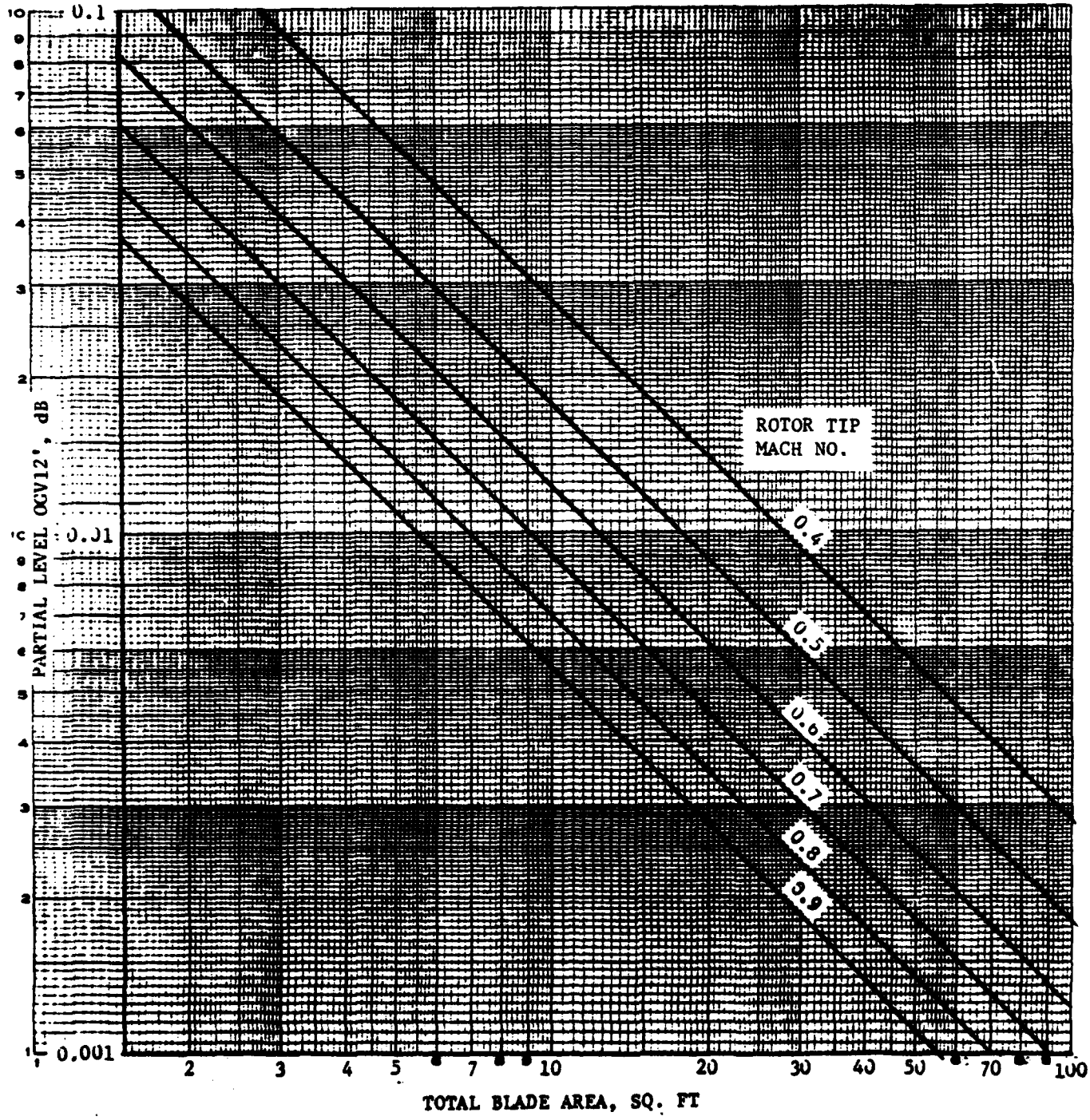

FIGURE B-3 REVISED FIGURE OGV13. ROTOR BROADBAND PARTIAL LEVEL BASED ON ROTOR BLADE AREA AND TIP MACH NUMBER

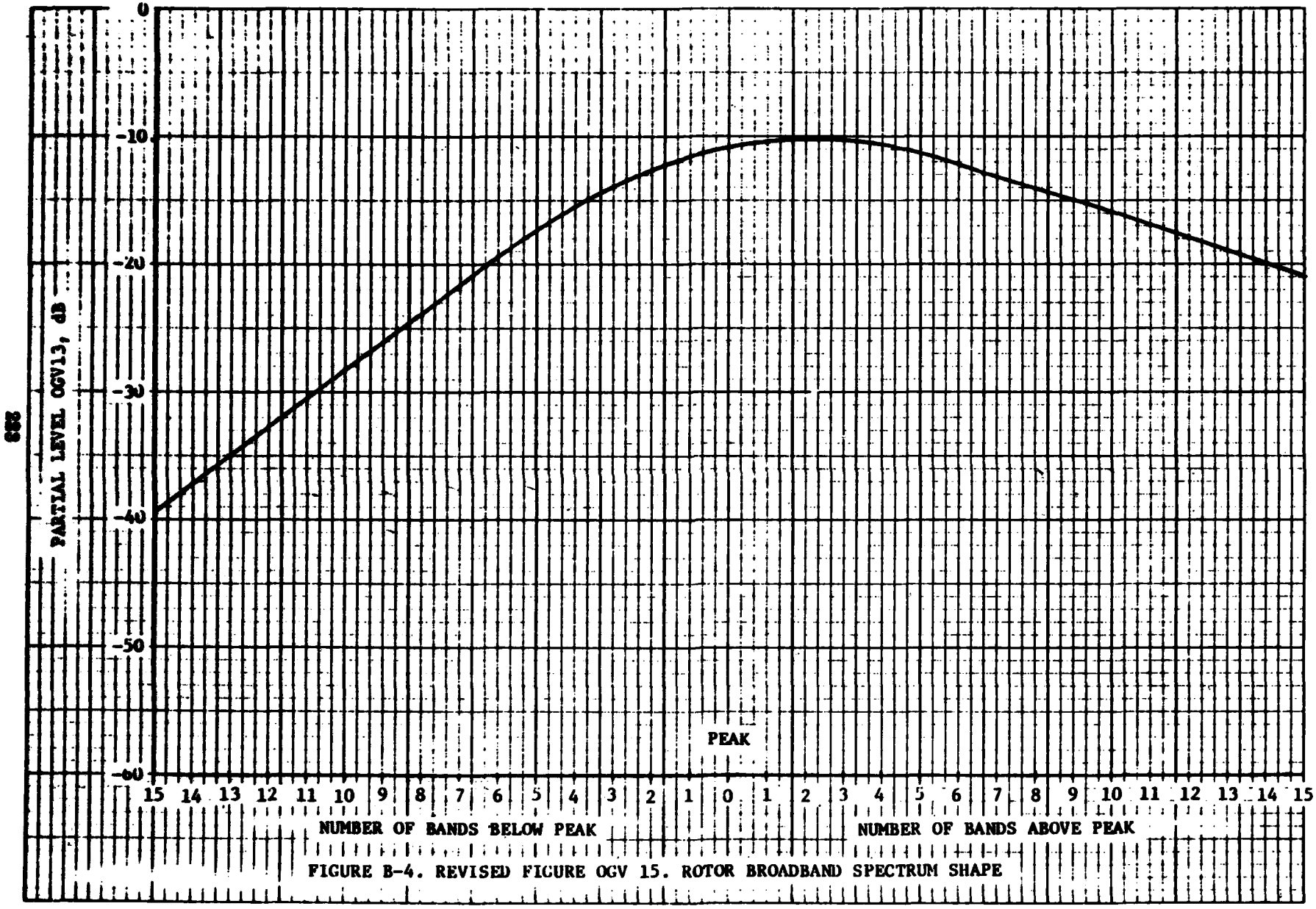

FIGURE B-4. REVISED FIGURE OGV 15. ROTOR BROADBAND SPECTRUM SHAPE

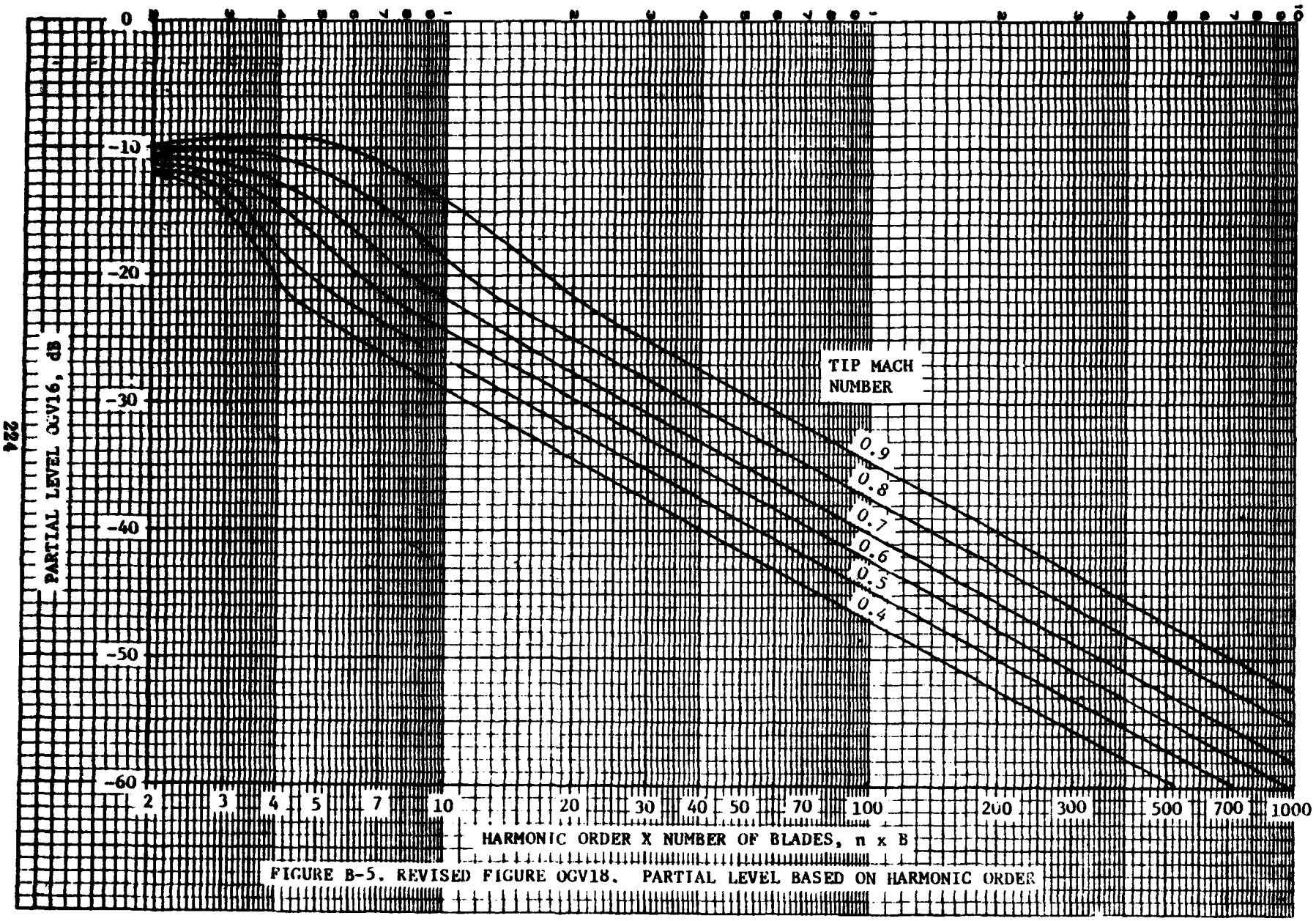

FIGURE B-5. REVISED FIGURE OGV18. PARTIAL LEVEL BASED ON HARMONIC ORDER

Helicopter Rotors

A chart for the dependence of helicopter rotor tone noise on rotor diameter was left out. Figure B-6 shows the partial noise levels for thrust and torque components based on rotor diameter and should be added as figure HEL29 to the helicopter rotor noise graphical calculation procedure. The consequence of inserting this figure, is that a step must be inserted between steps 6 and 7 on page 144. Thus, insert the following step:

Step 6A. Use figure HEL29 to obtain partial levels HEL11 for thrust and HEL12 for torque based on rotor diameter.

Step 7 should then be revised to include HEL11 in the list of partial levels to be summed for thrust components and to include HEL12 in the list of partial levels to be summed for torque components.

Also, in step 5 the axis of rotation and plane of rotation are mislabelled. σ is 0 degrees in the plane of rotation and 90 degrees on the axis of rotation, as correctly indicated in figure HEL7, page 152.

Finally, figures HEL7 through HEL26 are mislabelled. These are not SPL at 200 ft, but are the partial levels HEL7 and HEL8, as indicated in step 5.

Jets

The forward-flight effects on jet noise were revised. This revision resulted in new values for the flight exponent. Figure B-7 shows the revised curves for the flight exponent and for the flight correction, JET4. This figure replaces figure JET4 and figure JET5, page 213.

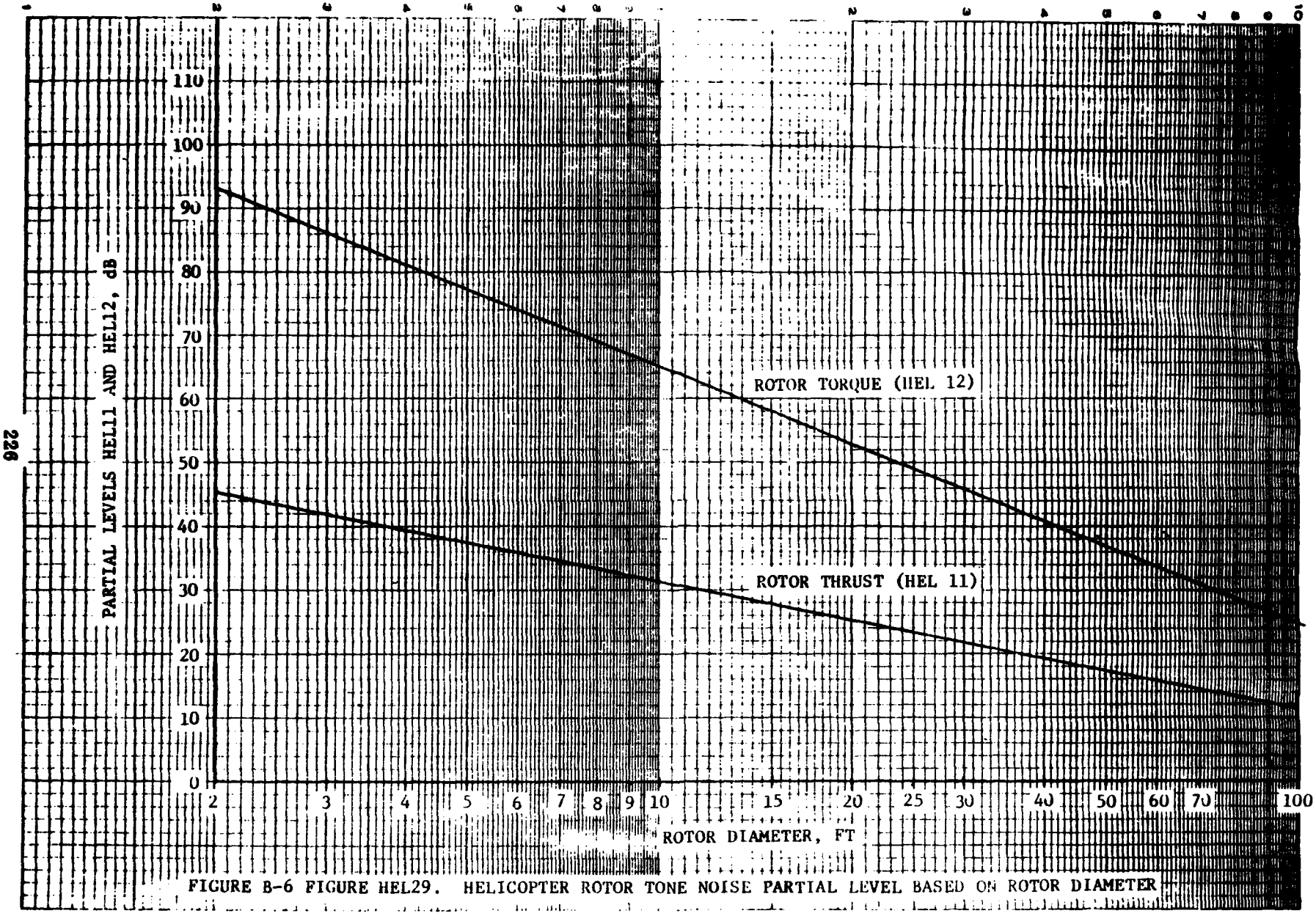

FIGURE B-6 FIGURE HEL29. HELICOPTER ROTOR TONE NOISE PARTIAL LEVEL BASED ON ROTOR DIAMETER

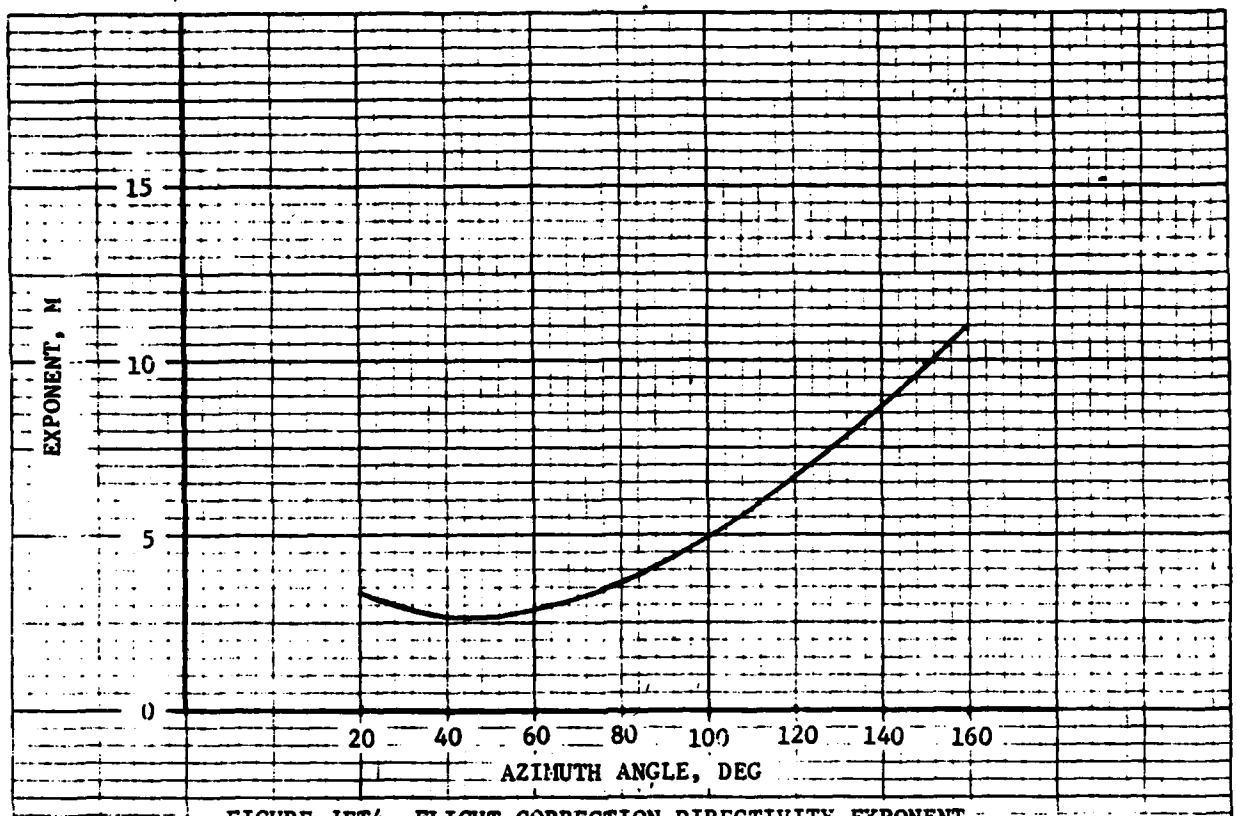

FIGURE JET4. FLIGHT CORRECTION DIRECTIVITY EXPONENT

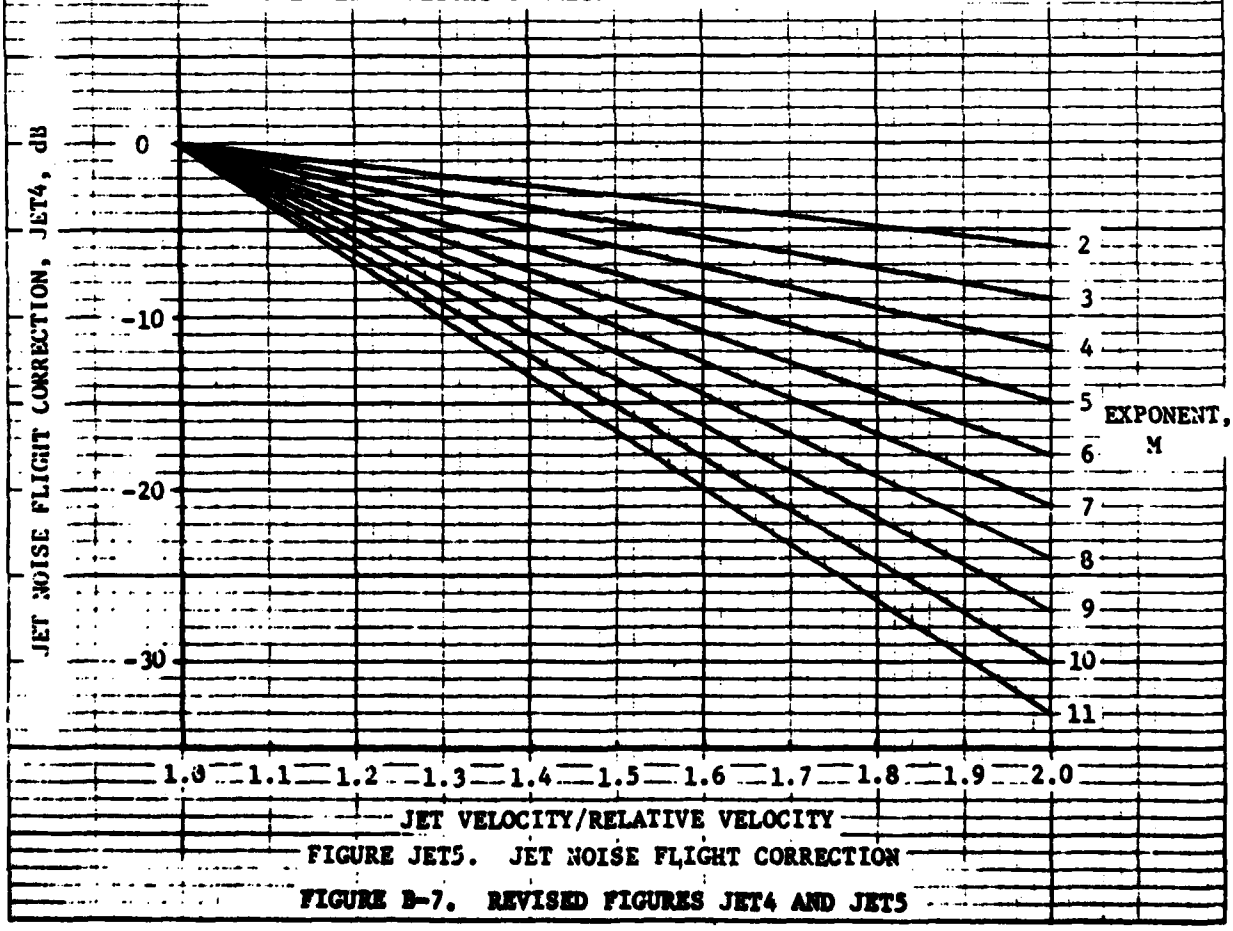

FIGURE JET5. JET NOISE FLIGHT CORRECTION

FIGURE B-7. REVISED FIGURES JET4 AND JET5

REFERENCES

1. Magliozzi, B., V/STOL Rotary Propulsion Systems Noise Prediction and Reduction, Report No. FAA-RD-76-49, 3 Volumes, May 1976.

2. Magliozzi, B., The Influence of Forward Flight on Propeller Noise, NASA CR-145105, Feb. 1977.

3. Anon., Standard Values of Atmospheric Absorption as a Function of Temperature and Humidity, ARP 866, Society of Automotive Engineers, Oct. 1973.

4. Hodder, B.K., The Effects of Forward Speed on Fan Inlet Turbulence and Its Relation to Tone Noise Generation, NASA TMX-62381 Aug 1974.

5. Hodder, B.K., "An Investigation of Possible Causes for the Reduction of Fan Noise in Flight," AIAA Paper 76-585, July, 1976.

6. Kaman Aerospace Corporation, Unpublished Measurements of HH-43B External Noise, Oct. 1964.

7. Bushell, K.W., "Measurement and Prediction of Jet Noise in Flight," AIAA Paper 75-461, March 1975.

8. Anon., Acoustic Effects Produced by a Reflecting Plane, AIR 1327, Society of Automotive Engineers, Sept. 1975.

9. Barry, F.W. and Magliozzi, B., Noise Detectability Prediction Method for Low Tip Speed Propellers, AFAPL-TR-71-37, June 1971.

10. Magliozzi, B. and Ganger, T.G., Advanced V/STOL Propeller Technology - Far-Field Noise Investigation, AFFDL-TR-71-88, Volume XIII, Mar. 1972.

11. Dietrich, D.A., et. al., "Acoustic Signatures of a Model Fan in the NASA-Lewis Anechoic Wind Tunnel," AIAA Paper 77-59, Los Angeles, Calif., 1977.

12. Magliozzi, B., et. al., Noise and Wake Structure Measurements in a Subsonic Tip Speed Fan, NASA CR-2323, Nov. 1973. Also, Tabulation and Plots of Test Data, NASA CR-132259, July 1973.

13. Rice, E.J., et. al., Acoustic and Aerodynamic Performance of a 6-Foot Diameter Fan for Turbofan Engines - III - Performance with Noise Suppressors, NASA TN D-6178, Feb. 1971.

14. Pegg, R.J. and Shidler, P.A., "Exploratory Wind Tunnel Investigation of the Effect of the Main Rotor Wake on Tail Rotor Noise," In the NASA Conference Publication 2052, Part I - Helicopter Acoustics, May, 1978.

15. Detroit Diesel Allison, Unpublished T-56 Engine Noise Data Transmitted to Hamilton Standard by Letter Dated Sept. 19, 1978.